Global and local strength analysis in equivalent quasi-static head waves, for a tanker ship structure, based on full length and 2-3 cargo holds 3D-FEM models

Cioarec Dan Sebastian

Master Thesis

presented in partial fulfilment
of the requirements for the double degree:
“Advanced Master in Naval Architecture” conferred by University of Liege
"Master of Sciences in Applied Mechanics, specialization in Hydrodynamics, Energetics and Propulsion” conferred by Ecole Centrale de Nantes

developed at "Dunarea de Jos" University of Galati
in the framework of the

“EMSHIP”
Erasmus Mundus Master Course
in “Integrated Advanced Ship Design”

Ref. 159652-1-2009-1-BE-ERA MUNDUS-EMMC

Supervisor: Prof. Leonard Domnisoru, "Dunarea de Jos" University of Galati

Reviewer: Prof. André Hage, University of Liege

Galati, February 2013

CONTENTS

DECLARATION OF AUTHORSHIP

Declaration of Authorship

I declare that this thesis and the work presented in it are my own and have been generated by me as the result of my own original research.

Where I have consulted the published work of others, this is always clearly attributed.

Where I have quoted from the work of others, the source is always given. With the exception of such quotations, this thesis is entirely my own work.

I have acknowledged all main sources of help.

Where the thesis is based on work done by myself jointly with others, I have made clear exactly what was done by others and what I have contributed myself.

This thesis contains no material that has been submitted previously, in whole or in part, for the award of any other academic degree or diploma.

I cede copyright of the thesis in favour of the University "Dunarea de Jos", of Galati, Romania

Date: 21.01.2013 *Signature*

ABSTRACT

Global and local strength analysis in equivalent quasi-static head waves, for a tanker ship structure, based on full length and 2-3 cargo holds 3D-FEM models

By **Cioarec Dan Sebastian**

The main objective of the thesis is to provide the specific knowledge concerning the methods for global and local ship hull structure strength analysis, under equivalent quasi-static head wave loads. The numerical results have to stress out the adequacy of structural models, with different complexity levels, developed for ship hull strength assessment.

For the analysis has been selected a chemical tanker ship with double hull, granted by the Ship Design Group, Galati, during the internship. The following ship data are required for the strengths analysis: hull offset lines, structural characteristics over several transversal sections, material characteristics, mass distribution over the ship length.

The ship hull offset lines is based on the chemical tanker ship and the transversal sections structure scantlings are according to the Bureau Veritas Classification Society Hull Rules. The mass distribution is based on the full 3D-CAD/FEM model developed in the study (for hull steel mass group) and the prototype ship onboard masses groups. The ship hull model has been developed using three different modelling levels: a 3D-FEM model full extended over the ship length; a 3D-FEM model extended on the two cargo holds compartments from the ship central part (coarse and fine mesh size) and a 1D-Equivalent Beam model (as reference for the 3D-FEM Models).

The global - local ship hull strength analysis based on 3D-FEM model full extended over the ship length, one sided, includes the following steps: the 3D-CAD of the ship hull offset lines, the 3D-CAD/FEM mesh (coarse) of the ship hull structure, the boundary conditions, the gravity loads from structure and other onboard masses, cargo and cargo tanks structure considered as local pressure applied on the double bottom shell in the cargo holds area, the equivalent quasi-static head wave pressure loads applied on the hull external shell, using an iterative procedure for the free floating and trim conditions equilibrium, implemented with user subroutines in the FEM solver. The results are obtained from the 3D-FEM model with post-processing user subroutines, as follows: normal, tangential and vonMises stresses. The strength assessment includes the safety factor in reference to the yield stress limit criteria. The 3D- FEM model has been developed with Solid Works Cosmos/M 2007 program, based on a 3D-CAD model developed with AutoCAD, with iterative analysis and post processing user subroutines developed for Cosmos/M solver, at Galati Naval Architecture Faculty.

The global ship strengths analysis based on 1D-equivalent ship girder model, under equivalent quasi-static head waves, is carried on with an iterative algorithm for free floating and trim equilibrium conditions, using an in-house made code from Galati Naval Architecture Faculty.

The global - local ship hull strength analysis based on 3D-FEM model extended on two cargo holds compartments (central ship part), with coarse mesh size, for cargo holds structural strength analysis, was performed with Solid Works Cosmos/M 2007, having the same local loads as the 3D-FEM Full extended model and at both model ends the global displacement and rotation are taken from the previous 1D-equivalent girder model. In order to apply the external pressure on the ship hull, from the equivalent quasi-static wave, and the global displacements and rotations at both model ends, there were used specific user subroutines implemented in Solid Works Cosmos/M 2007 Solver.

The 3D-FEM Model extended on two cargo hold compartments has been refined, in order to include some selected structural details (hot-spots domains). The boundary condition and the global-local loads are the same as for the previous coarse mesh size model. The strength assessment includes also hot-spot factor evaluation for the deck and bottom structural panels.

Comparison between deformations and stress values based on the four structural models, having different complexity levels, was performed. The numerical FEM analysis provides reliable data for the ship strength assessment, with a good concordance between the structural models developed in this study, taking into account the specific models sensitivity.

1. INTRODUCTION

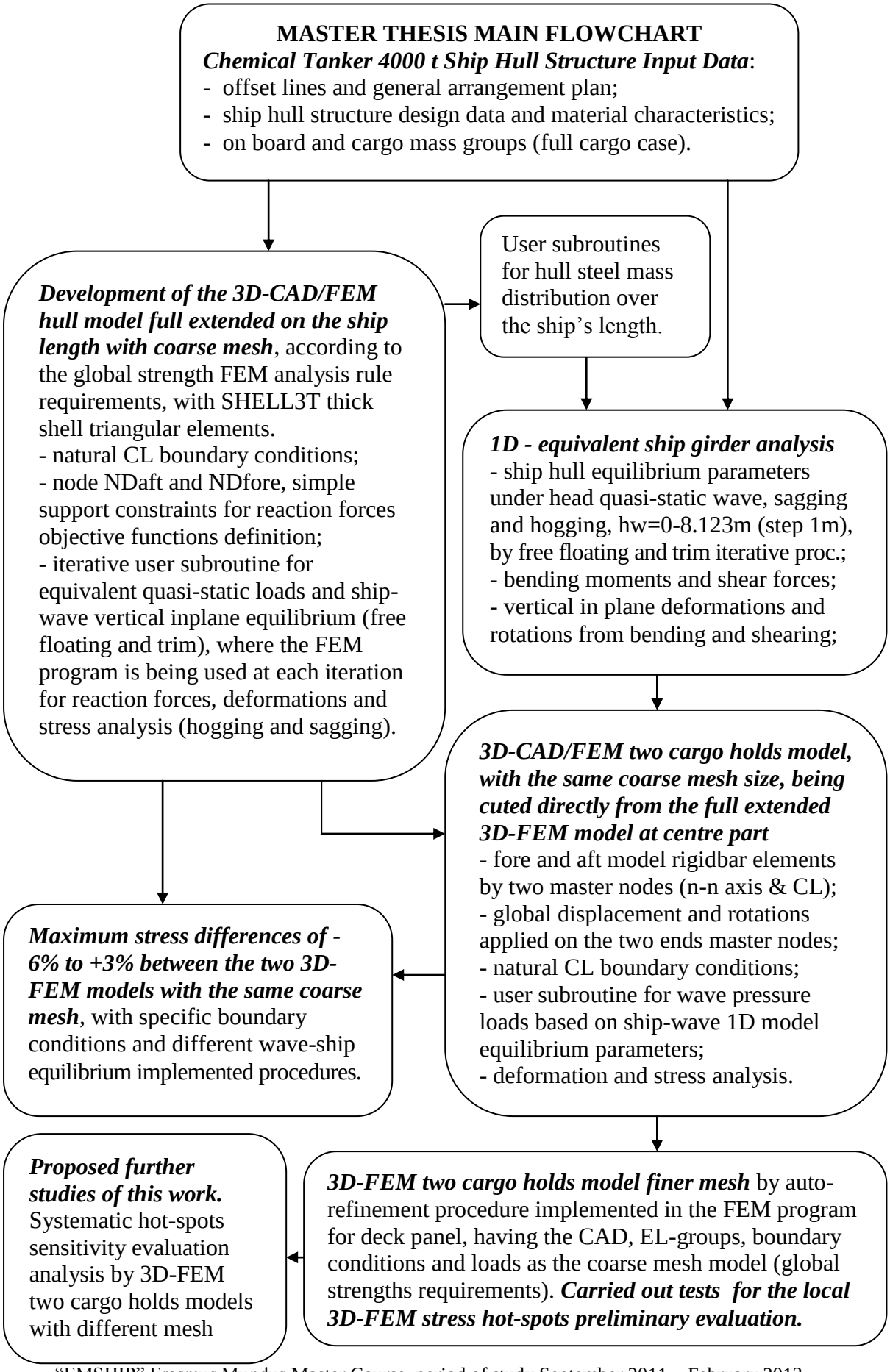

The finite element method was initial applied to the aircrafts construction, the structures been idealised through simple beam grids models. The finite element method knew a quick development in tandem with the increase of the computational capacities and it has enforced as a general numerical method of solving engineering problems from different areas, inclusively the ship structures domain.

Generally, a structural analysis has the following steps:

• the objectives settlement, the type and the size of the analysis;

• the modelling of structures and the boundary conditions;

• the settlement of type and the modelling of the loads;

• the analysis and the evaluation of the results.

The type and the size of the analysis depend on the nature of the structural response that is to be obtained. Generally, for the global-local strength analysis are obtained the stresses and deformations distributions, under dynamic or equivalent quasi-static wave loads.

The loads at the analysis of ship structures include: forces and external pressures, forces that arise from own ship weight and from the cargo, external wave pressures, etc.

At the ship structures the deformations and the stresses can be divided in the following categories, depending on the analysed problem:

• global deformations and stresses of the ships girder and main structural elements;

• local deformations and stresses of the main and secondary structural elements;

• hot-spot stress domains of the structural elements (details).

The requirements of the present day ship structural analyses impose to develop three-dimensional (3D) models, based on the FEM - Finite Element Method (Frieze and Shenoi 2006). In order to increase the accuracy of the global strength analysis of ship structure, a major step is to use the 3D-FEM full extended over the ship length models (Lehmann 1998, Rozbicki et al. 2001, Domnisoru 2006), instead of models extended only over several cargo holds (Hughes 1988, Domnisoru 2001, Servis et al. 2003). In this study, the global-local strength analysis is carried on a chemical-tanker ship, provided by the Ship Design Group, Galati Company, granted during the Internship activity. The study is focused on the full cargo loading case, under equivalent quasi-static head wave external loads. The numerical structural analyses are based on the following models: ship 1D-Equivalent Beam Model, 3D-FEM Full Extended Model (with coarse mesh) and also 3D-FEM two cargo holds compartments model (with coarse and fine mesh), using in-house program codes (Domnisoru 2006) and SolidWorks Cosmos/M (2007) FEM commercial program, involving also user subroutines for pre, post processing and analysis.

2.THEORETICAL BACKGROUND

In the following, there is presented the theoretical method for global strengths analysis of the ship hull, in the vertical plane, under own weight, cargo, still water and equivalent quasi-static head wave loads. There are considered three types of analysis models: the 1D-equivalent ship girder, the 3D-FEM model extended on several cargo holds compartments at the ship centre part and the 3D-FEM model full extended over the ship length. It is pointed out that the 3D-FEM models make possible to obtain better results for the global - local stress distribution at the ship strengths analysis and also it can reveal (locate) the hot-spot stress domains (Carlos Guedes Soares, Purnendu K. Das, 2007; Frieze, Shenoi, 2006; Domnisoru, 2006).

2.1. The Global Ship Strengths Analysis Based on 1D-Equivalent Beam Method

In this sub-chapter there is presented the 1D-Equivalent Beam ship hull model for global strengths analysis (Domnisoru 2006), which is used for the comparison with the methods based on 3D-FEM models.

2.1.1. The Ship 1D-Equivalent Beam Model - Still Water Loads

The ship weight distribution is obtained based on the ship mass distribution over the ship length, with the following relation:

$$g_x(x) = g \cdot \mu(x) \quad x \in [-L/2, L/2] \quad \Rightarrow \quad g_{xi} = g \cdot \mu_i \quad i = 1, n \tag{2.1.1}$$

where: L ship length, g gravity acceleration, μ(x) mass distribution, n ship girder elements over the 1D-beam model.

Obs. In order to simplify the integrals calculation with trapeze method, there are considered the significant ship hull transversal sections disposed at the middle of the „n" elements.

$$x_1 = -\frac{L}{2} + \frac{\delta x}{2} \quad , \quad x_{i+1} = x_i + \delta x \quad i = 1, n-1; \delta x = L/n; \int_{-L/2}^{L/2} f(x)dx = \delta x \cdot \sum_{i=1}^{n} f(x_i) \tag{2.1.2}$$

In order to obtain the ship still water equilibrium position it is necessary to use an iterative algorithm for a given $V = c_B LBd$ and x_G (from $\mu(x)$), as following:

$$iter=0 \qquad d_i^{(0)}=d \;\rightarrow\; A_{Ti}^{(0)} \;\; i=1,n \;\; x_F^{(0)};R^{(0)} \quad \textit{from ship offset lines}$$

$$V^{(0)}=\int_{-L/2}^{L/2}A_T^{(0)}(x)dx=\delta x\sum_{i=1}^{n}A_{T\,i}^{(0)} \qquad M_y^{(0)}=\int_{-L/2}^{L/2}x\cdot A_T^{(0)}(x)dx=\delta x\sum_{i=1}^{n}x_i A_{T\,i}^{(0)} \qquad x_B^{(0)}=\frac{M_y^{(0)}}{V^{(0)}}$$

$$d_{pp}^{(1)}=d-\left(\frac{L}{2}+x_F^{(0)}\right)\frac{x_G-x_B^{(0)}}{R^{(0)}} \qquad d_{pv}^{(1)}=d+\left(\frac{L}{2}-x_F^{(0)}\right)\frac{x_G-x_B^{(0)}}{R^{(0)}}$$

$$iter=k \qquad d_i^{(k)}=d_{pp}^{(k)}+\frac{d_{pv}^{(k)}-d_{pp}^{(k)}}{L}\left(x_i+\frac{L}{2}\right)\rightarrow \;\; A_{Ti}^{(k)} \;\; i=1,n \;\; x_F^{(k)};R^{(k)} \quad \textit{from ship offset lines}$$

$$V^{(k)}=\int_{-L/2}^{L/2}A_T^{(k)}(x)dx=\delta x\sum_{i=1}^{n}A_{T\,i}^{(k)} \qquad M_y^{(k)}=\int_{-L/2}^{L/2}x\cdot A_T^{(k)}(x)dx=\delta x\sum_{i=1}^{n}x_i A_{T\,i}^{(k)} \qquad x_B^{(k)}=\frac{M_y^{(k)}}{V^{(k)}}$$

$$d_{pp}^{(k+1)}=d_{pp}^{(k)}+\frac{V^{(k)}-V^{(k-1)}}{A_{WL}^{(k)}}-\left(\frac{L}{2}+x_F^{(k)}\right)\frac{x_G-x_B^{(k)}}{R^{(k)}} \;\; ; \;\; d_{pv}^{(k+1)}=d_{pv}^{(k)}+\frac{V^{(k)}-V^{(k-1)}}{A_{WL}^{(k)}}+\left(\frac{L}{2}-x_F^{(k)}\right)\frac{x_G-x_B^{(k)}}{R^{(k)}}$$

The convergence criteria are: $\left|V-V^{(k)}\right|<0.004V \qquad \left|x_G-x_B^{(k)}\right|<0.001L$ (2.1.3)

and also the longitudinal trim angle is: $\left(d_{pv}^{(k)}-d_{pp}^{(k)}\right)/L$.

Obs. There are noted above (2.1.3) the following:

$$I_y=\int_{-L/2}^{L/2}x^2b(x)dx=\delta x\cdot\sum_{i=1}^{n}x_i^2b_i \;\; ; \;\; R=\frac{I_y}{V} \; ; x_F=\frac{M_{yWL}}{A_{WL}} \; ; x_G=\int_{-L/2}^{L/2}x\cdot g_x(x)dx \Big/ \int_{-L/2}^{L/2}g_x(x)dx$$
$$A_{WL}=\int_{-L/2}^{L/2}b(x)dx=\delta x\cdot\sum_{i=1}^{n}b_i \;\; ; M_{yWL}=\int_{-L/2}^{L/2}x\cdot b(x)dx=\delta x\cdot\sum_{i=1}^{n}x_i\,b_i \qquad (2.1.4)$$

where: B ship breadth, d medium draught amidships, c_B block coefficient, b(x) water plane breadth, x_G the gravity centre abscise.

The still water vertical force per unit length results from the following relation:

$$a_{cx}(x)=\rho g A_T(x) \quad x\in[-L/2,L/2] \;\Rightarrow\; a_{cxi}=\rho g A_{T\,i}^{(k)} \quad i=1,n \qquad (2.1.5)$$

The ship still water loads results from the following relation:

$$p_{cx}(x)=g_x(x)-a_{cx}(x) \qquad x\in[-L/2,L/2] \;\Rightarrow\; p_{cxi}=g_{xi}-a_{cxi} \qquad i=1,n \qquad (2.1.6)$$

The still water shear forces and bending moments results from the following relations:

$$T_c(x)=\int_{-L/2}^{x}p_{cx}(x)dx \;\; ; \;\; M_c(x)=\int_{-L/2}^{x}T_c(x)dx \qquad (2.1.7)$$

2.1.2. The Supplementary Ship 1D-Equivalent Beam Model Loads From Equivalent Quasi-static Head Waves

There are considered the loads from equivalent quasi-static head waves, with the wave length equal to the ship length ($\lambda = L$). The amplitude of the equivalent quasi-static wave $a_w=h_w/2$, with Smith correction, based on Bureau Veritas, 2010 Rules, it results according to the following expression:

$$h_w = \left[\frac{L}{25} + 4.1\right] \cdot c_{RW} \ \ [m] \ ; \quad L < 90m$$
$$h_w = \left[10.75 - \left(\frac{300 - L}{100}\right)^{3/2}\right] \cdot c_{RW} \ [m] \ ; \quad 90 \le L \le 300m \tag{2.1.8}$$

where $c_{RW} \in \{1.00 \quad 0.90 \quad 0.75 \quad 0.66 \quad 0.60\}$ is the zone navigation coefficient. In the case of the studied chemical tanker ship $c_{RW}=1$.

In order to take into account the real ship hull offset lines, analogue to the case of still water, there it is used a non-linear iterative procedure with two steps.

In this case d_m, d_{pp},d_{pv}, trim become the parameters that can define the position of the median plane of the equivalent quasi-static head wave, taking as reference the base plane of the ship hull.

For the considered loading case there are known: Δ , V, x_G , L , the offset lines, the ship hydrostatics, Bonjean diagram.

Obs. The coordinates system origin is considered at the aft ship $x \in [0, L]$.

$$x_1 = \frac{\delta x}{2} \ , \ x_{i+1} = x_i + \delta x \quad i = 1, n-1; \ \delta x = L/n \tag{2.1.9}$$

Step I – the floating condition

$$iter = 0 \quad d_m^{(0)} = 0 \ \Rightarrow \ d_i^{(0)} = d_m^{(0)} \pm \frac{h_w}{2}\cos\left(\frac{2\pi x_i}{L}\right) \ \rightarrow \ A_{Ti}^{(0)} \quad i = 1, n \quad from\ Bonjean$$
$$V^{(0)} = \int_0^L A_T^{(0)}(x)dx = \delta x \sum_{i=1}^{n} A_{Ti}^{(0)} \qquad M_y^{(0)} = \int_0^L x \cdot A_T^{(0)}(x)dx = \delta x \sum_{i=1}^{n} x_i A_{Ti}^{(0)} \qquad x_B^{(0)} = \frac{M_y^{(0)}}{V^{(0)}} \tag{2.1.10}$$
$$iter = k \quad d_m^{(k)} = d_m^{(k-1)} + 0.001 \ \Rightarrow \ d_i^{(k)} = d_m^{(k)} \pm \frac{h_w}{2}\cos\left(\frac{2\pi x_i}{L}\right) \ \rightarrow \ A_{Ti}^{(k)} \quad i = 1, n \quad from\ Bonjean$$
$$V^{(k)} = \int_0^L A_T^{(k)}(x)dx = \delta x \sum_{i=1}^{n} A_{Ti}^{(k)} \qquad M_y^{(k)} = \int_0^L x \cdot A_T^{(k)}(x)dx = \delta x \sum_{i=1}^{n} x_i A_{Ti}^{(k)} \qquad x_B^{(k)} = \frac{M_y^{(k)}}{V^{(k)}}$$

and the iteration is made until $V^{(k)} \ge V$.

The solution is refined, using the half domain method, so that at the last iteration „m" it is achieved the convergence criteria $\left|V - V^{(m)}\right| < 0.001V$.

At the end of the first step, it results the following parameters:

$$x_B^I = x_B^{(m)} \qquad d_m^I = d_m^{(m)} \;\rightarrow\; x_F^I \;,\; A_{wL}^I \tag{2.1.11}$$

- Step II – the trim condition

$$x_G > x_B^I \;\rightarrow\; \delta trim = 0.00001 \quad \text{or} \quad x_G < x_B^I \;\rightarrow\; \delta trim = -0.00001$$

$$iter = 0 \quad d_m^{(0)} = d_m^I \qquad x_F^{(0)} = x_F^I \qquad A_{wL}^{(0)} = A_{wL}^I \qquad trim^{(0)} = \delta trim$$

$$d_{pp}^{(0)} = d_m^{(0)} - x_F^{(0)} \cdot trim^{(0)} \qquad d_{pv}^{(0)} = d_m^{(0)} + \left(L - x_F^{(0)}\right) \cdot trim^{(0)}$$

$$d_i^{(0)} = d_{pp}^{(0)} + \left(d_{pv}^{(0)} - d_{pp}^{(0)}\right)\frac{x_i}{L} \pm \frac{h_w}{2}\cos\left(\frac{2\pi x_i}{L}\right) \;\rightarrow\; A_{Ti}^{(0)} \quad i = 1, n \quad \textit{from Bonjean}$$

$$V^{(0)} = \int_0^L A_T^{(0)}(x)dx = \delta x \sum_{i=1}^{n} A_{Ti}^{(0)} \qquad M_y^{(0)} = \int_0^L x \cdot A_T^{(0)}(x)dx = \delta x \sum_{i=1}^{n} x_i A_{Ti}^{(0)} \qquad x_B^{(0)} = \frac{M_y^{(0)}}{V^{(0)}}$$

$$x_G > x_B^{(0)} \;\rightarrow\; \delta trim = 0.00001 \quad \text{or} \quad x_G < x_B^{(0)} \;\rightarrow\; \delta trim = -0.00001$$

$$iter = k \quad d_m^{(k)} = d_m^{(k-1)} + \frac{V - V^{(k-1)}}{A_{wL}^{(k-1)}} \;\rightarrow\; x_F^{(k)} \;,\; A_{wL}^{(k)} \qquad trim^{(k)} = trim^{(k-1)} + \delta trim \tag{2.1.12}$$

$$d_{pp}^{(k)} = d_m^{(k)} - x_F^{(k)} \cdot trim^{(k)} \qquad d_{pv}^{(k)} = d_m^{(k)} + \left(L - x_F^{(k)}\right) \cdot trim^{(k)}$$

$$d_i^{(k)} = d_{pp}^{(k)} + \left(d_{pv}^{(k)} - d_{pp}^{(k)}\right)\frac{x_i}{L} \pm \frac{h_w}{2}\cos\left(\frac{2\pi x_i}{L}\right) \;\rightarrow\; A_{Ti}^{(k)} \quad i = 1, n \quad \textit{from Bonjean}$$

$$V^{(k)} = \int_0^L A_T^{(k)}(x)dx = \delta x \sum_{i=1}^{n} A_{Ti}^{(k)} \qquad M_y^{(k)} = \int_0^L x \cdot A_T^{(k)}(x)dx = \delta x \sum_{i=1}^{n} x_i A_{Ti}^{(k)} \qquad x_B^{(k)} = \frac{M_y^{(k)}}{V^{(k)}}$$

$$x_G > x_B^{(k)} \;\rightarrow\; \delta trim = 0.00001 \quad \text{or} \quad x_G < x_B^{(k)} \;\rightarrow\; \delta trim = -0.00001$$

and it is iterated until $\delta trim$ is changing the sign.

The solution is refined with the half domain method, so that at the last iteration „m" there are satisfied the convergence criteria: $\left|V - V^{(m)}\right| < 0.001V \qquad \left|x_G - x_B^{(m)}\right| < 0.001L$.

At the end of the second step there result the following data:

$$d_m = d_m^{(m)} \;,\; d_{pp} = d_{pp}^{(m)} \;,\; d_{pv} = d_{pv}^{(m)} \;,\; trim = trim^{(m)} \;,\; A_{Ti} = A_{Ti}^{(m)} \quad i = 1, n \tag{2.1.13}$$

The total vertical load from equivalent quasi-static head wave has the expression:

$$p_{xi} = g_{xi} - \rho g A_{Ti} \quad i = 1, n \;\rightarrow\; p_x(x) \quad x \in [0, L] \tag{2.1.14}$$

The total shear forces and bending moments from equivalent quasi-static head wave have the following expressions:

$$T(x) = \int_0^x p_{cx}(x)dx \,;\; M(x) = \int_0^x T(x)dx \qquad x \in [0, L] \tag{2.1.15}$$

Obs. In the above relations the sign $\pm$ make possible to select the hogging (+) and sagging (-) wave loads cases. Based on the above 1D-Equivalent Beam Model, the in-house program P_ACASV version 5, (Domnisoru, 2006) has been developed as a standalone code.

2.2. The Global - Local Ship Strengths Analysis Based on 3D-FEM Full Extended Models

The enhanced method of ship global - local strengths analysis is based on 3D-FEM models developed over the full length of the ship (Domnisoru, 2006).

In compare to the 1D Equivalent Beam Model (Chapter 2.2.1) the approach based on 3D-FEM models has the following main advantages:

- the real ship 3D structure is taken into account, with the corresponding geometries and material proprieties;
- reduced number of boundary conditions (compared to partial extended models);
- the 3D stress and deformations distributions in the ship structure are obtained, pointing out also the local hot-spots domains;
- with no restrictions to the ship hull offset lines form, the floating and trim equilibrium position is obtained at still water and equivalent quasi-static statistical head waves.

2.2.1 The 3D-CAD of the Ship Hull Offset Lines

In the first step there is developed the ship hull offset lines CAD, using specialized program Rhinoceros, 2006. This CAD models are exported as neutral DXF files format.

2.2.2. The 3D-CAD of the Ship Hull Structure

The second step includes the 3D-CAD ship hull geometry modelling, extended over the full ship length. This approach is based on the ship offset lines CAD files, which can be developed on general CAD programs as AutoCAD, 2011(Autodesk), with export of DXF files format, or directly using the FEM program CAD pre-processing procedures, as those existing in Solid Works Cosmos/M 2007.

2.2.3 The 3D-FEM Mesh of the Ship Hull Structure

The third step of the ship strengths analysis includes the generation of the 3D-FEM models, based on the parametric or auto-mesh options that are usual included in the FEM programs.

2.2.4 The Boundary Conditions on the 3D-FEM Model of the Ship Hull Structure

At the fourth analysis step there are modelled the boundary conditions for the 3D-FEM ship hull model full extended over the length, that are of two types:

- the symmetry conditions at the nodes disposed in the centre line plane of the ship, the model being developed only on one side (for head waves loads case);
- the vertical support conditions at two nodes disposed at the ship hull structure extremities (in the centre line plane), noted NDpp at the stern (aft) and NDpv at the bow (fore). At the vertical equilibrium conditions, for still water or equivalent quasi-static head waves, the reactions forces in the two vertical supports must become zero.

2.2.5 The Loading Conditions. Numerical Analysis Based on 3D-FEM Models

At the fifth analysis step there are considered the modelling of the loads conditions and the effective numerical analysis of the 3D-FEM model developed over the full ship length, in order to obtain the deformations and stress distributions at the ship global-local strengths analysis.

The loads acting over the ship hull are of three types (considering Solid Works Cosmos/M 2007 implementation):

- the gravity loads from the own structures weight and other onboard mass components of the displacement, except the cargo masses (and cargo tank independent structure);
- the cargo loads plus the cargo tanks independent structure, considered as local pressures uniform distributed over the double bottom shell;
- the equivalent quasi-static head wave pressure loads for the following cases: $h_w = 0$ (still water) and $h_w \neq 0$ (according the statistical values from Classification Societies Rules), using an iterative procedure for the free floating and trim condition equilibrium (see Fig.2.2.1.), implemented with GEO macro-commands files in the Solid Works Cosmos/M 2007 FEM program.

In figure 2.2.1 there is presented the principal flow chart of the GEO macro commands files (Domnisoru 2006), where the Solid Works Cosmos/M 2007 FEM is used as solver for linear static structural analysis of the 3D-FEM model at each iteration.

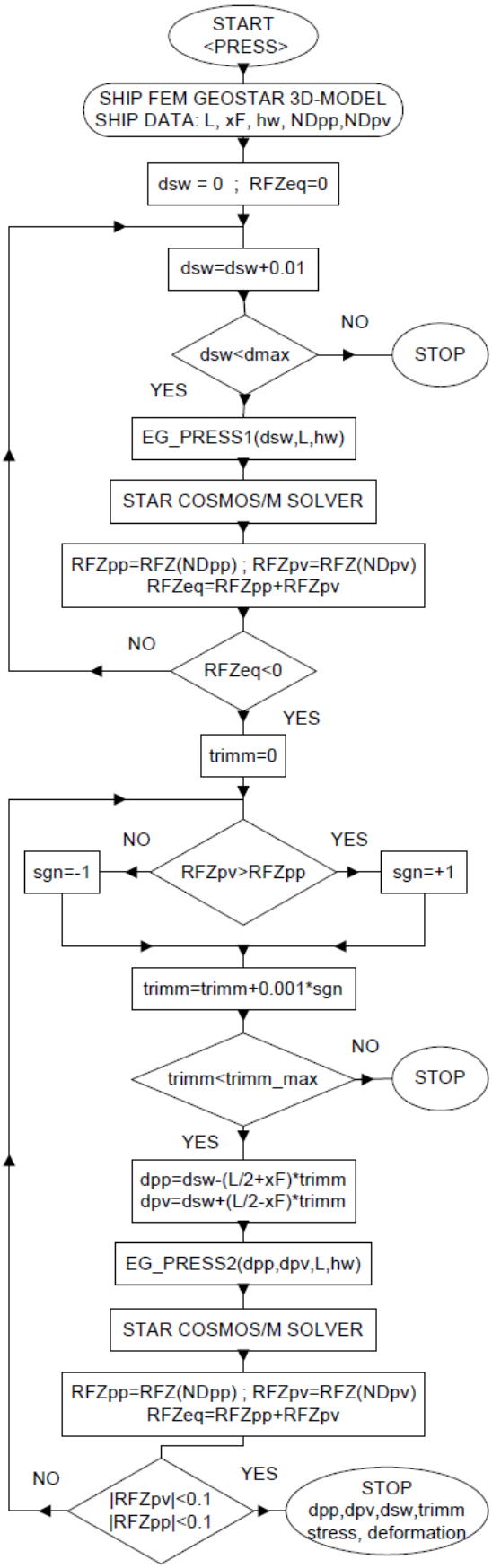

Fig. 2.2.1 Flow chart of GEO macro-commands files (Domnisoru, 2006)

The iterative procedure includes two main parts:

- the free floating condition, having as objective numerical function the sum of vertical reaction forces at the two nodes at ship extremities that has to become zero;
- the free trim and floating condition, having as objective numerical functions the vertical reactions forces at each two nodes at ship extremities that have to become zero.

Based on the algorithm from figure 2.2.1, in the following appendixes there are presented the numerical procedures developed using GEO macro-commands programming language from the Solid Works Cosmos/M 2007 program.

- in Appendix A.1.1 there is presented the "press_full.geo" file GEO macro-commands for the iterative procedure of free floating and trim equilibrium;
- in Appendix A.1.3 there is presented the "geomacro.mac" file GEO procedures library developed for the support of GEO macro-commands "hst.geo" and "press_full.geo" that must be located in the directory "c:\CosmosM".

2.2.6. The Numerical Results Evaluation

At the sixth step of the global-local ship strengths analysis, based on 3D-FEM Models, there are obtained the following numerical results:

- the free floating & trim equilibrium parameters (draught and trim angle of the reference plane, still water plane of wave medium plane);
- the global and local deformations of the ship hull structure;
- the global and local (hot-spots stress domains) stress distributions over the full ship hull length.

For the ship deck (D) and bottom (B) shells (σ_z=0) 3D-FEM model, the equivalent vonMises stress σ_{von} results smaller as the longitudinal normal stress σ_x (in global coordinates), because the transversal normal stress has non-zero value $\sigma_y < \sigma_x$, correlated also with almost zero tangential stresses $\tau_{xy} \approx \tau_{yz} \approx \tau_{xz} \approx 0$ presented in equation (2.2.1). In the side panels (neutral axis) the dominant stresses are the tangential components.

$$\sigma_{von}|_{D,B} = [\sigma_x^2 + \sigma_y^2 - \sigma_x\sigma_y + 3(\tau_{xy}^2 + \tau_{yz}^2 + \tau_{xz}^2)]^{1/2} \leq |\sigma_x|_{D,B} \quad (2.2.1)$$

For a selected panel of the 3D-FEM model (Deck, Bottom, Side) and a given longitudinal section the maximum stress value result from the equation 2.2.2:

$$\sigma, \tau_{max} = max(\sigma, \tau)|Nodes\ (panel, section) \quad (2.2.2.)$$

2.3. The Two Cargo Hold Compartments 3D-FEM Model

In order to reduce the complexity of the 3D-FEM Model full extended over the ship length, for practical purpose of global-local ship strength analysis in the centre part, the classification society rules recommend the use of 3D-FEM Models partially extended over the ship length, as those corresponding to the cargo hold compartments. In this case the equilibrium condition (Ship-equivalent quasi-static wave) cannot be any longer obtained directly on the two cargo holds structural model, as for 1D and 3D Models iterative procedures (Sub-Chapters 2.1 and 2.2), being necessary to apply the requested global vertical equilibrium position based on a previous 1D Equivalent Beam Model analysis results.

A coarse mesh size will be used, for cargo holds structural strength analysis, the same as for the 3D-FEM Full Extended Model. The loads are based on the previous 1D-Equivalent Beam Model (with the iterative algorithm for the vertical in-plane equilibrium).

The main advantage of partially extended 3D-FEM Models is that the structural model can have also a finer mesh on several details, without involving excessive time resources for supplementary equilibrium conditions calculations (Domnisoru et al., 2005)

2.3.1. Vertical Deflection of the Ship Hull Based on the 1D-Equivalent Elastic Beam Model

In order to compute the rotations and displacements conditions of the partially extended 3D FEM Model, at both end extremities, the 1D-Equivalent Beam Model vertical deflection analysis results are used. The ship girder is modelled with n beam elements as follows:

$$x_0 = 0, \quad x_{i+1} = x_i + \delta x \qquad i = 0, n-1 \qquad x_n = L \tag{2.3.1}$$

We consider for deformation computation the shear forces T(x) and bending moment M(x) in the vertical plane for the equivalent head wave condition (equation 2.1.15).

The total displacement resulting from the bending moment and the shearing force has the following expression:

$$w(x) = w_m(x) + w_t(x) \qquad x \in [0, L] \tag{2.3.2}$$

where: $w_m(x)$ is the vertical deflection from bending and $w_t(x)$ is the vertical deflection from shearing.

On the basis of the equation for the bending and the shearing 1D equivalent beam deflection, it results the following equations:

$$w_m(x) = \frac{1}{E}\left[\int_0^x \int_0^x \frac{M(x)}{I(x)} dxdx - \frac{x}{L}\int_0^L \int_0^L \frac{M(x)}{I(x)} dxdx\right]$$
$$\int_0^x \int_0^x \frac{M(x)}{I(x)} dxdx = x\int_0^x \frac{M(x)}{I(x)} dxdx - \int_0^x \frac{M(x)}{I(x)} dx = x \cdot Int_1 - Int_2 \tag{2.3.3}$$

$$\frac{1}{L}\int_0^L \int_0^x \frac{M(x)}{I(x)}dxdx = \int_0^L \frac{M(x)}{I(x)}dx - \frac{1}{L}\int_0^L \frac{M(x)}{I(x)}dx = \alpha$$

$$w_m(x) = \frac{1}{E}(x \cdot Int_1 - Int_2 - x \cdot \alpha)$$

$$w_t(x) = \frac{1}{G}\left[\frac{x}{L}\int_0^L \frac{T(x)}{A_f(x)}dx - \int_0^x \frac{T(x)}{A_f(x)}dx\right]$$

$$\int_0^x \frac{T(x)}{A_f(x)}dx = Int_3 \; ; \; \frac{1}{L}\int_0^L \frac{T(x)}{A_f(x)}dx = \beta$$

$$w_t(x) = \frac{1}{G}[x \cdot \beta - Int_3]$$

Based on the elastic 1D Equivalent Beam Model deformation results, it is possible also to have a preliminary check of the ship hull girder using the admissible values for the maximum vertical deflection:

$$w_{max} = \max_{x\in[0,L]}|w(x)|_{(\mu=0)} \leq w_{adm} = \frac{L}{500} \tag{2.3.4}$$

Based on equations (2.3.2-3), through derivation operation the rotation angles distribution is obtained over the length of the ship 1D-girder.

2.3.2.Boundary Conditions on Two Cargo Holds Compartments Model

The boundary conditions are of two types: symmetry condition (natural condition); the rotation and displacement conditions from the global 1D-model at both model end extremities (global condition).

The symmetry conditions is referring to all the nodes in the centre line plane, and this condition is due to the fact that the 3D-FEM model of the ship was developed in Portside only (head wave case).

The boundary conditions for the Aft part of the model are given by a single node, ND_AFT, situated at specific coordinates: x at the AFT extremity point of the model, y=0 and z at the neutral axis position of the AFT extremity transversal section. Based on the user subroutine presented in the Appendix A.3.1, points are created on all the nodes available in the AFT part of the model. Afterwards based on the user subroutine in the Appendix A.3.2, lines are created for all the nodes into connection with the previously created ND_AFT. The CAD lines objects previously created will be meshed as rigid beam elements (RBAR type in SolidWorks Cosmos/M). Similar rigid elements are developed for the Fore node, ND_FORE placed at the FORE extremity of the model.

The boundary conditions at ND_AFT and ND_FORE are presented in table 2.3.2.

Table.2.3.2. Boundary conditions applied on the two cargo holds compartments 3D FEM Model

Boundary Conditions						
Restrictions	U_x	U_y	U_z	R_x	R_y	R_z
Nodes at symmetry plane	-	x	-	x	-	-
ND_AFT Aft model node	x	x	-	x	-	x
ND_FORE Aft model node	-	x	-	x	-	x

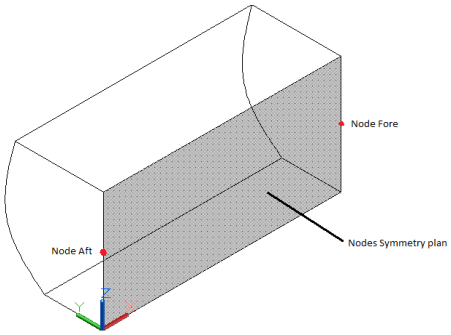

Figure.2.3.2. Nodes to apply the boundary conditions on the two cargo holds compartments 3D-FEM Model

The two cargo hold compartments 3D-FEM Model has the FEM structure and the mass groups the same as for the 3D-FEM full extended model, selected for the central part according to the model extension.

The global rotations and the displacements (Uzpp, Rypp and Uzpv, Rypv) applied on the model in ND_AFT and ND_FORE nodes, are based on the 1D Equivalent Beam Model vertical deformation analysis (chapter 2.3.1). On the external shell of the model, bottom, bilge and side shells, the pressure is applied from the equivalent quasi-static wave, for the parameters from global equilibrium in vertical plane calculated with the 1D Equivalent Beam Model (chapter 2.1), using the procedures presented in Appendix A3.1. and A.3.2. This type of model has further refinements for some structural details, in order to obtain better resolution of the maximum stress values in the selected hot-spot areas. Usually, it is expected that the maximum stresses are obtained into the deck panel elements at hatchway or other similar geometrical details (with significant geometric gradient).

On the basis of the equation (2.3.5), a linear extrapolation of the normal stresses and equivalent vonMises stresses is made for a hot-spot area (Bureau Veritas,2010),

$$\sigma_{hs}=1.5\sigma_{0.5t}-0.5\sigma_{1.5t} \tag{2.3.5}$$

where t is equal to maximum between t_1 and t_2 as it is presented in the figure 2.3.3.

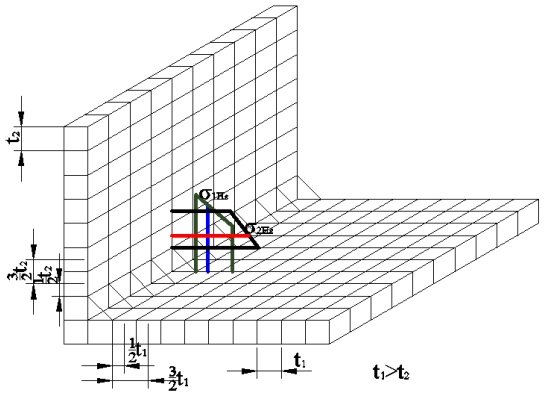

Fig 2.3.3 Structural joint hotspot stress evaluation (Bureau Veritas,2010)

Based on the 3D-FEM partially extended model, with the same meshing element size and the global equilibrium parameters along with the beam rotations and deformations resulting from the 1D Equivalent Beam Model, if the geometry and the mass distributions are modelled with accuracy for the analyzed ship model, it should result analogous stress distributions and deformation as for the 3D-FEM full extended ship model, at the centre part. For the analyzed chemical-tanker, the results from chapters 5, 6, 7 are pointing out this correlation between the numerical results of the three structural models. In this case a 3D-FEM partially extended model, having refinements of the mesh at several details, can be used in order to obtain with higher sensitivity the hot-spots stress factors (see chapter 8).

3.THE SHIP STRUCTURE DESCRIPTION, BASED ON THE CHEMICAL TANKER 4000 TONES PROTOTYPE SHIP

The analysis carried on in this study are focused on a test ship type tanker with double hull, based on the Chemical Tanker 4000 prototype ship, granted during the internship at Ship Design Group, Galati.

The following ship data are required for the strength analysis: general arrangement, offset lines, structural characteristics over several transversal and longitudinal sections, material characteristics, mass distribution over the ship length, shell expansion.

The ship hull offset lines is based on the prototype ship and the transversal sections structure scantlings are according to the Bureau Veritas, 2010 Rules. The mass distribution is based on the full ship hull 3D-CAD/FEM model and the tanker prototype ship.

The ship main dimensions and the frame spacing are displayed below:

Main dimensions:

Length Over All : 109.62 m

Length Between Perpendiculars: 106.20 m

Breadth moulded: 13.50 m

Design draught: 5.45 m

Depth at side (moulded): 8.60 m

Frame spacing over the ship length (Table.3.1)

Table.3.1. Frame spacing (Ship Design Group 2007)

FRAME		mm
-4	26	600
26	29	570
29	46	706
46	47	805
47	77	706
77	78	805

FRAME		mm
78	80	760
80	81	805
81	113	706
113	114	805
114	135	706
135	143	625
143	158	600

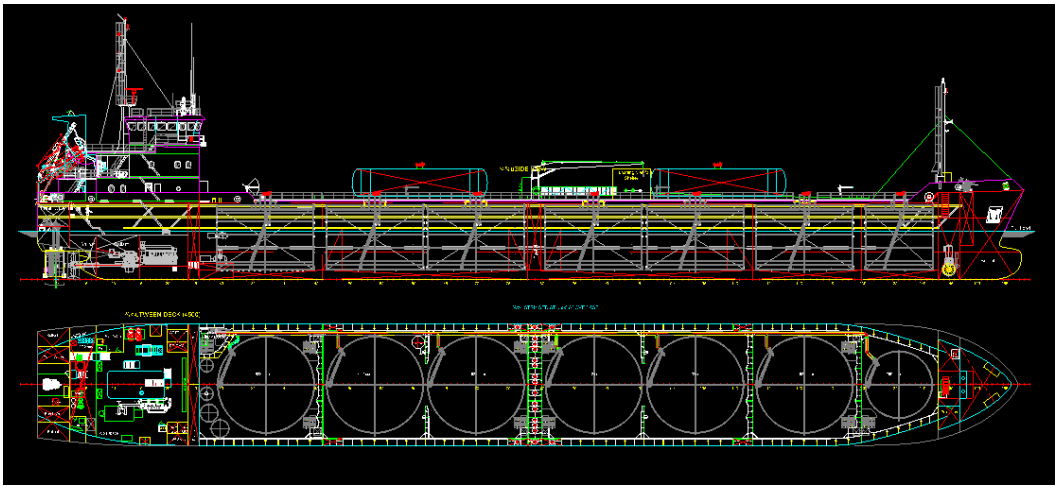

Fig.3.1. General Arrangement (granted by Ship Design Group Galati, 2007)

As it can be observed from the General Arrangement (Fig.3.1.), the cylindrical part of the ship is extended over 80 % of the ship length, covering the cargo holds compartments area. The cargo bays area includes 7 cylindrical structural independent tanks for liquid cargo, resulting a total of 3950.6 m^3 Net Volume.

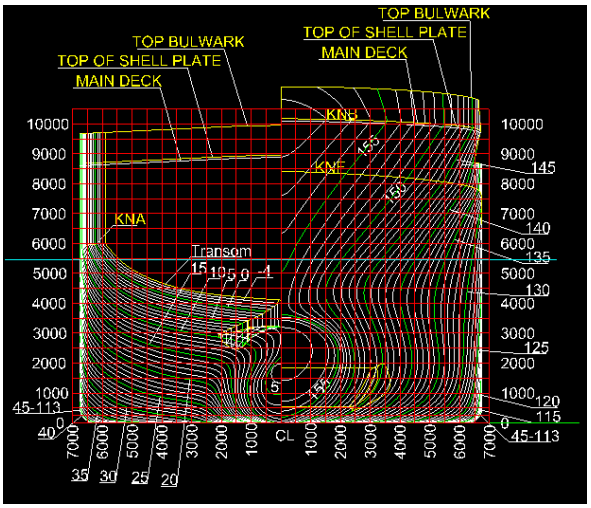

Fig.3.2. The 2D - Offset Lines (granted by Ship Design Group Galati, 2007)

Starting from the original 2D hull offset lines, I had developed the 3D offset lines, using AutoCAD. Following, I have developed the external shell surfaces of the 3D-CAD Model, providing the best accuracy for the geometry.

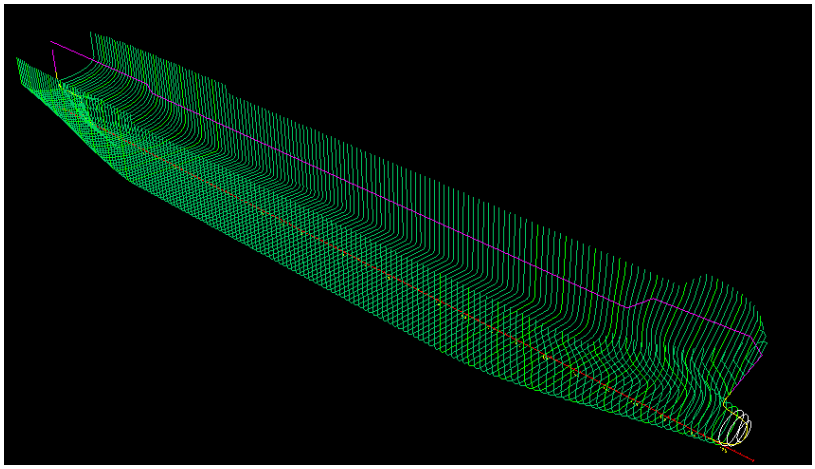

Fig.3.3. The 3D-CAD Offset Lines

Fig.3.4. Chemical Tanker 4000 Tones prototype ship (granted by Ship Design Group 2007)

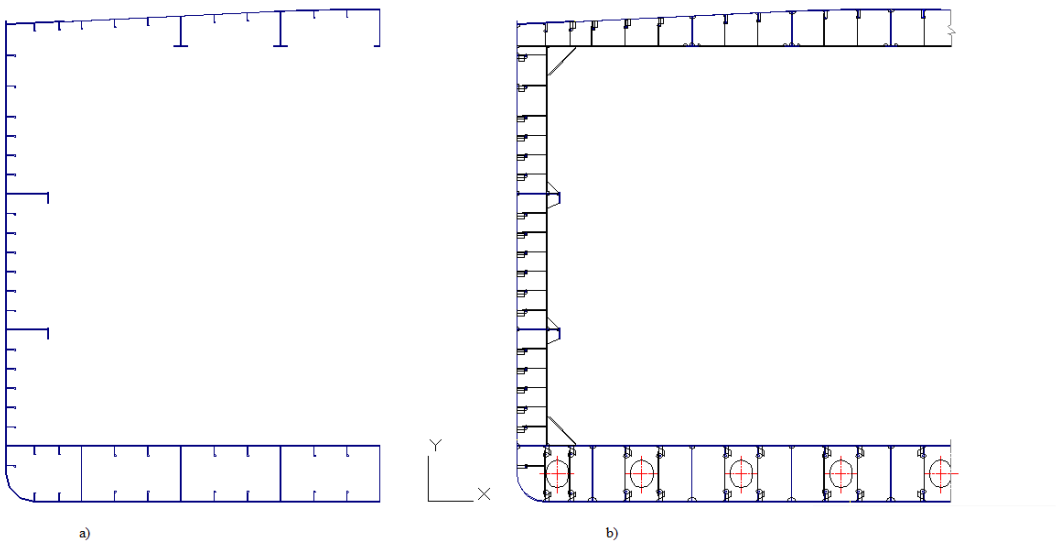

Fig.3.5. Chemical Tanker 4000 Tones prototype ship amidships a) normal frame transverse section b) web frame transverse section (granted by Ship Design Group 2007)

4. GENERATION OF 3D-CAD/FEM MODEL FULL EXTENDED ON THE SHIP'S LENGTH

In order to develop the 3D-CAD model, the entire length of the ship was divided into 7 main blocks, which are AFT block, Amidships area (block 2, 3, 4, 5, 6) and FORE block. By using the initial scantlings information and the structural transversal and longitudinal sections, the model was developed in the AutoCAD 2011 by using 3D faces and multiple layers, according to the corresponding thickness of the plating.

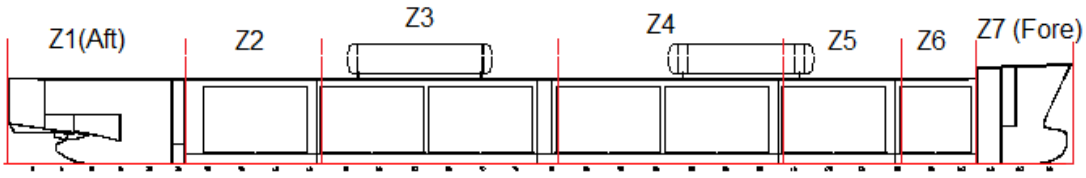

Fig.4.1. Dividing the ship to blocks (Ship Design Group 2007)

All the layers used in the 3D-CAD modelling, with the corresponding thickness, will be further used in the 3D-FEM model as geometric properties, in order to define the plates thickness in the FEM Solid Works Cosmos/M 2007 program. Each layer was developed for a specific component of the hull structure of the ship, with a thickness and a colour label assigned, therefore it will facilitate the thickness description in Solid Works Cosmos/M 2007. Each layer was exported as a DXF file, so the FEM software can import all the layers with the correct thickness.

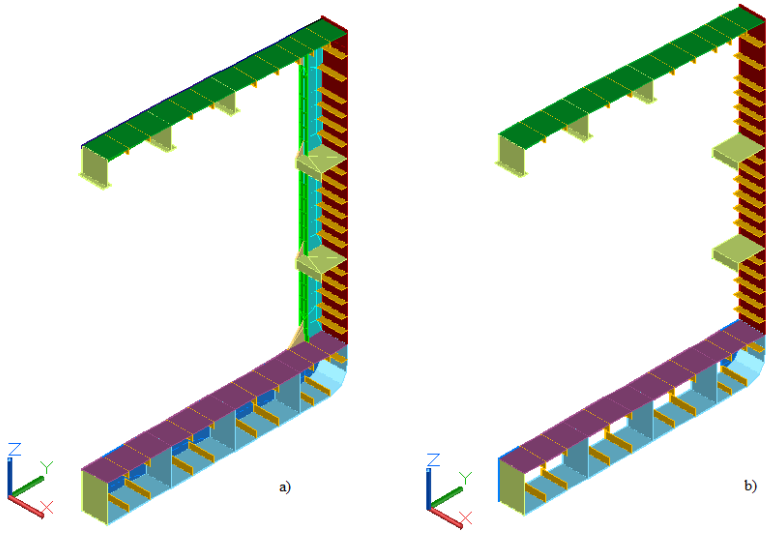

Fig.4.2.The 3D-CAD part of the Amidships section between two frames

a) Web Frame; b) Normal Frame

In the following figures are presented 3D-CAD/FEM models, as well for the afferent tables with the plate thickness for each block.

Table.4.1.Figures with 3D - CAD /FEM models of the ship, based on full extended model

Block	3D CAD Model	3D FEM Model	Thickness table
1 (AFT)	Fig.4.3.	Fig.4.4.	Appendix 4, Table.A.4.1.
2	Fig.4.5.	Fig.4.6.	Appendix 4, Table.A.4.2.
3	Fig.4.7.	Fig.4.8.	Appendix 4, Table.A.4.3.
4	Fig.4.9.	Fig.4.10.	Appendix 4, Table.A.4.4.
5	Fig.4.11.	Fig.4.12.	Appendix 4, Table.A.4.5.
6	Fig.4.13.	Fig.4.14.	Appendix 4, Table.A.4.6.
7 (Fore)	Fig.4.15.	Fig.4.16.	Appendix 4, Table.A.4.7.
Full size Model	Fig.4.17.	Fig.4.19.	

As ship structure materials are selected A and AH40-type grade steel (AH40 fore upper ship flange panel), with the following characteristics, according to Bureau Veritas (2010):

Tab.4.2. The ship structure materials A, AH40-type grade Steel Characteristics

Property Name	Symbol	Value
Young's Modulus	E	$2.1\ 10^8$ (kN/m^2)
Poisson Ratio	υ	0.3
Density	ρ	7.7 (t/m^3)
Yield stress A	ReH	235 MPa
Yield stress AH40	ReH	390 MPa
Admissible stress A	adm_GS	σ=175 MPa; τ=110 MPa
Admissible stress AH40	adm_GS	σ=265 MPa; τ=165 MPa

The 3D - FEM model has been developed by Solid Works Cosmos/M 2007 program, having NDmax=49508 nodes and ELmax=110558 Triangle Thick Shell elements (SHELL3T element type, membrane and thick shell with Mindlin formulation). Each shell element has the corresponding thickness, according to the tanker ship initial scantlings, defined as Real Constants Sets in appendix A.4.

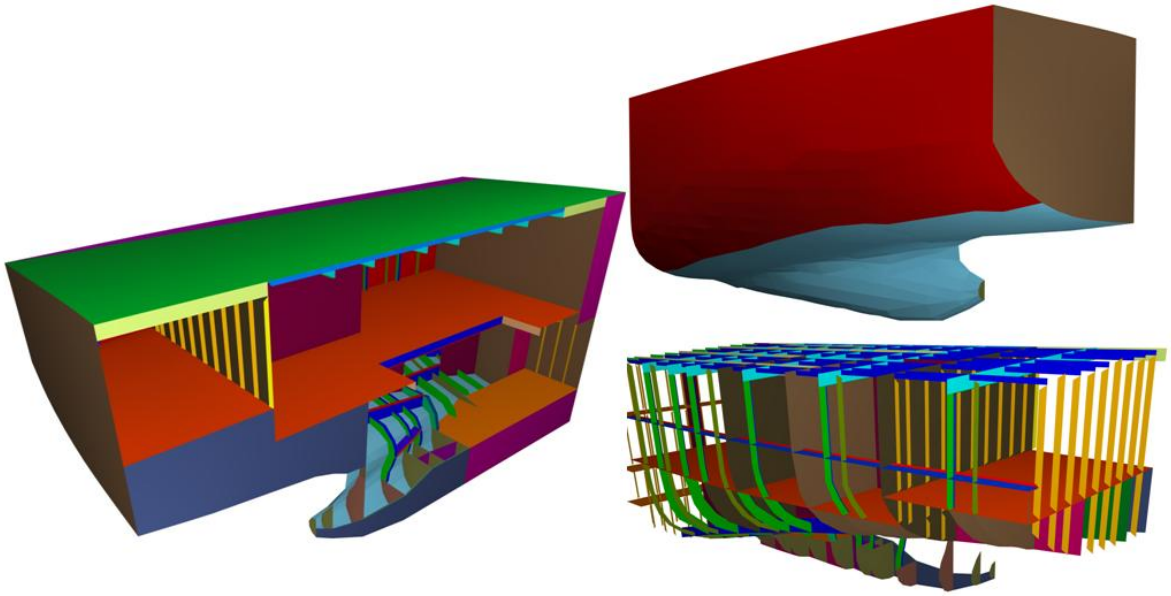

Fig.4.3. Aft block of the 3D - CAD model (PS only)

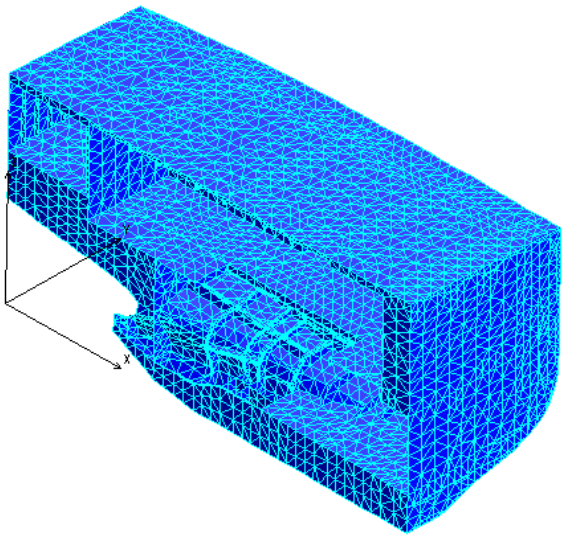

Fig.4.4. Aft block of the 3D - FEM model (PS only)

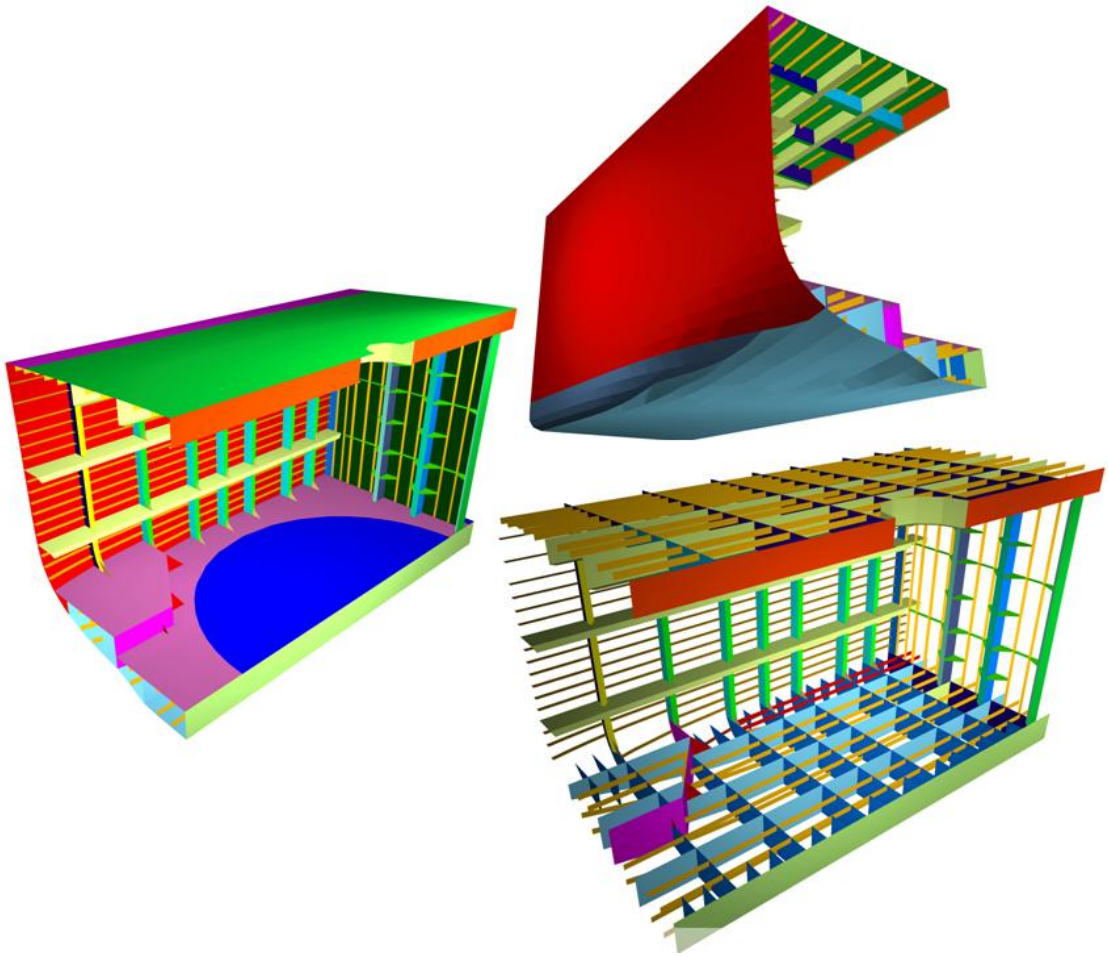

Fig.4.5. Amidships block 2 of the 3D - CAD model (PS only)

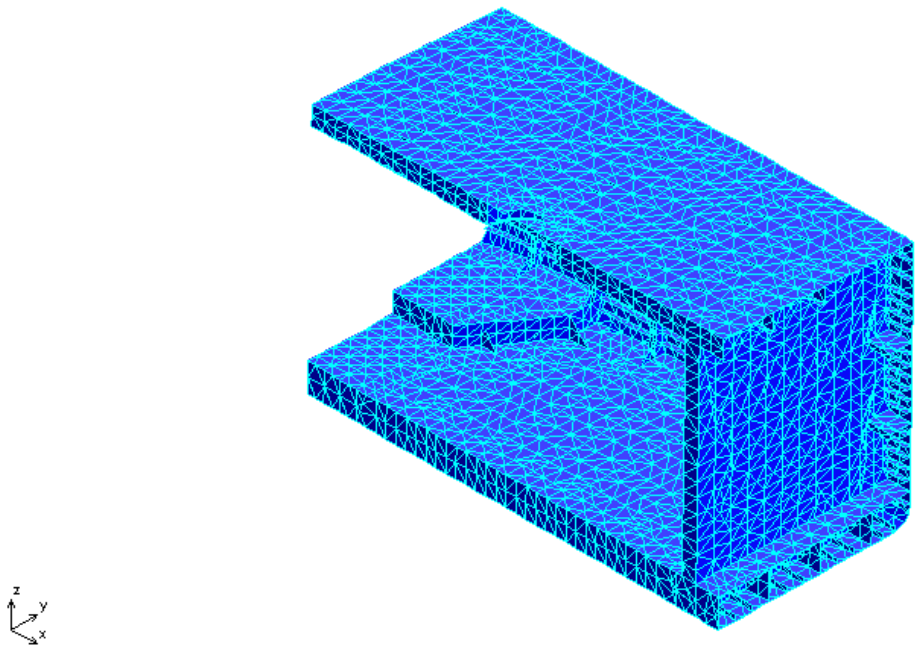

Fig.4.6. Amidships block 2 of the 3D - FEM model (PS only)

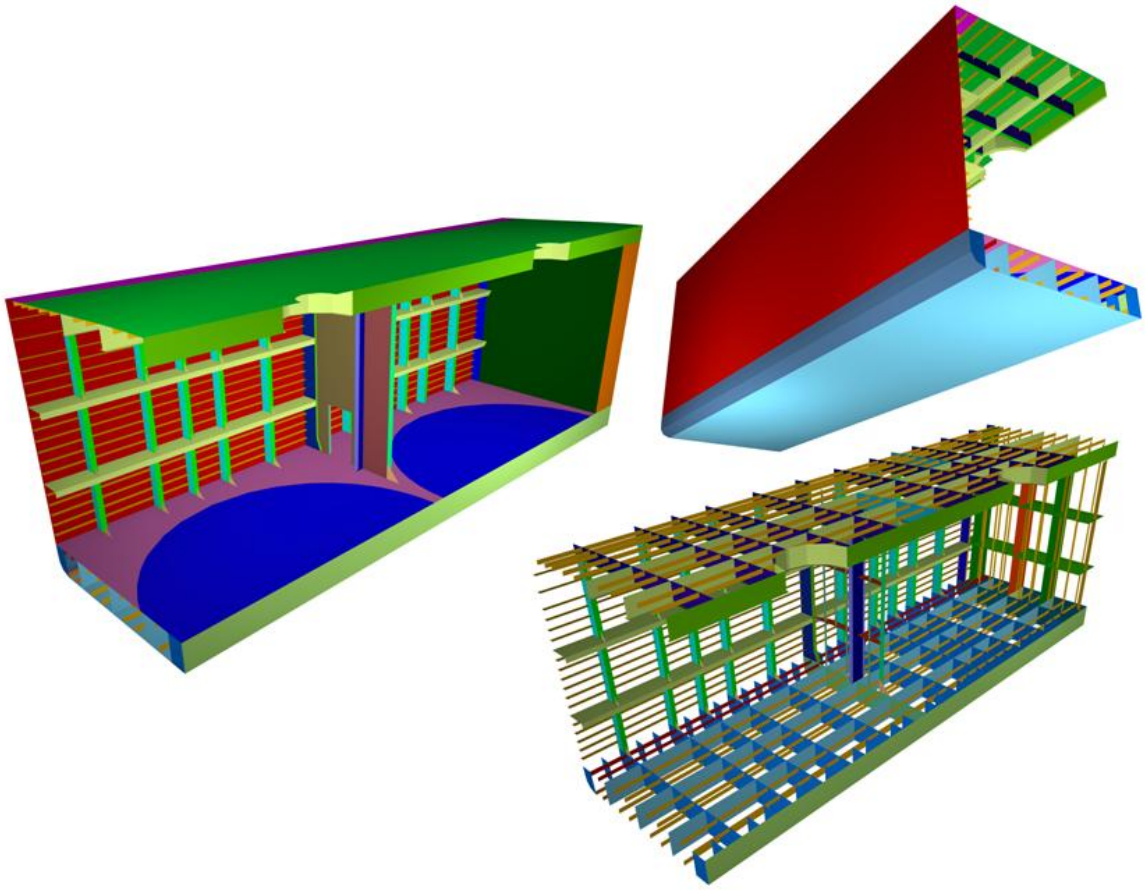

Fig.4.7. Amidships block 3 of the 3D - CAD model (PS only)

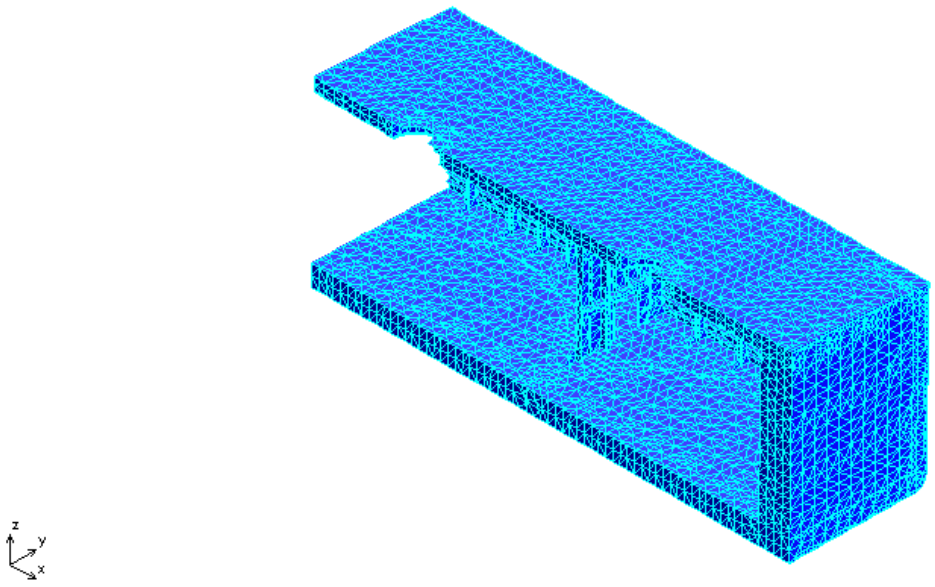

Fig.4.8. Amidships block 3 of the 3D - FEM model (PS only)

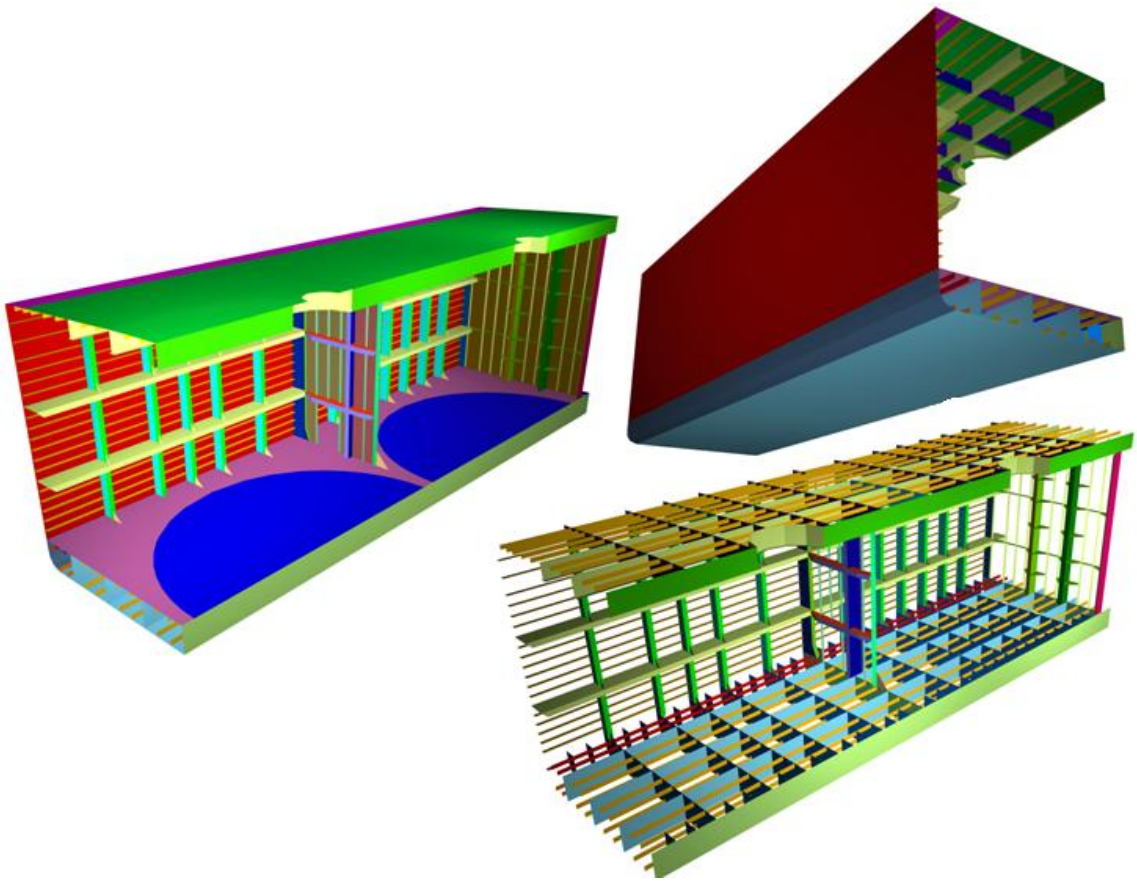

Fig.4.9. Amidships block 4 of the 3D - CAD model (PS only)

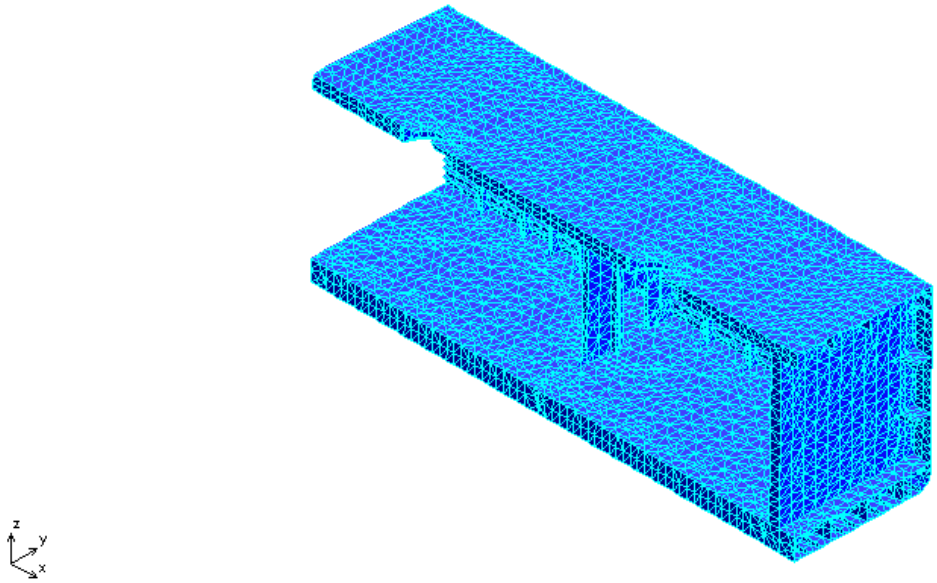

Fig.4.10. Amidships block 4 of the 3D - FEM model (PS only)

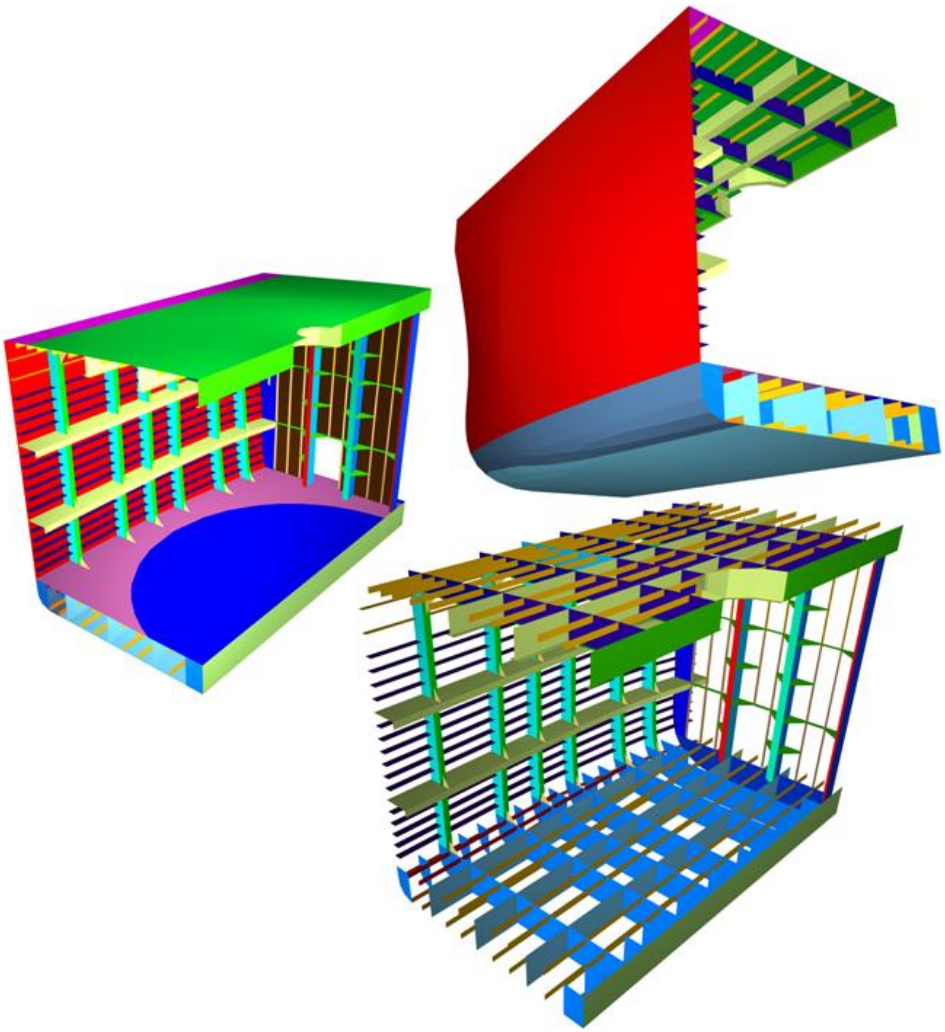

Fig.4.11. Amidships block 5 of the 3D - CAD model (PS only)

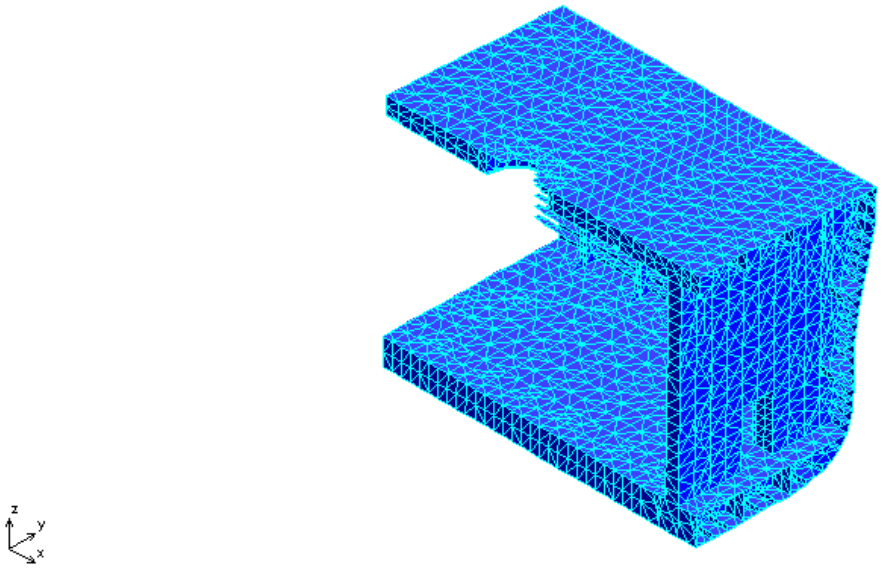

Fig.4.12. Amidships block 5 of the 3D - FEM model (PS only)

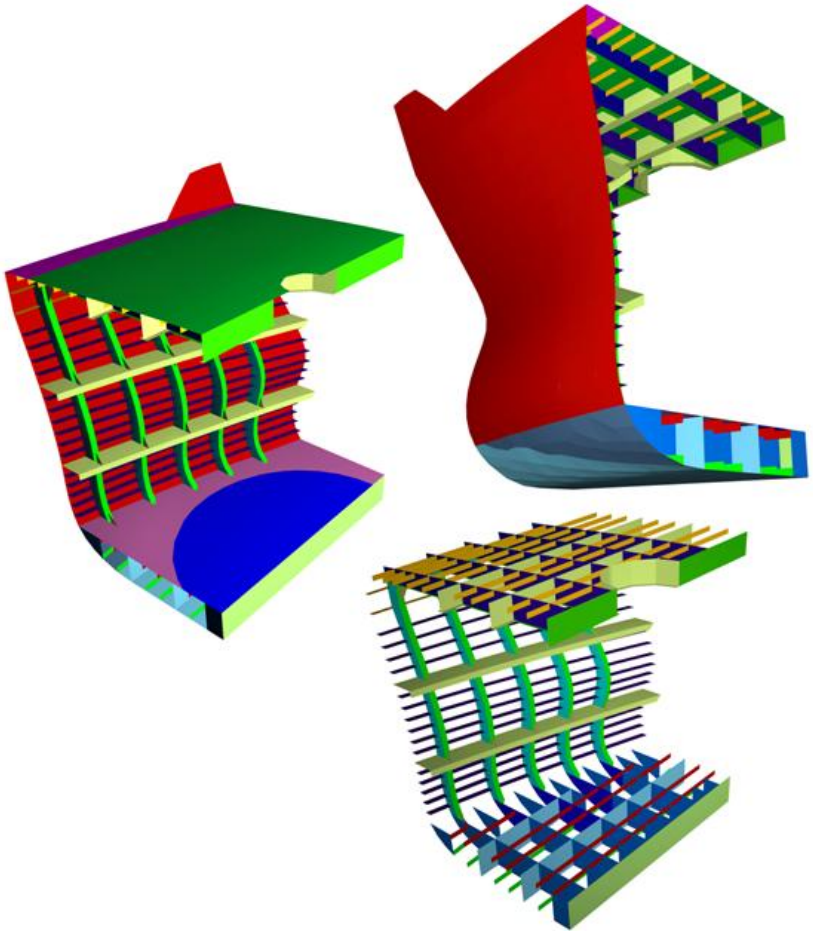

Fig.4.13. Amidships block 6 of the 3D - CAD model (PS only)

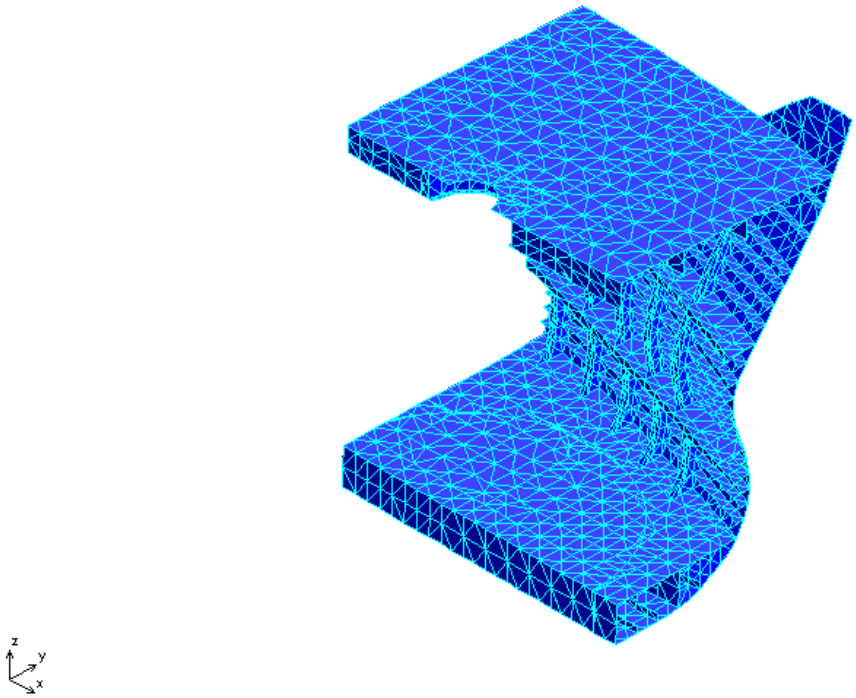

Fig.4.14. Amidships block 6 of the 3D - FEM model (PS only)

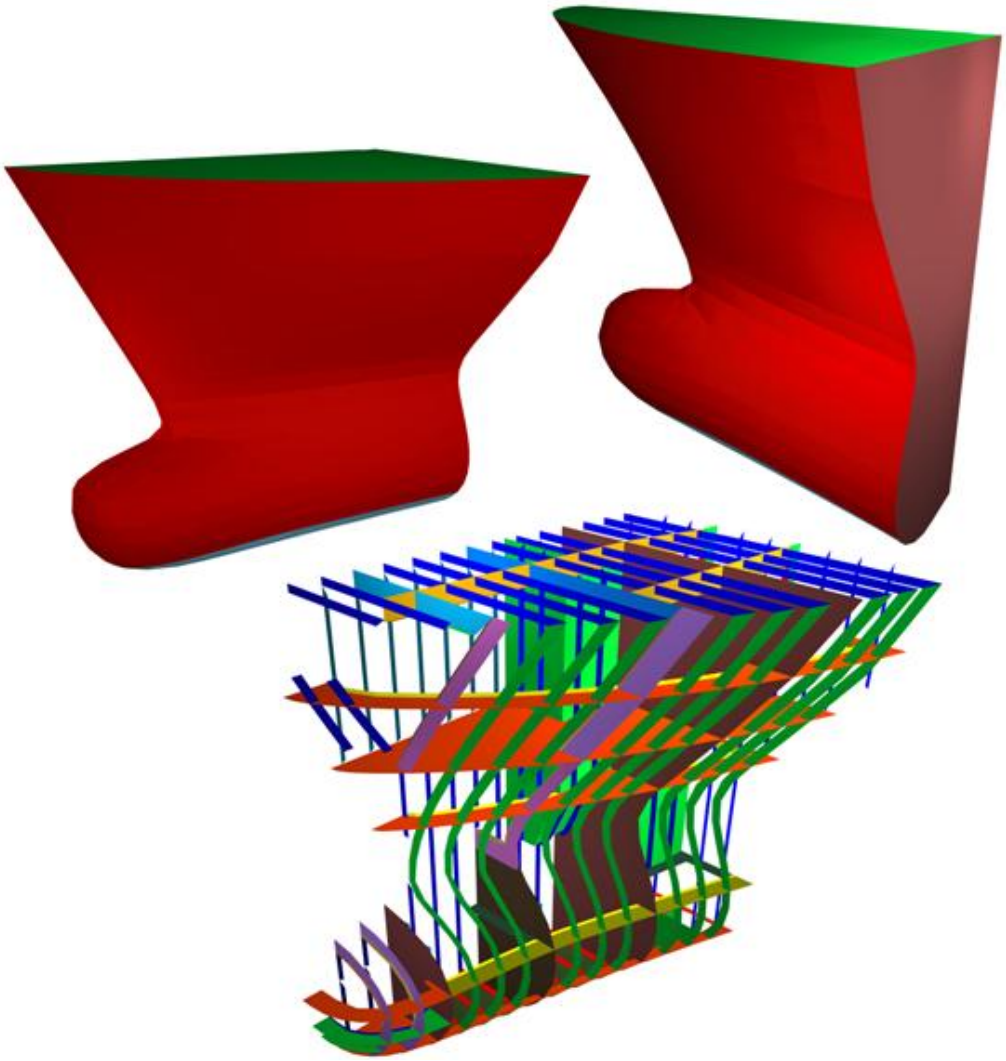

Fig.4.15. Fore block 7 of the 3D - CAD model (PS only)

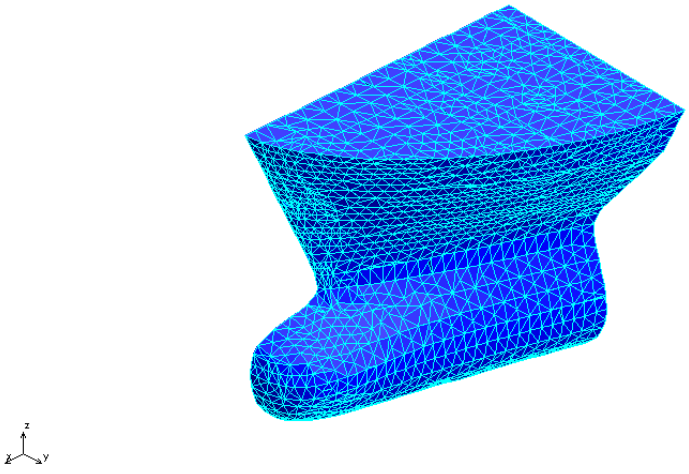

Fig.4.16. Fore block 7 of the 3D - FEM model (PS only)

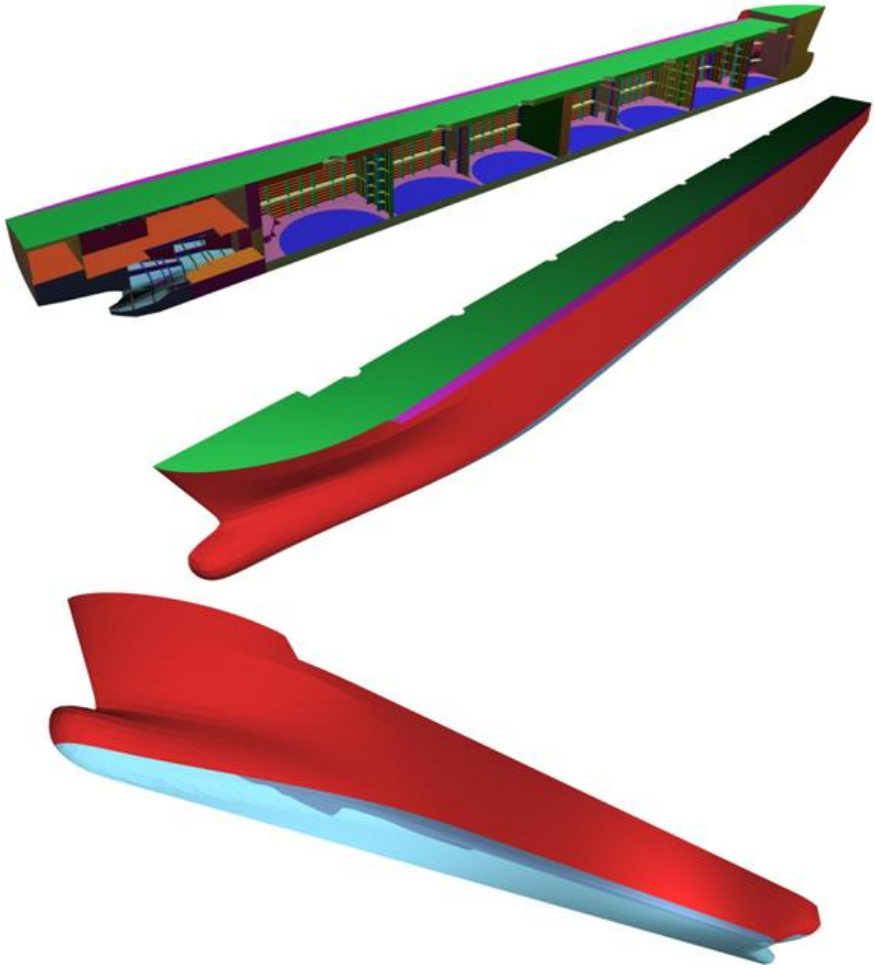

Fig.4.17. Full sized 3D - CAD model (PS only)

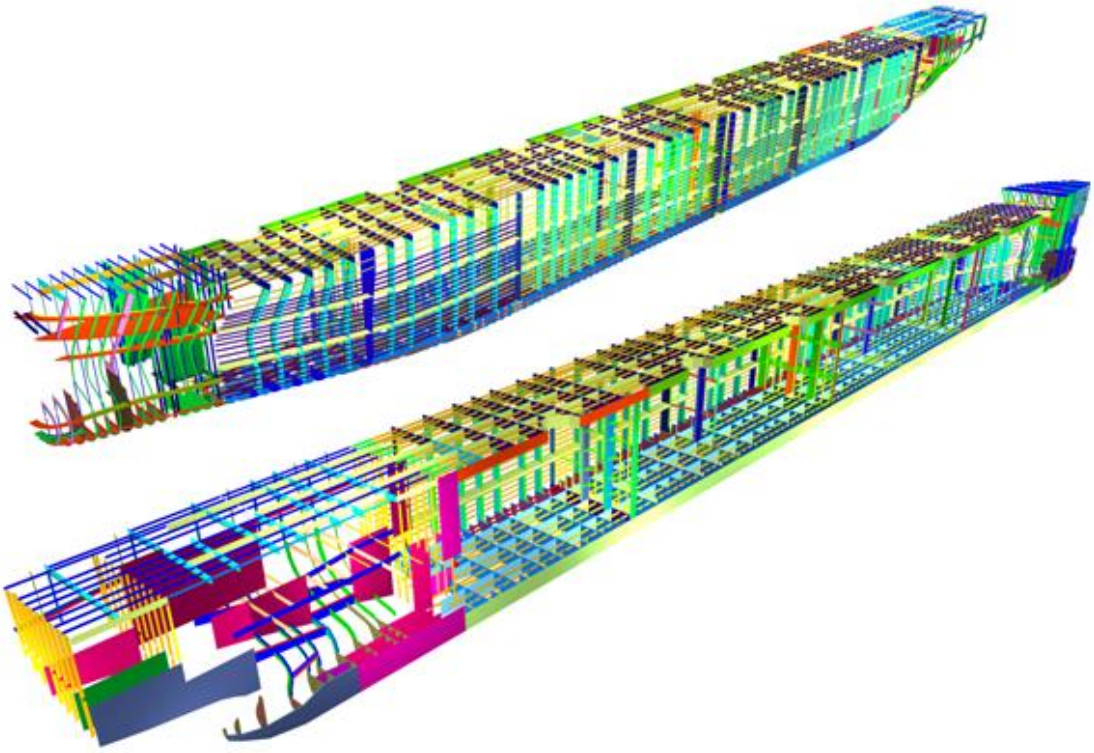

Fig.4.18. Full sized 3D - CAD model without shell plating (PS only)

Based on the 3D-FEM model previously generated (see Fig.4.4., Fig.4.6., Fig.4.8., Fig.4.10., Fig.4.12., Fig.4.14. and Fig.4.16.), each of the ship structural panels were checked, in order to be in conformity with the geometry provided in the technical drawings, such as transversal and longitudinal sections and shell expansion. For each block, a neutral GFM file was created, including only the FEM objects of the block model. The total 3D-FEM model is obtained in the Solid Works Cosmos/M 2007 program, by assembling all the GFM files, corresponding to the block model FEM objects.

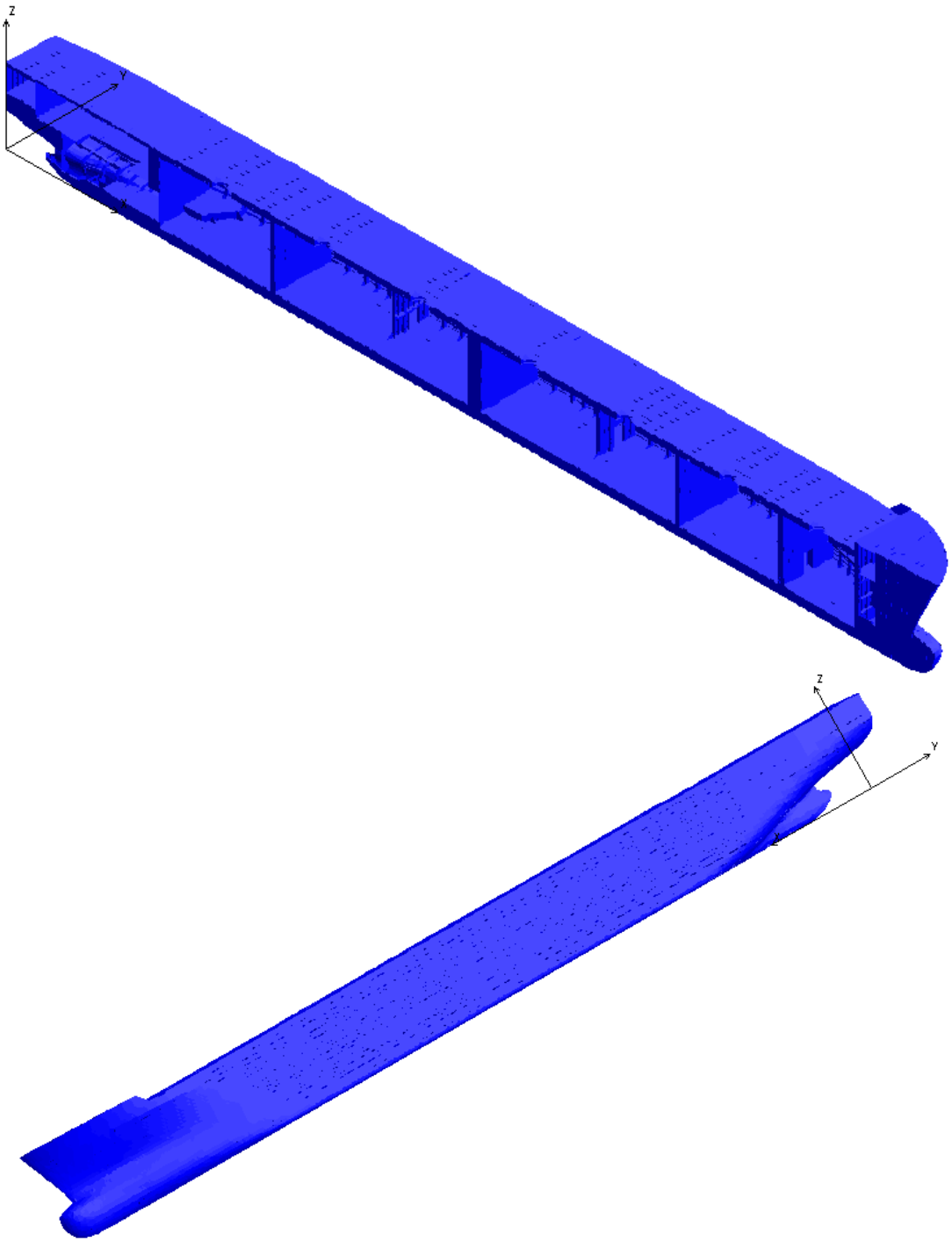

Fig.4.19. The 3D-FEM Model extended over the entire ship Length (PS only)

5. THE GLOBAL SHIP STRENGTHS ANALYSIS BASED ON 1D-EQUIVALENT BEAM MODEL, UNDER EQUIVALENT QUASI - STATIC HEAD WAVES.

5.1. The 1D Equivalent Beam Model

The 1D Equivalent Beam Model for the ship hull is selected for an evaluation of the global strength at the initial design stage, without the possibility to include the local hot-spots stress domains.

The ship hull offset lines with geometrical nonlinearities (Fig.3.2. The 2D - Offset Lines), require to obtain the equilibrium conditions of the ship girder in vertical plane using an nonlinear iterative procedure (Domnisoru, 2006).

The ship girder is considered to have loads from equivalent quasi-static head waves (having the length of the wave equal to the total length of the ship L), with the statistic height of the wave in conformity with the classification societies rules (Bureau Veritas, 2010).

The numerical analysis is carried out based on the theoretical model, presented in subchapter 2.1.

The 1D Equivalent Beam Model analysis is performed by P_ACASV program (Domnisoru, 2006), developed at the Galati Naval Architecture Department (UGAL).

The input data for the 1D analysis is presented in Appendix 5.1, Table A.5.1, which contains the mass distribution diagram along the ship's length and the equivalent beam transversal sections strength characteristics. The height of the equivalent quasi-static head wave is considered to be in the range $h_w = 0 – 8.123$ m, with the step increment $\Delta h_w = 1$ m.

The maximum height of the equivalent-quasi static head wave is $h_{wmax} = 8.123$ m, in conformity with the Bureau Veritas Rules, 2010, for analysis being selected the hogging and sagging ship-wave relative positions cases.

5.2. Results by the 1D Equivalent Beam Model Numerical Computation in Hogging Conditions

The iterative procedure at the global-local ship strength, based on 1D Equivalent Beam Model, has converged to the following wave medium plane vertical position parameters (see Table 5.2.1).

Table.5.2.1. Vertical position parameters of the wave medium plane, in hogging conditions, based on 1D Equivalent Beam Model

Wave height case [m]	Vertical position amidships [m]	Trim in the longitudinal plane [rad]
0	4.41235	0.00280000
1	4.34453	0.00093000
2	4.26554	0.00005000
3	4.17685	0.00009000
4	4.07410	0.00121000
5	3.96386	0.00273000
6	3.84601	0.00448000
7	3.71806	0.00645000
8	3.57505	0.00870000
8.123	3.55606	0.00900000

In the following figures are presented the stress distributions obtained at the global-local strength analysis based on the 1D-Equivalent Beam Model, under Hogging conditions.

- Fig.5.2.1 is presenting the Bending moment M for 1D computation in hogging wave conditions
- Fig.5.2.2. is presenting the Shear force T for 1D computation in hogging wave conditions
- Fig.5.2.3. and Appendix A.5.2, Table.A.5.2.1. are presenting the Normal Deck Stresses, σ_X [MPa] in Hogging wave conditions, 1D computation, and the stress check according to the admissible stress limit adm_GS
- Fig.5.2.4. and Appendix A.5.2, Table.A.5.2.2. are presenting the Normal Bottom Stresses, σ_X [MPa] in Hogging wave conditions, 1D computation, and the stress check according to the admissible stress limit adm_GS
- Fig. 5.2.5. and Appendix A.5.2, Table. A.5.2.3. are presenting the Tangential side stresses τ_{xz} [MPa] in Hogging wave conditions, 1D computation, and the stress check according to the admissible stress limit adm_GS

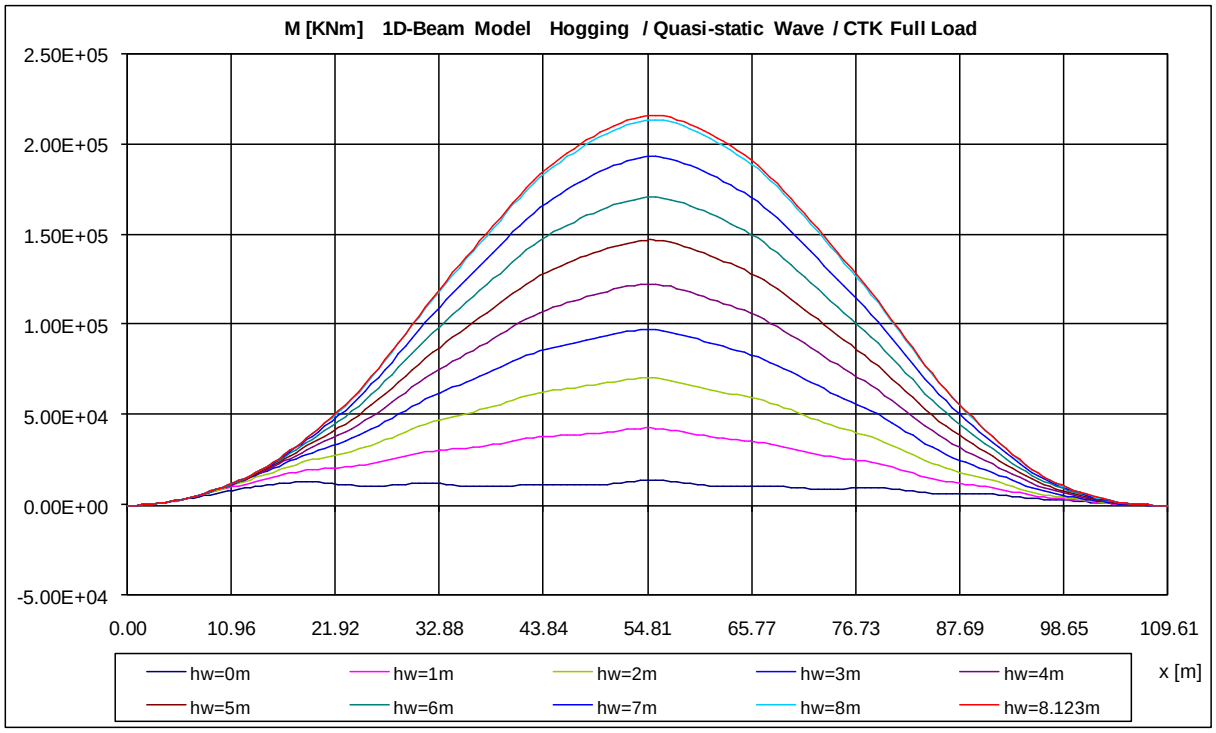

Fig.5.2.1. Bending moment M [kNm] for 1D computation in hogging wave conditions

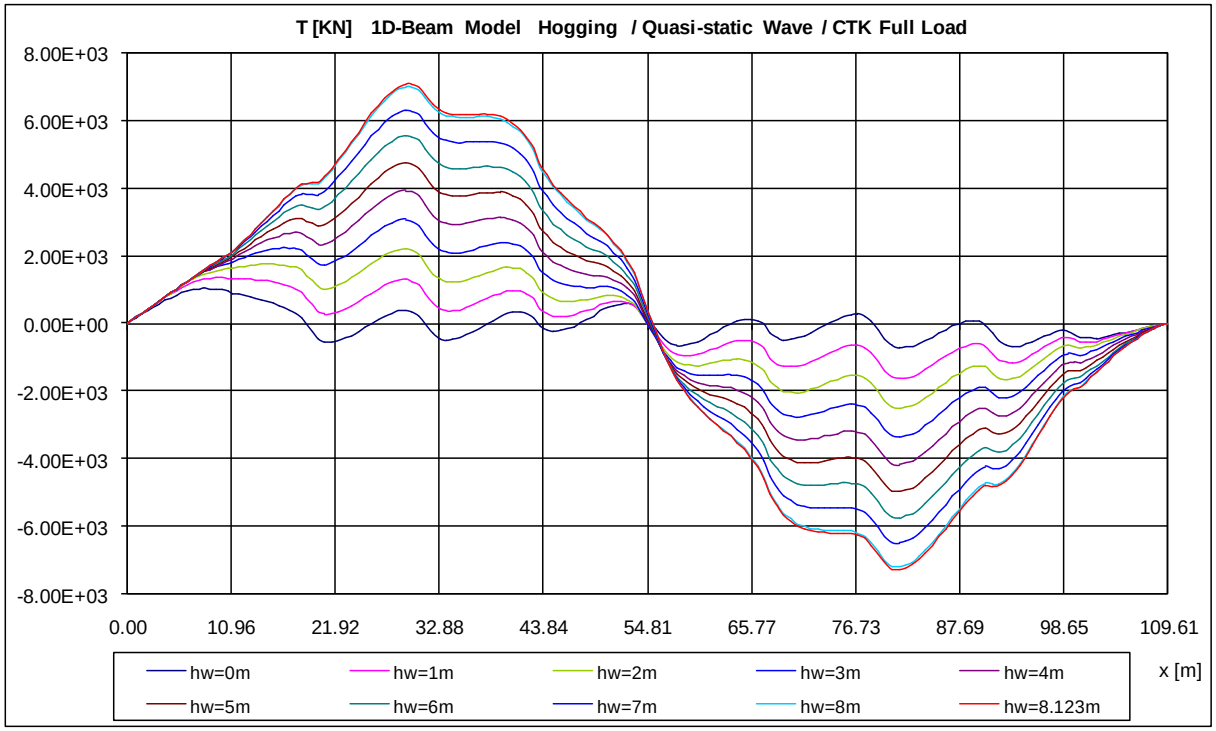

Fig.5.2.2. Shear force T [kN] for 1D computation in hogging wave conditions

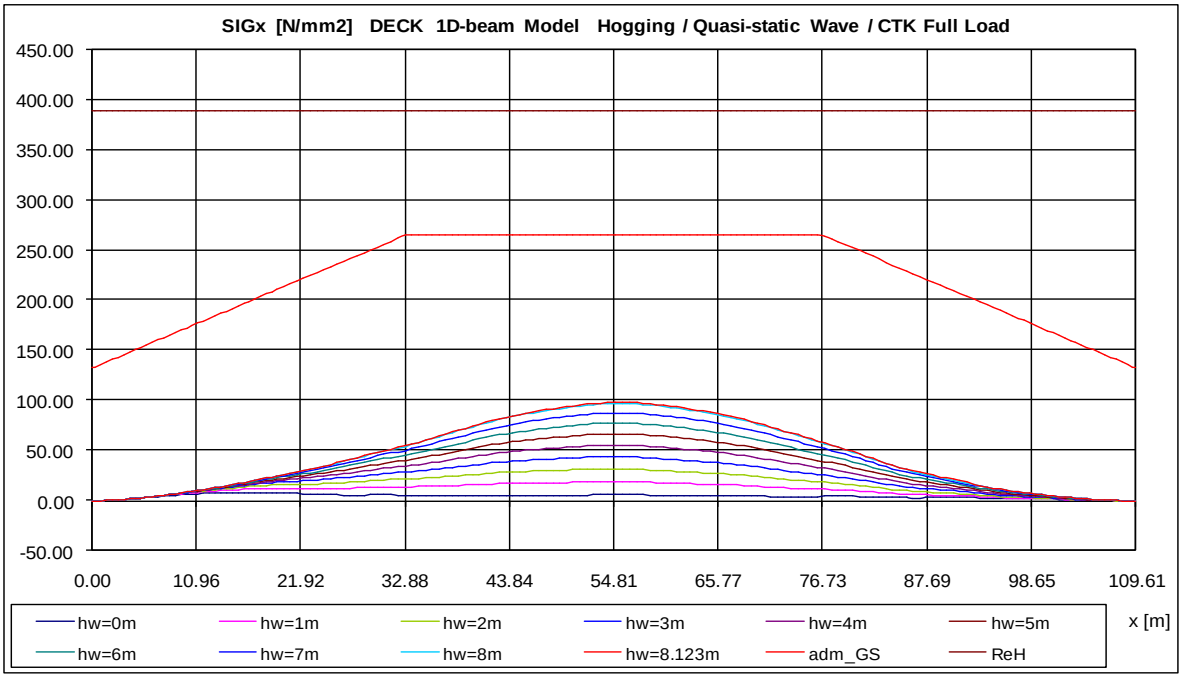

Fig.5.2.3. Normal Deck Stress, σ_X [MPa] in Hogging wave conditions, 1D computation

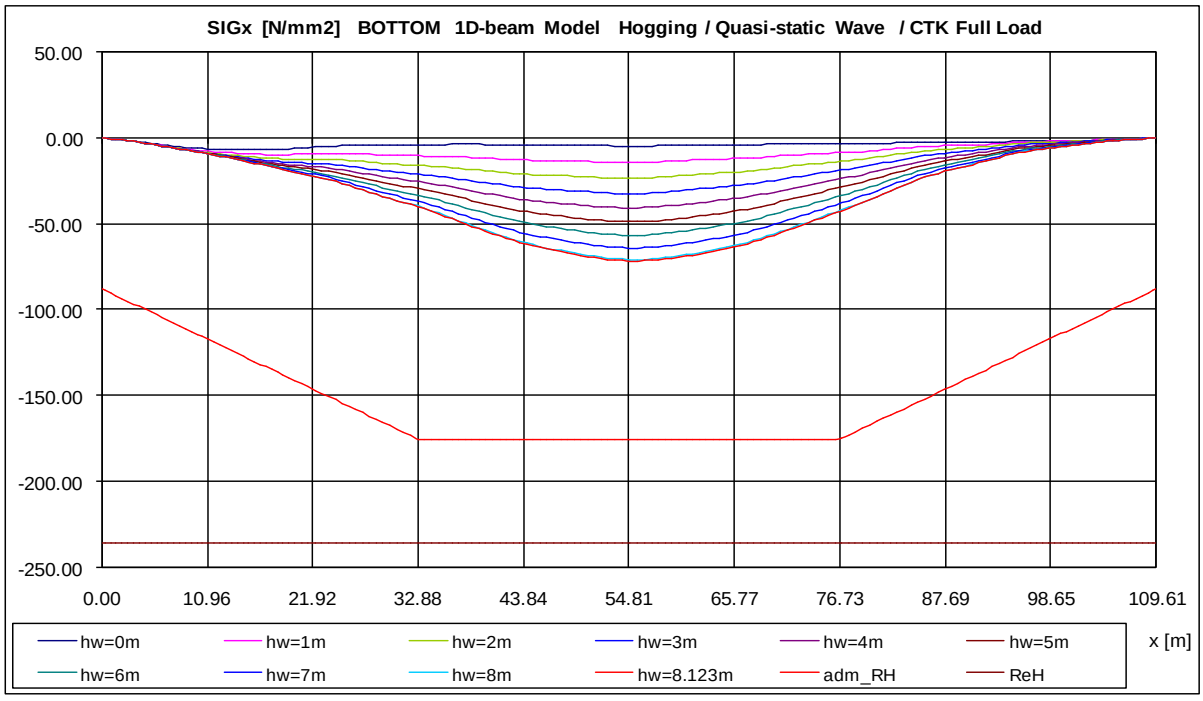

Fig.5.2.4. Normal Bottom Stress, σ_X [MPa] in Hogging wave conditions, 1D computation

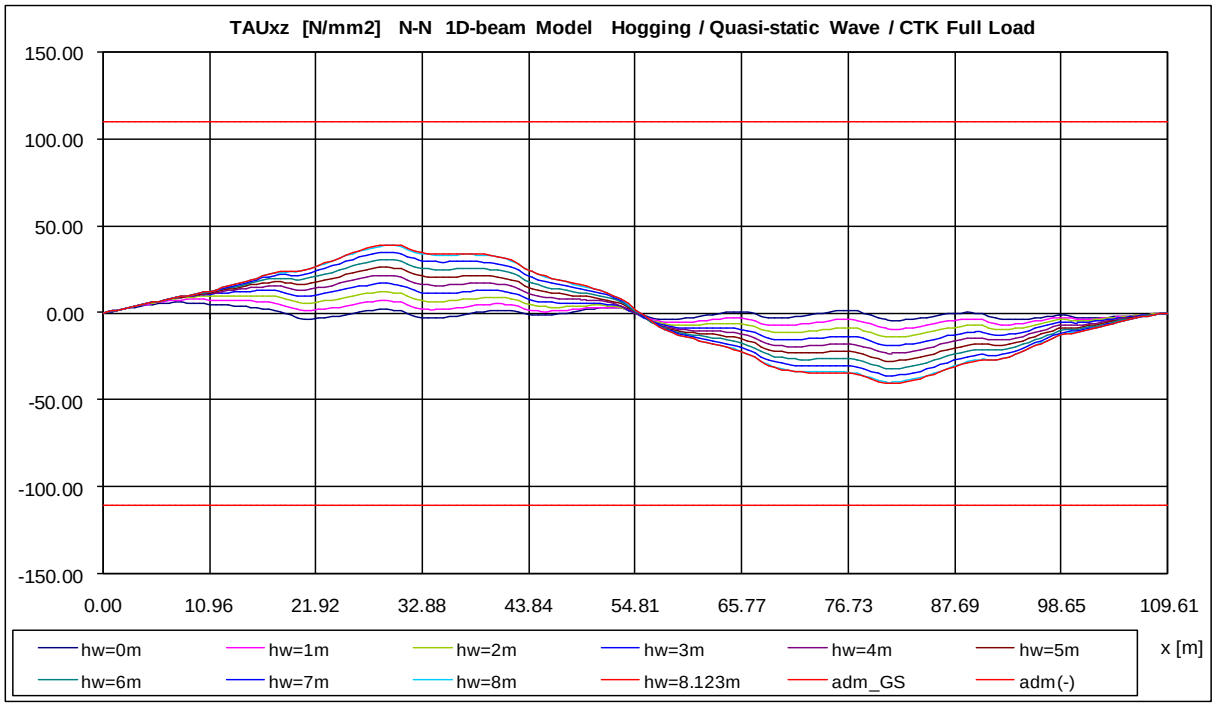

Fig. 5.2.5. Tangential side stress τ_{xz} [MPa] in Hogging wave conditions, 1D computation

Based on the numerical data from the Appendix Table. A.5.1.1, A.5.1.2 and A.5.1.3. for the reference wave height h_{wBV}=8.123 m it results the following synthesis data:

Table.5.2.4. Maximum Hogging stresses based on 1D-Equivalent Beam Model, h_w=8.123 m

Panel stress	Stress max 1D [MPa]	Stress adm_GS [MPa]	max/adm_GS
Maximum σ_x deck	98.25	265	0.37
Maximum σ_x bottom	71.27	175	0.41
Maximum τ_{xz} side	40.9	110	0.37

- The vertical position of the equivalent quasi-static head wave medium plane is changing from 4.41235 m (h_w=0 m) to 3.55606 m (h_w=8.123 m), representing a typical condition for the hogging case, having also an increase of the trim from 0.00280000 rad (h_w=0 m) to 0.00900000 (h_w=8.123 m).
- The maximum stresses are smaller than the admissible values, the highest ratio being recorded for the bottom, max/adm_{GS}=0.41.

5.3. Results by the 1D Equivalent Beam Model Numerical Computation in Sagging Conditions

The iterative procedure at the global-local ship strength, based on 1D Equivalent Beam Model, has converged to the following wave medium plane vertical position parameters.

Table.5.3.1. Vertical position parameters of the wave medium plane, in sagging conditions, based on 1D Equivalent Beam Model

Wave height case [m]	Vertical position amidships [m]	Trim in the longitudinal plane [rad]
0	4.41235	0.00280000
1	4.46923	0.00508000
2	4.51777	0.00733000
3	4.55919	0.00942000
4	4.59453	0.01129000
5	4.62491	0.01292000
6	4.65089	0.01428000
7	4.67334	0.01542000
8	4.69267	0.01637000
8.123	4.69483	0.01648000

In the following figures are presented the stress distributions obtained at the global-local strength analysis based on 1D-Equivalent Beam Model, under Sagging conditions.

- Fig.5.3.1 is presenting the Bending moment M for 1D computation in sagging wave conditions
- Fig.5.3.2. is presenting the Shear force T for 1D computation in sagging wave conditions
- Fig.5.3.3. and Appendix A.5.3, Table.A.5.3.1. are presenting the Normal Deck Stresses, σ_X [MPa] in Sagging wave conditions, 1D computation, and the stress check according to the admissible stress limit adm_GS
- Fig.5.3.4. and Appendix A.5.3, Table.A.5.3.2. are presenting the Normal Bottom Stresses, σ_X [MPa] in Sagging wave conditions, 1D computation, and the stress check according to the admissible stress limit adm_GS
- Fig. 5.3.5. and Appendix A.5.3, Table. A.5.3.3. are presenting the Tangential side stresses τ_{xz} [MPa] in Sagging wave conditions, 1D computation, and the stress check according to the admissible stress limit adm_GS.

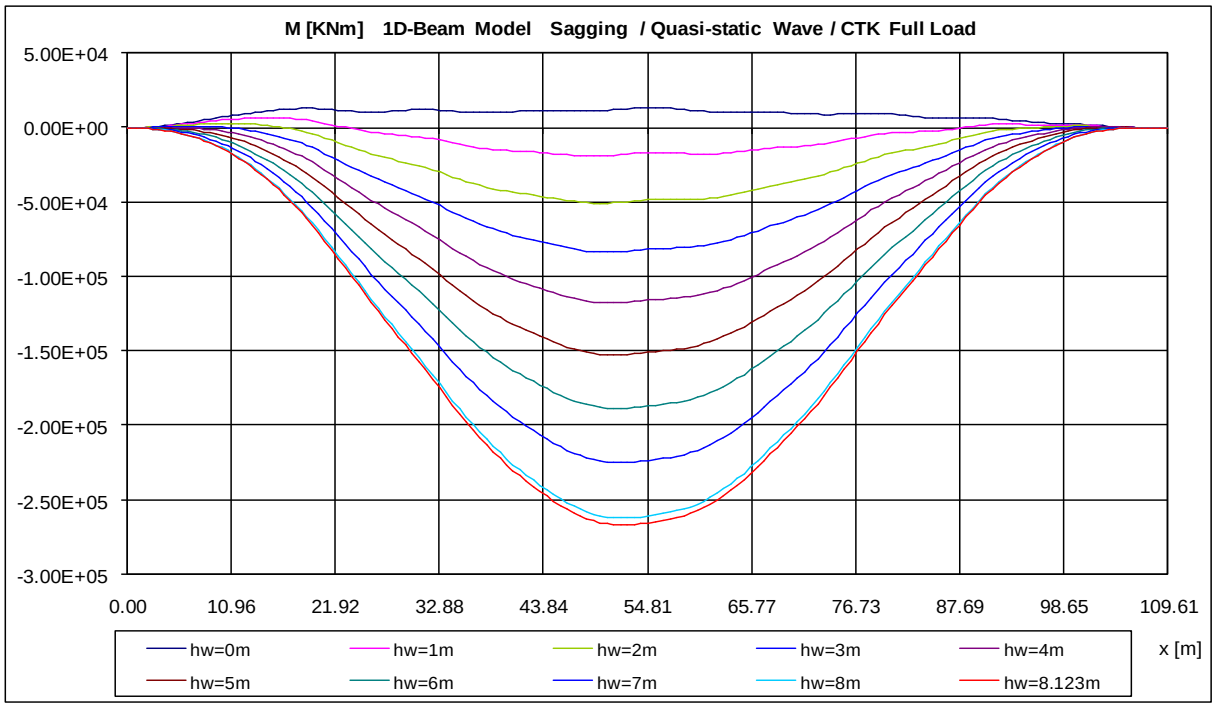

Fig.5.3.1Bending moment M [kNm] for 1D computation in sagging wave conditions

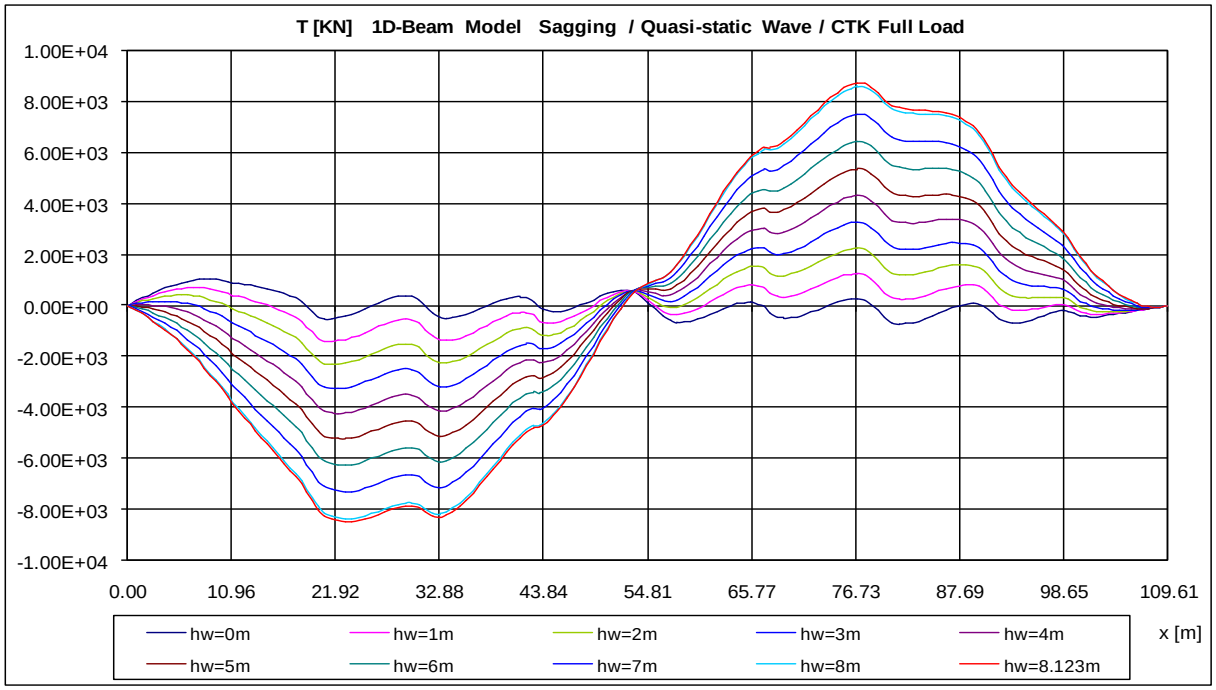

Fig.5.3.2. Shear force T [kN] for 1D computation in sagging wave conditions

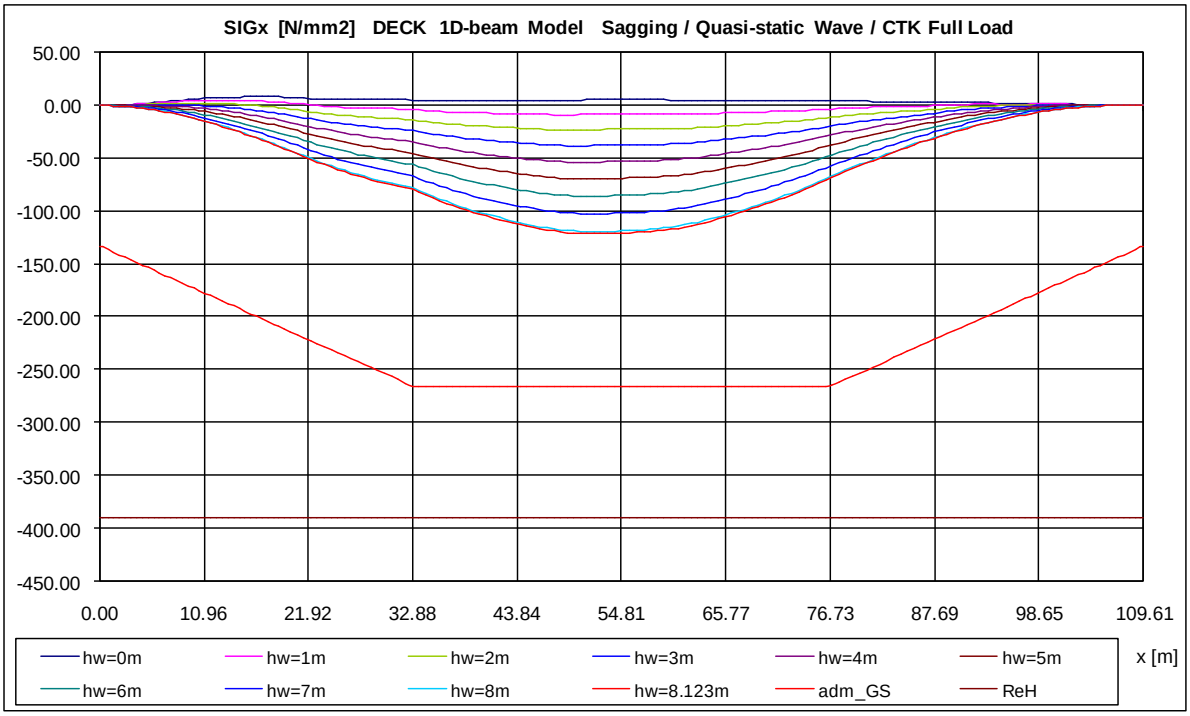

Fig.5.3.3. Normal Deck Stress, σ_X [MPa] in Sagging wave conditions, 1D computation

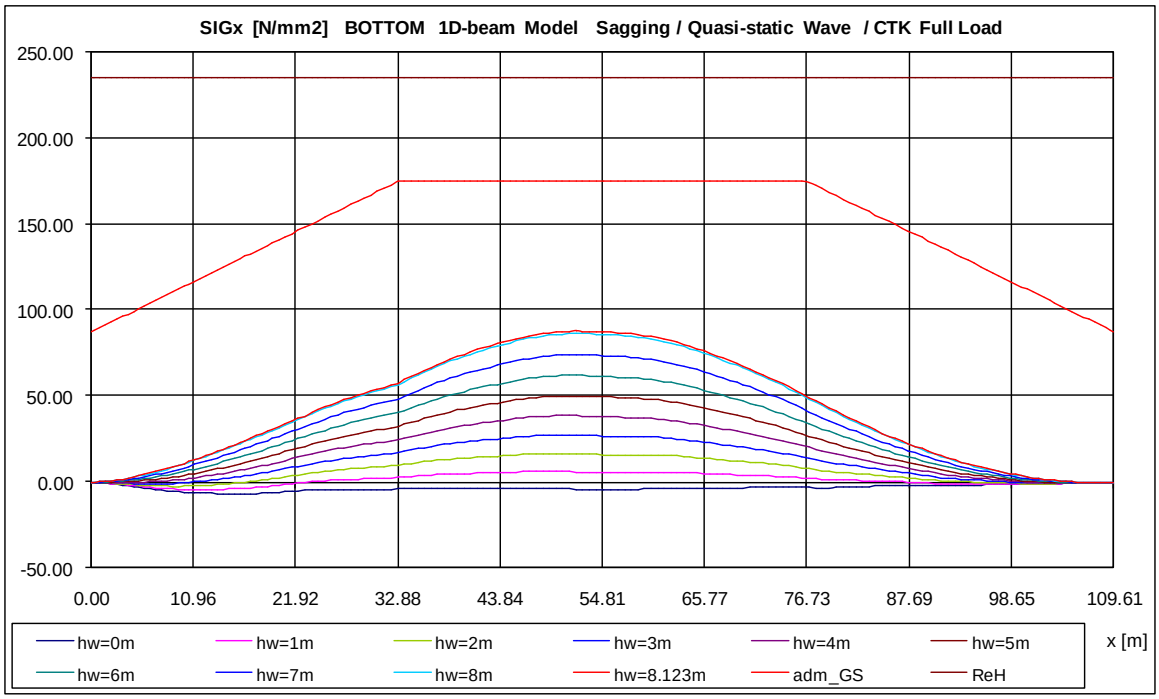

Fig.5.3.4. Normal Bottom Stress, σ_X [MPa] in Sagging wave conditions, 1D computation

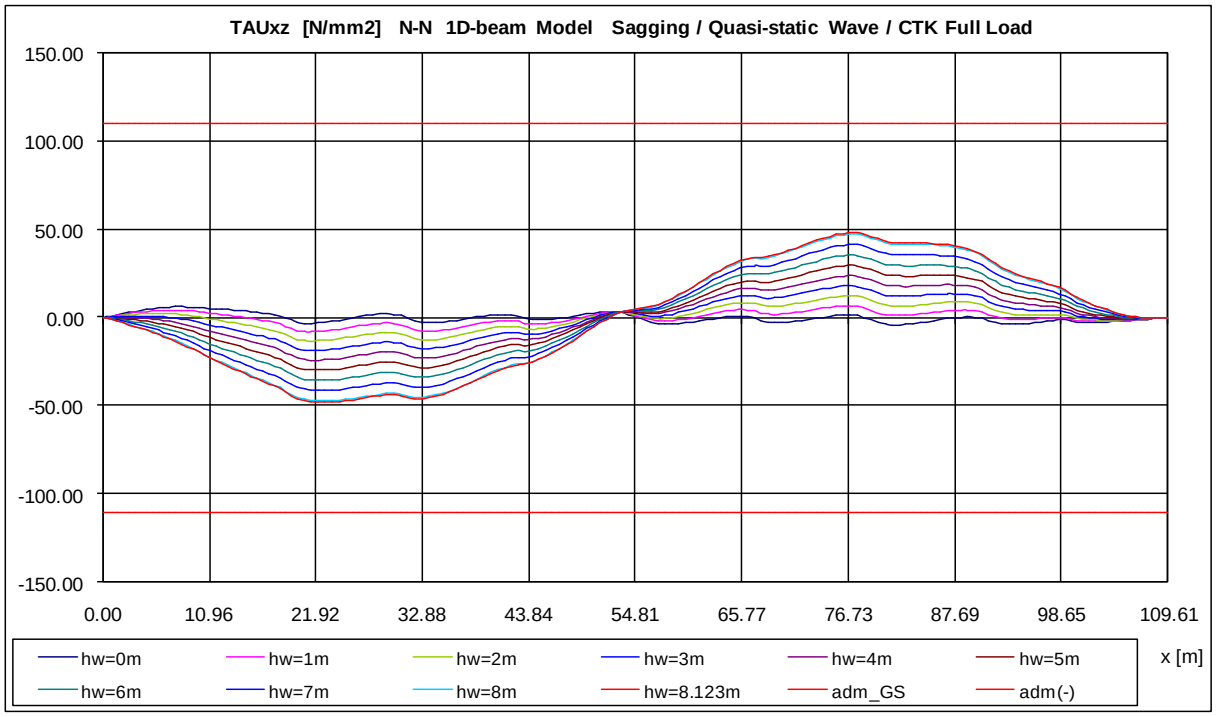

Fig. 5.3.5. Tangential side stress τ_{xz} [MPa] in Sagging wave conditions, 1D computation

Based on the numerical data from Appendix Tables. A.5.2.1, A.5.2.2 and A.5.2.3 for the reference wave height h_{wBV}=8.123 m it results the following synthesis data:

Table.5.3.4. Maximum Sagging stresses based on 1D-Equivalent Beam Model, h_w=8.123 m

Panel stress	Stress max 1D [MPa]	Stress adm_GS [MPa]	max/adm_GS
Maximum σ_x deck	121.17	265	0.46
Maximum σ_x bottom	87.90	175	0.50
Maximum τ_{xz} side	48.27	110	0.44

- The vertical position of the equivalent quasi-static head wave medium plane is changing from 4.41235 m (h_w=0 m) to 4.69483m (h_w=8.123 m), representing a typical condition for the sagging case, having an increase of the trim from 0.00280000 rad (h_w=0 m) to 0.01648000 (h_w=8.123 m).
- The maximum stresses are smaller than the admissible values, the highest ratio being recorded for the bottom, max/adm_{GS}=0.50.

6. THE NUMERICAL ANALYSIS OF GLOBAL-LOCAL SHIP HULL STRENGTH, BASED ON 3D-FEM MODEL FULL EXTENDED OVER THE SHIP LENGTH

According to the theoretical method presented in sub-chapter 2.2, the equivalent quasi-static head wave pressure loads will be applied on the hull external shell using an iterative procedure for the free floating and trim conditions equilibrium, implemented with user subroutines in the FEM solver.

In order to extract the results from the 3D-FEM model post-processing user subroutines are used for the following data: normal, tangential and vonMises stresses, deformations, etc.

At the ship global strength analysis, compared as to the simplified method, based on 1D-Equivalent Beam Model, the approach based on 3D-FEM Model extended over the whole ship length, has the main advantage of direct 3D results distribution.

6.1. Boundary and Loading Conditions

In order to proceed to the numerical analysis, the boundary conditions and the loadings are defined. Since the model is developed only on Portside, taking into account the head wave load condition, the following boundary conditions are considered:

Table.6.1. Boundary conditions definition 3D-FEM Full Extended Model

Boundary Conditions			
Nodes	Node nr.	Constraints	Type
ND_AFT	31067	U_X	Neutral
		U_Z	Forced, for equilibrium objective function definition
ND_FORE	46022	U_Z	Forced, for equilibrium objective function definition
CENTRE PLANE	All nodes	U_Y; R_X	Symmetry, natural

The neutral boundary condition is referring to the AFT node, ND_AFT. Also for this specific node, a forced boundary condition U_z was applied. For the Fore part of the ship, the boundary conditions were applied to ND_FORE, forced condition with constraint on U_z D.O.F. The symmetry condition (natural) is referring to all the nodes in the centre line plane and this condition is due to the fact that the ship 3D-FEM model is developed only in Portside (PS).

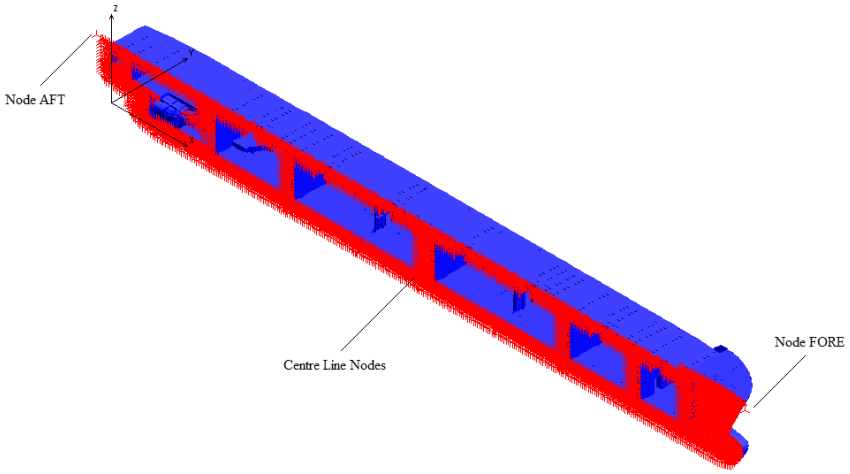

Fig.6.1. Applying the Boundary Conditions on the 3D-FEM Full Extended Model

In order to obtain an accurate structural analysis, the appropriate loads have to be applied on the 3D-FEM Model. The lightship mass diagram is obtained based on the steel hull 3D-FEM full extended model and it is presented in Fig.6.2.

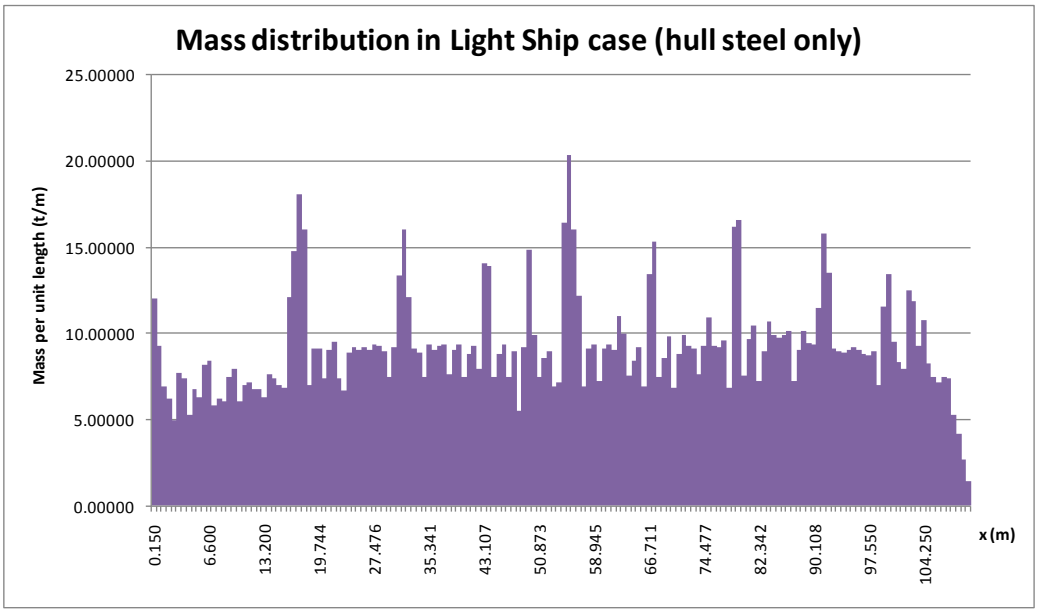

Fig.6.2. Lightship Mass distribution, based on 3D-FEM full extended model

The total light ship mass obtained based on the 3D-FEM Model is 1017.282 tones, using the elements constitutive mass properties.

In order to obtain the entire Hull mass, the onboard mass groups presented in Table 6.2, have to be considered, applied on the 3D-FEM Model as equivalent uniform pressures over the corresponding surfaces.

Table.6.2. Equivalent pressures for onboard mass components
(according to prototype ship from Ship Design Group, Galati 2007)

Chapter	Mass [t]	Pressure P (kN/m^2)
HULL Steel	1017.282	
Cargo tanks and systems	271.3	6.79
Miscellaneous	64.3	
Hull Outfitting	121.8	13.49
Machinery	68.1	22.31
Accommodation	85.7	5
Systems	71.1	5.5
Electrical	27.7	6.04
TOTAL	**1727.282**	

All of the equivalent pressures from Table 6.2, are applied according to their specific location, according to the ship's general arrangement plane (Fig.3.1.) and the stability booklet. Also the weight of the liquid cargo plus the cargo tank structural independent is applied as uniform pressure distributed on the corresponding supporting surfaces, on the double bottom (according to the cylindrical cargo tanks geometry Fig.6.5.b). Since not all the cargo tanks/compartments of the ship are the same , in Table 6.3. are presented the corresponding pressures. In order to consider for analysis the model weight, the gravity acceleration g=9.81 [m/s^2] has to be included in the input data, in order to generate the gravity loads.

Figure 6.4 presents the mass distribution over the ship length in the case of full cargo loading. The ship's displacement at full cargo loading case is 5380.18 tones.

Figure 6.5. a) presents the equivalent pressure distribution over the 3D-FEM model, for onboard and cargo masses modelling, corresponding to the full cargo loading case. Also it can be noticed in detail the distribution surface for the cylindrical cargo tanks with independent structure (Fig.6.5.b).

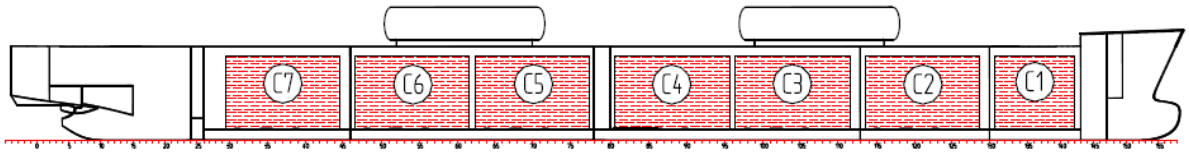

Fig.6.3. The cargo tanks position over the ship's length (Ship Design Group 2007)

Table.6.3 The equivalent pressure from independent filled up structural cargo tanks

Position	Mass (t)	Pressure P (kN/m^2)
CARGO Tank 1	326	62.6
CARGO Tank 2	679	61.1
CARGO Tank 3	679	
CARGO Tank 4	679	
CARGO Tank 5	679	
CARGO Tank 6	679	
CARGO Tank 7	679	

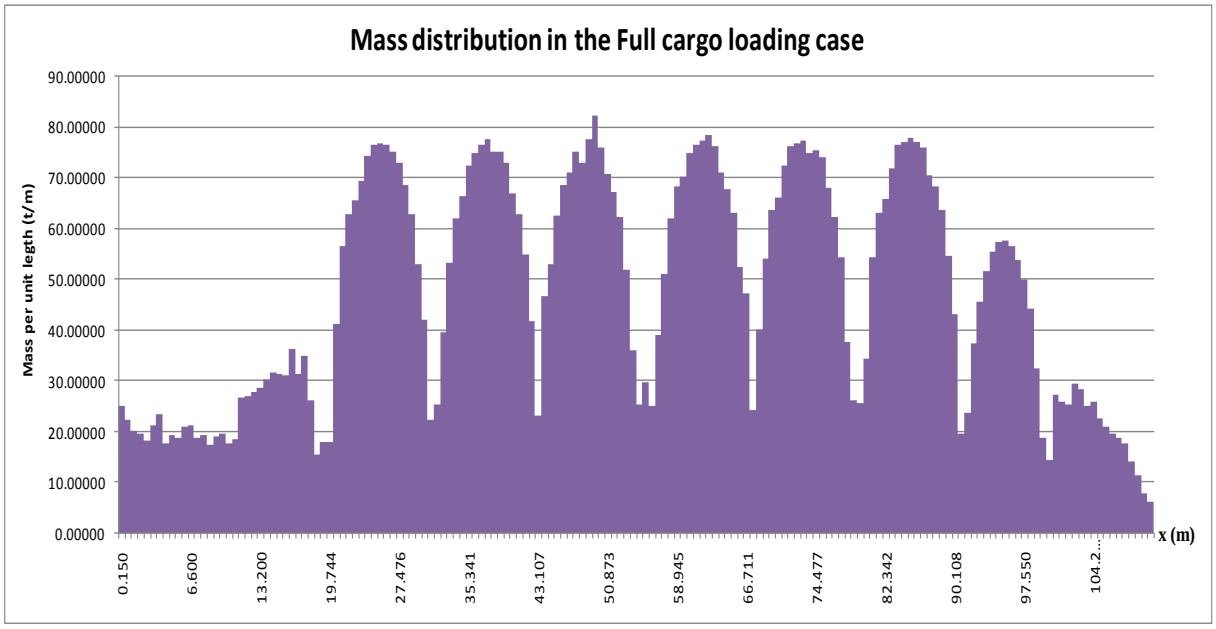

Fig. 6.4. Mass distribution in Full cargo loading case, 3D-FEM Full Extended Model

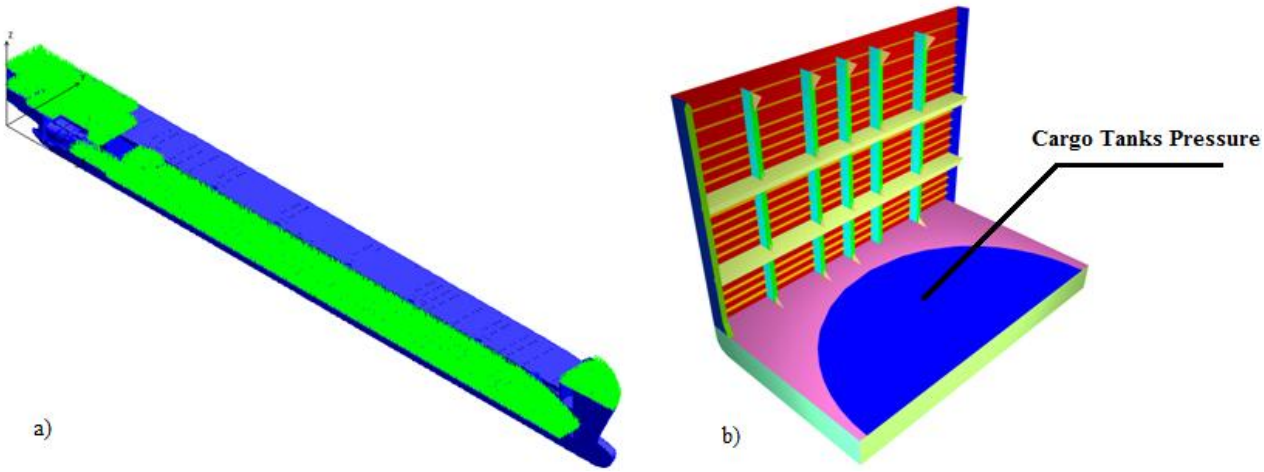

Fig.6.5. a) Equivalent Pressure applied on 3D-FEM Model, for onboard and cargo masses modelling, b) Distribution surface for the cylindrical cargo tanks

6.2 Numerical Analysis in Still Water Condition. Hydrostatic Water Pressure, Deformation and Stress Distributions

The still water equilibrium condition is obtained based on the theoretical model presented in subchapter 2.2, using the macro-command files procedures, implemented in Solid Works Comos/ M 2007 software, presented in Appendix A.1.1 and A.1.2, for h_w=0. The external hydrostatic water pressure is applied on bottom, bilge and side shells, during the iterative procedure for establishing the still water equilibrium condition.

In the following figures are presented the results from the numerical global-local strength analysis in still water condition (h_w=0):

- Fig.6.2.1. External hydrostatic water pressure on the ship hull at still water condition
- Fig.6.2.2. Vertical deflection at the ship girder at still water condition
- Fig.6.2.3. Equivalent vonMises Stress distribution in the cargo compartments (x=18.57 m to 99.42 m) at still water condition.

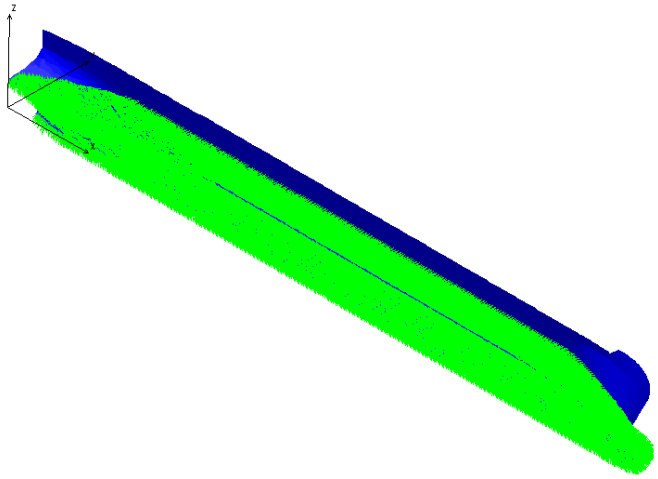

Fig.6.2.1 External water Hydrostatic Pressure [N/mm^2] applied on the shell plating in Still Water condition

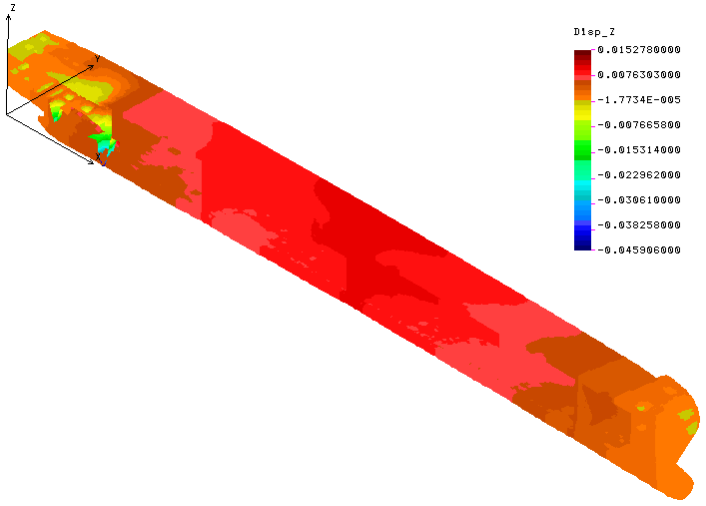

Fig.6.2.2. Vertical deflection on Z direction [m] in Still Water condition

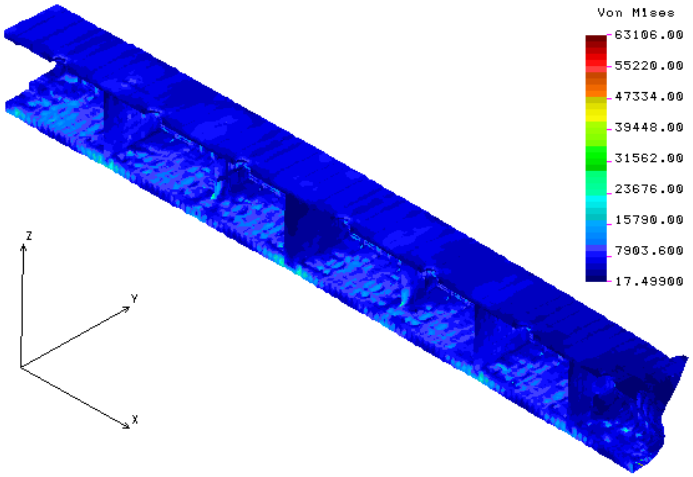

Fig.6.2.3. Equivalent vonMises stress distribution [kN/m^2] in Still Water condition, the cargo holds compartments part (x=18.57 m to 99.42 m)

6.3. Numerical Analysis in Hogging Conditions. Equivalent Quasi-static Wave Pressure, Deformation and Stress Distributions (Wave height 0-8.123 m)

In the following figures are presented the numerical results obtained at the global-local strength analysis based on the full extended 3D-FEM Model, under Hogging condition, using the theoretical method with iterative procedure for ship-wave vertical equilibrium, from subchapter 2.2. and the macro commands files from appendix A.1.1 and A.1.2 implemented in the Solid Works Cosmos/M 2007 FEM software.

Table.6.3.1.Figures List with numerical results at the global local strength analysis in hogging conditions, based on 3D-FEM full extended model

Wave height case [m]	Wave pressure distribution	Total vertical deflection	vonMises stress distributions
1	Fig.6.3.3	Fig.6.3.4	Fig.6.3.5
2	Fig.6.3.6	Fig.6.3.7	Fig.6.3.8
3	Fig.6.3.9	Fig.6.3.10	Fig.6.3.11
4	Fig.6.3.12	Fig.6.3.13	Fig.6.3.14
5	Fig.6.3.15	Fig.6.3.16	Fig.6.3.17
6	Fig.6.3.18	Fig.6.3.19	Fig.6.3.20
7	Fig.6.3.21	Fig.6.3.22	Fig.6.3.23
8	Fig.6.3.24	Fig.6.3.25	Fig.6.3.26
8.123	Fig.6.3.27	Fig.6.3.28	Fig.6.3.29

The iterative procedure at the global-local ship strength, based on 3D-FEM full extended model, has converged to the following wave medium plane vertical position parameters (see Table.6.3.2.)

Table.6.3.2. Vertical position parameters of the wave medium plane, in hogging conditions, based on 3D-FEM full extended model

Wave height case [m]	Vertical position amidships [m]	Trim in the longitudinal plane [rad]
0	4.41196	0.00318826
1	4.34431	0.00141595
2	4.26268	0.000254517
3	4.17222	0.00047057
4	4.07518	0.0013809
5	3.97264	0.00263539
6	3.86422	0.00406041
7	3.74648	0.00567603
8	3.6132	0.00761187
8.123	3.59531	0.0078738

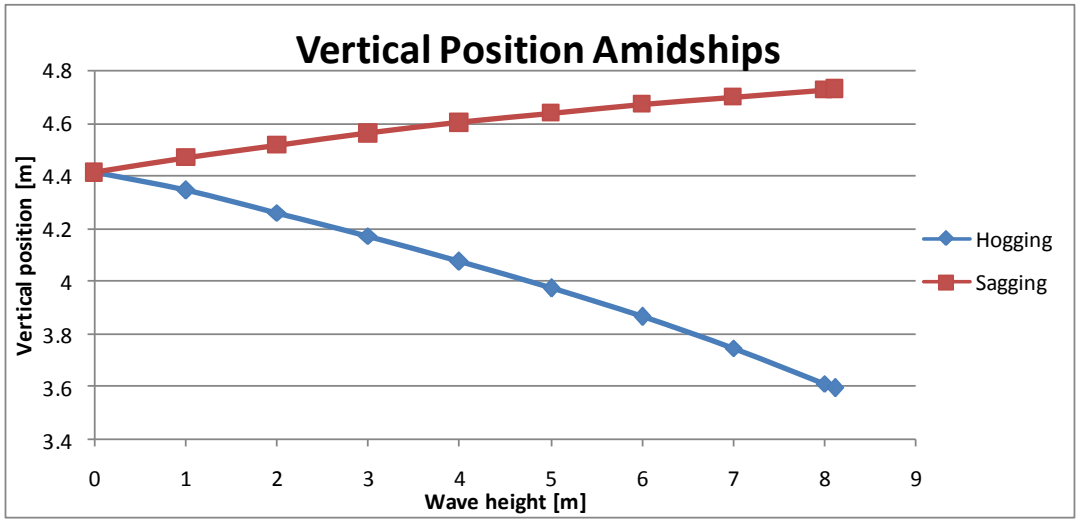

Fig.6.3.1. Vertical Position Amidships in Hogging and Sagging Wave conditions, based on 3D-FEM full extended model

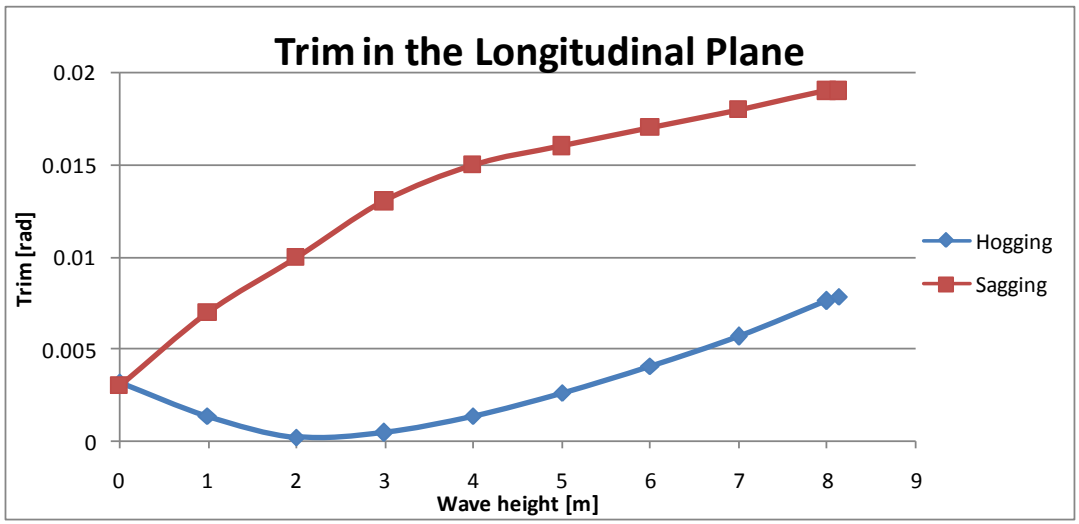

Fig.6.3.2. Trim in the Longitudinal Plane in Hogging and Sagging Wave conditions, based on 3D-FEM full extended model

- **Hogging conditions h_w=1 m equivalent quasi-static head wave height**

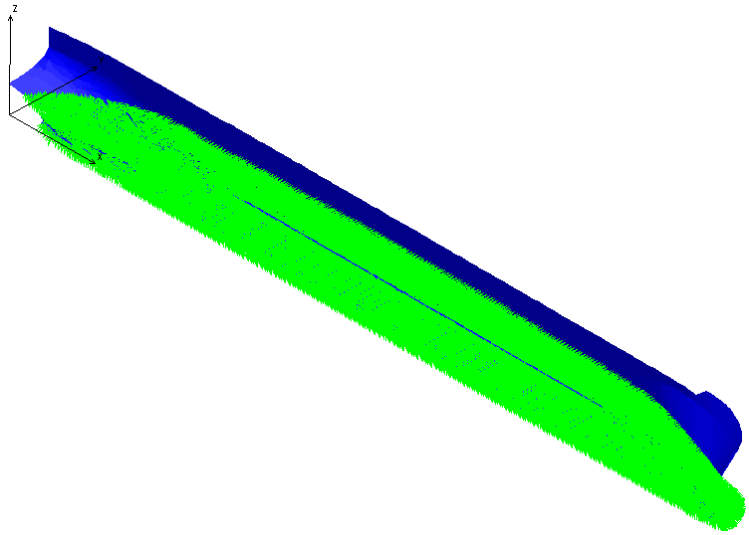

Fig.6.3.3 Hydrostatic Pressure from the external equivalent quasi-static wave applied on the ship hull, Wave height 1 m, Hogging condition

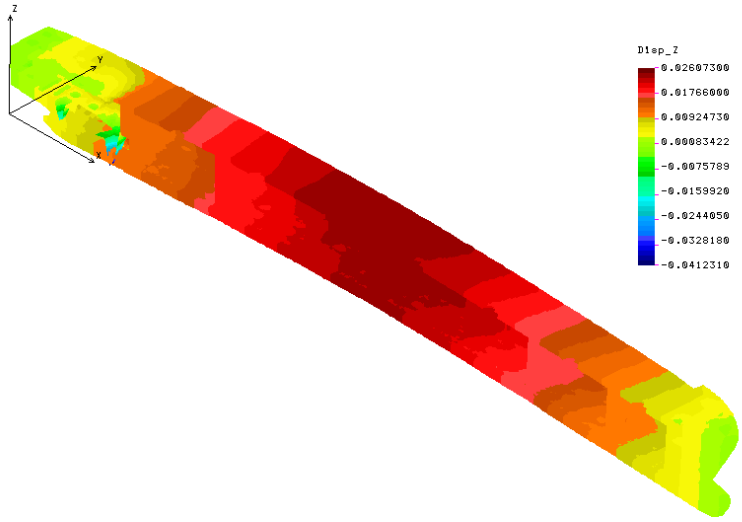

Fig.6.3.4. Vertical deflection on Z direction (m), Wave height 1 m, Hogging condition

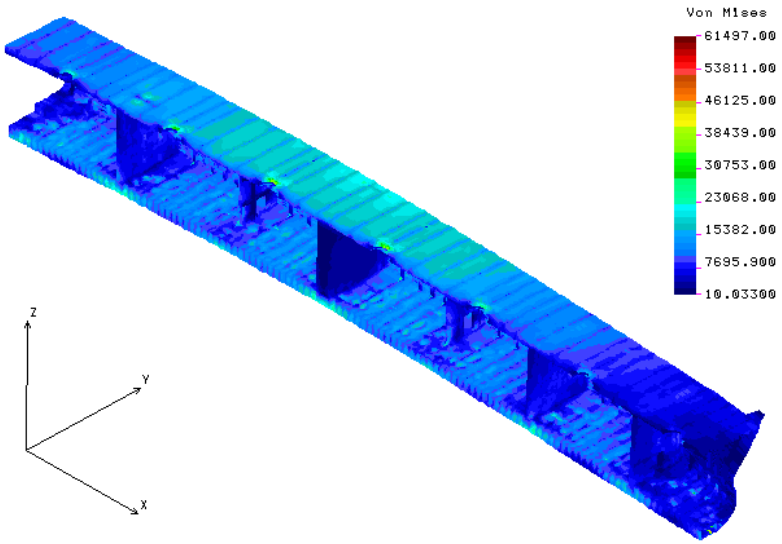

Fig.6.3.5. Equivalent vonMises stress distribution [kN/m^2] ,at the cargo compartments part (x=18.57 m to 99.42 m), Wave height 1 m, Hogging condition

- **Hogging conditions h_w=2 m equivalent quasi-static head wave height**

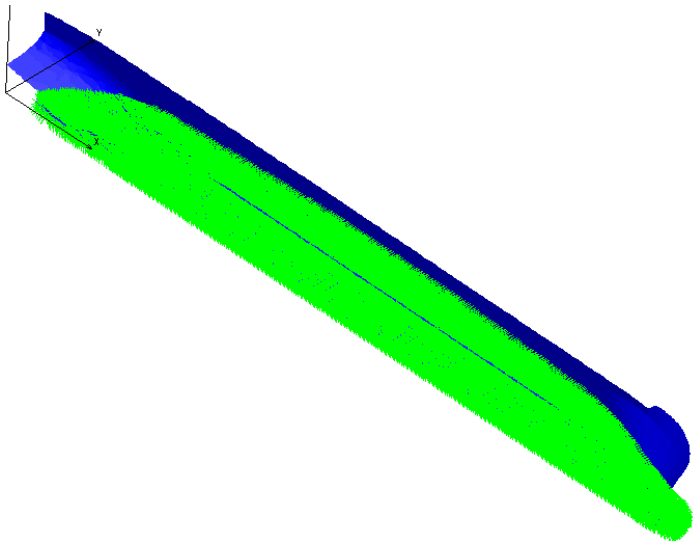

Fig.6.3.6. Hydrostatic Pressure from the external equivalent quasi-static wave applied on the ship hull, Wave height 2 m, Hogging condition

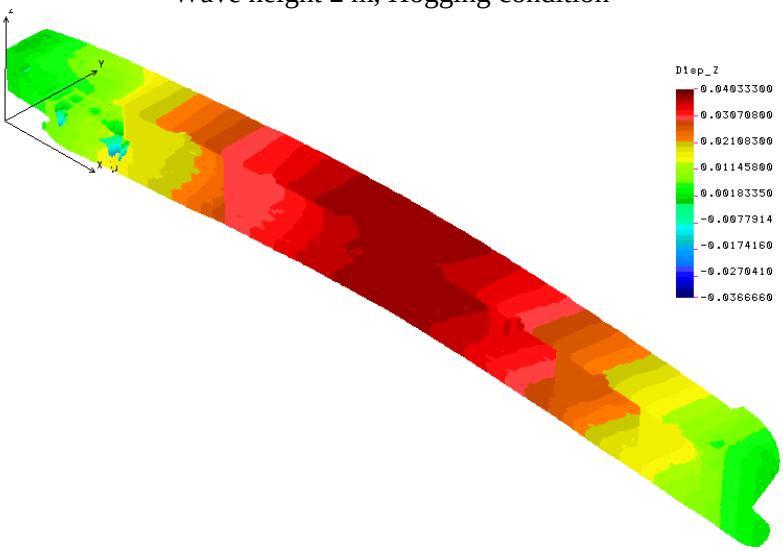

Fig.6.3.7. Vertical deflection on Z direction (m), Wave height 2 m, Hogging condition

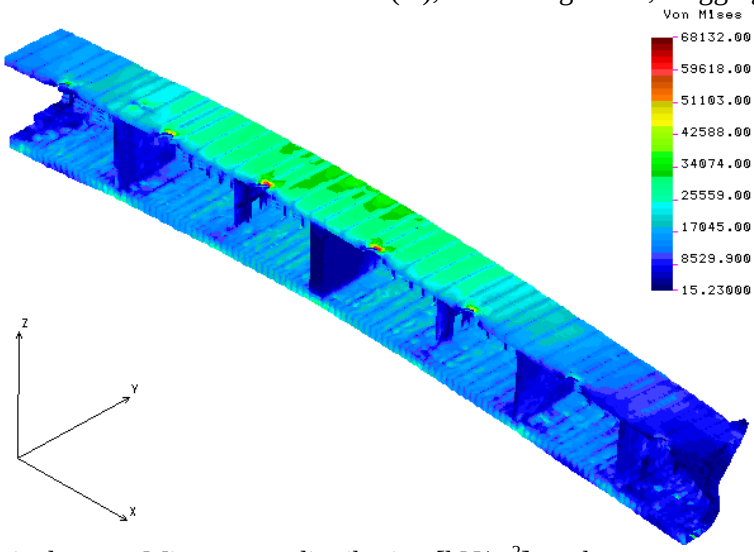

Fig.6.3.8. Equivalent vonMises stress distribution [kN/m^2] ,at the cargo compartments part (x=18.57 m to 99.42 m), Wave height 2 m, Hogging condition

- **Hogging conditions h_w=3 m equivalent quasi-static head wave height**

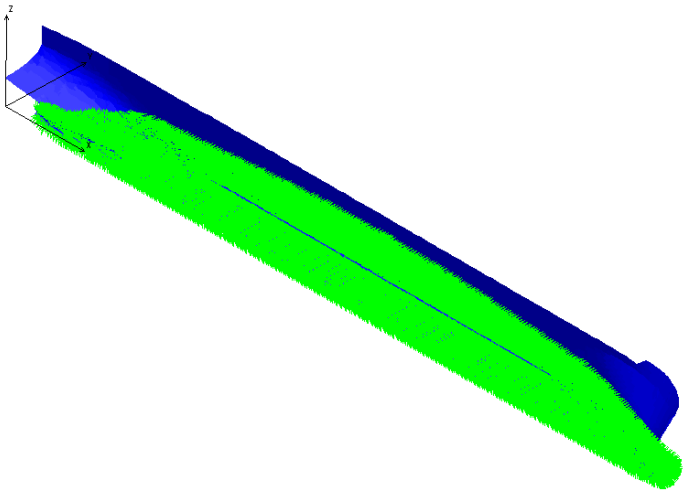

Fig.6.3.9 Hydrostatic Pressure from the external equivalent quasi-static wave applied on the ship hull, Wave height 3 m, Hogging condition

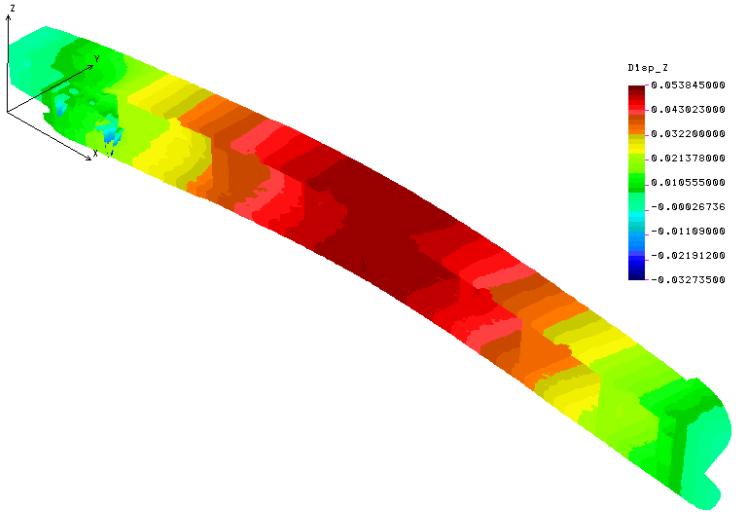

Fig.6.3.10. Vertical deflection on Z direction (m), Wave height 3 m, Hogging condition

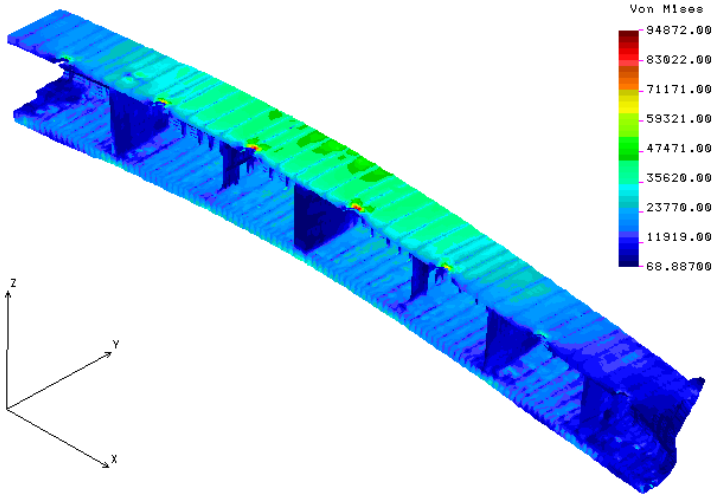

Fig.5.3.11. Equivalent vonMises stress distribution [kN/m^2] ,at the cargo compartments part (x=18.57 m to 99.42 m), Wave height 3 m, Hogging condition

- **Hogging conditions h_w=4 m equivalent quasi-static head wave height**

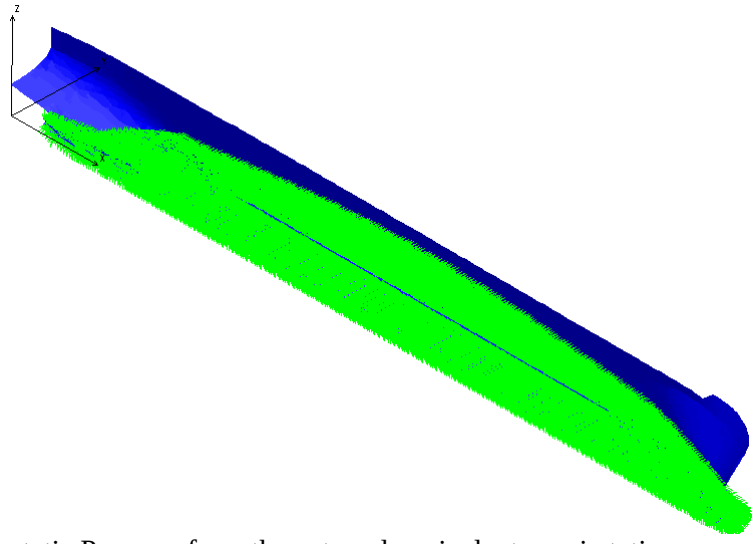

Fig.6.3.12. Hydrostatic Pressure from the external equivalent quasi-static wave applied on the ship hull, Wave height 4 m, Hogging condition

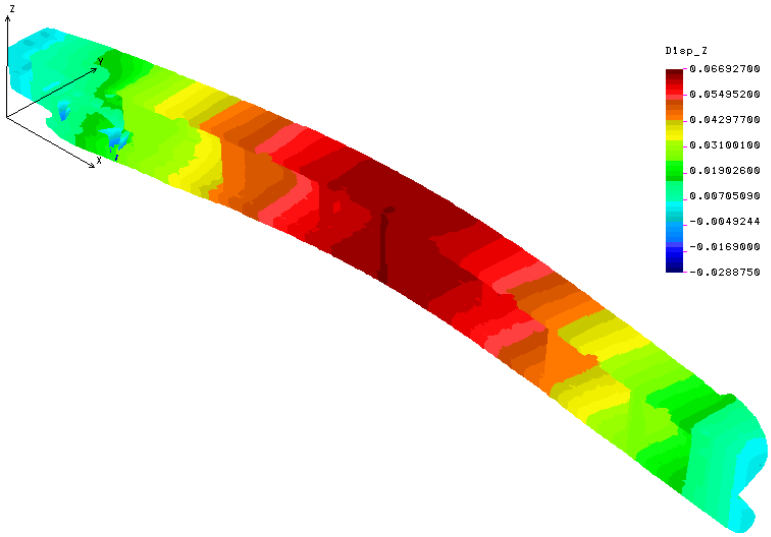

Fig.6.3.13. Vertical deflection on Z direction (m), Wave height 4 m, Hogging condition

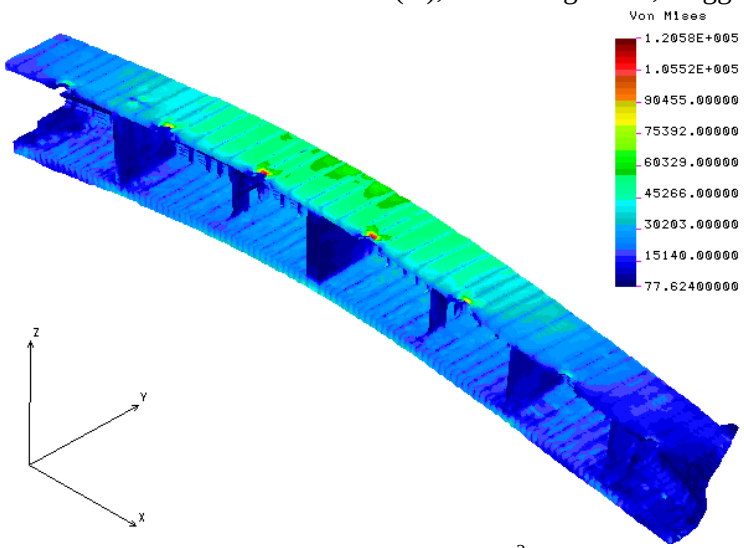

Fig.6.3.14. Equivalent vonMises stress distribution [kN/m^2] ,at the cargo compartments part (x=18.57 m to 99.42 m), Wave height 4 m, Hogging condition

- **Hogging conditions h_w=5 m equivalent quasi-static head wave height**

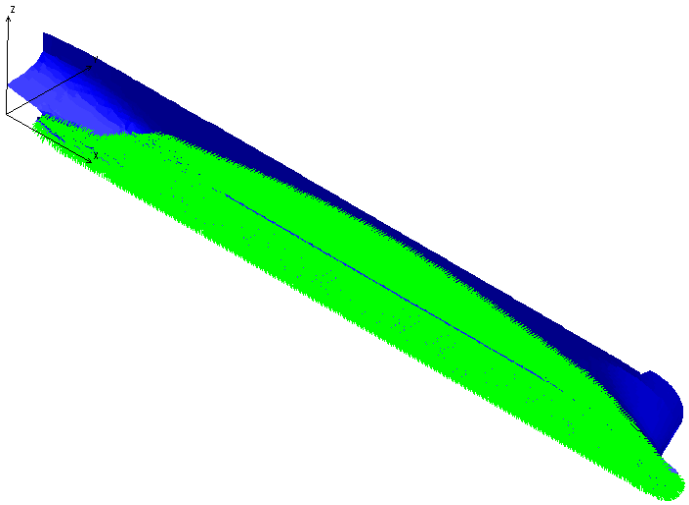

Fig.6.3.15 Hydrostatic Pressure from the external equivalent quasi-static wave applied on the ship hull, Wave height 5 m, Hogging condition

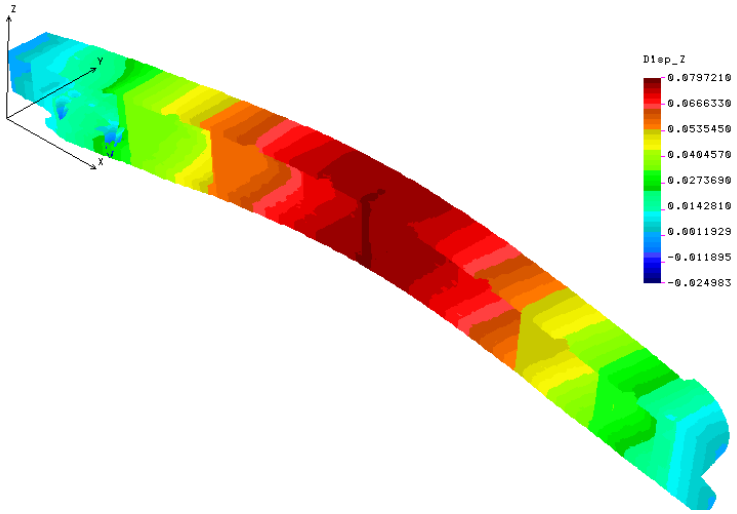

Fig.6.3.16. Vertical deflection on Z direction (m), Wave height 5 m, Hogging condition

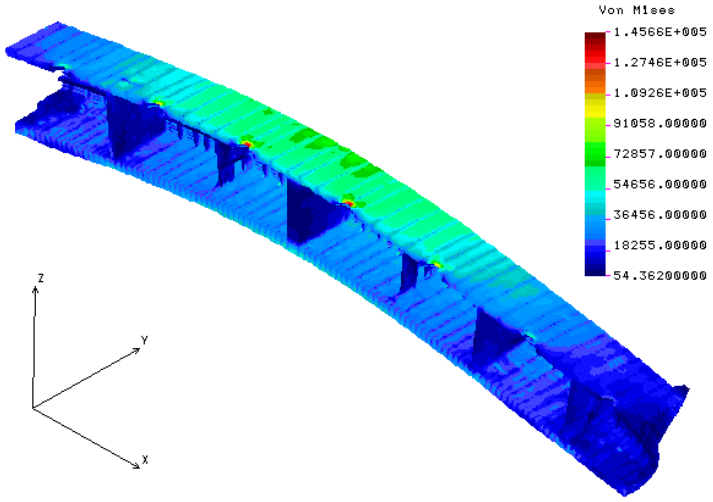

Fig.6.3.17. Equivalent vonMises stress distribution [kN/m^2] ,at the cargo compartments part (x=18.57 m to 99.42 m), Wave height 5 m, Hogging condition

- **Hogging conditions h_w=6 m equivalent quasi-static head wave height**

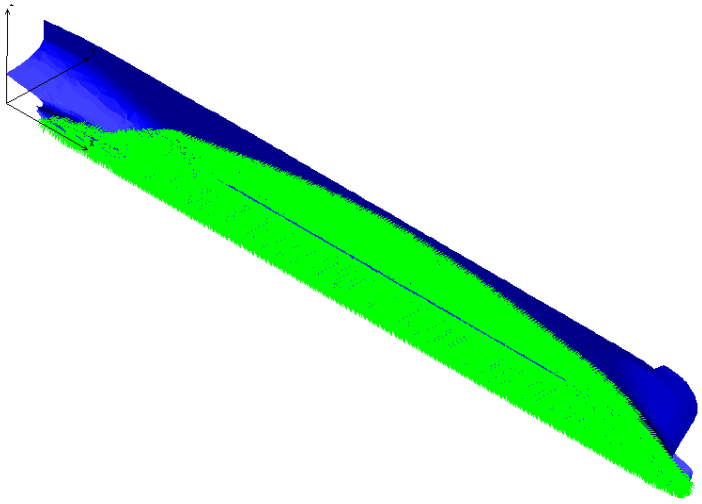

Fig.6.3.18. Hydrostatic Pressure from the external equivalent quasi-static wave applied on the ship hull, Wave height 6 m, Hogging condition

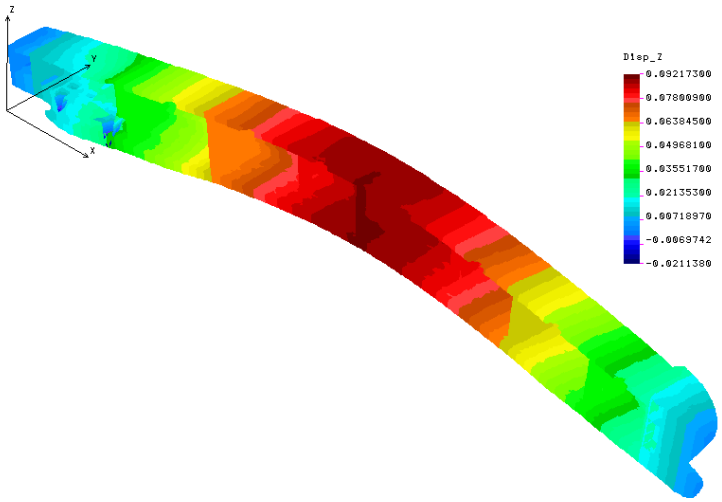

Fig.6.3.19. Vertical deflection on Z direction (m), Wave height 6 m, Hogging condition

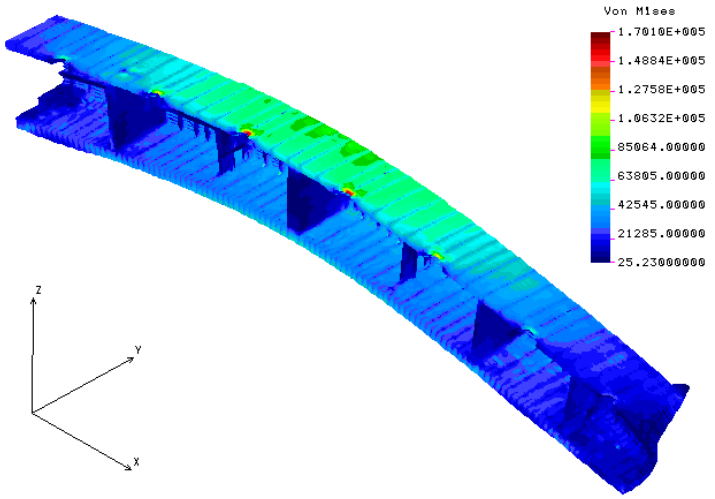

Fig.6.3.20. Equivalent vonMises stress distribution [kN/m^2] ,at the cargo compartments part (x=18.57 m to 99.42 m), Wave height 6 m, Hogging condition

- **Hogging conditions h_w=7 m equivalent quasi-static head wave height**

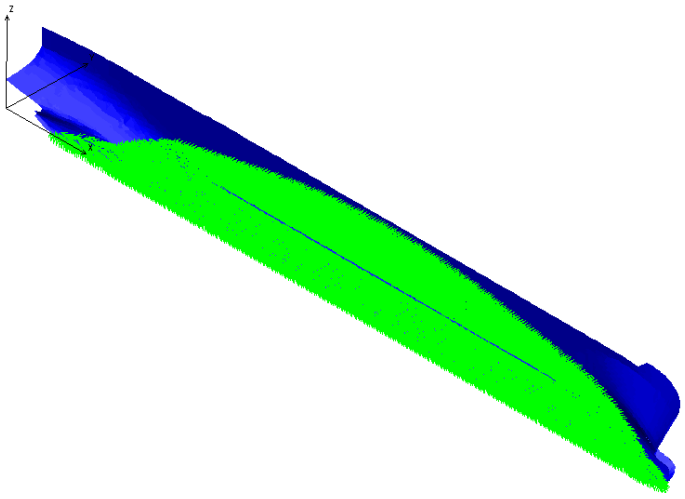

Fig.6.3.21. Hydrostatic Pressure from the external equivalent quasi-static wave applied on the ship hull, Wave height 7 m, Hogging condition

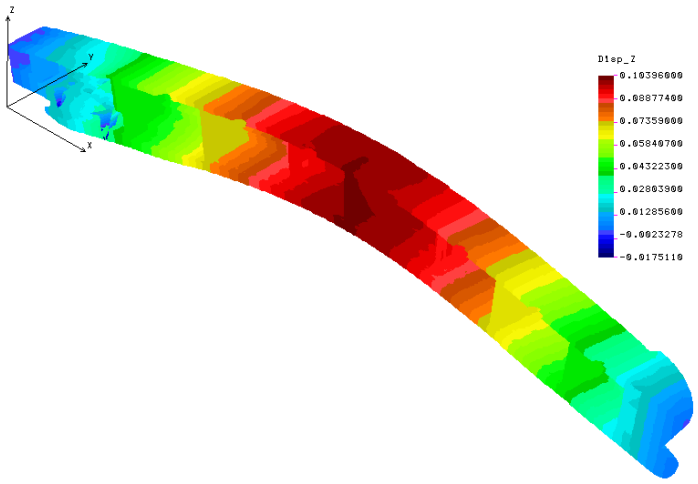

Fig.6.3.22. Vertical deflection on Z direction (m), Wave height 7 m, Hogging condition

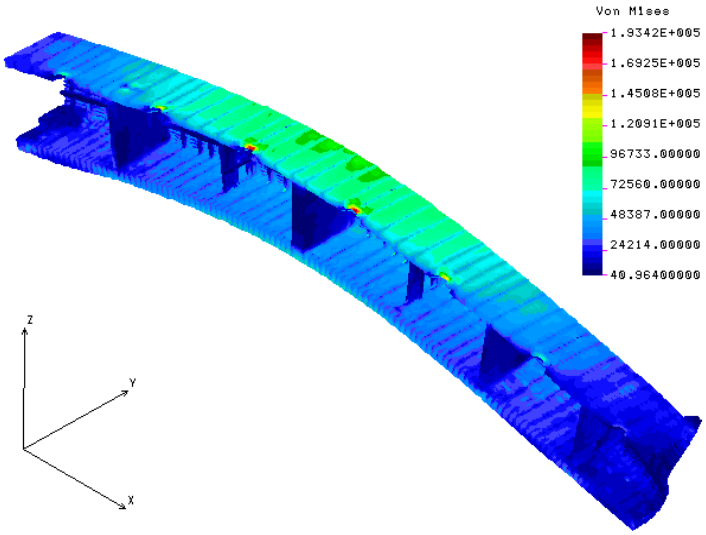

Fig.6.3.23. Equivalent vonMises stress distribution [kN/m^2] ,at the cargo compartments part (x=18.57 m to 99.42 m), Wave height 7 m, Hogging condition

- **Hogging conditions h_w= 8 m equivalent quasi-static head wave height**

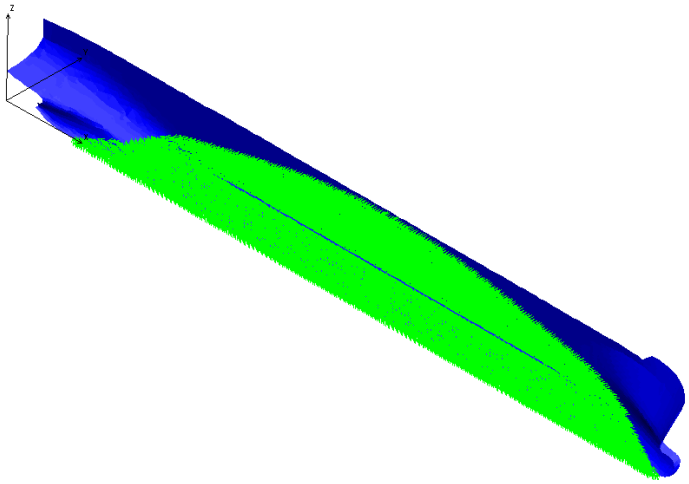

Fig.6.3.24. Hydrostatic Pressure from the external equivalent quasi-static wave applied on the ship hull, Wave height 8 m, Hogging condition

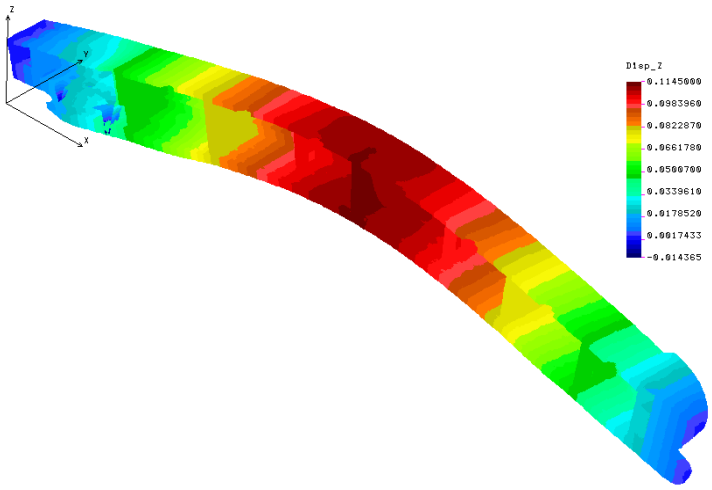

Fig.6.3.25. Vertical deflection on Z direction (m), Wave height 8 m, Hogging condition

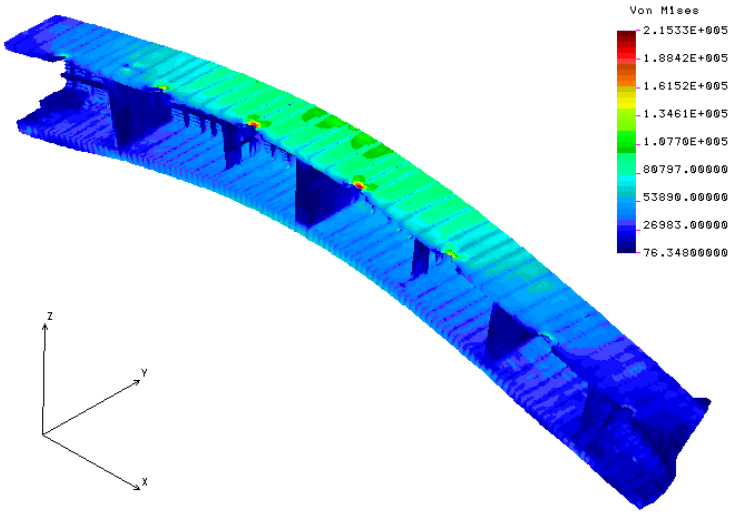

Fig.6.3.26. Equivalent vonMises stress distribution [kN/m^2] ,at the cargo compartments part (x=18.57 m to 99.42 m), Wave height 8 m, Hogging condition

- **Hogging conditions h_w=8.123 m equivalent quasi-static head wave height**

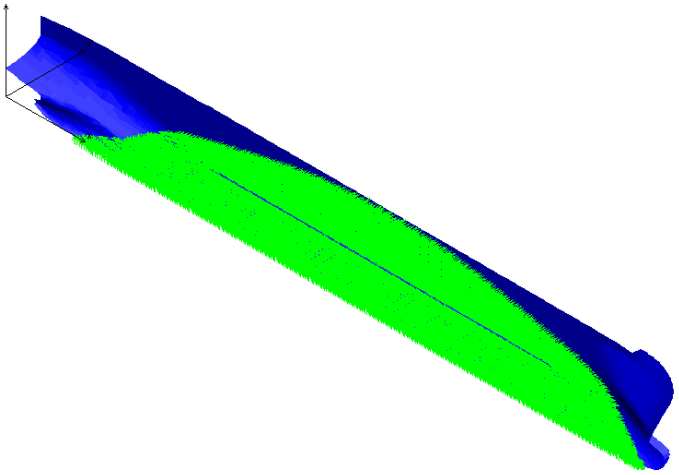

Fig.6.3.27. Hydrostatic Pressure from the external equivalent quasi-static wave applied on the ship hull, Wave height 8.123 m, Hogging condition

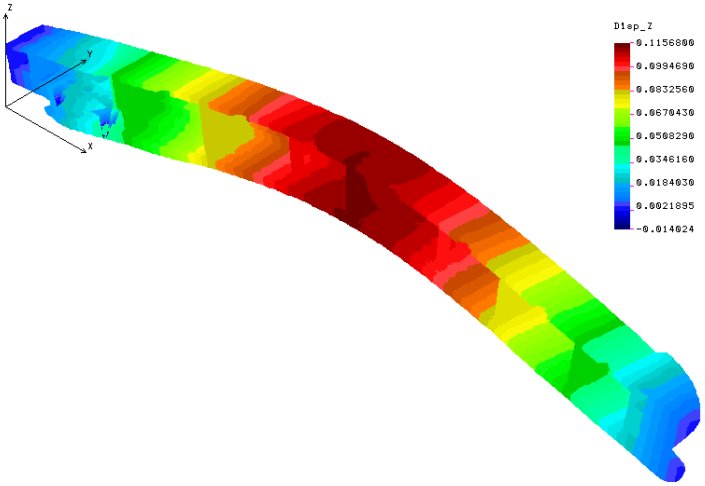

Fig.6.3.28. Vertical deflection on Z direction (m), Wave height 8.123 m, Hogging condition

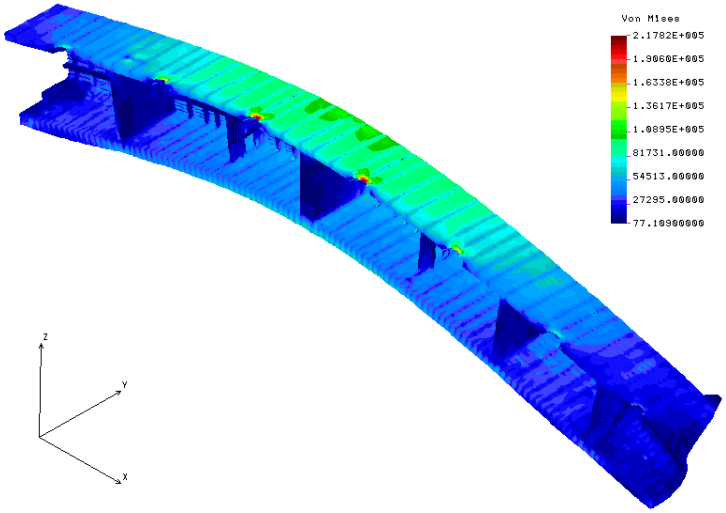

Fig.6.3.29. Equivalent vonMises stress distribution [kN/m^2], at the cargo compartments part (x=18.57 m to 99.42 m), Wave height 8.123 m, Hogging condition

6.4. Discussions and Conclusions for the Numerical Computation in Hogging Conditions, Based on Full Extended 3D-FEM Model

In the following figures are presented the maximum values for stress distributions obtained at the global- local strength analysis, based on the full extended 3D-FEM Model, in Hogging conditions. For selected panels (Deck, Bottom, Side) and a given transversal section the maximum stress value result from the equation 2.2.2:

- Fig. 6.4.1 and Appendix A.6.1, Table A.6.1.1. are presenting the Maximum Normal Deck Stress, σ_x [MPa] in Hogging wave conditions, 3D-FEM full extended model, and the safety coefficients Cs according to the yield stress limit ReH.
- Fig.6.4.2. and Appendix A.6.1, Table.A.6.1.2. are presenting the Maximum Equivalent vonMises Deck Stress, σ_{von} [MPa] in Hogging wave conditions, 3D-FEM full extended model, and the safety coefficients Cs according to the yield stress limit ReH.
- Fig.6.4.3. and Appendix A.6.1, Table.A.6.1.3. are presenting the Maximum Normal Bottom Stress, σ_x [MPa] in Hogging wave conditions, 3D-FEM full extended model, and the safety coefficients Cs according to the yield stress limit ReH.
- Fig.6.4.4. and Appendix A.6.1, Table.A.6.1.4. are presenting the Maximum Equivalent vonMises Bottom Stress, σ_{von} [MPa] in Hogging wave conditions, 3D-FEM full extended model, and the safety coefficients Cs according to the yield stress limit ReH.
- Fig.6.4.5. and Appendix A.6.1, Table.A.6.1.5. are presenting the Maximum Tangential side stress τ_{xz} [MPa] in Hogging wave conditions, 3D-FEM full extended model.

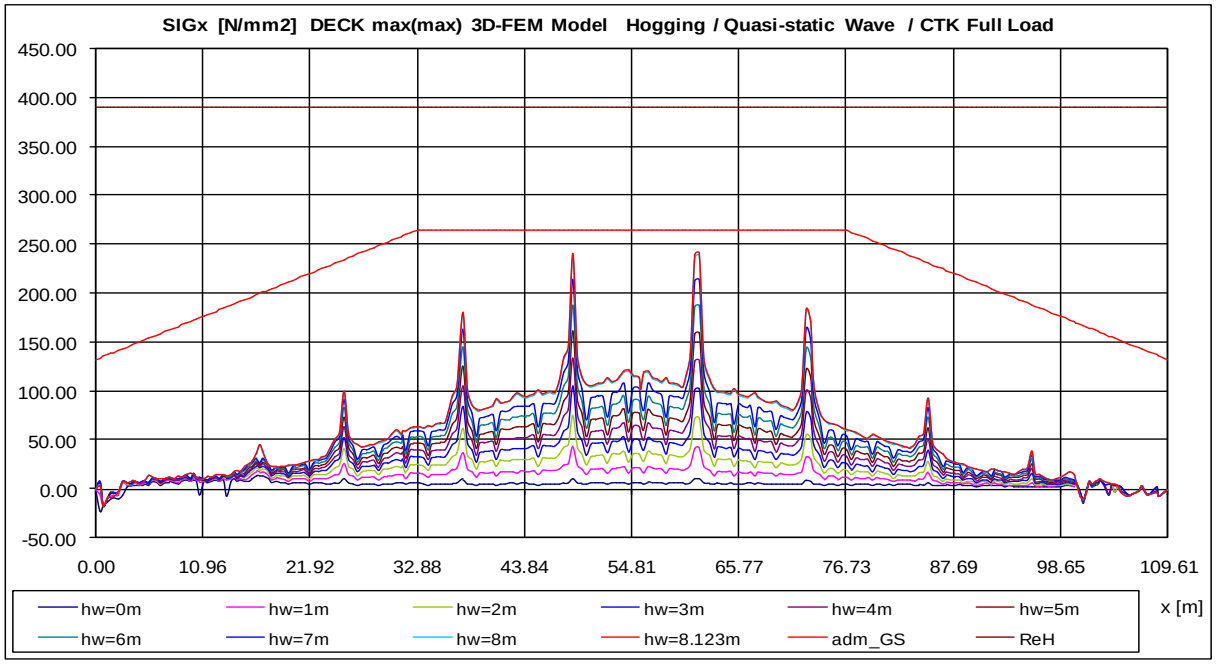

Fig.6.4.1. Maximum Normal Deck Stress, σ_X [MPa] in Hogging wave conditions, 3D-FEM full extended model

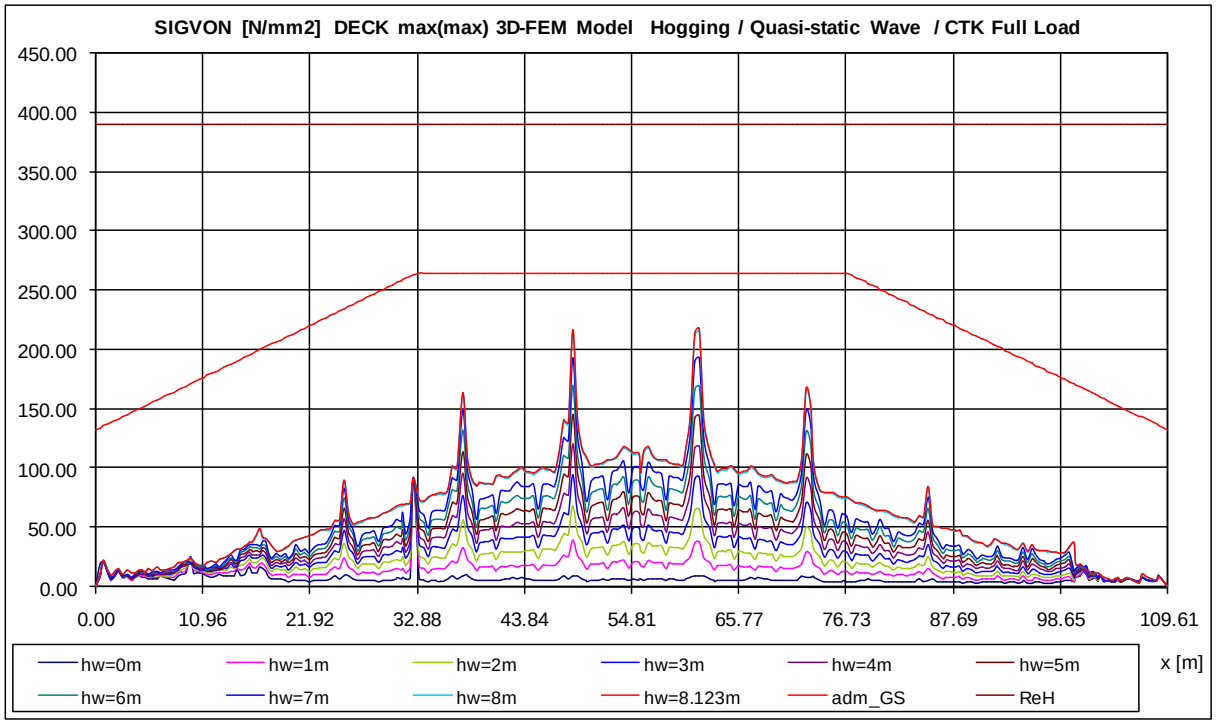

Fig.6.4.2. Maximum Equivalent vonMises Deck Stress, σ_{von} [MPa] in Hogging wave conditions, 3D-FEM full extended model

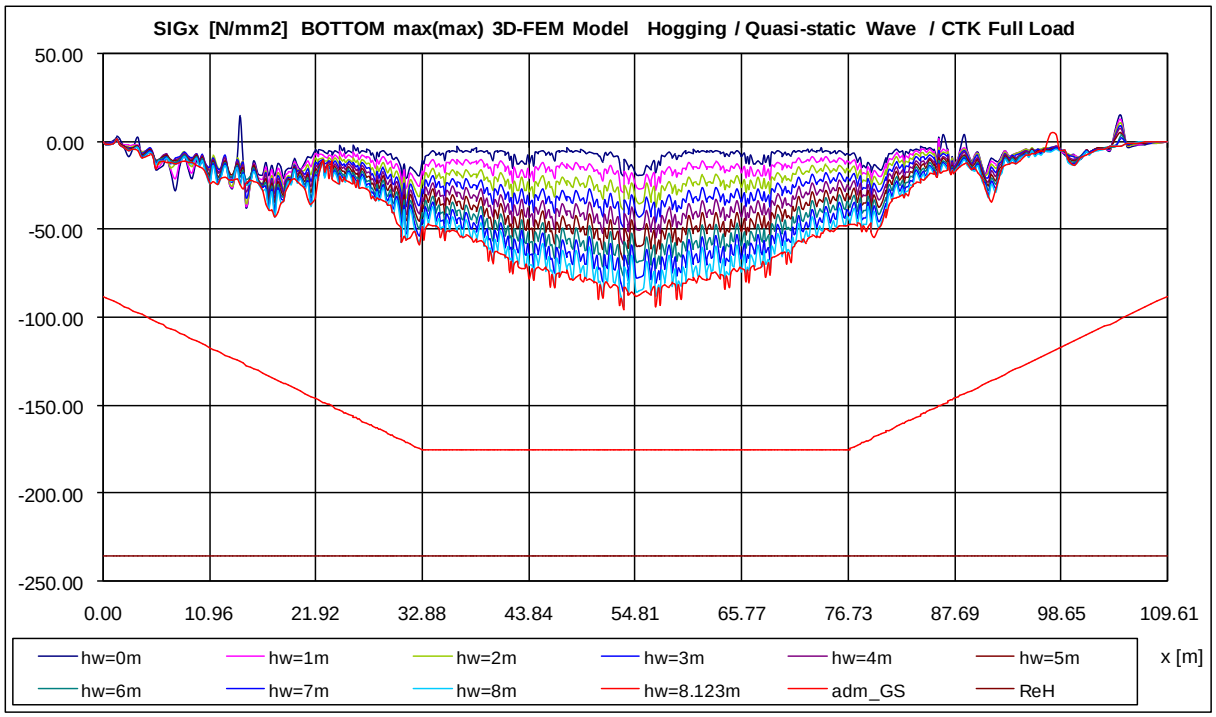

Fig.6.4.3. Maximum Normal Bottom Stress, σ_X [MPa] in Hogging wave conditions, 3D-FEM full extended model

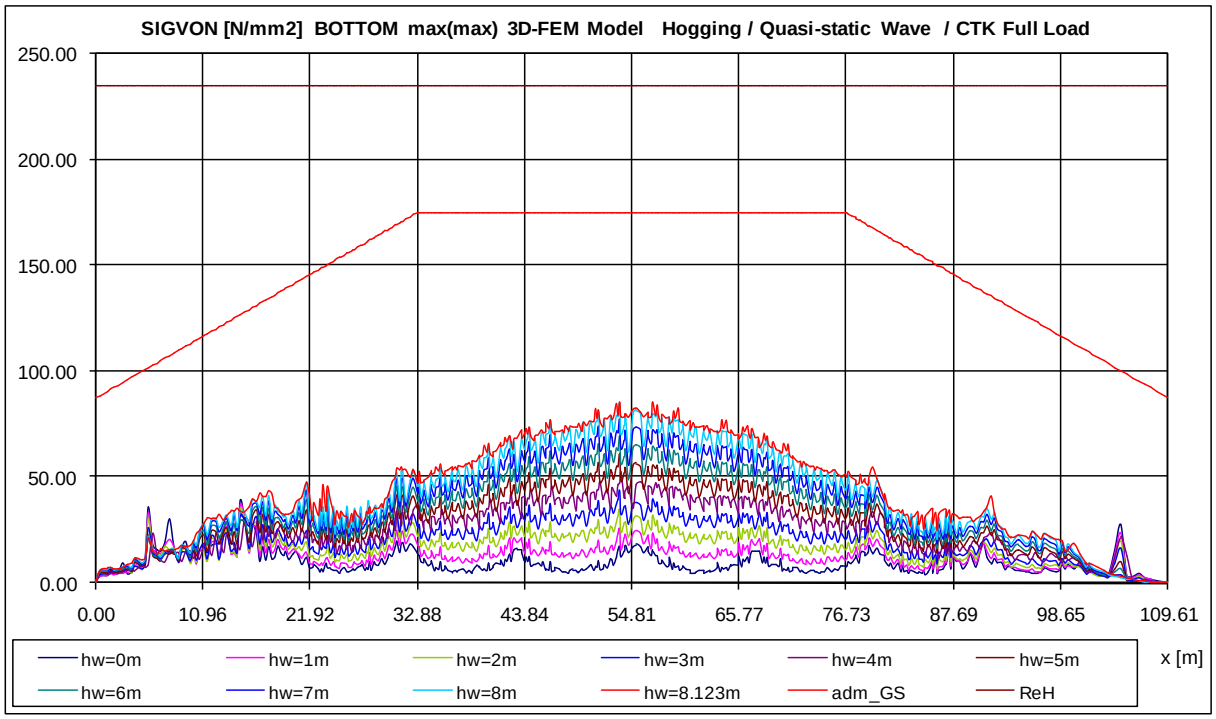

Fig.6.4.4. Maximum Equivalent vonMises Bottom Stress, σ_{von} [MPa] in Hogging wave conditions, 3D-FEM full extended model

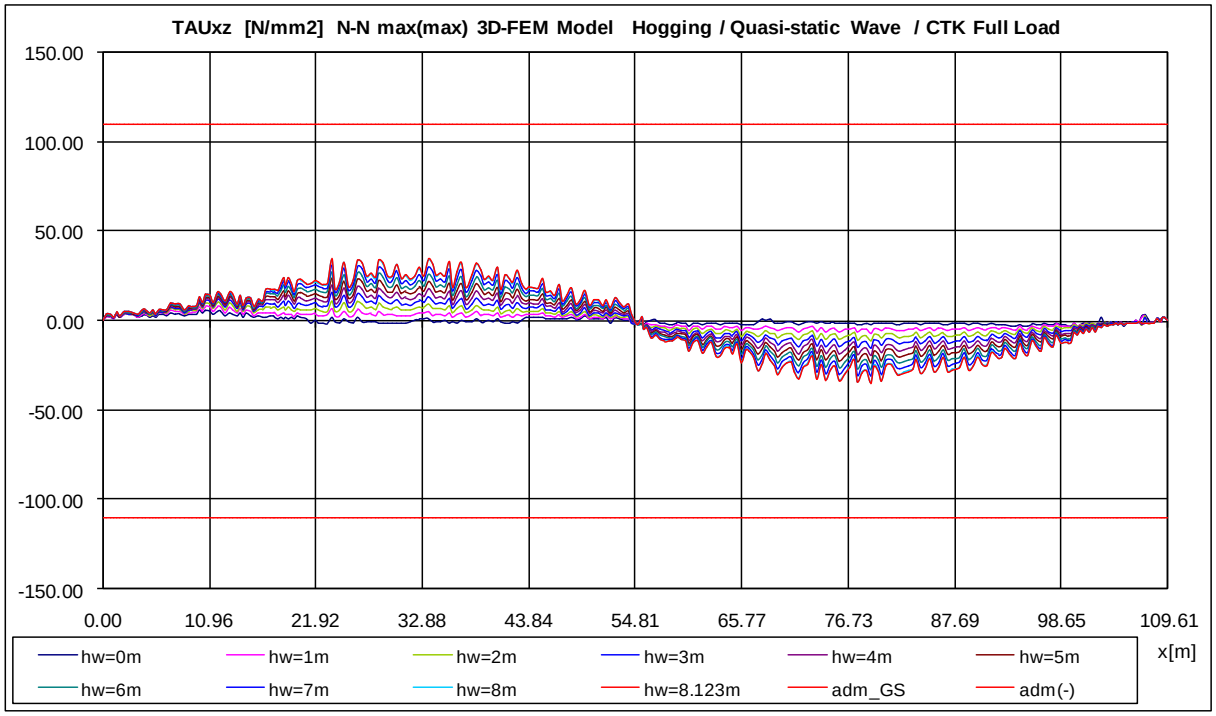

Fig.6.4.5. Maximum Tangential side stress τ_{xz} [MPa] in Hogging wave conditions, 3D-FEM full extended model

Based on figures Fig.6.3.4; Fig.6.3.7; Fig.6.3.10; Fig.6.3.13; Fig.6.3.16; Fig.6.3.19; Fig.6.3.22; Fig.6.3.25; Fig.6.3.28, in Table 6.4.6 the global vertical deflections are presented for the ship hull structure in Hogging condition.

Table.6.4.6. Maximum vertical deflections based on 3D-FEM full extended model in Hogging condition

h_w [m]	w_{max} [m]	$w_{adm}=L/500$ [m]	$\lvert w_{max}\rvert/w_{adm}$
0	-0.0459	0.2192	0.209397
1	-0.0412		0.187956
2	0.0403		0.183832
3	0.0538		0.245413
4	0.0669		0.30517
5	0.0797		0.363558
6	0.0921		0.420122
7	0.1039		0.473949
8	0.1145		0.522302
8.123	0.1156		0.527319

The maximum deflection (Table 6.4.6) is smaller than the addmisible value (0.527 < 1).

Based on the numerical data from Appendix Tables A.6.1.1, A.6.1.2, A.6.1.3, A.6.1.4 and A.6.1.5, for the reference wave height h_{wBV}=8.123 m it results the following synthesis data:

Table.6.4.7. Maximum Hogging stresses based on 3D-FEM full extended model, h_w=8.123 m

Panel stress	**Stress 3D [MPa]**	**ReH [MPa]**	**Cs=ReH/Stress_3D**	**Stress 1D [MPa]**	**3D/1D**
Maximum σ_x deck	241.20	390	1.617	98.25	2.45
Maximum σ_{vonM} deck	217.80	390	1.791	98.25	2.21
Maximum σ_x bottom	94.89	235	2.477	71.27	1.33
Maximum σ_{vonM} bottom	85.62	235	2.745	71.27	1.20
Panel stress	**τ_{3D} [MPa]**	**τ_{adm} [MPa]**	**3D / adm**	**τ_{1D} [MPa]**	**3D/1D**
Maximum τ_{xz} side	34.70	110	0.315	40.09	0.86

where Cs represents the strength safety coefficient for deck (D) and bottom (B) panels, (on upper and lower ship girder panels the normal stresses are dominant, equation 2.2.1) taking as reference the steel yield stress ReH limit, for the resulting maximum 3D-FEM stresses.

Based on the numerical data from chapter 5.2., and tables (Table.6.4.6, Table.6.4.7.and Table.6.3.2 with the equilibrium parameters) it results the following conclusions at Hogging conditions:

- The vertical position of the equivalent quasi-static wave medium plane is changing from 4.412 m (h_w=0 m) to 3.595 m (h_w=8.123 m), representing a typical condition for the hogging case, coupled with the increase of the trim from 0.003188 rad (h_w=0 m) to 0.007873 (h_w=8.123 m). Those values are in good agreement with the equilibrium parameters based on 1D Equivalent Beam model (chapter 5, Table.5.2.1.).
- The maximum vonMises stresses are smaller than the normal σ_x stresses in the ship extreme fibre panels (deck and bottom), according to equation 2.2.1. chapter 2.2.6.
- The maximum stresses result at the deck panel, with significant hot spots around the liquid cargo tank hatch. More accurate hotspots stress factors will be computed based on a finer mesh model (chapter 8).
- All the stress safety coefficients having the yield stress limit reference are higher than 1, the smallest value being recorded for the deck around the hatch hotspot area 1.617>1.
- Comparing the maximum stresses between the 3D FEM full extended model and the 1D Equivalent BEAM model, it results that the 3D - FEM Model stresses are 2.21 - 2.45 times larger than the 1D model, for the deck, 1.20- 1.33 times larger for the bottom and smaller on the tangential side stresses (without significant hotspots).
- The ratio between 3D/1D stress values are pointing clear that the deck panel has significant hotspots areas, even if the 3D-FEM model has a coarse mesh size.

6.5. Numerical Analysis in Sagging Conditions. Equivalent Quasi-static Wave Pressure, Deformation and Stress Distributions (Wave height 0-8.123 m)

In the following figures are presented the numerical results obtained at the global-local strength analysis based on the full extended 3D-FEM Model, under Sagging condition, using the theoretical method with iterative procedure for ship-wave vertical equilibrium, from subchapter 2.2, and the macro commands files from Appendix A.1.1 and A.1.2. implemented in the SolidWorks Cosmos/M 2007 FEM software.

Table.6.5.1.Figures List with numerical results at the global local strength analysis in Sagging conditions, based on 3D-FEM full extended model

Wave height case [m]	Wave pressure distribution	Total vertical deflection	vonMises stress distributions
1	Fig.6.5.1	Fig.6.5.2	Fig.6.5.3
2	Fig.6.5.4	Fig.6.5.5	Fig.6.5.6
3	Fig.6.5.7	Fig.6.5.8	Fig.6.5.9
4	Fig.6.5.10	Fig.6.5.11	Fig.6.5.12
5	Fig.6.5.13	Fig.6.5.14	Fig.6.5.15
6	Fig.6.5.16	Fig.6.5.17	Fig.6.5.18
7	Fig.6.5.19	Fig.6.5.20	Fig.6.5.21
8	Fig.6.5.22	Fig.6.5.23	Fig.6.5.24
8.123	Fig.6.5.25	Fig.6.5.26	Fig.6.5.27

The iterative procedure at the global-local ship strength, based on 3D-FEM full extended model, has converged to the following wave medium plane vertical position parameters.

Table.6.5.2. Vertical position parameters of the wave medium plane, in sagging conditions, based on 3D-FEM full extended model

Wave height case [m]	Vertical position amidships [m]	Trim in the longitudinal plane[rad]
0	4.412	0.003
1	4.469	0.007
2	4.518	0.010
3	4.562	0.013
4	4.602	0.015
5	4.638	0.016
6	4.671	0.017
7	4.700	0.018
8	4.726	0.019
8.123	4.729	0.019

with graphical presentation in Fig.6.3.1 for Vertical position amidships and Fig.6.3.2 for Trim in the longitudinal plane.

- **Sagging conditions h_w=1 m equivalent quasi-static head wave height**

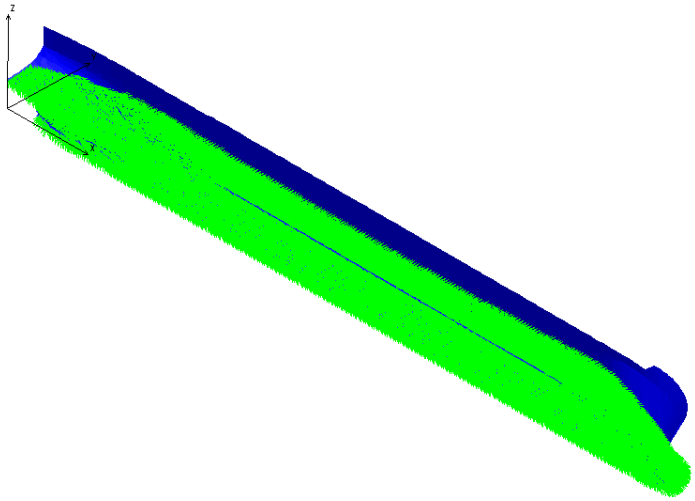

Fig.6.5.1. Hydrostatic Pressure from the external equivalent quasi-static wave applied on the ship hull, Wave height 1 m, Sagging condition

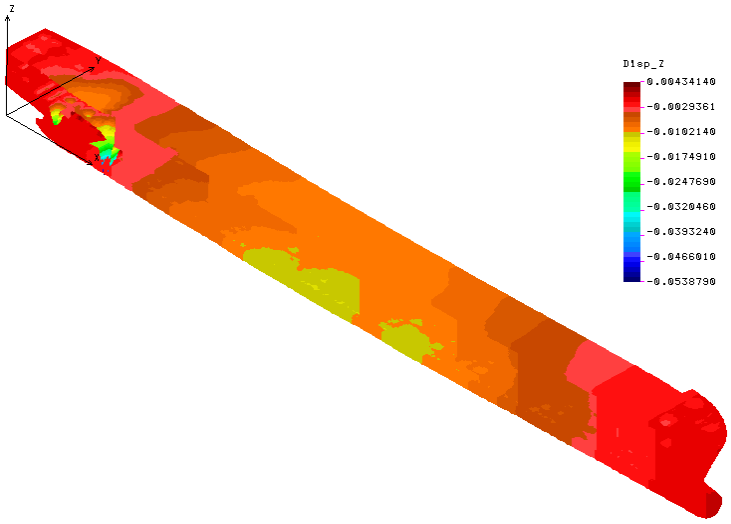

Fig.6.5.2. Vertical deflection on Z direction (m), Wave height 1 m, Sagging condition

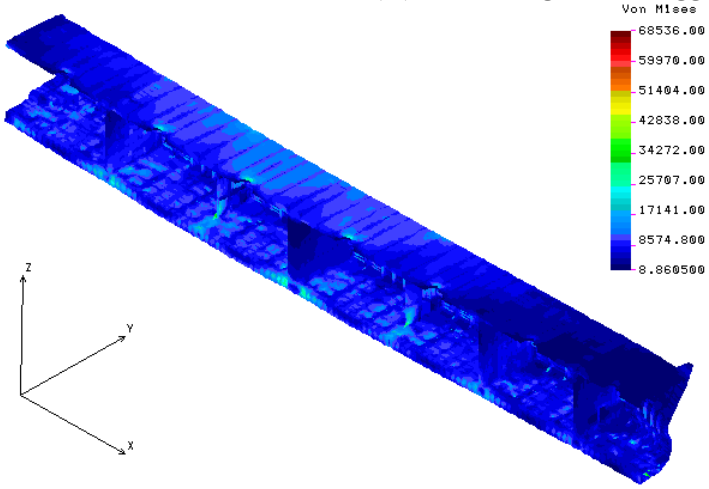

Fig.6.5.3. Equivalent vonMises stress distribution [kN/m^2] ,at the cargo compartments part (x=18.57 m 99.42 m), Wave height 1 m, Sagging condition

- **Sagging conditions h_w=2 m equivalent quasi-static head wave height**

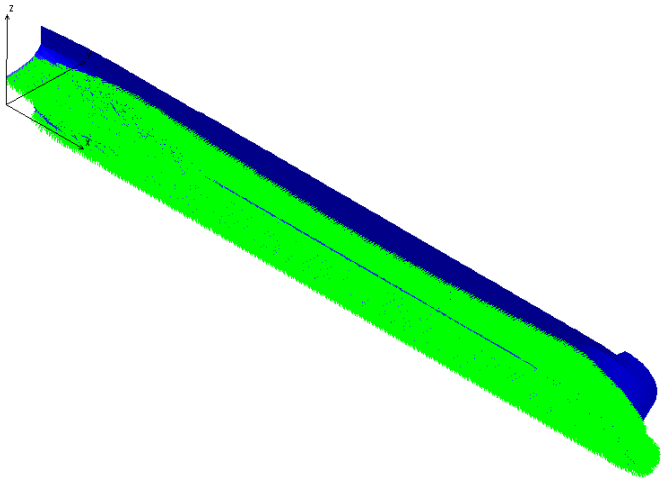

Fig.6.5.4. Hydrostatic Pressure from the external equivalent quasi-static wave applied on the ship hull, Wave height 2 m, Sagging condition

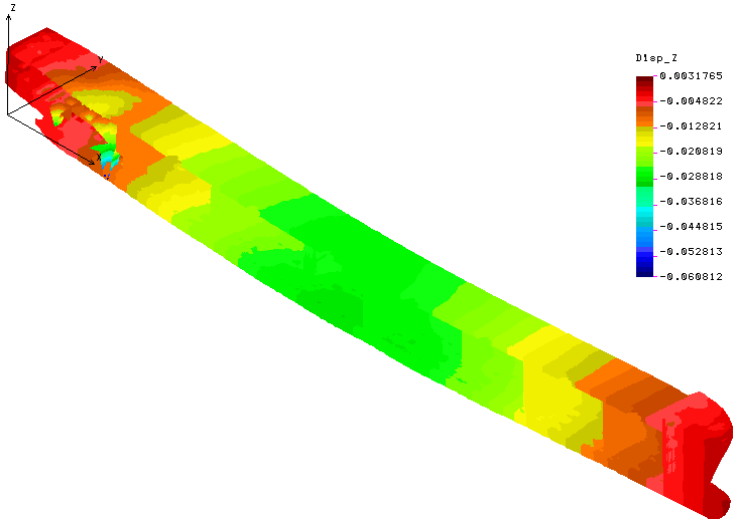

Fig.6.5.5. Vertical deflection on Z direction (m), Wave height 2 m, Sagging condition

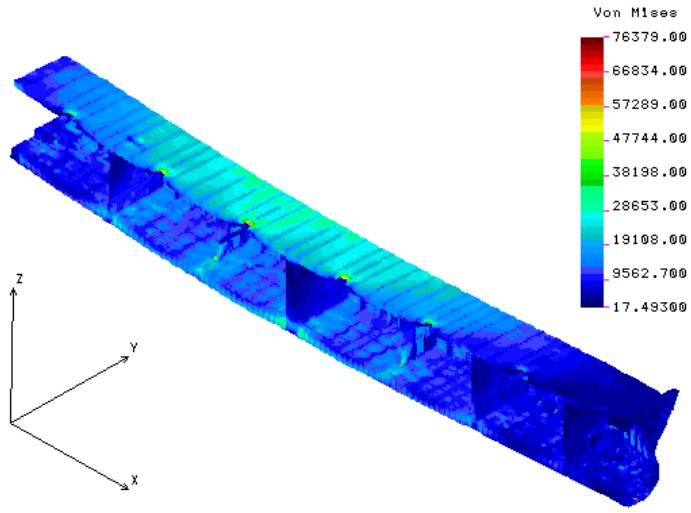

Fig.6.5.6. Equivalent vonMises stress distribution [kN/m^2] ,at the cargo compartments part (x=18.57 m to 99.42 m), Wave height 2 m, Sagging condition

- **Sagging conditions h_w=3 m equivalent quasi-static head wave height**

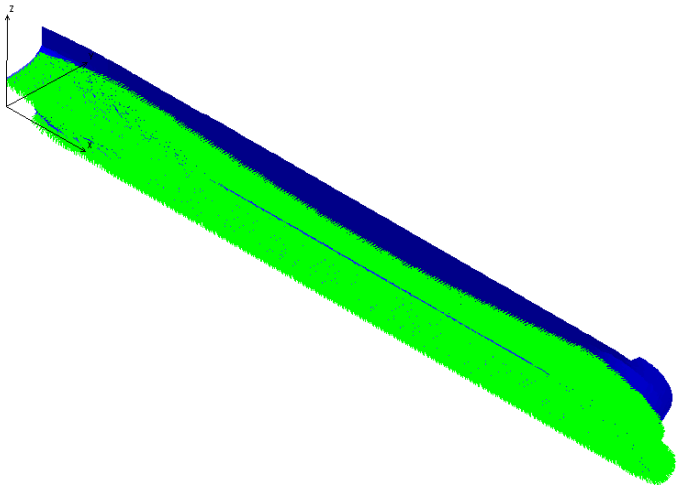

Fig.6.5.7. Hydrostatic Pressure from the external equivalent quasi-static wave applied on the ship hull, Wave height 3 m, Sagging condition

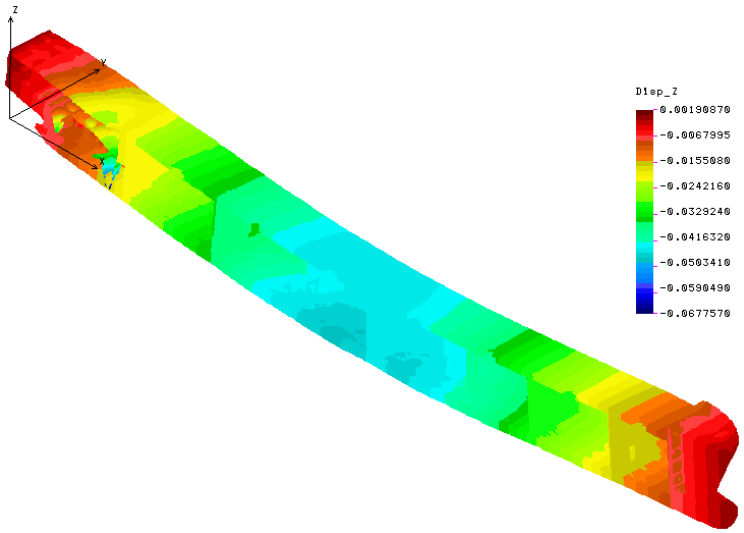

Fig.6.5.8. Vertical deflection on Z direction (m), Wave height 3 m, Sagging condition

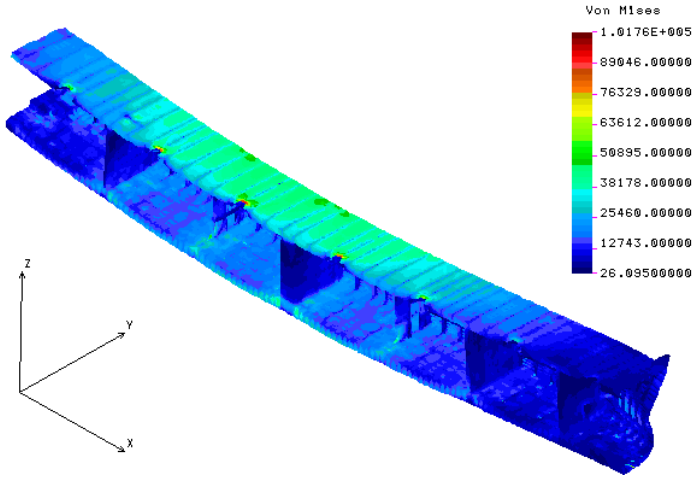

Fig.6.5.9. Equivalent vonMises stress distribution [kN/m^2] ,at the cargo compartments part (x=18.57 m to 99.42 m), Wave height 3 m, Sagging condition

- **Sagging conditions h_w=4 m equivalent quasi-static head wave height**

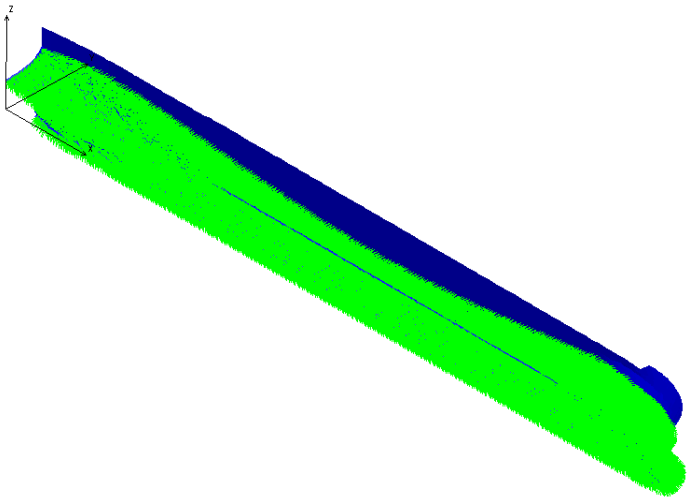

Fig.6.5.10. Hydrostatic Pressure from the external equivalent quasi-static wave applied on the ship hull, Wave height 4 m, Sagging condition

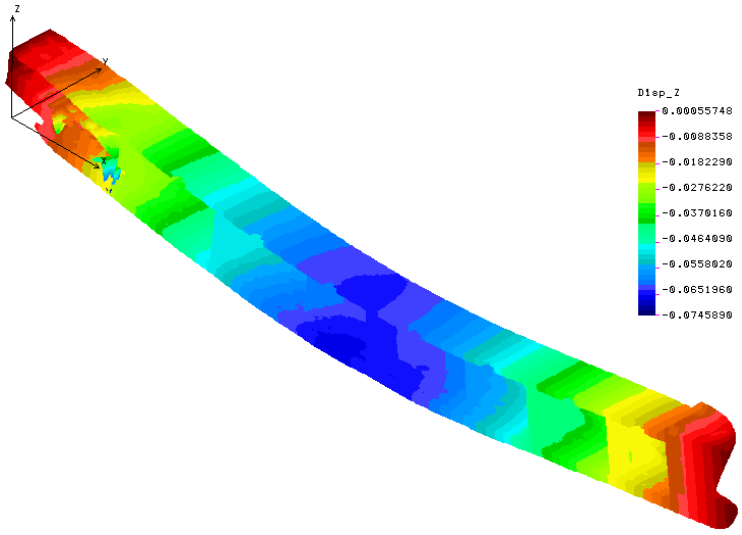

Fig.6.5.11. Vertical deflection on Z direction (m), Wave height 4 m, Sagging condition

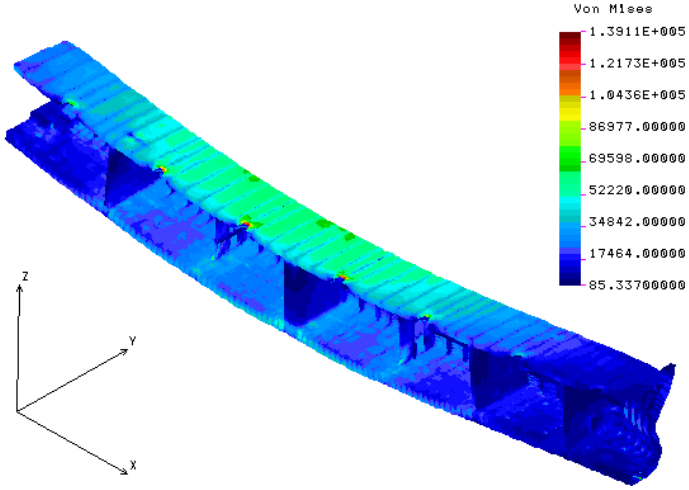

Fig.6.5.12. Equivalent vonMises stress distribution [kN/m^2] ,at the cargo compartments part (x=18.57 m to 99.42 m), Wave height 4 m, Sagging condition

- **Sagging conditions h_w=5 m equivalent quasi-static head wave height**

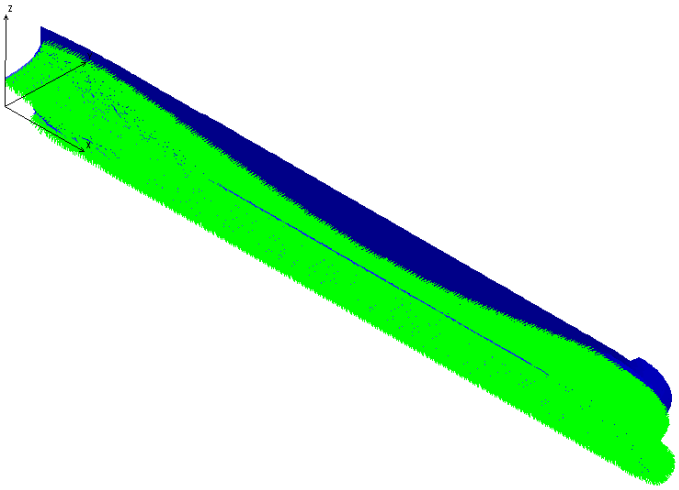

Fig.6.5.13. Hydrostatic Pressure from the external equivalent quasi-static wave applied on the ship hull, Wave height 5 m, Sagging condition

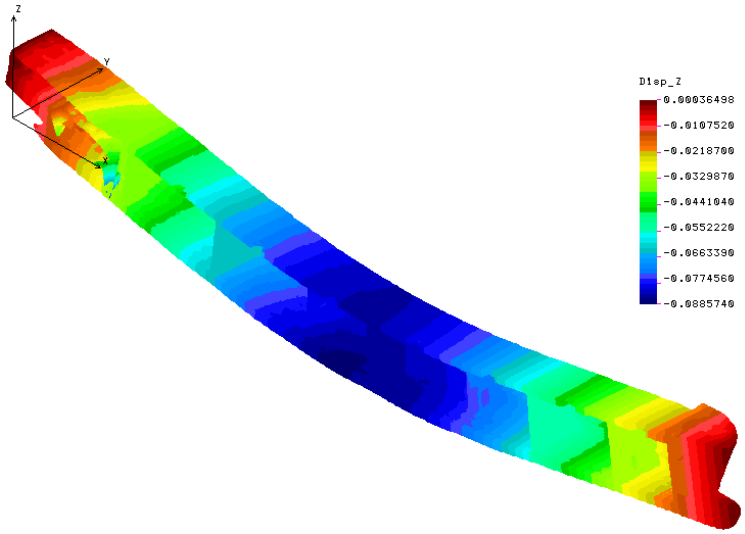

Fig.6.5.14. Vertical deflection on Z direction (m), Wave height 5 m, Sagging condition

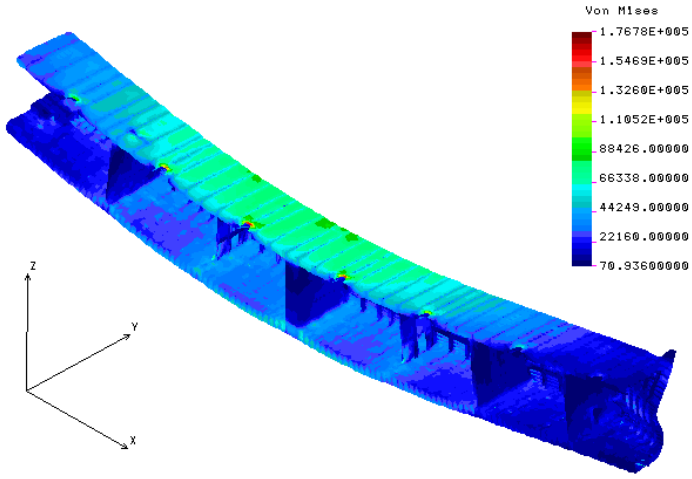

Fig.6.5.15. Equivalent vonMises stress distribution [kN/m^2] ,at the cargo compartments part (x=18.57 m to 99.42 m), Wave height 5 m, Sagging condition

- **Sagging conditions h_w=6 m equivalent quasi-static head wave height**

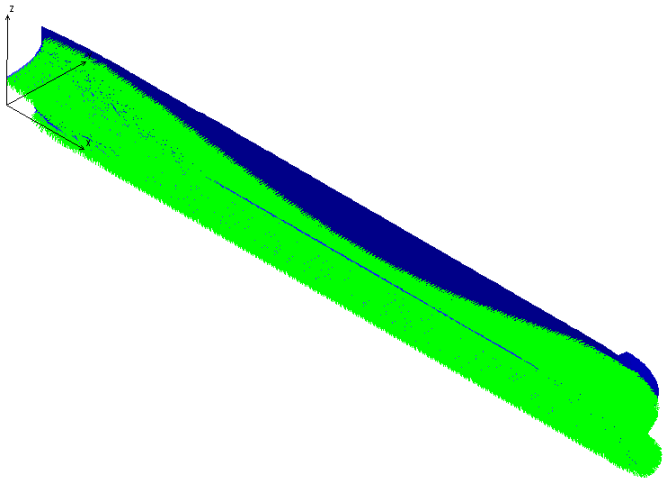

Fig.6.5.16. Hydrostatic Pressure from the external equivalent quasi-static wave applied on the ship hull, Wave height 6 m, Sagging condition

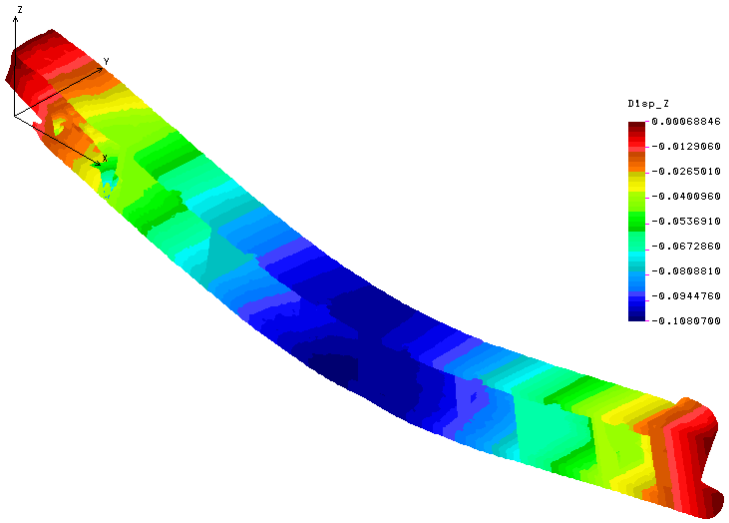

Fig.6.5.17. Vertical deflection on Z direction (m), Wave height 6 m, Sagging condition

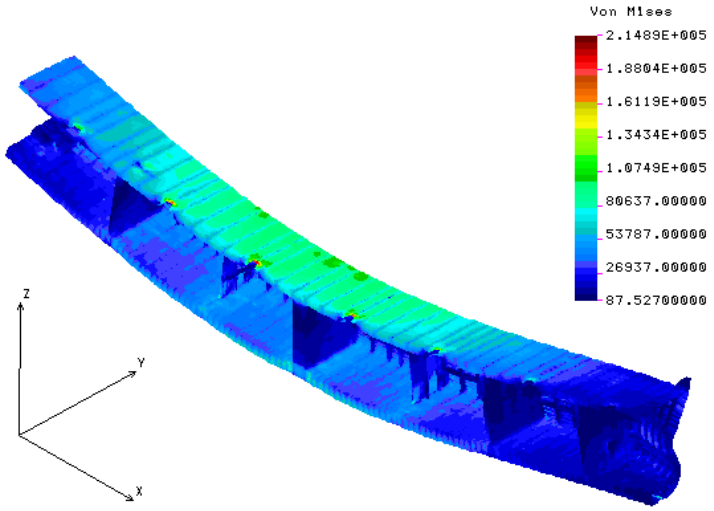

Fig.6.5.18. Equivalent vonMises stress distribution [kN/m^2] ,at the cargo compartments part (x=18.57 m to 99.42 m), Wave height 6 m, Sagging condition

- **Sagging conditions h_w=7 m equivalent quasi-static head wave height**

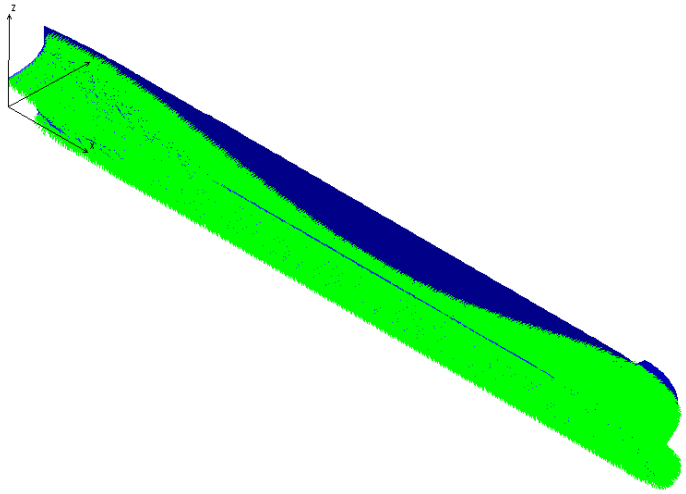

Fig.6.5.19. Hydrostatic Pressure from the external equivalent quasi-static wave applied on the ship hull, Wave height 7 m, Sagging condition

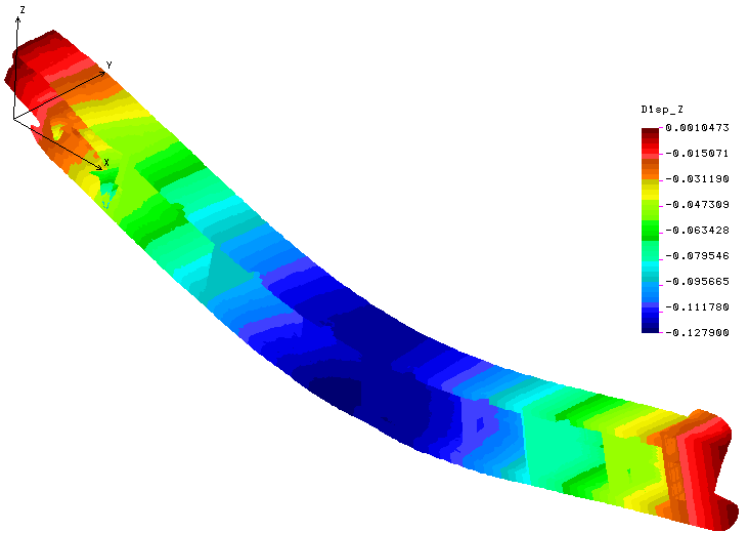

Fig.6.5.20. Vertical deflection on Z direction (m), Wave height 7 m, Sagging condition

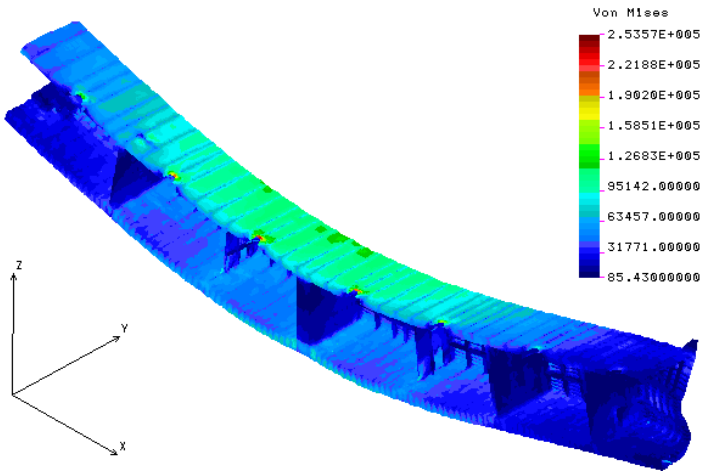

Fig.6.5.21. Equivalent vonMises stress distribution [kN/m^2] ,at the cargo compartments part (x=18.57 m to 99.42 m), Wave height 7 m, Sagging condition

- **Sagging conditions h_w=8 m equivalent quasi-static head wave height**

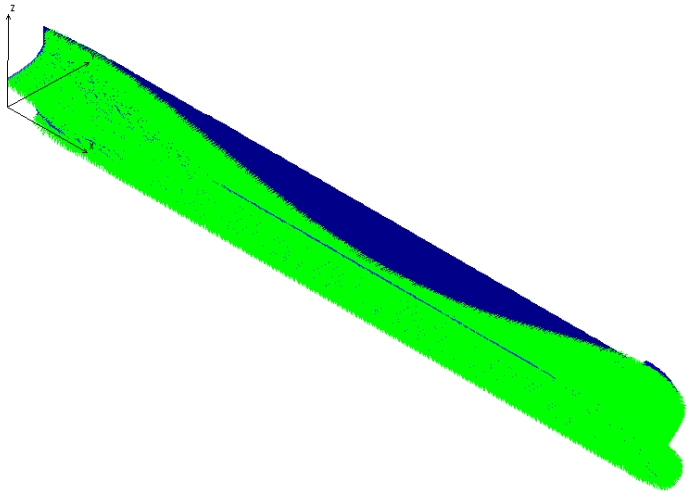

Fig.6.5.22. Hydrostatic Pressure from the external equivalent quasi-static wave applied on the ship hull, Wave height 8 m, Sagging condition

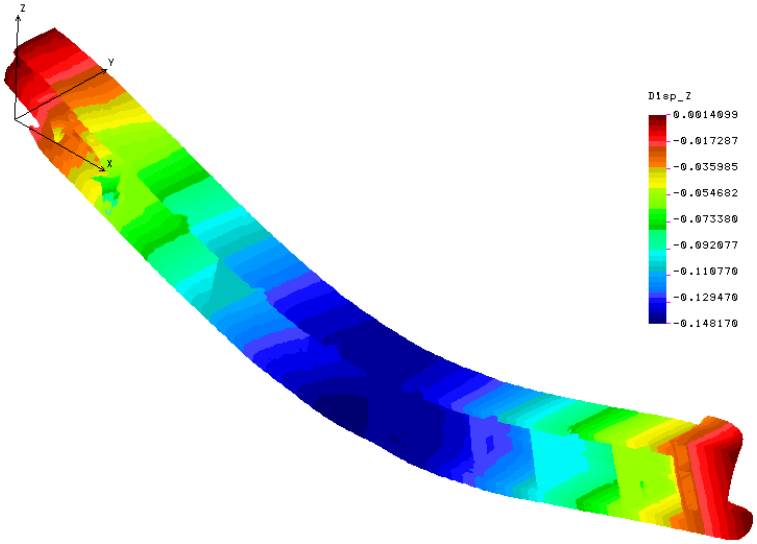

Fig.6.5.23. Vertical deflection on Z direction (m), Wave height 8 m, Sagging condition

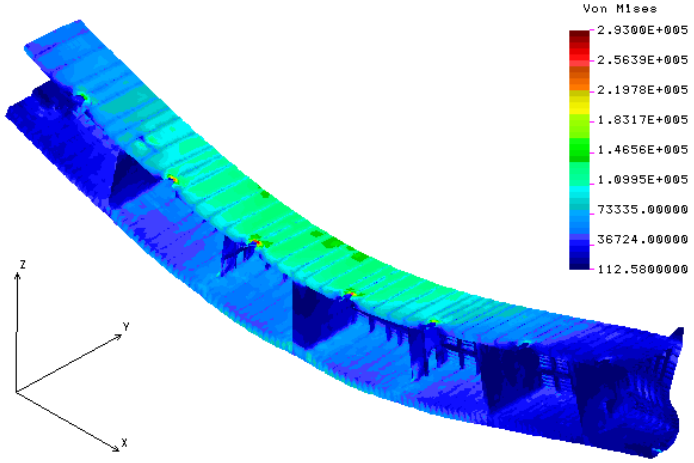

Fig.6.5.24. Equivalent vonMises stress distribution [kN/m^2] ,at the cargo compartments part (x=18.57 m to 99.42 m), Wave height 8 m, Sagging condition

- **Sagging conditions h_w=8.123 m equivalent quasi-static head wave height**

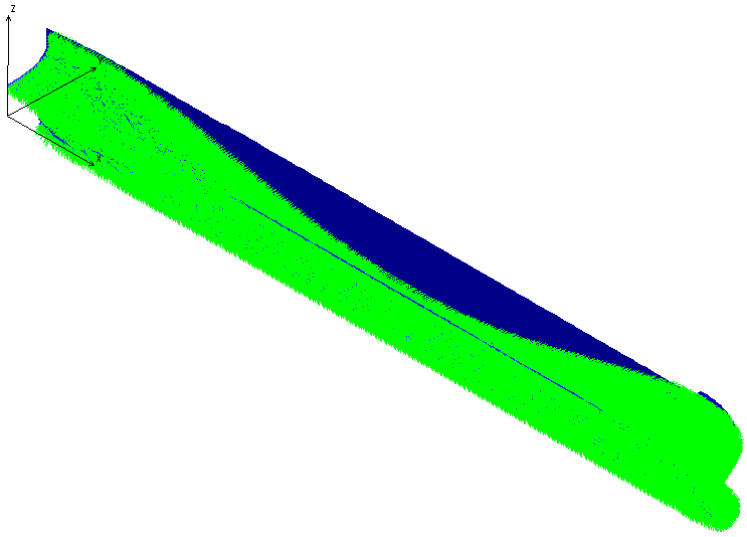

Fig.6.5.25. Hydrostatic Pressure from the external equivalent quasi-static wave applied on the ship hull, Wave height 8.123 m, Sagging condition

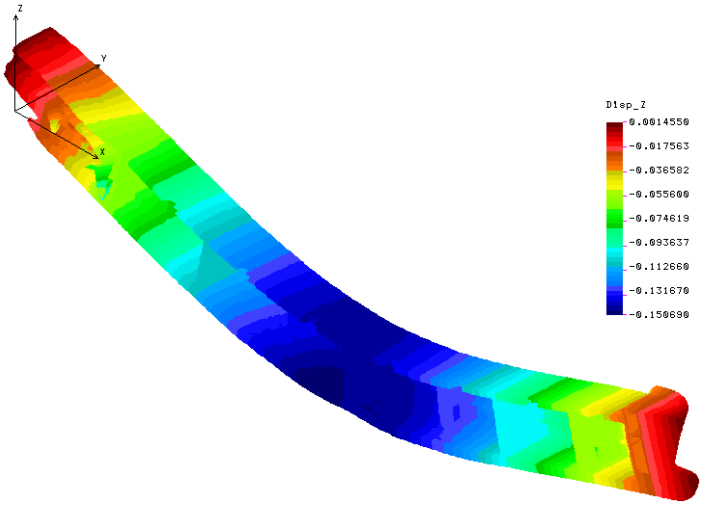

Fig.6.5.26. Vertical deflection on Z direction (m), Wave height 8.123 m, Sagging condition

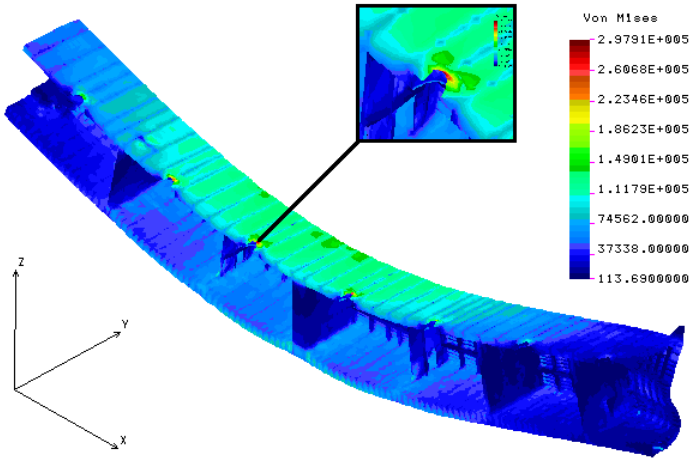

Fig.6.5.27. Equivalent vonMises stress distribution [kN/m^2] ,at the cargo compartments part (x=18.57 m to 99.42 m), Wave height 8.123 m, Sagging condition

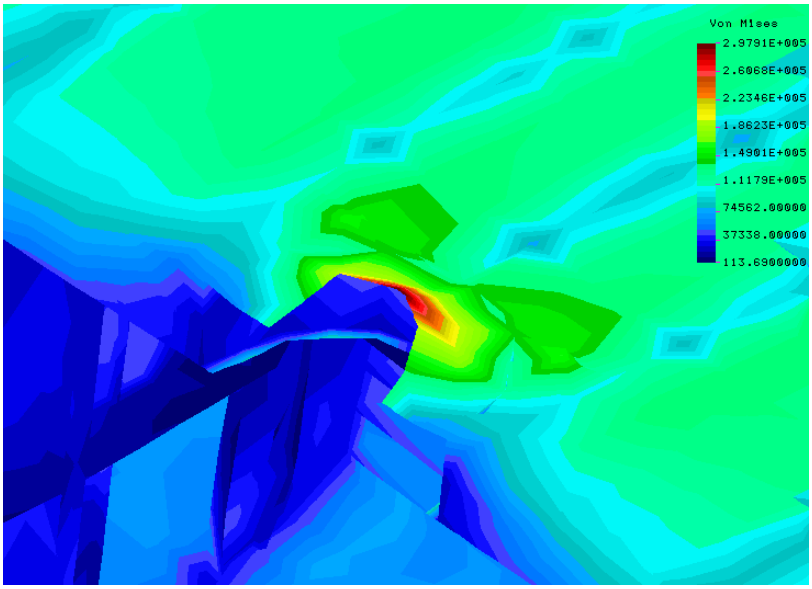

Fig.6.5.28. Equivalent vonMises stress distribution detail [kN/m^2] ,at the cargo compartments part, Wave height 8.123 m, Sagging condition

6.6. Discussions and Conclusions for the Numerical Computation in Sagging Conditions, Based on Full Extended 3D-FEM Model

In the following figures are presented the maximum values for stress distributions obtained at the global- local strength analysis based on the full extended 3D-FEM Model, under Sagging conditions. For selected panels (Deck, Bottom, Side) and a given transversal section the maximum stress value, according to equation 2.2.2.:

- Fig. 6.6.1 and Appendix A.6.2, Table A.6.2.1. are presenting the Maximum Normal Deck Stress, σ_X [MPa] in Sagging wave conditions, 3D-FEM full extended model, and the safety coefficients Cs according to the yield stress limit ReH.
- Fig.6.6.2. and Appendix A.6.2, Table.A.6.2.2. are presenting the Maximum Equivalent vonMises Deck Stress, σ_{von} [MPa] in Sagging wave conditions, 3D-FEM full extended model, and the safety coefficients Cs according to the yield stress limit ReH.
- Fig.6.6.3. and Appendix A.6.2, Table.A.6.2.3. are presenting the Maximum Normal Bottom Stress, σ_X [MPa] in Sagging wave conditions, 3D-FEM full extended model, and the safety coefficients Cs according to the yield stress limit ReH.
- Fig.6.6.4. and Appendix A.6.2, Table.A.6.2.4. are presenting the Maximum Equivalent vonMises Bottom Stress, σ_{von} [MPa] in Sagging wave conditions, 3D-FEM full extended model, and the safety coefficients Cs according to the yield stress limit ReH.
- Fig.6.6.5. and Appendix A.6.2, Table.A.6.2.5. are presenting the Maximum Tangential side stress τ_{xz} [MPa] in Sagging wave conditions, 3D-FEM full extended model.

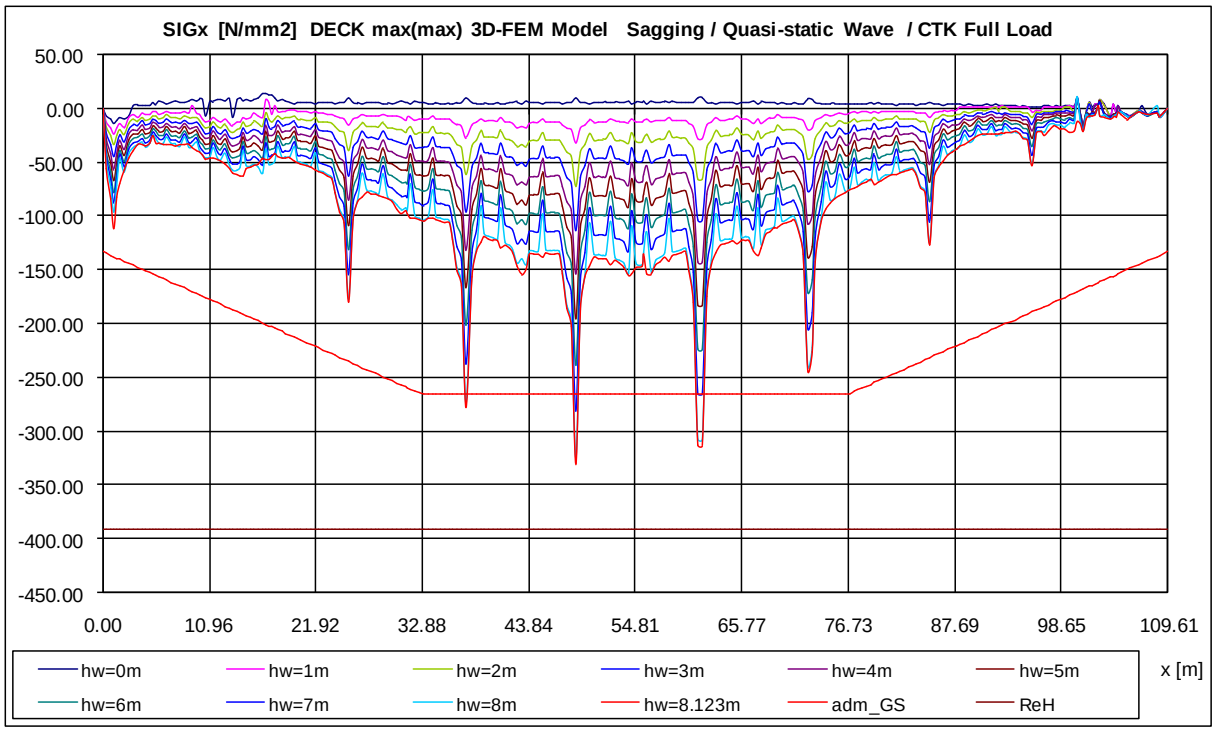

Fig.6.6.1. Maximum Normal Deck Stress, σ_X [MPa] in Sagging wave conditions, 3D-FEM full extended model

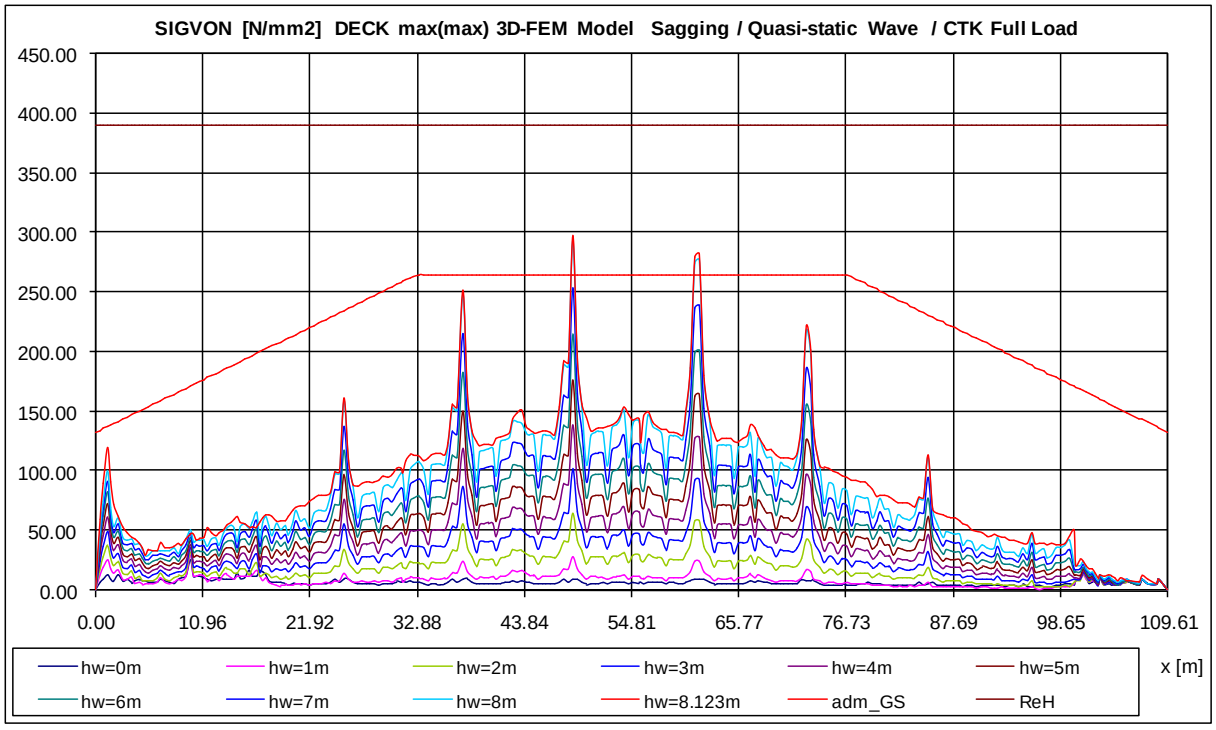

Fig.6.6.2. Maximum Equivalent vonMises Deck Stress, σ_{von} [MPa] in Sagging wave conditions, 3D-FEM full extended model

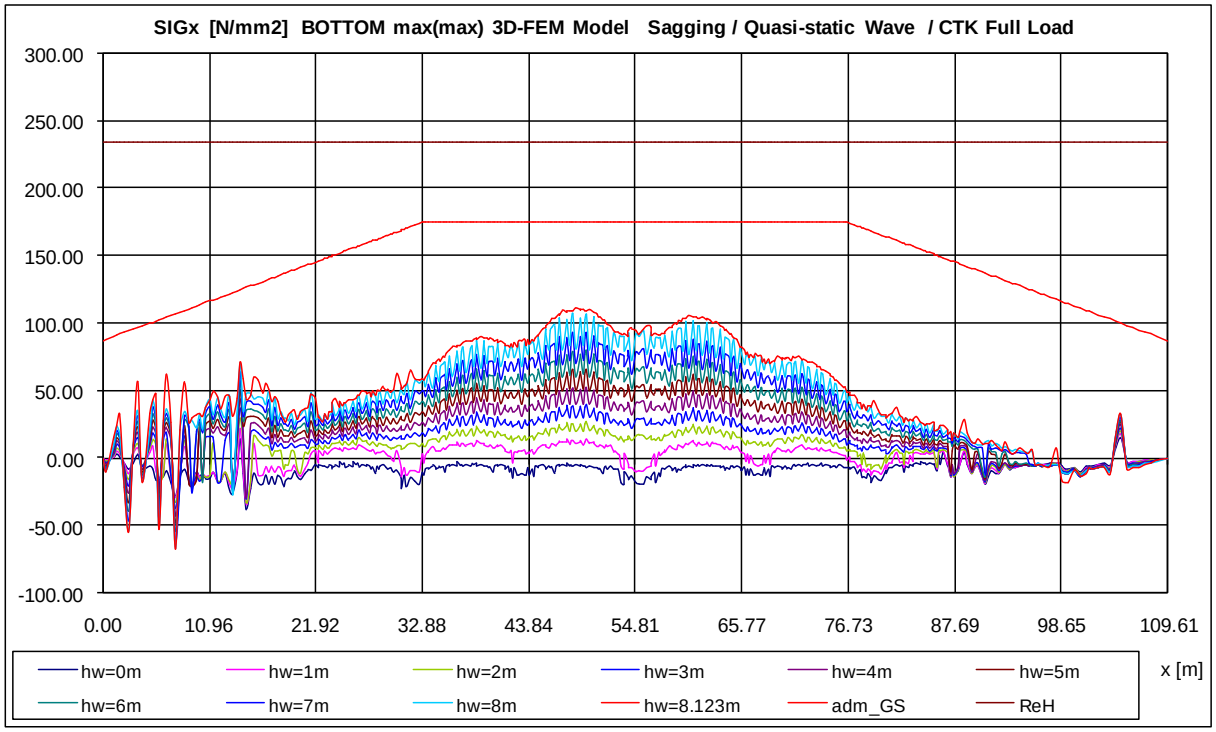

Fig.6.6.3. Maximum Normal Bottom Stress, σ_X [MPa] in Sagging wave conditions, 3D-FEM full extended model

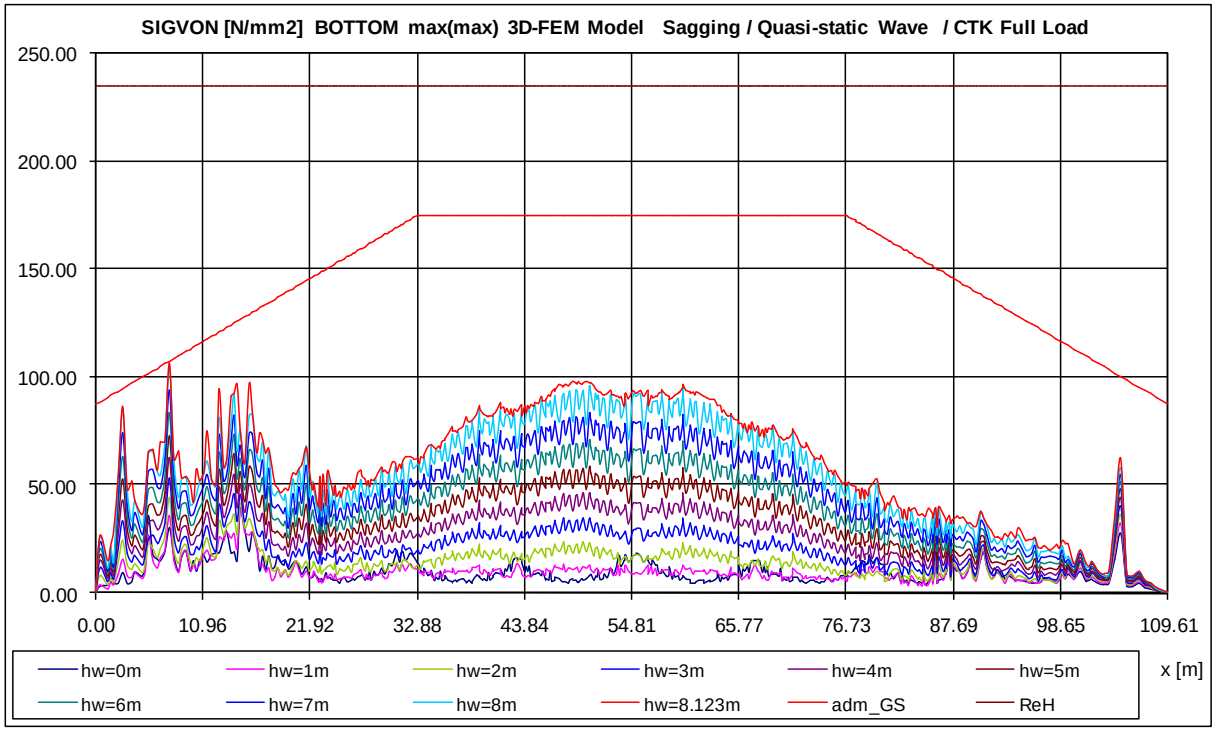

Fig.6.6.4. Maximum Equivalent vonMises Bottom Stress, σ_{von} [MPa] in Sagging wave conditions, 3D-FEM full extended model

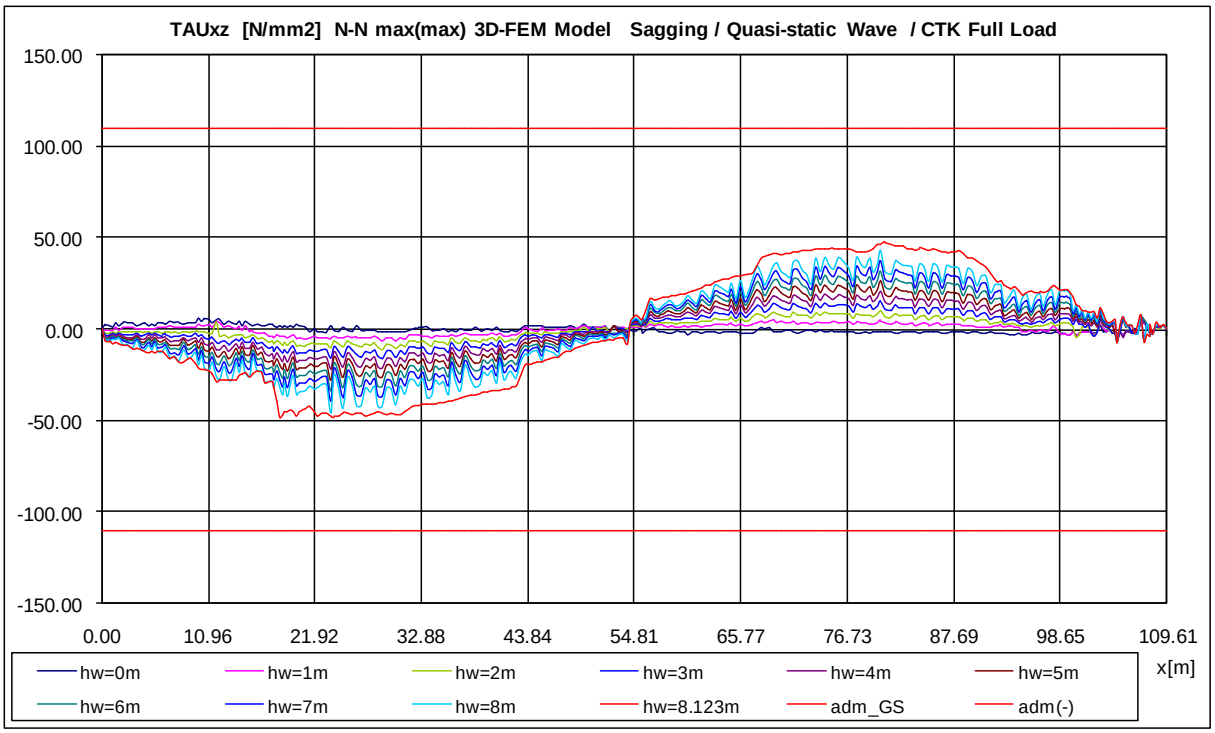

Fig.6.6.5. Maximum Tangential side stress τ_{xz} [MPa] in Sagging wave conditions, 3D-FEM full extended model

Based on figures (Fig.6.5.2; Fig.6.5.5; Fig.6.5.8; Fig.6.5.11; Fig.6.5.14; Fig.6.5.17; Fig.6.5.20; Fig.6.5.23; Fig.6.5.26) in Table 6.6.6, the global vertical deflections are presented for the ship hull structure in Sagging conditions.

Table.6.6.6. Maximum vertical deflections based on 3D-FEM full extended model in Sagging conditions

h_w [m]	w_{max} [m]	w_{adm}=L/500 [m]	$\lvert w_{max}\rvert/w_{adm}$
0	-0.045906	0.2192	0.20939
1	-0.053879		0.24579
2	-0.060812		0.27743
3	-0.067775		0.30919
4	-0.074589		0.34028
5	-0.088574		0.40408
6	-0.108070		0.49302
7	-0.127900		0.58349
8	-0.148170		0.67596
8.123	-0.150690		0.68745

Based on the numerical data from the tables(Appendix Table A.6.2.1, A.6.2.2, A.6.2.3, A.6.2.4 and A.6.2.5) for the reference wave height h_{wBV}=8.123 m it results the following synthesis data:

Table.6.6.7. Maximum Sagging stresses based on 3D-FEM full extended model, h_w=8.123 m

Panel stress	**Stress 3D [MPa]**	**ReH [MPa]**	**Cs=ReH/Stress_3D**	**Stress 1D [MPa]**	**3D/1D**
Maximum σ_x deck	329.90	390	1.18	121.17	2.72
Maximum σ_{vonM} deck	297.90	390	1.30	121.17	2.46
Maximum σ_x bottom	111.30	235	2.11	87.90	1.27
Maximum σ_{vonM} bottom	106.50	235	2.207	87.90	1.21
Panel stress	**τ_{3D} [MPa]**	**τ_{adm} [MPa]**	**3D / adm**	**τ_{1D} [MPa]**	**3D/1D**
Maximum τ_{xz} side	47.85	110	0.435	48.27	0.99

Based on the numerical data from chapter 5.3, and tables (Table.6.6.6, Table.6.6.7. and Table.6.5.2 with the equilibrium parameters) it results the following conclusions at Sagging conditions:

- The maximum deflection (Table 6.6.6) is smaller than the admissible value (0.687 < 1).
- The vertical position of the equivalent quasi-static wave medium plane is changing from 4.412 m (h_w=0 m) to 4.729 m (h_w=8.123 m), representing a typical condition for the sagging case, coupled with the increase of the trim from 0.003188 rad (h_w=0 m) to 0.019032 (hw=8.123 m). Those values are in good agreement with the equilibrium parameters based on 1D Equivalent Beam model (chapter 5, Table.5.3.1.).
- The maximum vonMises stresses are smaller than the normal σ_x stresses in the ship extreme fibre panels (deck and bottom) according to equation 2.2.1. chapter 2.2.6.
- The maximum stresses results in the deck panel, with significant hot spots around the liquid cargo tank hatch. More accurate hotspots stress factors will be computed based on finer mesh model (chapter 8).
- All the Cs stress safety coefficients, having the yield stress limit reference, are higher than 1, the smallest value being recorded for the deck around the hotspot area 1.18 - 1.30 > 1.
- Comparing the maximum stresses between the 3D-FEM full extended model and the 1D Equivalent Beam model, it results that the 3D-FEM Model stresses are 2.46 - 2.72 times larger than the 1D model, for the deck, 1.21- 1.27 times larger for the bottom and similar on the tangential side stresses, with a value of 0.99 ≅ 1.
- The ratio between 3D/1D stress values are pointing clear that the deck panel has significant hatch hotspots areas, even if the 3D-FEM model has a coarse mesh size.

7. THE GLOBAL - LOCAL SHIP HULL STRENGTH ANALYSIS BASED ON 3D-FEM MODEL EXTENDED ON TWO CARGO HOLDS COMPARTMENTS (CENTRAL SHIP PART, COARSE MESH SIZE).

The model was developed by using two cargo holds compartments, each containing two main cargo cylinders as in the figure below:

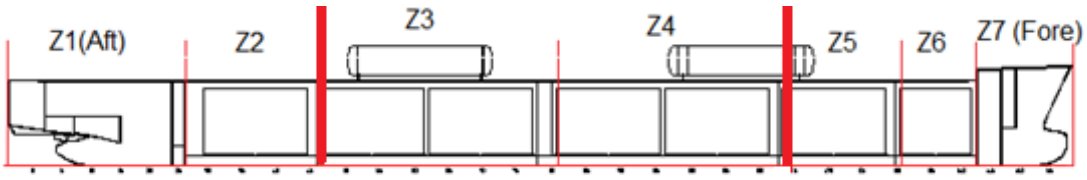

Fig. 7.1. The two cargo holds compartments of the Ship (Ship Design Group 2007)

The longitudinal coordinates along X axis of the two cargo holds model are from 31.772 m to 80.224 m, including the bulkhead at the end of the second cargo hold. The model was extracted from the full extended 3D - FEM, presented in the chapter 6, in order to compare the new results by using the corresponding boundary conditions that are going to be implemented on this two cargo holds compartments 3D-FEM model.

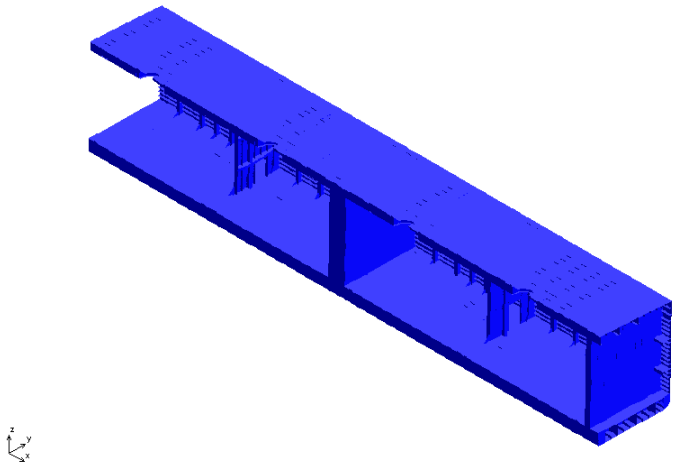

Fig.7.2. The 3D- FEM of the two cargo holds model

The boundary conditions (natural) for the symmetry will remain the same as in the full extended 3D- FEM model, which is referring to all the nodes in the centre line plane. The boundary conditions for the Aft part of the model are driven by a single nod, ND_AFT, situated at the following coordinates: x=31.712 m, y=0 m and z=3.73167 m, where the z value represents vertical position of the neutral axis location at amidships. The user subroutine, presented in the Appendix A.3.1, creates points for all the nodes available in the x coordinate of the Aft part of the model. Afterwards the user subroutine in the Appendix A.3.2**,** creates lines from all the nodes, to the node previously created ND_AFT.

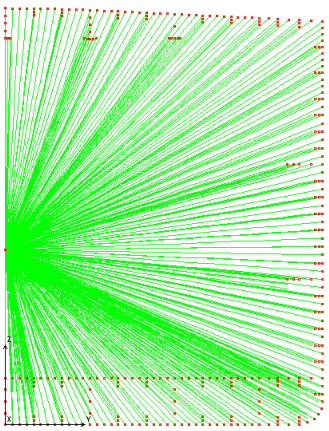

Fig.7.3. Nodes and lines for the Boundary Conditions of the two cargo holds 3D-FEM model

Similar steps were applied for the Fore node, ND_FORE, with the longitudinal coordinate x=80.224 m. Afterwards there was defined a new element group RigidBar for those lines, in order to generate the link elements.

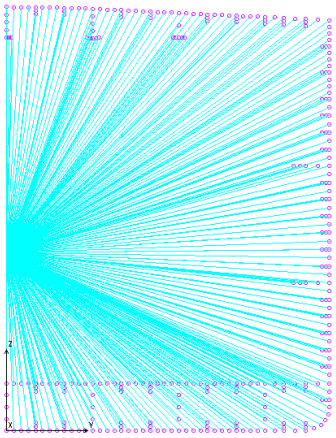

Fig.7.4. Elements RigidBar for the Boundary Conditions of the two cargo holds 3D-FEM model

The constraints to each node are displayed in the table 7.1., with the type of the boundary condition displayed next to the node.

Table.7.1. Boundary conditions definition for two cargo holds 3D-FEM model

Boundary Conditions			
Nodes	Node nr.	Constraints	Type
ND_AFT	95436	UX	Neutral
		UY; RX	Symmetry, Natural
		RZ	Neutral
ND_FORE	95437	RZ	Neutral
		UY; RX	Symmetry, Natural
CENTRE LINE PLANE	All nodes	UY; RX	Symmetry, Natural

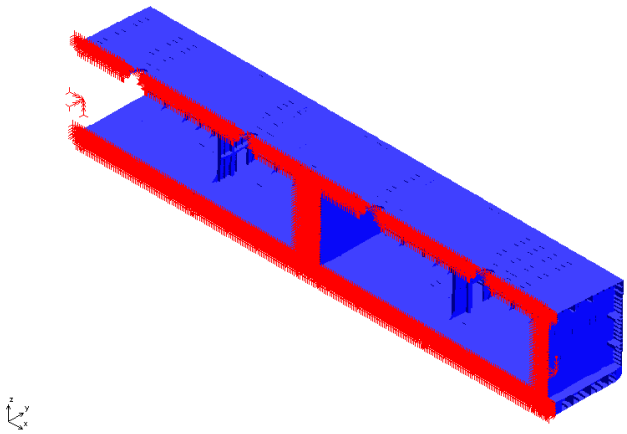

Fig.7.5.Boundary conditions on the two Cargo holds 3D-FEM model

Similar pressures were applied, as in the case of the Full extended 3D FEM model. Along the two cargo holds compartments model only the cargo pressure P =61.1 [kN/m^2] and the onboard equivalent pressure P=6.79 [kN/m^2] were applied (from Table.6.3.).

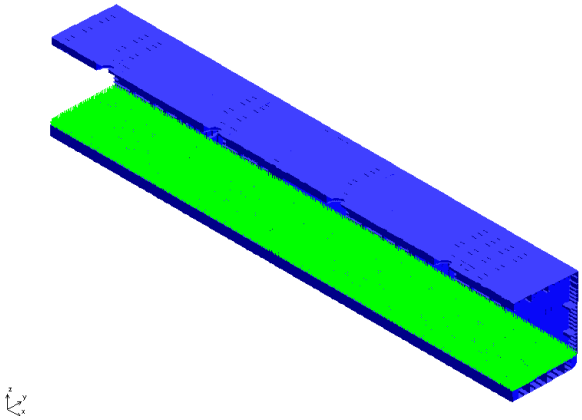

Fig.7.6. Applying the equivalent pressure for onboard masses and cargo,
on the two cargo holds compartments 3D-FEM Model

As in the case of the full extended model, the equivalent quasi-static wave pressure was applied using the updated user subroutine presented in Appendix A.2.2, and the selection of the specific shell plating was performed with the user subroutine presented in Appendix A.2.1.

Also displacements and rotations were imposed on the two cargo holds compartment 3D-FEM model, computed with the 1D-Equivalent Beam Model, chapter 5, from global equilibrium condition, based on the controlling nodes, ND_AFT, ND_FORE (see Table.7.2.), taking into account their longitudinal position over the ship length.

Table.7.2. Displacements and Rotations applied as global constraints, on the two cargo holds compartments 3D-FEM Model, at the aft and fore peak reference nodes

Global conditions	**Still water**		**Hogging wave height 8.123**		**Sagging wave height 8.123**	
Node location	Node AFT	Node FORE	Node AFT	Node FORE	Node AFT	Node FORE
Coordinate [m]	31.712	80.224	31.712	80.224	31.712	80.224
Displacement w [m]	0.006580	0.005363	0.072170	0.067611	-0.095999	-0.084755
Rotation Θ[rad]	0.000089	0.000147	-0.001891	0.002052	0.002367	-0.002599

7.1. Numerical Analysis in Still Water Condition. Hydrostatic Water Pressure, Deformation and Stress Distributions

The still water equilibrium condition is obtained based on the theoretical model presented in subchapter 2.3, using the macro-command files procedures, implemented in Solid Works Comos/ M 2007 software, presented in Appendix A.2.1 and A.2.2. The external hydrostatic water pressure is applied on bottom, bilge and side shells, based on the global equilibrium conditions presented in Table.7.2.

In the following figures are presented the results from the numerical global-local strength analysis in still water condition:

- Fig 7.1.1. External hydrostatic water pressure on the ship hull at still water condition
- Fig.7.1.2. Vertical deflection at the ship girder at still water condition
-Fig 7.1.3. Equivalent vonMises Stress distribution in the cargo compartments (x=31.772 m to 80.224 m)

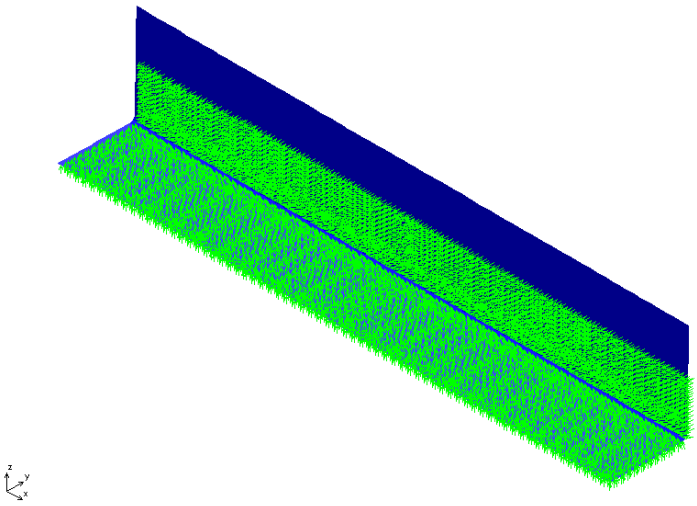

Fig.7.1.1 External water Hydrostatic Pressure [N/mm^2] applied on the shell plating in Still Water condition, 3D-FEM 2C model with coarse mesh size

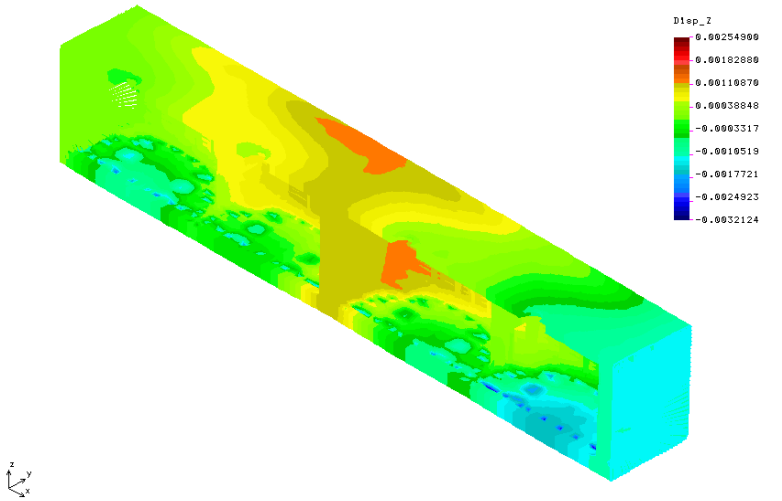

Fig.7.1.2. Vertical deflection on Z direction [m] in Still Water condition, model with coarse mesh size

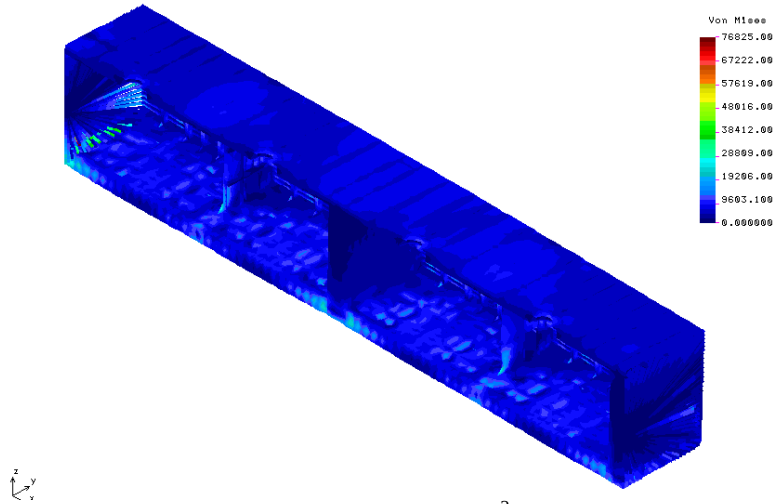

Fig.7.1.3. Equivalent vonMises stress distribution [kN/m^2] in Still Water condition, the cargo compartments part (x=31.772 m to 80.224 m), 3D-FEM 2C model with coarse mesh size

7.2. Numerical Analysis in Hogging and Sagging Conditions. Equivalent Quasi-static Wave Pressure, Deformation and Stress Distributions

In the following figures are presented the numerical results obtained at the global-local strength analysis based on the two cargo holds compartments 3D-FEM Model, with coarse mesh size, under Hogging and Sagging conditions, using the theoretical method for the ship-wave vertical equilibrium, from subchapter 2.3, and the macro commands files from appendix A.2.1. and A.2.2. implemented in the Solid Works Cosmos/M 2007 FEM software.

Table.7.2.1.Figure List with numerical results at the global local strength analysis in hogging conditions, based on two cargo holds compartments 3D-FEM Model coarse mesh size

Wave height case [m]	Wave pressure distribution	Total vertical deflection	vonMises stress distributions
Hogging 8.123	Fig.7.2.1.	Fig.7.2.2.	Fig.7.2.3.
Sagging 8.123	Fig.7.2.4.	Fig.7.2.5.	Fig.7.2.6.

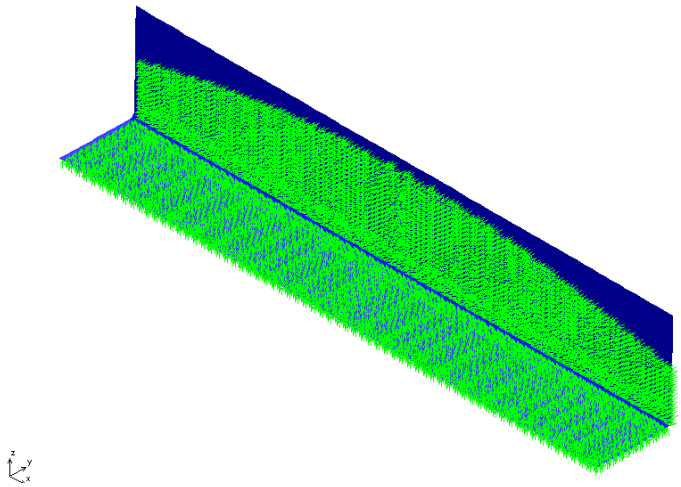

Fig.7.2.1 Hydrostatic Pressure from the external equivalent quasi-static wave applied on the ship hull, Wave height 8.123 m, Hogging condition, 3D-FEM 2C model with coarse mesh size

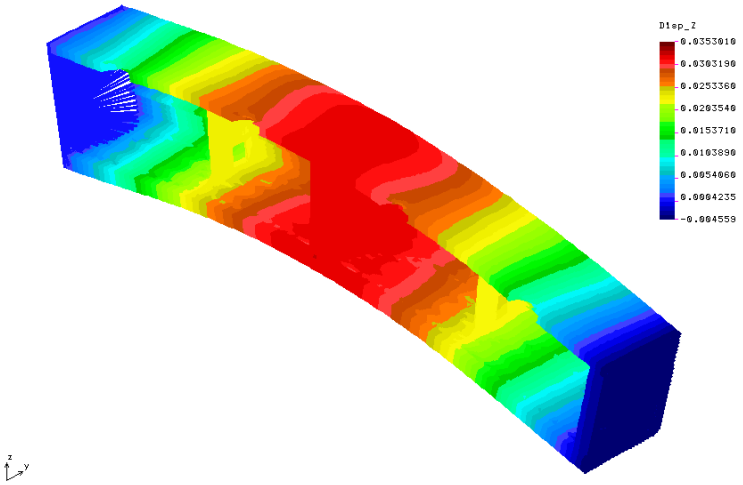

Fig.7.2.2. Vertical deflection on Z direction (m), Wave height 8.123 m, Hogging condition, 3D-FEM 2C model with coarse mesh size

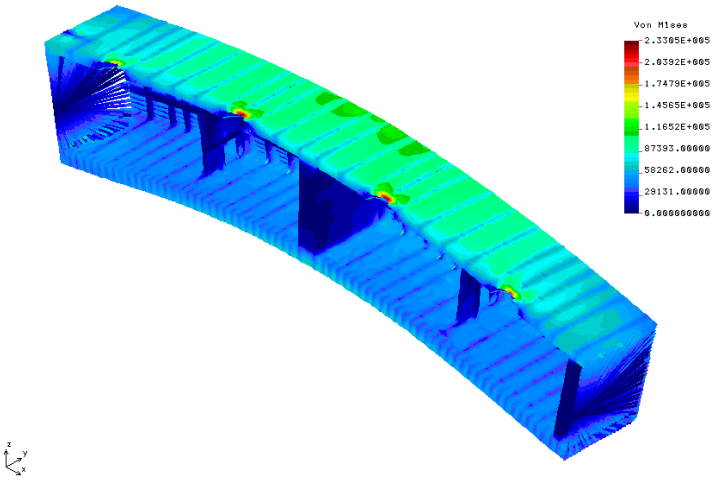

Fig.7.2.3. Equivalent vonMises stress distribution [kN/m^2] ,at the cargo compartments part (x=31.772 m to 80.224 m), Wave height 8.123 m, Hogging condition, 3D-FEM 2C model with coarse mesh size

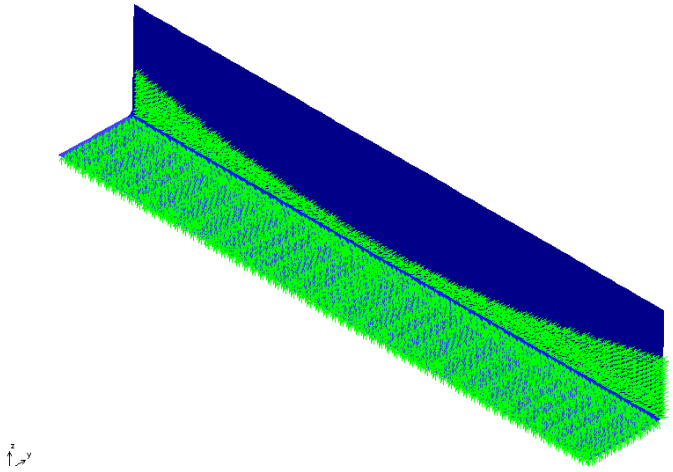

Fig.7.2.4 Hydrostatic Pressure from the external equivalent quasi-static wave applied on the ship hull, Wave height 8.123 m, Sagging condition, 3D-FEM 2C model with coarse mesh size

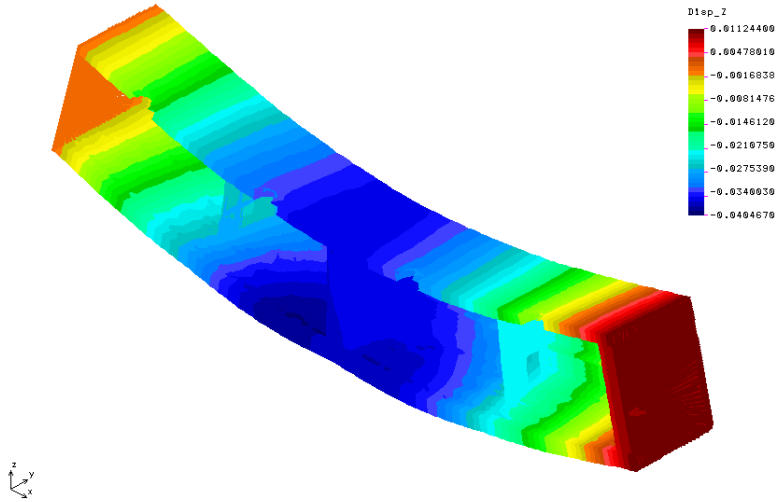

Fig.7.2.5. Vertical deflection on Z direction (m), Wave height 8.123 m, Sagging condition, 3D-FEM 2C model with coarse mesh size

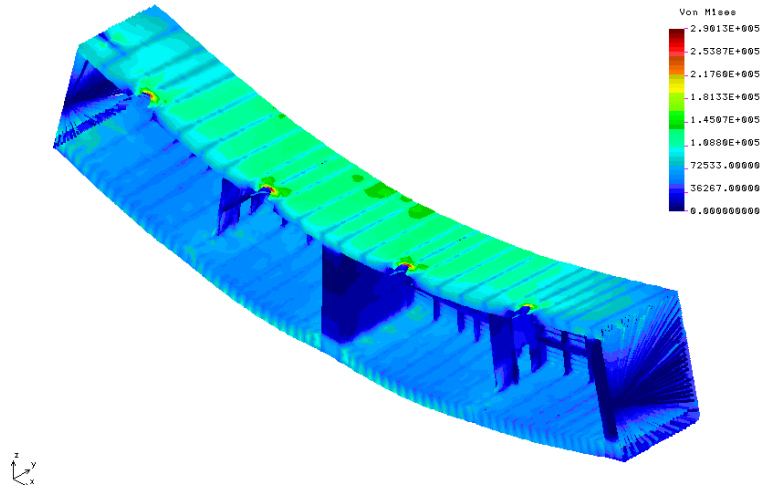

Fig.7.2.6. Equivalent vonMises stress distribution [kN/m^2] ,at the cargo compartments part (x=31.772 m to 80.224 m), Wave height 8.123 m, Sagging condition, 3D-FEM 2C model with coarse mesh size

7.3. Discussions and Conclusions for the Numerical Computation in Hogging and Sagging Conditions, Two Cargo Holds Compartments 3D-FEM Model, With Coarse Size Mesh

In the following figures are presented the maximum values for stress distributions obtained at the global- local strength analysis based on the two cargo holds compartments 3D-FEM Model (2C), with coarse mesh size, under Hogging and Sagging conditions. For selected panels (Deck, Bottom, Side) and a given longitudinal section the maximum stress value result from the equation 2.2.2.

- Fig.7.3.1. and Appendix A.7,Table A.7.1. are presenting the Maximum Normal Deck Stress, σ_X [MPa] in Hogging wave conditions, two cargo holds compartments 3D-FEM model with coarse mesh size, and the safety coefficients Cs according to the yield stress limit ReH.
- Fig.7.3.2. and Appendix A.7, Table.A.7.2. are presenting the Maximum Equivalent vonMises Deck Stress, σ_{von} [MPa] in Hogging wave conditions, two cargo holds compartments 3D-FEM model with coarse mesh size, and the safety coefficients Cs according to the yield stress limit ReH.
- Fig.7.3.3. and Appendix A.7, Table.A.7.3. are presenting the Maximum Normal Bottom Stress, σ_X [MPa] in Hogging wave conditions, two cargo holds compartments 3D-FEM model with coarse mesh size, and the safety coefficients Cs according to the yield stress limit ReH.
- Fig.7.3.4. and Appendix A.7, Table.A.7.4. are presenting the Maximum Equivalent vonMises Bottom Stress, σ_{von} [MPa] in Hogging wave conditions, two cargo holds compartments 3D-FEM model with coarse mesh size, and the safety coefficients Cs according to the yield stress limit ReH.
- Fig.7.3.5. and Appendix A.7, Table.A.7.5. are presenting the Maximum Tangential side stress τ_{xz} [MPa] in Hogging wave conditions, two cargo holds compartments 3D-FEM model with coarse mesh size.
- Fig. 7.3.6 and Appendix A.7, Table A.7.6. are presenting the Maximum Normal Deck Stress, σ_X [MPa] in Sagging wave conditions, two cargo holds compartments 3D-FEM model with coarse mesh size, and the safety coefficients Cs according to the yield stress limit ReH.
- Fig.7.3.7. and Appendix A.7, Table.A.7.7. are presenting the Maximum Equivalent vonMises Deck Stress, σ_{von} [MPa] in Sagging wave conditions, two cargo holds compartments 3D-FEM model with coarse mesh size, and the safety coefficients Cs according to the yield stress limit ReH.
- Fig.7.3.8. and Appendix A.7, Table.A.7.8. are presenting the Maximum Normal Bottom Stress, σ_X [MPa] in Sagging wave conditions, two cargo holds compartments 3D-FEM model with coarse mesh size, and the safety coefficients Cs according to the yield stress limit ReH.

- Fig.7.3.9. and Appendix A.7, Table.A.7.9. are presenting the Maximum Equivalent vonMises Bottom Stress, σ_{von} [MPa] in Sagging wave conditions, two cargo holds compartments 3D-FEM model with coarse mesh size, and the safety coefficients Cs according to the yield stress limit ReH.
- Fig.7.3.10. and Appendix A.7, Table.A.7.10. are presenting the Maximum Tangential side stress τ_{xz} [MPa] in Sagging wave conditions, two cargo holds compartments 3D-FEM model with coarse mesh size.

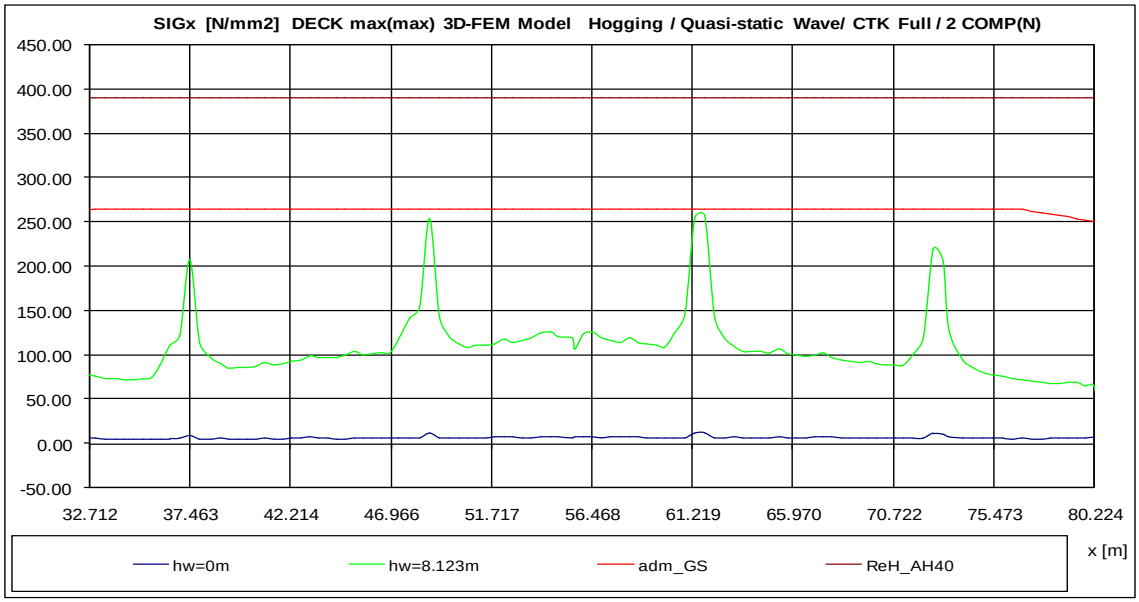

Fig.7.3.1. Maximum Normal Deck Stress,σ_X [MPa] in Hogging wave conditions, two cargo holds compartments 3D-FEM model with coarse mesh size

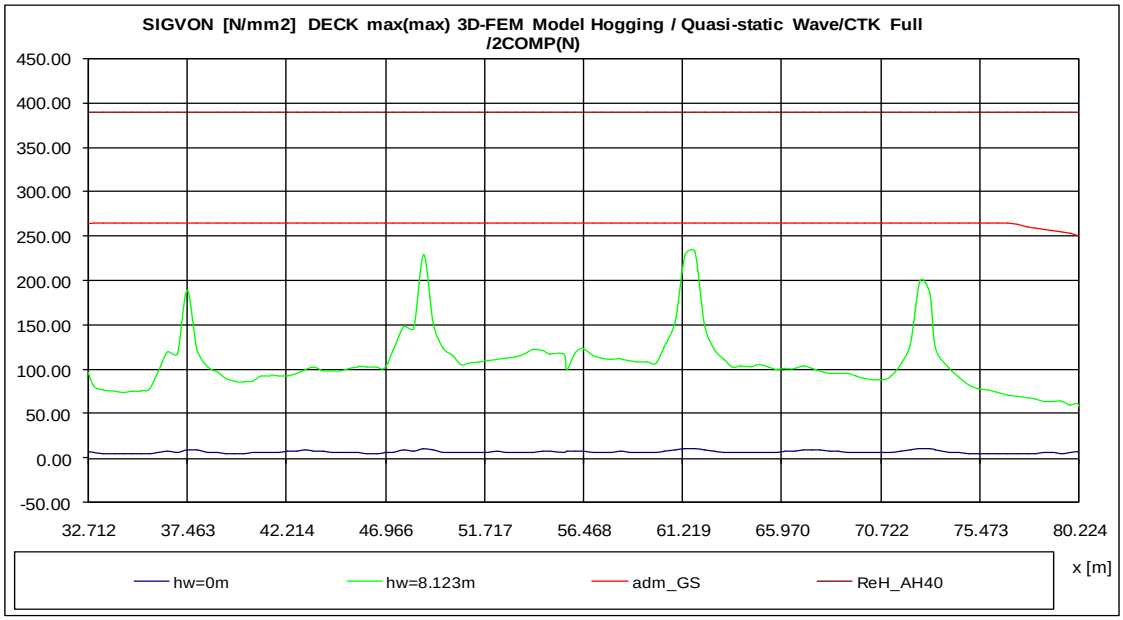

Fig.7.3.2. Maximum Equivalent vonMises Deck Stress,σ_{von} [MPa] in Hogging wave conditions, two cargo holds compartments 3D-FEM model with coarse mesh size

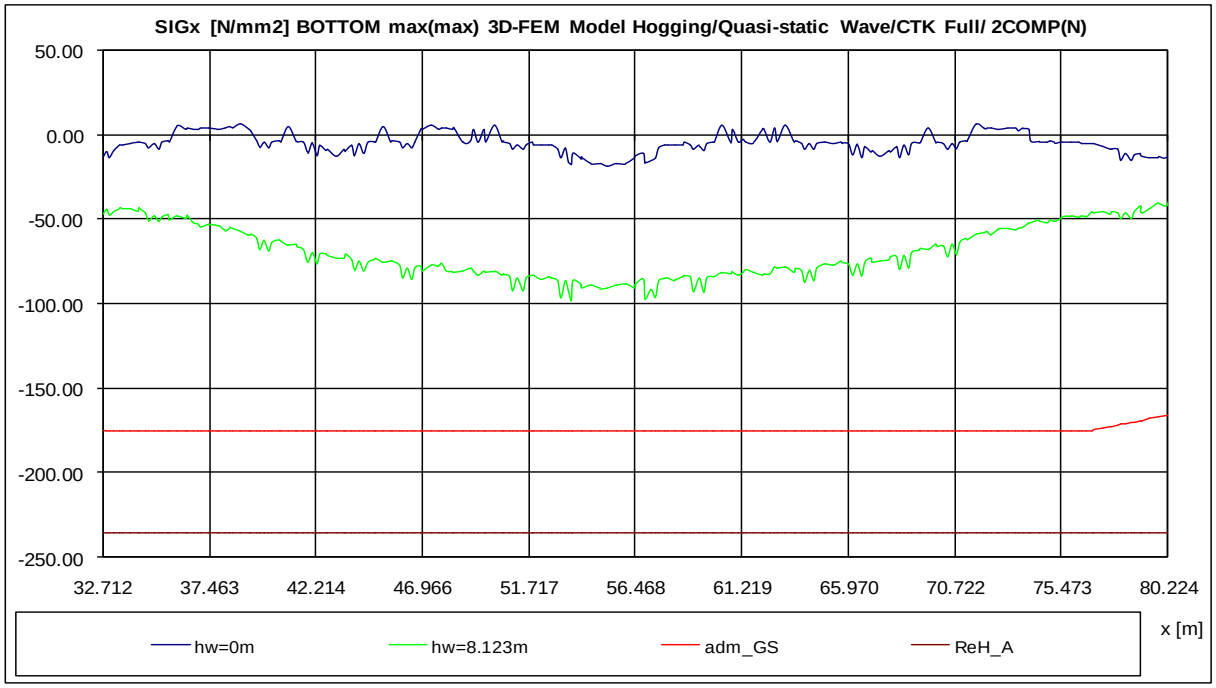

Fig. 7.3.3. Maximum Normal Bottom Stress, σ_X [MPa] in Hogging wave conditions, two cargo holds compartments 3D-FEM model with coarse mesh size

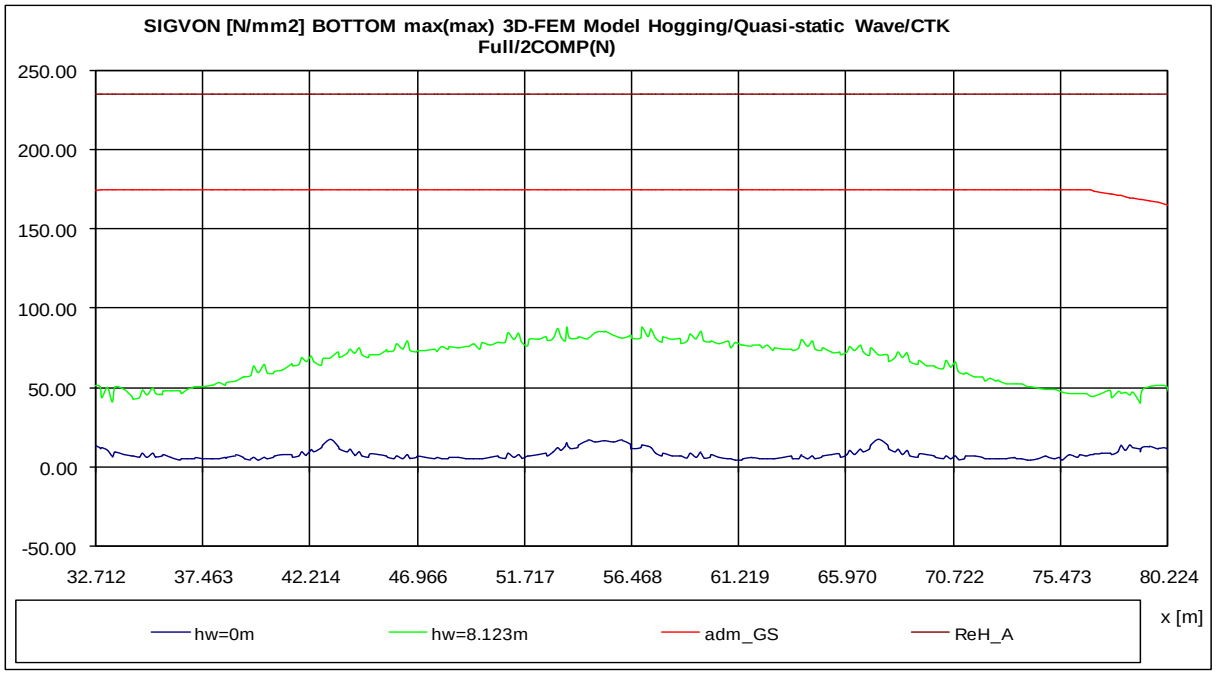

Fig. 7.3.4. Maximum equivalent vonMises Bottom Stress, σ_{von} [MPa] in Hogging wave conditions, two cargo holds compartments 3D-FEM model with coarse mesh size

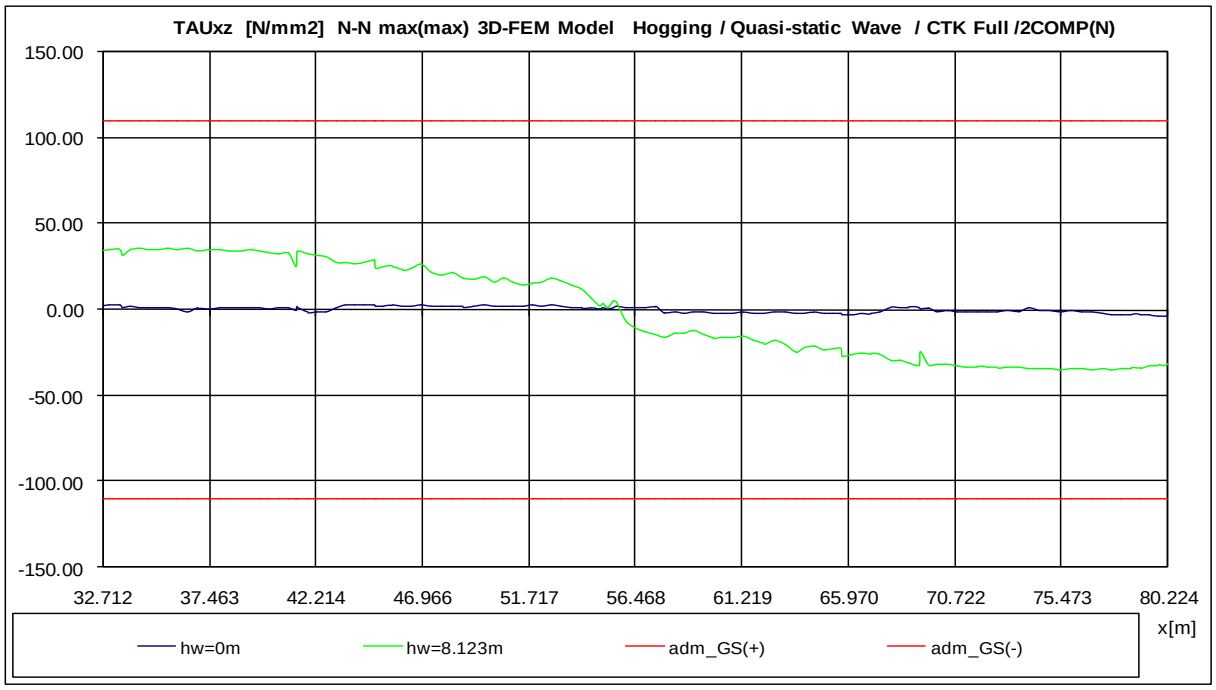

Fig. 7.3.5. Maximum Tangential side stress τ_{xz} [MPa] in Hogging wave conditions, two cargo holds compartments 3D-FEM model with coarse mesh size

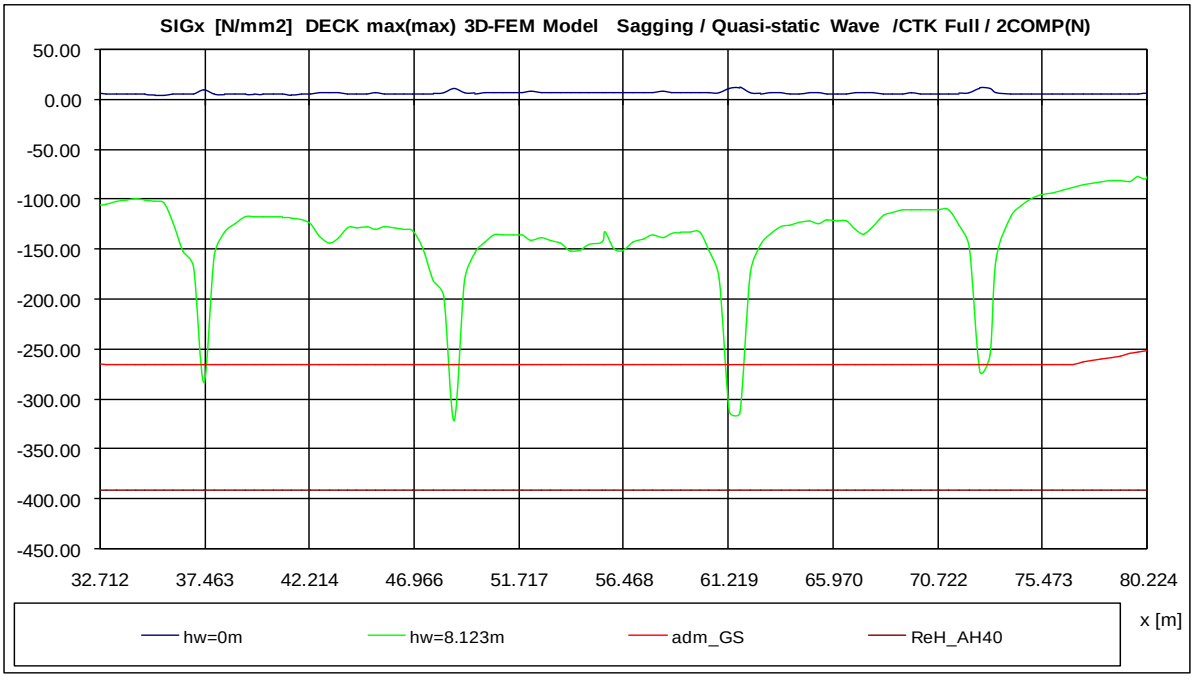

Fig.7.3.6. Maximum Normal Deck Stress, σ_X [MPa] in Sagging wave conditions, two cargo holds compartments 3D-FEM model with coarse mesh size

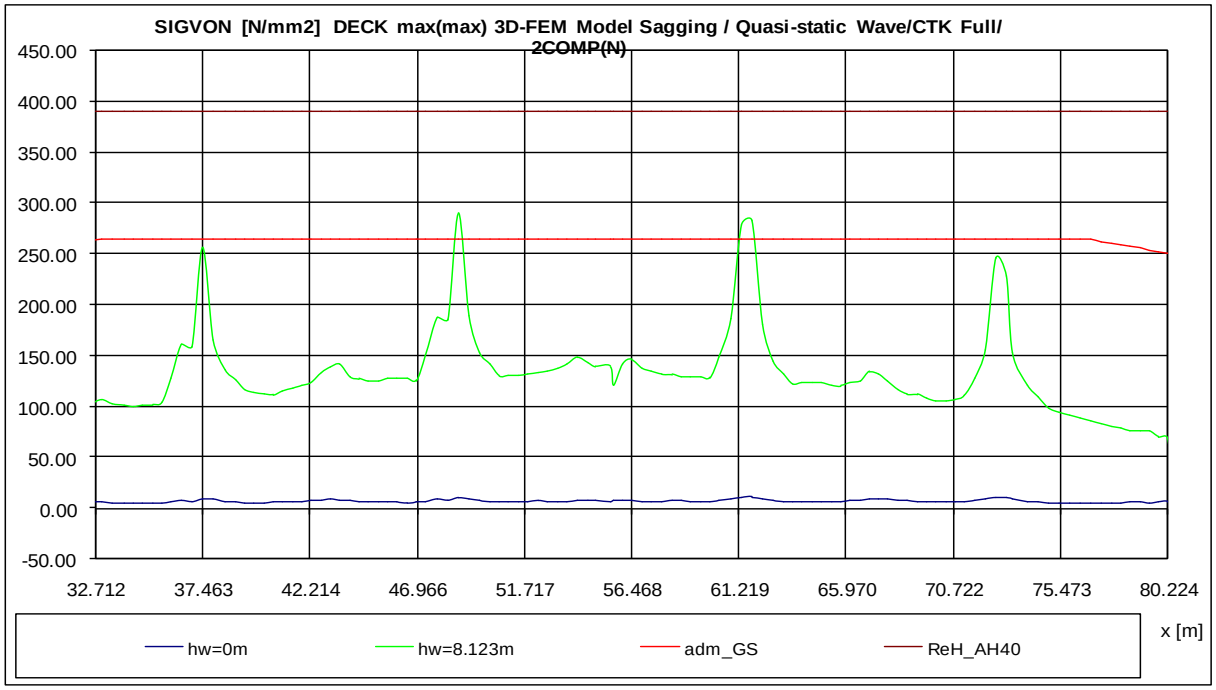

Fig.7.3.7. Maximum Equivalent vonMises Deck Stress, σ_{von} [MPa] in Sagging wave conditions, two cargo holds compartments 3D-FEM model with coarse mesh size

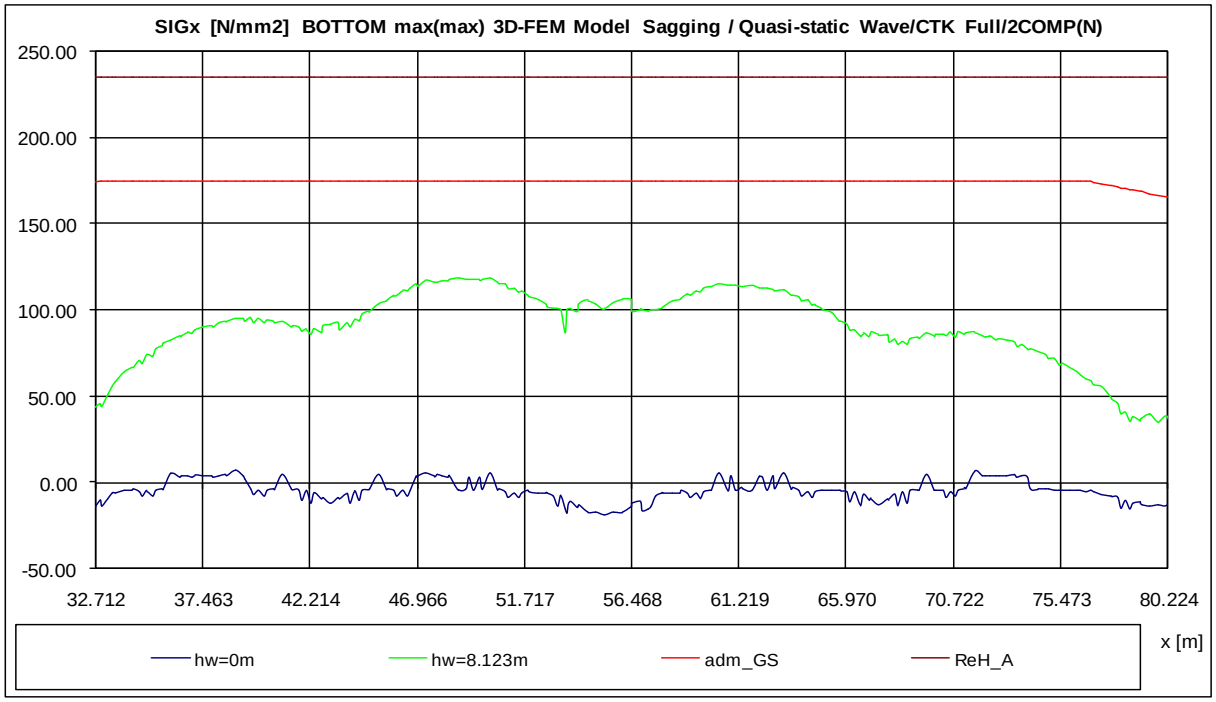

Fig. 7.3.8. Maximum Normal Bottom Stress, σ_X [MPa] in Sagging wave conditions, two cargo holds compartments 3D-FEM model with coarse mesh size

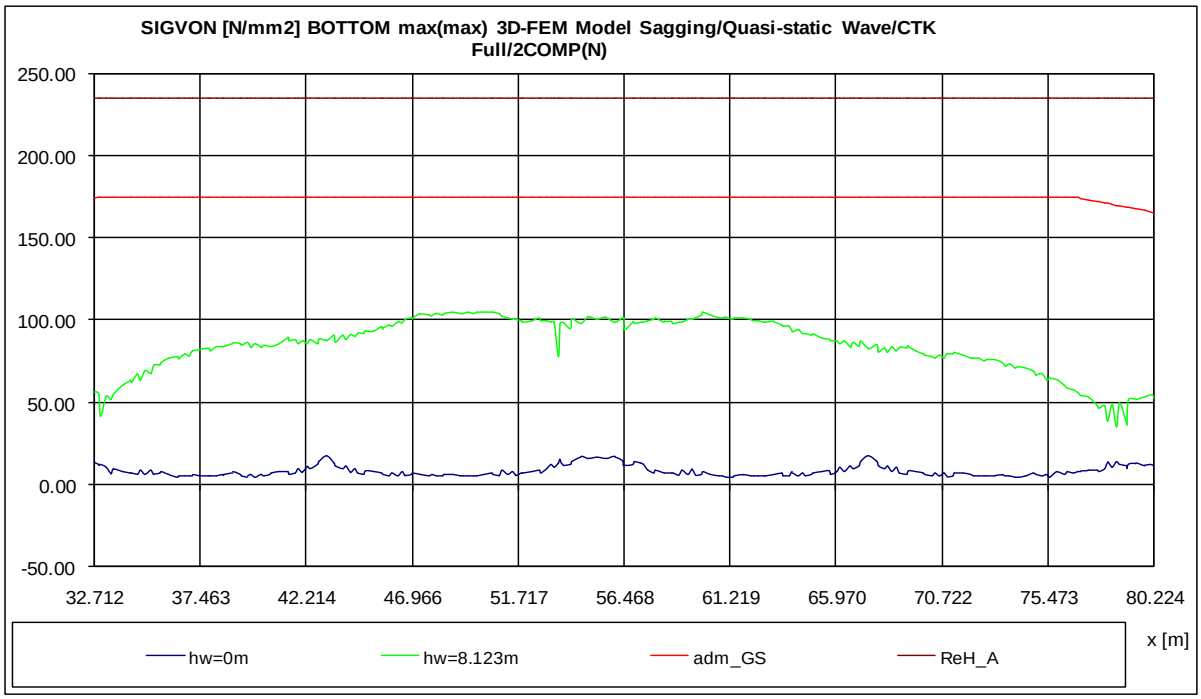

Fig. 7.3.9. Maximum Equivalent vonMises Bottom Stress, σ_{von} [MPa] in Sagging wave conditions, two cargo holds compartments 3D-FEM model with coarse mesh size

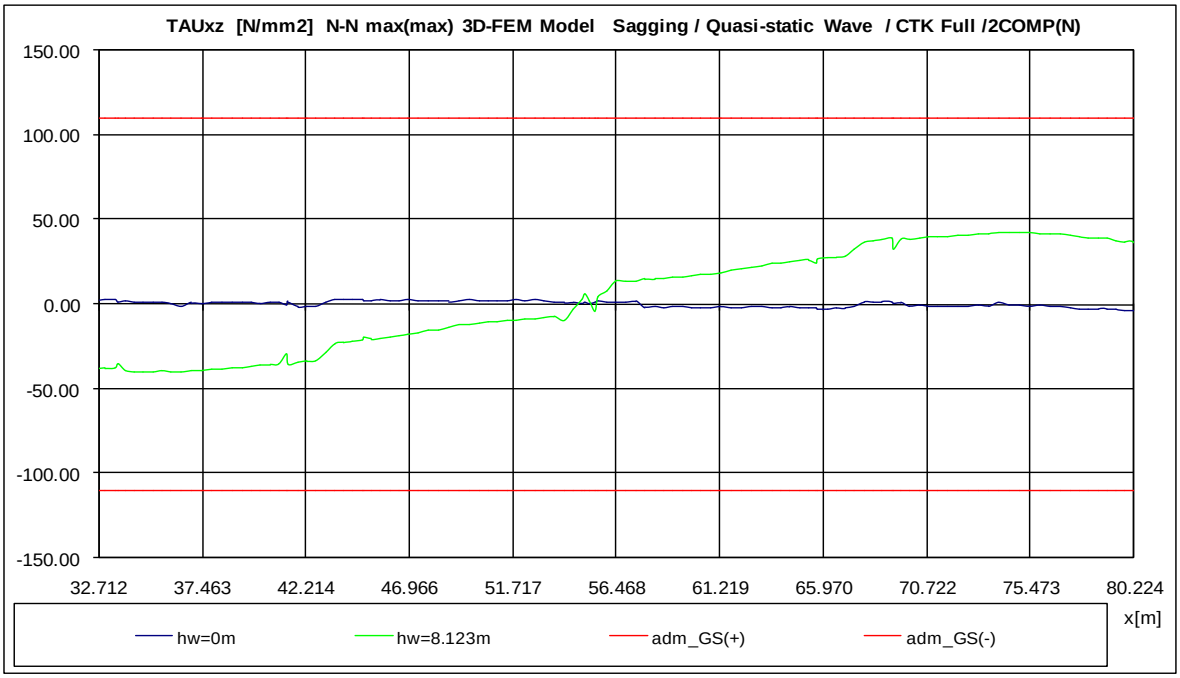

Fig. 7.3.10. Maximum Tangential side stress τ_{xz} [MPa] in Sagging wave conditions, two cargo holds compartments 3D-FEM model with coarse mesh size

Based on the numerical data from the tables (Appendix Table. A.7.1. to A.7.10) for the reference wave height h_{wBV}=8.123 m it results the following synthesis data:

Table.7.3.12. Maximum Hogging stresses based on two cargo holds compartments 3D-FEM model with coarse mesh size, h_w=8.123 m

Panel stress	**Stress 3D [MPa]**	**ReH [MPa]**	$C_s = \frac{ReH}{Stress_{3D}}$	**Stress 1D [MPa]**	$\frac{3D}{1D}$
Maximum σ_x deck	257.90	390	1.512	98.25	2.624936
Maximum σ_{vonM} deck	233.00	390	1.674	98.25	2.371501
Maximum σ_x bottom	98.01	235	2.398	71.27	1.375193
Maximum σ_{vonM} bottom	88.60	235	2.652	71.27	1.24316
Panel stress	**τ_{3D} [MPa]**	**τ_{adm} [MPa]**	**3D / adm**	**τ_{1D} [MPa]**	**3D/1D**
Maximum τ_{xz} side	35.78	110	0.325	40.09	0.892492

Table.7.3.13. Maximum Sagging stresses based on two cargo holds compartments 3D-FEM model with coarse mesh size, h_w=8.123 m

Panel stress	**Stress 3D [MPa]**	**ReH [MPa]**	$C_s = \frac{ReH}{Stress_{3D}}$	**Stress 1D [MPa]**	$\frac{3D}{1D}$
Maximum σ_x deck	321.30	390	1.214	121.17	2.65
Maximum σ_{vonM} deck	290.10	390	1.344	121.17	2.39
Maximum σ_x bottom	118.90	235	1.976	87.90	1.35
Maximum σ_{vonM} bottom	105.46	235	2.230	87.90	1.20
Panel stress	**τ_{3D} [MPa]**	**τ_{adm} [MPa]**	**3D / adm**	**τ_{1D} [MPa]**	**3D/1D**
Maximum τ_{xz} side	42.36	110	0.385	48.27	0.87

In order to validate the corresponding boundary conditions and loads that were applied on the two cargo holds compartments 3D-FEM Model with coarse size mesh, a comparison has been made with the Full extended 3D-FEM model (coarse mesh). All the maximum values for σ_x , σ_{vonM} and τ_{xz} Stresses on the Deck, Bottom and Side were analysed (see Table.7.3.13, Table.7.3.14 and Table.7.3.15).

Table.7.3.13. Maximum Hogging and Sagging stresses , on Deck elements, based on comparison between the two cargo holds compartments 3D-FEM model and the Full extended 3D-FEM model, h_w=8.123 m

h_w	Maximum σ_x Stress 3D Full [MPa]	Maximum σ_x Stress 3D 2 Comp [MPa]	$\frac{\sigma x\ 3D\ Full}{\sigma x2\ Comp}$	Maximum σ_{vonM} Stress 3D Full [MPa]	Maximum σ_{vonM} Stress 3D 2 Comp [MPa]	$\frac{\sigma vonM\ 3D\ Full}{\sigma vonM\ 2\ Comp}$
Hogging 8.123	241.20	257.90	0.94	217.80	233.00	0.93
Sagging 8.123	329.90	321.30	1.03	297.90	290.10	1.03

Table.7.3.14. Maximum Hogging and Sagging stresses , on Bottom elements, based on comparison between the two cargo holds compartments 3D-FEM model and the Full extended 3D-FEM model, h_w=8.123 m

h_w	Maximum σ_x Stress 3D Full [MPa]	Maximum σ_x Stress 3D 2 Comp [MPa]	$\frac{\sigma x\ 3D\ Full}{\sigma x2\ Comp}$	Maximum σ_{vonM} Stress 3D Full [MPa]	Maximum σ_{vonM} Stress 3D 2 Comp [MPa]	$\frac{\sigma vonM\ 3D\ Full}{\sigma vonM\ 2\ Comp}$
Hogging 8.123	94.89	98.01	0.97	85.62	88.60	0.97
Sagging 8.123	111.30	118.90	0.94	106.50	105.46	1.01

Table.7.3.15. Maximum Hogging and Sagging stresses , on Side elements, based on comparison between the two cargo holds compartments 3D-FEM model and the Full extended 3D-FEM model, h_w=8.123 m

h_w	Maximum τ_{xz} Stress 3D Full [MPa]	Maximum τ_{xz} Stress 3D 2 Comp [MPa]	$\frac{\tau xz\ 3D\ Full}{\tau xz\ 2\ Comp}$
Hogging 8.123	34.70	35.78	0.97
Sagging 8.123	47.85	42.36	1.13

As it can be observed from Table.7.3.13, Table.7.3.14 and Table.7.3.15, the differences between the two model compared are very small, being ensured a very good agreement between the two cargo holds compartments 3D-FEM coarse size mesh model and the Full extended 3D-FEM model (see Fig.7.3.11, Fig.7.3.12 and Fig.7.3.13).

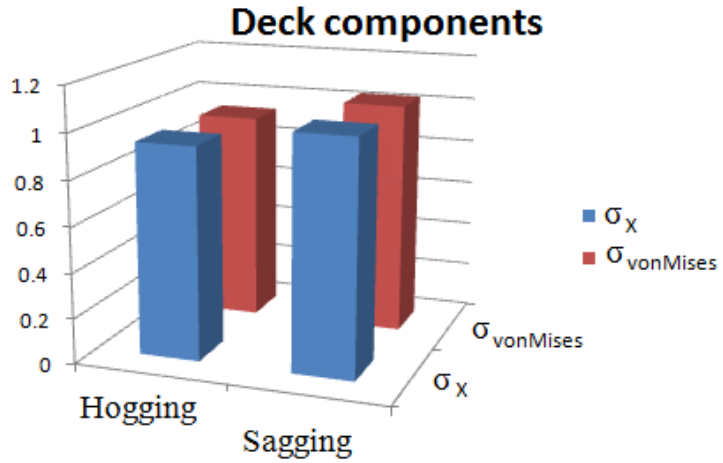

Fig 7.3.11. Hogging and Sagging stresses rapport , on Deck elements, based on comparison between the two cargo holds compartments 3D-FEM model with coarse mesh size and the Full extended 3D-FEM model, h_w=8.123 m

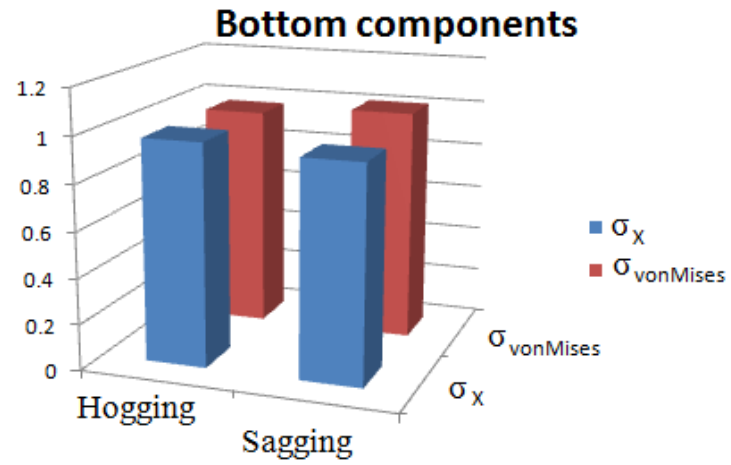

Fig 7.3.12. Hogging and Sagging stresses rapport , on Bottom elements, based on comparison between the two cargo holds compartments 3D-FEM model with coarse mesh size and the Full extended 3D-FEM model, h_w=8.123 m

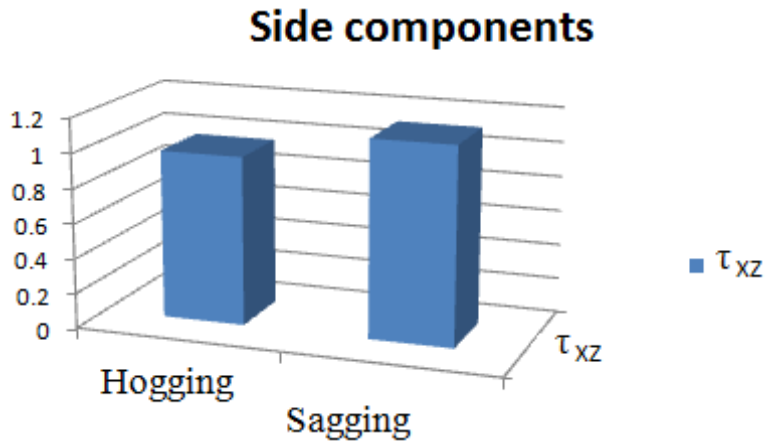

Fig 7.3.13. Hogging and Sagging stresses rapport , on Side elements, based on comparison between the two cargo holds compartments 3D-FEM model with coarse mesh size and the Full extended 3D-FEM model, h_w=8.123 m

The differences of -6 % + 3 % for the stress values between the two 3D-FEM models, having the same coarse mesh size may occur due to the following causes:

- for the two cargo holds compartments 3D-FEM model with coarse mesh size are used non-linear equilibrium parameters, based on the 1D Equivalent Beam Model, and not directly computed based on Full extended 3D-FEM model
- The equivalent transversal section's characteristics are used from the 1D model, and not directly those from the 3D-FEM structure, in the phase of the vertical deflections computation, used for the global constraints (aft and fore) of the two compartments model.

Due to the good agreement between the results obtained with full extended 3D-FEM Model and the two cargo holds compartments 3D-FEM Model with coarse mesh size, in chapter 8 for the partially extended model can be used the same boundary conditions and loads set, but with a finer mesh size structure.

8.THE GLOBAL - LOCAL SHIP HULL STRENGTH ANALYSIS BASED ON 3D-FEM FINE MESH MODEL EXTENDED ON TWO CARGO HOLDS COMPARTMENTS (CENTRAL SHIP PART).

A finer mesh mode was developed between the longitudinal coordinates of x=31.772 m to 80.224 m. The model was realised by using triangle shell elements (membrane and thick plates), having a total number of elements of 203171 and a total number of nodes of 95437.

The boundary conditions for the model remain as have been explained in detail in chapter 7, Table.7.1

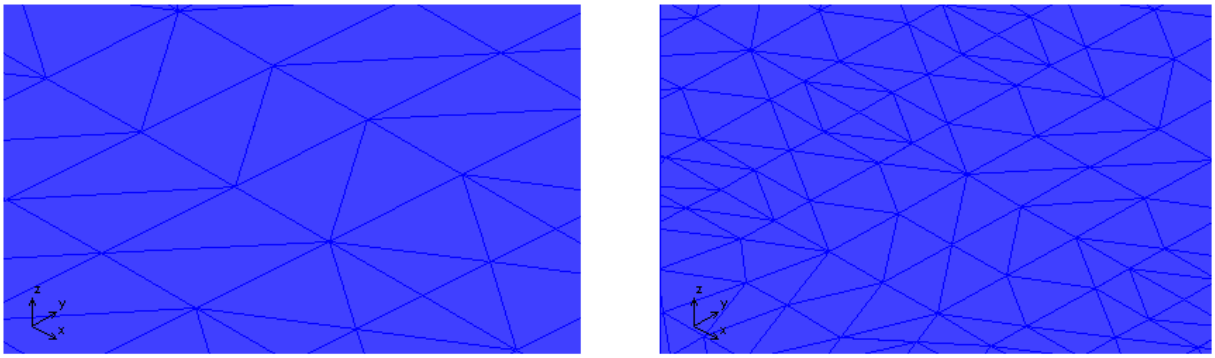

a) b)

Fig. 8.1. Mesh size coparison between a) coarse mesh size in 3D FEM full extended model and b) fine mesh size two cargo holds compartments 3D FEM Model

As in the case of the two cargo holds compartment 3D-FEM model with coarse mesh, the equivalent hydrostatic pressure was applied by the user subroutine presented in the Appendix A2.2, and the selection of the specific plating was performed with the Appendix A.2.1.Identical to the analysis presented in chapter 7, displacements and rotations (Table.7.2) were applied on the two cargo holds compartment 3D-FEM fine mesh model, being computed with the 1D Equivalent Beam Model.

8.1. Numerical Analysis in Still Water Condition. Hydrostatic Water Pressure, Deformation and Stress Distributions

The still water equilibrium condition is obtained based on the theoretical model presented in subchapter 2.3, using the macro-command files procedures, implemented in SolidWorks Comos/ M 2007 software, presented in Appendix A.2.1 and A.2.2. The external hydrostatic water pressure (h_w=0) is applied on bottom, bilge and side shells, based on the 1D-Equivalent Beam global equilibrium conditions (see table.7.2.).

In the following figures are presented the results from the numerical global-local strength analysis in still water condition:

- Fig 8.1.1. External hydrostatic water pressure on the ship hull at still water condition;
- Fig.8.1.2. Vertical deflection at the ship girder at still water condition;
- Fig 8.1.3. Equivalent vonMises Stress distribution in the cargo compartments (x=31.772 m to 80.224 m).

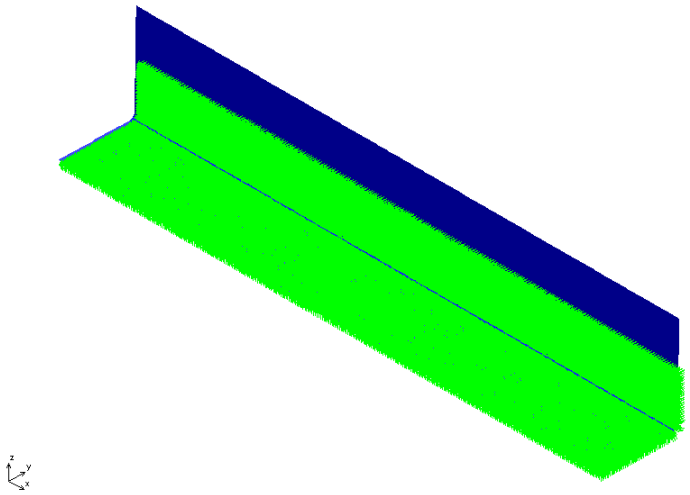

Fig.8.1.1 External water Hydrostatic Pressure [N/mm^2] applied on the shell plating in Still Water condition, 3D-FEM 2D-F fine mesh model

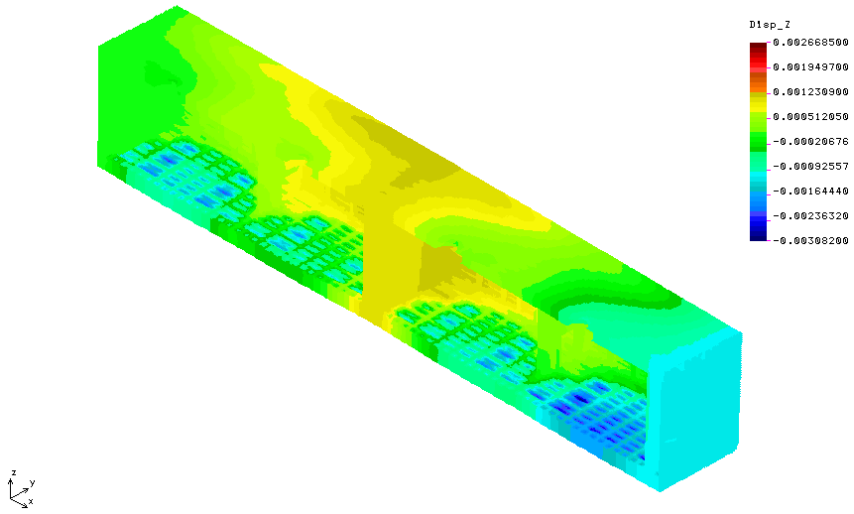

Fig.8.1.2. Vertical deflection on Z direction [m] in Still Water condition, 3D-FEM 2D-F fine mesh model

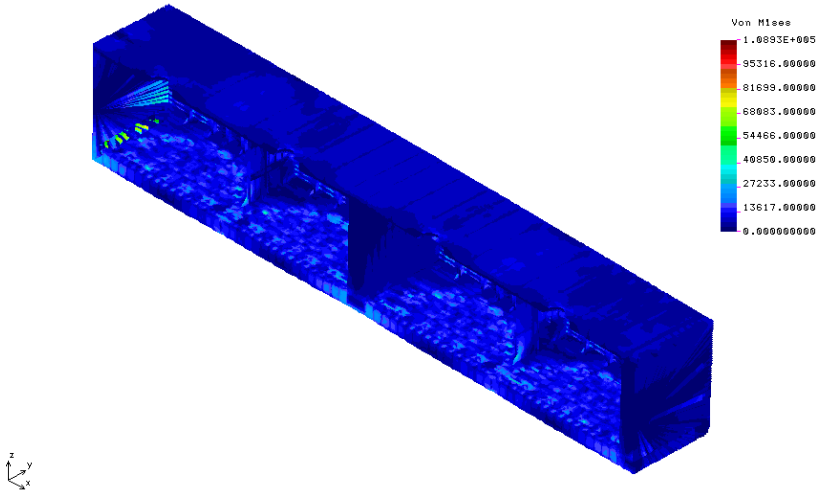

Fig.8.1.3. Equivalent VonMises stress distribution [kN/m^2] in Still Water condition, the cargo compartments part (x=31.772 m to 80.224 m), 3D-FEM 2D-F fine mesh model

8.2. Numerical Analysis in Hogging and Sagging Conditions. Equivalent Quasi-static Wave Pressure, Deformation and Stress Distributions

In the following figures are presented the numerical results obtained at the global-local strength analysis based on the two cargo holds compartments 3D-FEM fine mesh Model, under Hogging and Sagging conditions, using the macro commands files from Appendix A.2.1 and A.2.2. implemented in the Solid Works Cosmos/M 2007 FEM software.

Table.8.2.1.Figures List with numerical results at the global local strength analysis in hogging conditions, based on two cargo holds compartments 3D-FEM fine mesh Model

Wave height case [m]	Wave pressure distribution	Total vertical deflection	VonMises stress distributions
Hogging 8.123	Fig.8.2.1.	Fig.8.2.2.	Fig.8.2.3.
Sagging 8.123	Fig.8.2.4.	Fig.8.2.5.	Fig.8.2.6.

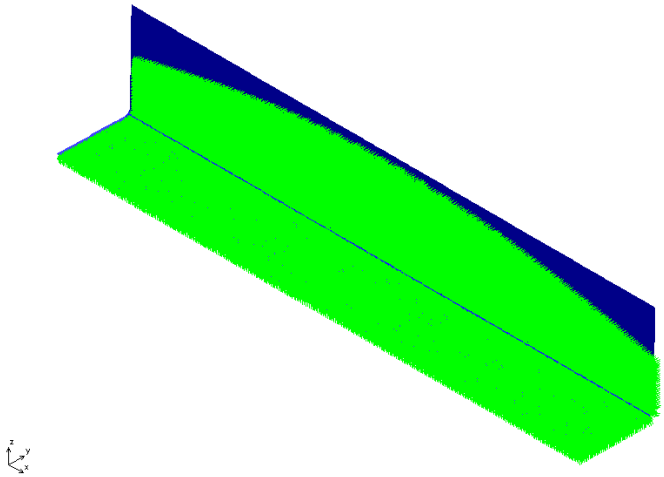

Fig.8.2.1 Hydrostatic Pressure from the external equivalent quasi-static wave applied on the ship hull, Wave height 8.123 m, Hogging condition, 3D-FEM 2D-F fine mesh model

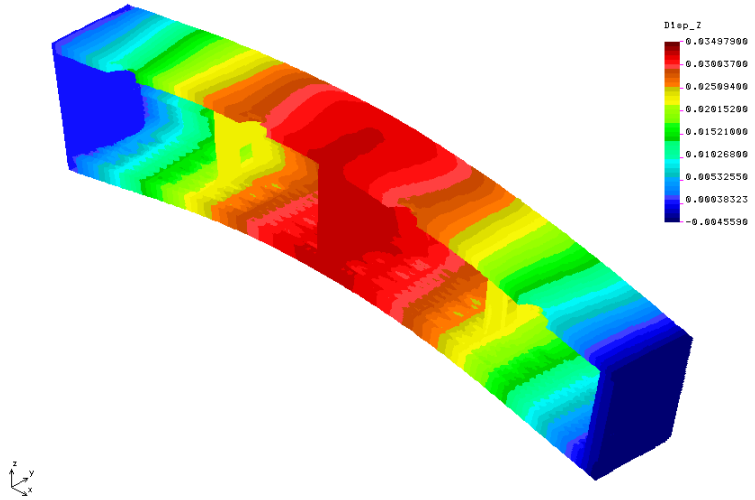

Fig.8.2.2. Vertical deflection on Z direction (m), Wave height 8.123 m, Hogging condition, 3D-FEM 2D-F fine mesh model

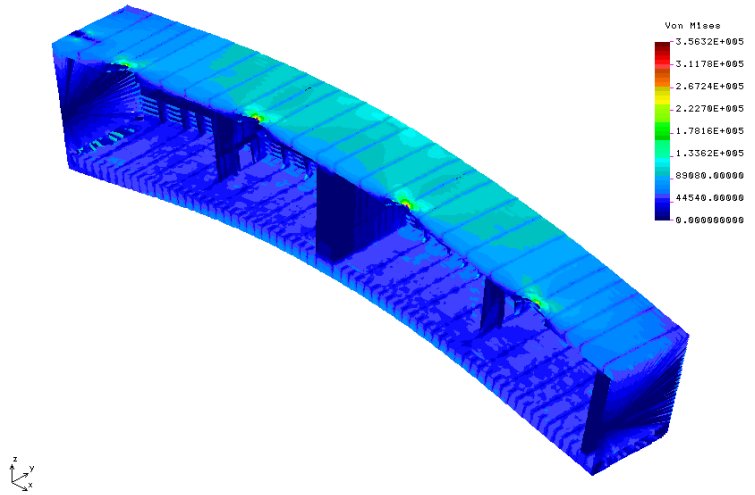

Fig.8.2.3. Equivalent VonMises stress distribution [kN/m^2] ,at the cargo compartments part (x=31.772 m to 80.224 m), Wave height 8.123 m, Hogging condition, 3D-FEM 2D-F fine mesh model

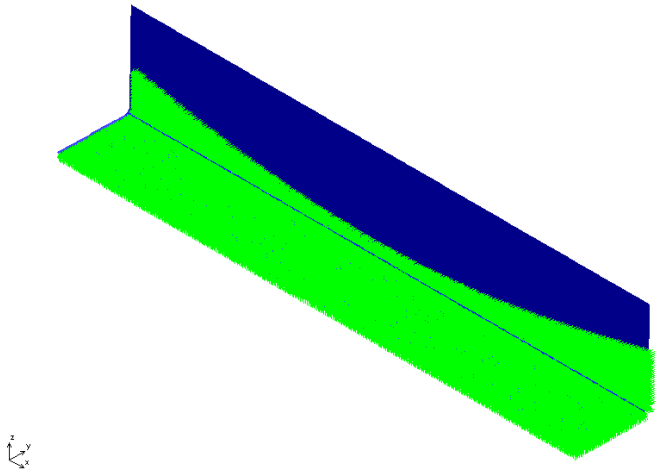

Fig.8.2.4 Hydrostatic Pressure from the external equivalent quasi-static wave applied on the ship hull, Wave height 8.123 m, Sagging condition, 3D-FEM 2D-F fine mesh model

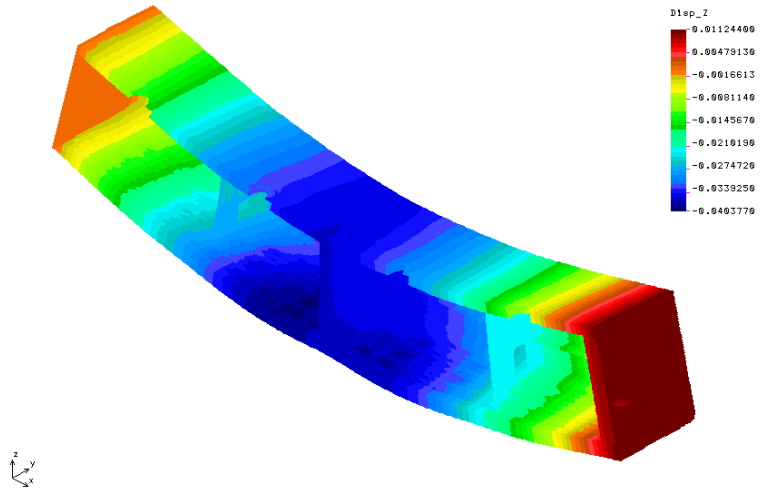

Fig.8.2.5. Vertical deflection on Z direction (m), Wave height 8.123 m, Sagging condition, 3D-FEM 2D-F fine mesh model

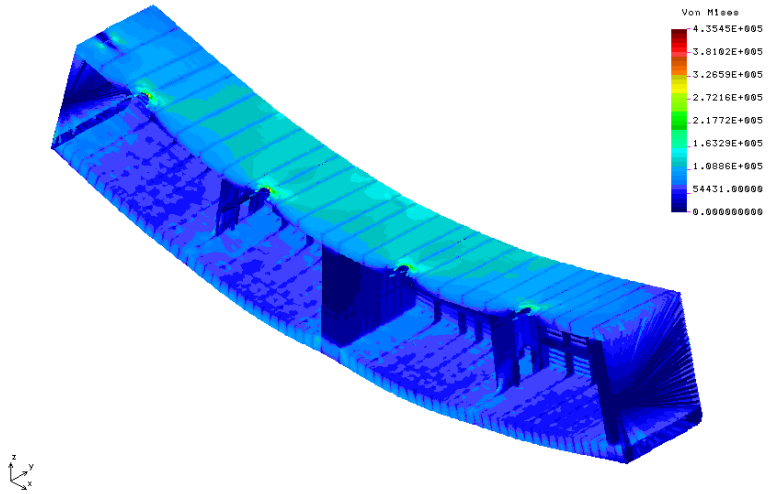

Fig.8.2.6. Equivalent vonMises stress distribution [kN/m^2] ,at the cargo compartments part (x=31.772 m to 80.224 m), Wave height 8.123 m, Sagging condition, 3D-FEM 2D-F fine mesh model

8.3. Discussions and Conclusions for the Numerical Computation in Hogging and Sagging Conditions, Two Cargo Holds Compartments 3D-FEM Model, With Fine Mesh Size

In the following figures are presented the maximum values for stress distributions obtained at the global- local strength analysis based on the two cargo holds compartments 3D-FEM fine mesh Model, under Hogging and Sagging conditions. For selected panels (Deck, Bottom, Side) and a given longitudinal section the maximum stress value result from the equation 2.2.2:

- Fig. 8.3.1 and Appendix A.8, Table A.8.1. are presenting the Maximum Normal Deck Stress, σ_X [MPa] in Hogging wave conditions, two cargo holds compartments 3D-FEM fine mesh model, and the safety coefficients Cs according to the yield stress limit ReH.
- Fig.8.3.2. and Appendix A.8, Table.A.8.2. are presenting the Maximum Equivalent vonMises Deck Stress, σ_{von} [MPa] in Hogging wave conditions, two cargo holds compartments 3D-FEM fine mesh model, and the safety coefficients Cs according to the yield stress limit ReH.
- Fig.8.3.3. and Appendix A.8, Table.A.8.3. are presenting the Maximum Normal Bottom Stress, σ_X [MPa] in Hogging wave conditions, two cargo holds compartments 3D-FEM fine mesh model, and the safety coefficients Cs according to the yield stress limit ReH.
- Fig.8.3.4. and Appendix A.8, Table.A.8.4. are presenting the Maximum Equivalent vonMises Bottom Stress, σ_{von} [MPa] in Hogging wave conditions, two cargo holds compartments 3D-FEM fine mesh model, and the safety coefficients Cs according to the yield stress limit ReH.
- Fig.8.3.5. and Appendix A.8, Table.A.8.5. are presenting the Maximum Tangential side stress τ_{xz} [MPa] in Hogging wave conditions, two cargo holds compartments 3D-FEM fine mesh model.

- Fig.8.3.6 and Appendix A.8, Table A.8.6. are presenting the Maximum Normal Deck Stress, σ_X [MPa] in Sagging wave conditions, two cargo holds compartments 3D-FEM fine mesh model, and the safety coefficients Cs according to the yield stress limit ReH.
- Fig.8.3.7. and Appendix A.8, Table.A.8.7. are presenting the Maximum Equivalent vonMises Deck Stress, σ_{von} [MPa] in Sagging wave conditions, two cargo holds compartments 3D-FEM fine mesh model, and the safety coefficients Cs according to the yield stress limit ReH.

- Fig.8.3.8. and Appendix A.8, Table.A.8.8. are presenting the Maximum Normal Bottom Stress, σ_X [MPa] in Sagging wave conditions, two cargo holds compartments 3D-FEM fine mesh model, and the safety coefficients Cs according to the yield stress limit ReH.
- Fig.8.3.9. and Appendix A.8, Table.A.8.9. are presenting the Maximum Equivalent vonMises Bottom Stress, σ_{von} [MPa] in Sagging wave conditions, two cargo holds compartments 3D-FEM fine mesh model, and the safety coefficients Cs according to the yield stress limit ReH.
- Fig.8.3.10. and Appendix A.8, Table.A.8.10. are presenting the Maximum Tangential side stress τ_{xz} [MPa] in Sagging wave conditions, two cargo holds compartments 3D-FEM fine mesh model.

- Fig.8.3.11. and Appendix A.8, Table.A.8.11. are presenting the Maximum Normal Deck Stress, σ_X [MPa] in Hogging wave conditions, two cargo holds compartments 3D-FEM fine mesh model, and the safety coefficients Cs according to the yield stress limit ReH, *with HotSpot correction (equation 2.3.5)*
- Fig.8.3.12. and Appendix A.8, Table.A.8.12 are presenting the Maximum Equivalent vonMises Deck Stress, σ_{von} [MPa] in Hogging wave conditions, two cargo holds compartments 3D-FEM fine mesh model, and the safety coefficients Cs according to the yield stress limit ReH, *with HotSpot correction (equation 2.3.5)*
- Fig.8.3.13. and Appendix A.8, Table.A.8.13. are presenting the Maximum Normal Deck Stress, σ_X [MPa] in Sagging wave conditions, two cargo holds compartments 3D-FEM fine mesh model, and the safety coefficients Cs according to the yield stress limit ReH. *with HotSpot correction (equation 2.3.5)*
- Fig.8.3.14. and Appendix A.8, Table.A.8.14. are presenting the Maximum Equivalent vonMises Deck Stress, σ_{von} [MPa] in Sagging wave conditions, two cargo holds compartments 3D-FEM fine mesh model, and the safety coefficients Cs according to the yield stress limit ReH, *with HotSpot correction (equation 2.3.5)*

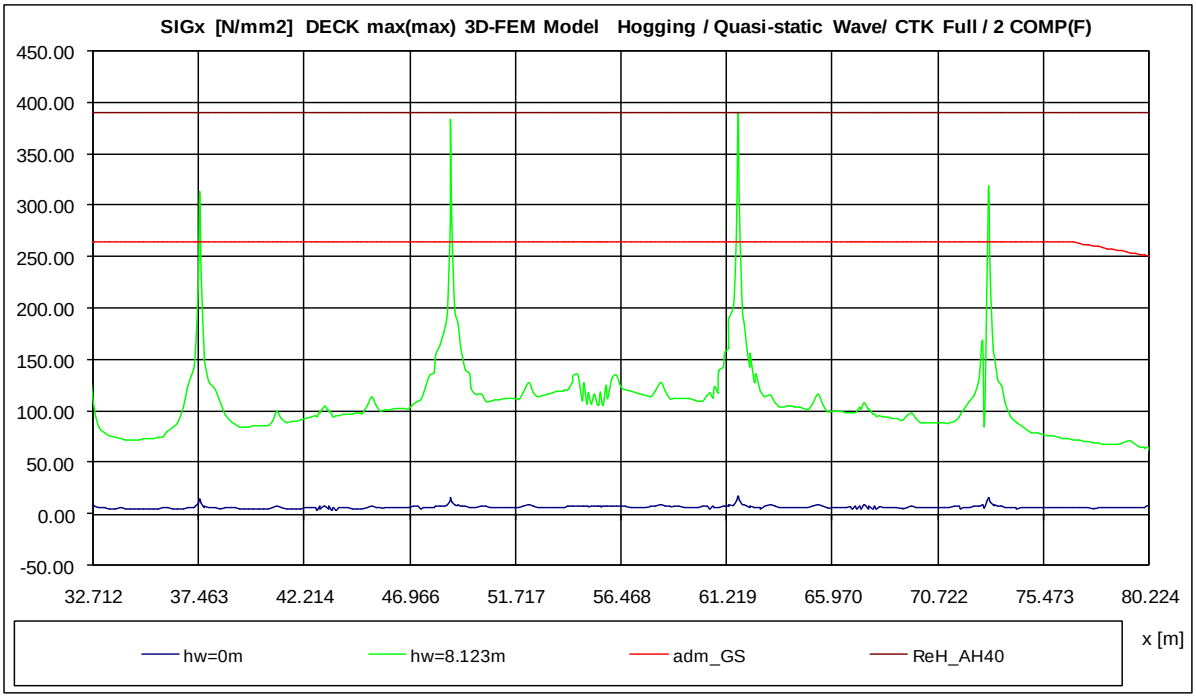

Fig.8.3.1. Maximum Normal Deck Stress, σ_X [MPa] in Hogging wave conditions, two cargo holds compartments 3D-FEM fine mesh model

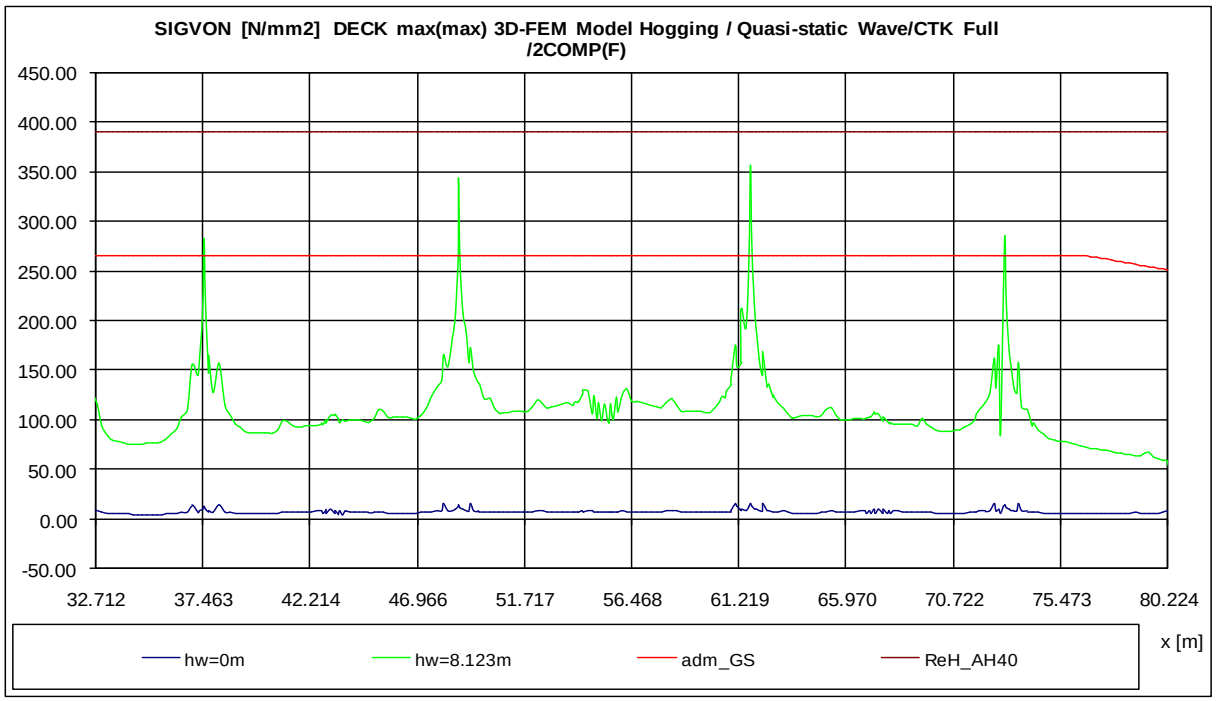

Fig.8.3.2. Maximum Equivalent vonMises Deck Stress, σ_{von} [MPa] in Hogging wave conditions, two cargo holds compartments 3D-FEM fine mesh model

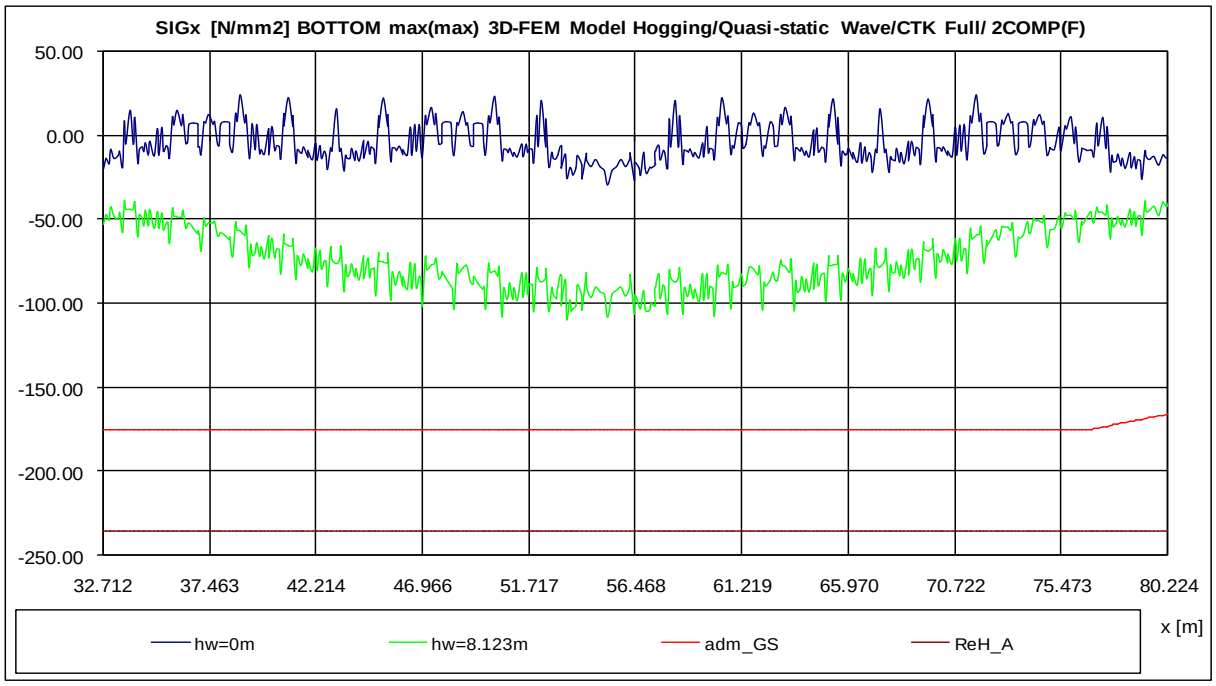

Fig.8.3.3. Maximum Normal Bottom Stress, σ_X [MPa] in Hogging wave conditions, two cargo holds compartments 3D-FEM fine mesh model

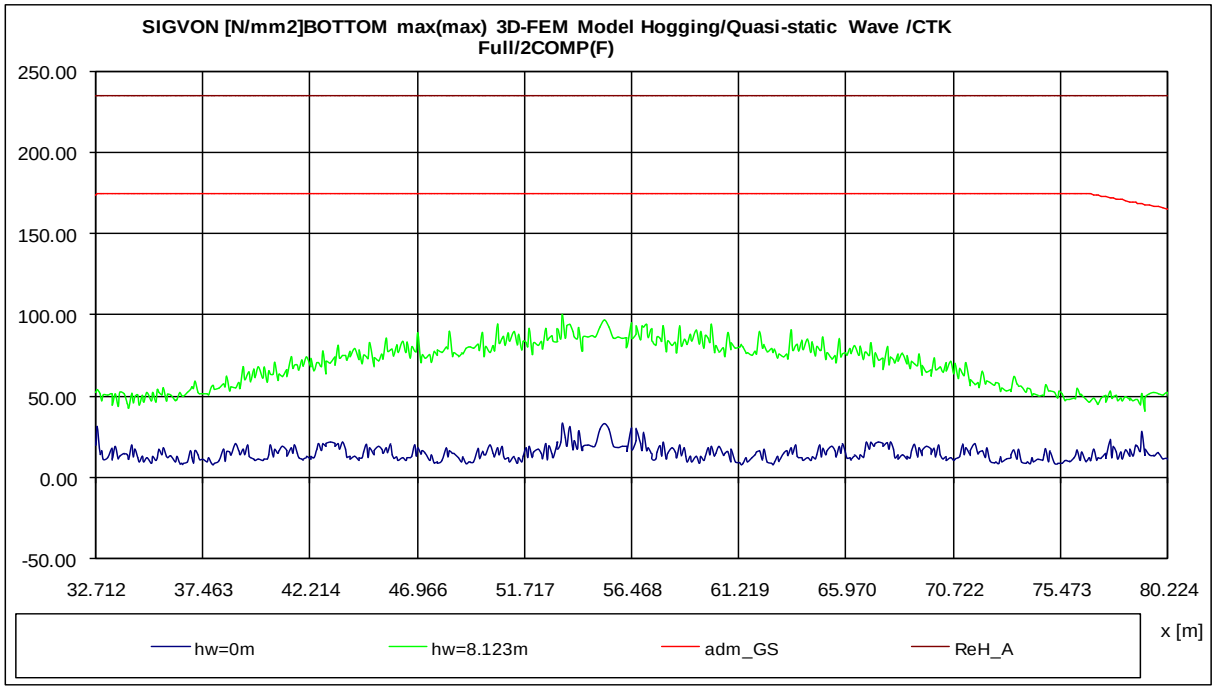

Fig. 8.3.4. Maximum Equivalent vonMises Bottom Stress, σ_{von} [MPa] in Hogging wave conditions, two cargo holds compartments 3D-FEM fine mesh model

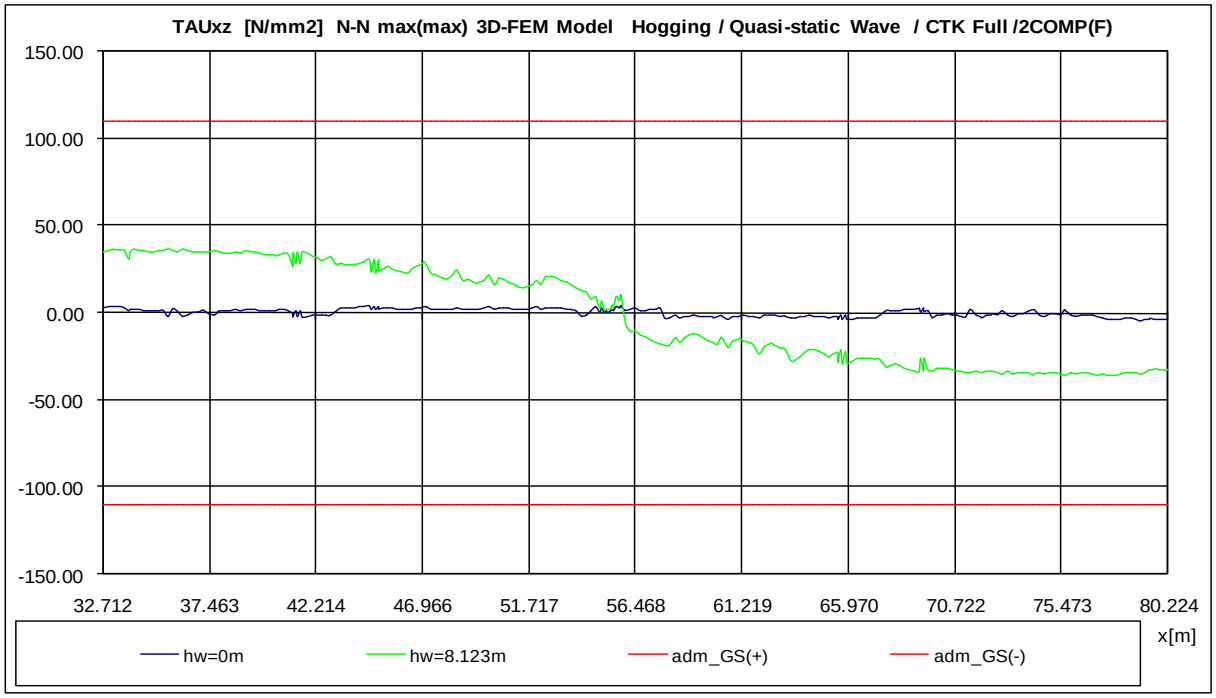

Fig. 8.3.5. Maximum Tangential side stress τ_{xz} [MPa] in Hogging wave conditions, two cargo holds compartments 3D-FEM fine mesh model

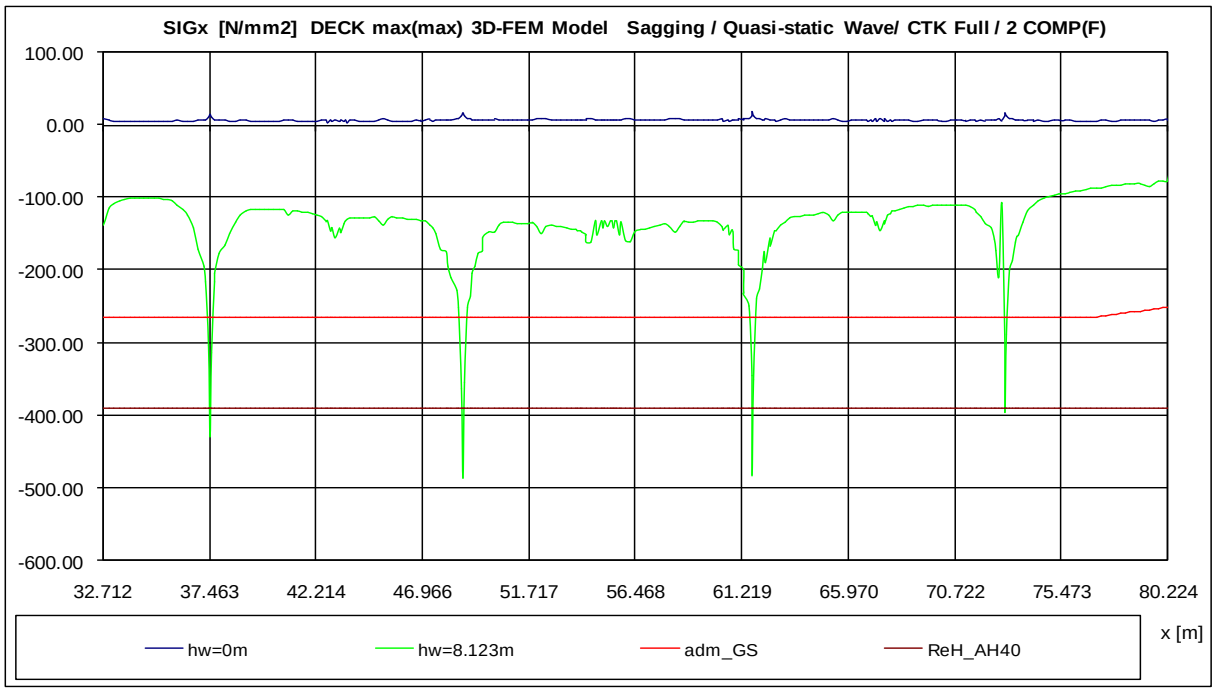

Fig.8.3.6. Maximum Normal Deck Stress, σ_X [MPa] in Sagging wave conditions, two cargo holds compartments 3D-FEM fine mesh model

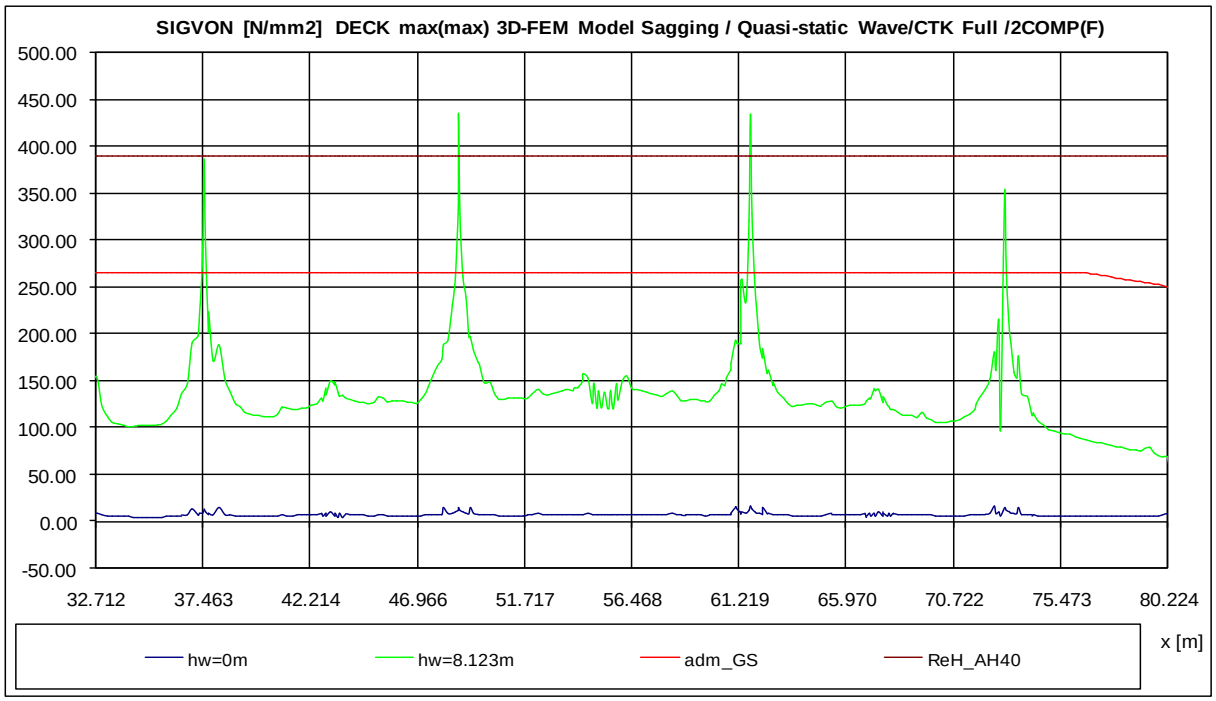

Fig.8.3.7. Maximum Equivalent vonMises Deck Stress, σ_{von} [MPa] in Sagging wave conditions, two cargo holds compartments 3D-FEM fine mesh model

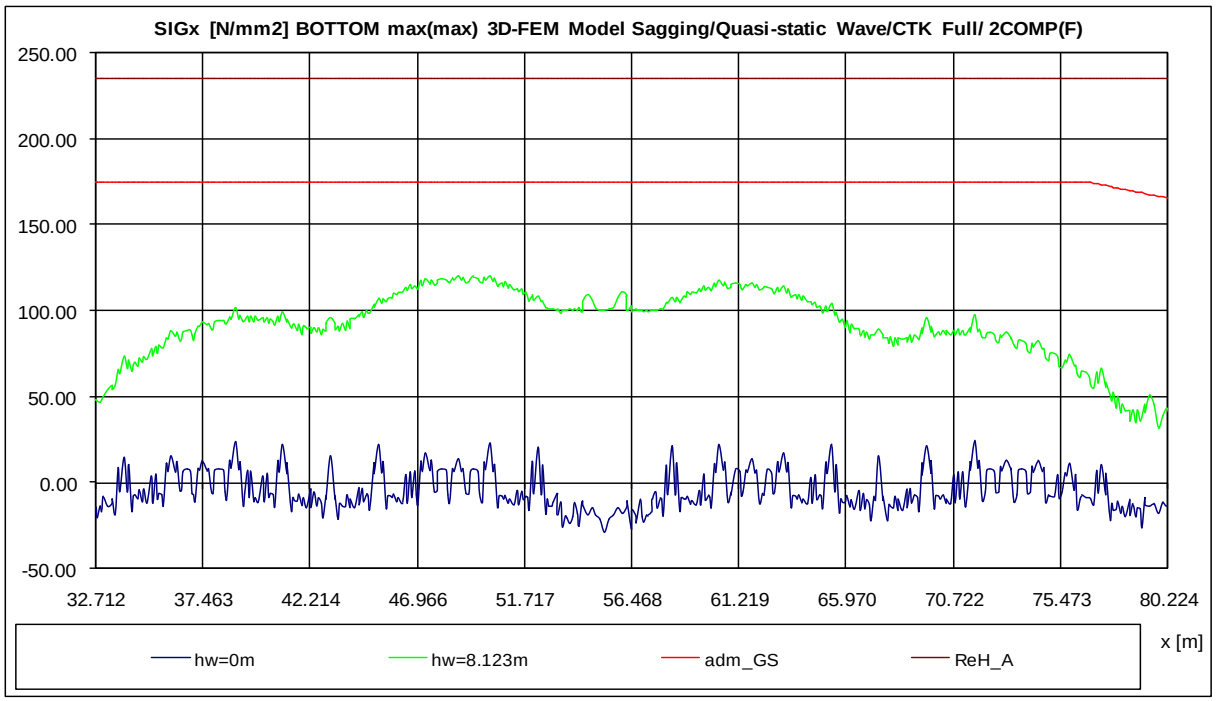

Fig. 8.3.8. Maximum Normal Bottom Stress, σ_X [MPa] in Sagging wave conditions, two cargo holds compartments 3D-FEM fine mesh model

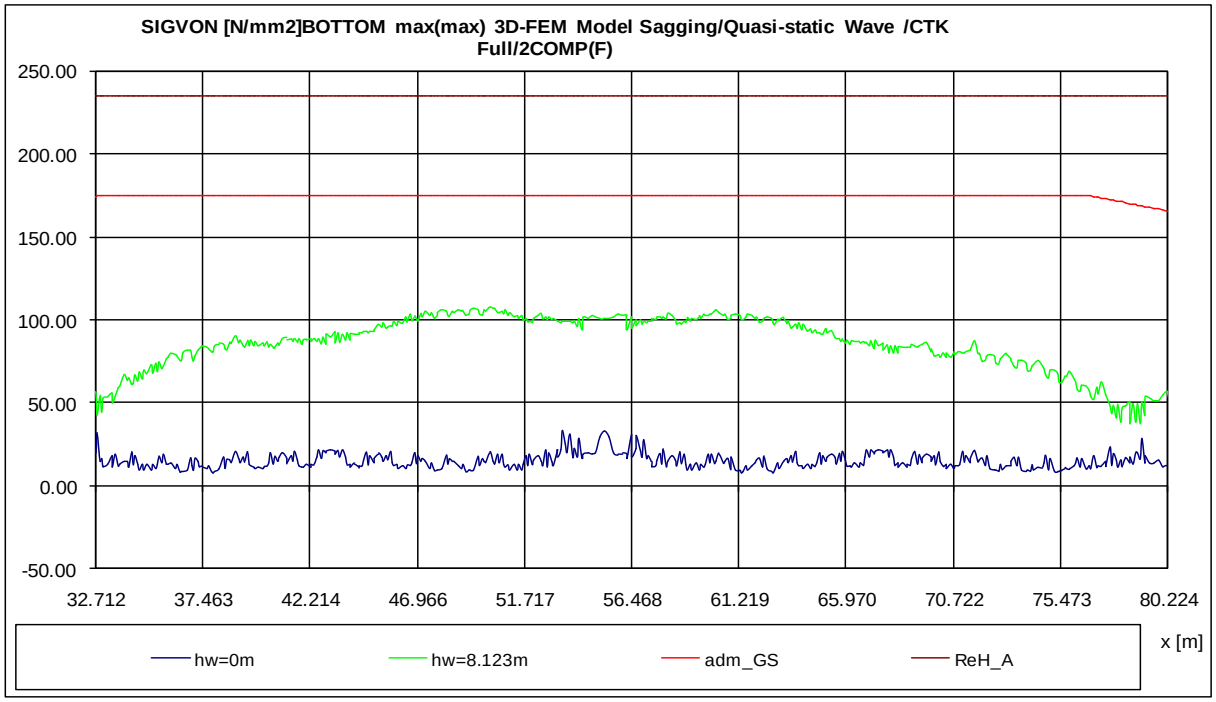

Fig. 8.3.9. Maximum Equivalent vonMises Bottom Stress, σ_{von} [MPa] in Sagging wave conditions, two cargo holds compartments 3D-FEM fine mesh model

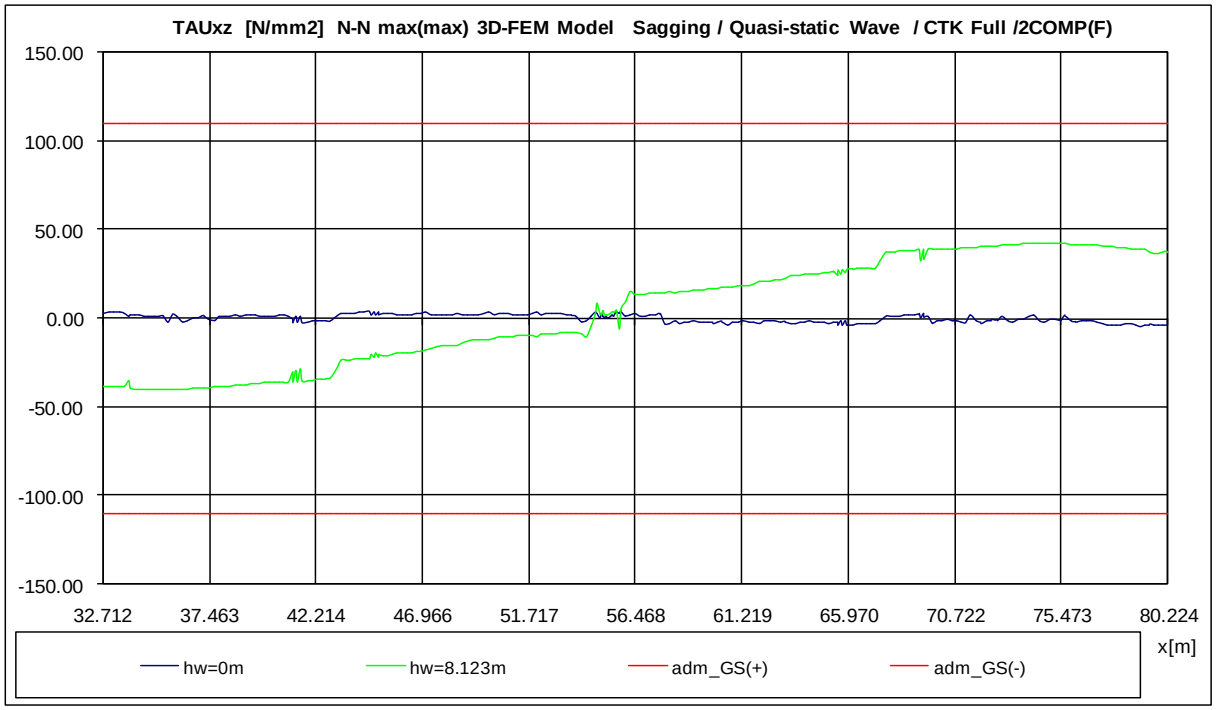

Fig. 8.3.10. Maximum Tangential side stress τ_{xz} [MPa] in Sagging wave conditions, two cargo holds compartments 3D-FEM fine mesh model

As it can be observed from the previous figures, the maximum values for the σ_x and σ_{vonM} components for the Deck elements exceed the yielding stress limit. In order to have the correct reading and interpretation of the results, the stress hotspots have to be evaluated according to Bureau Veritas 2010 rules, see equation 2.3.5, Figure.2.3.3. Therefore the corrected hotspot stress values for the σ_x and σ_{von} for the two cargo holds FEM fine mesh model are presented in the following figures.

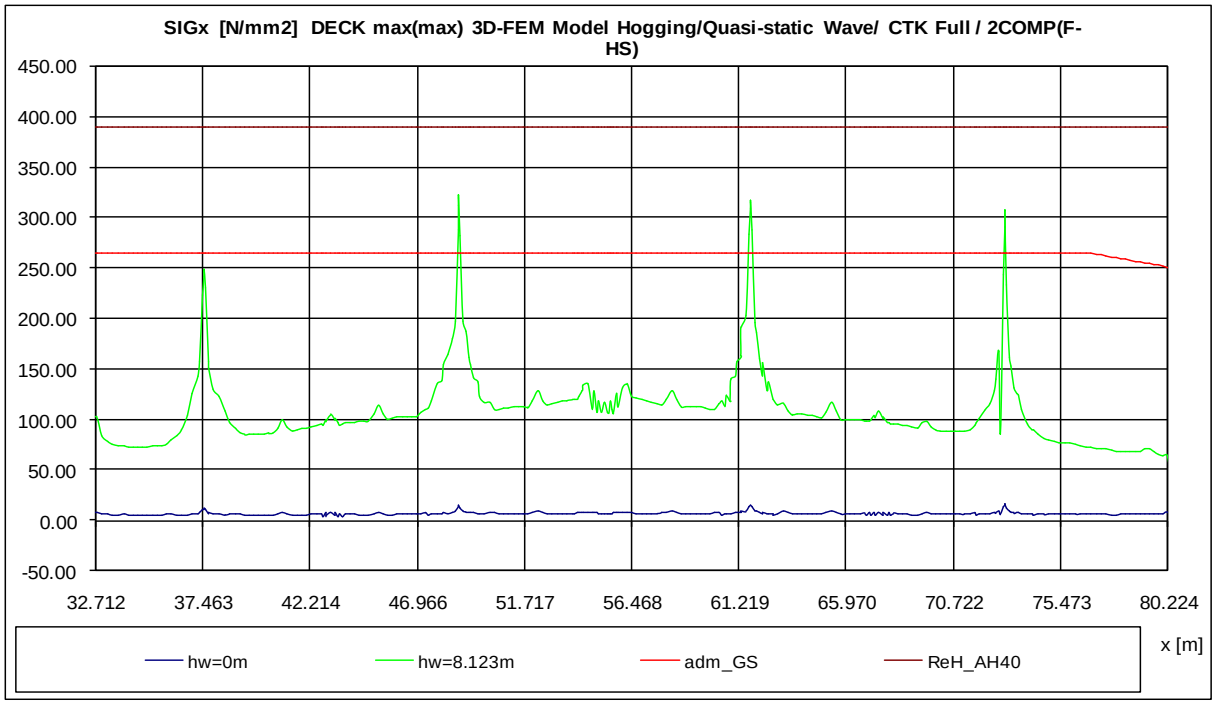

Fig.8.3.11. Maximum Normal Deck Stress, σ_X [MPa] in Hogging wave conditions, two cargo holds compartments 3D-FEM fine mesh model, with Hotspot correction (eq 2.3.5.)

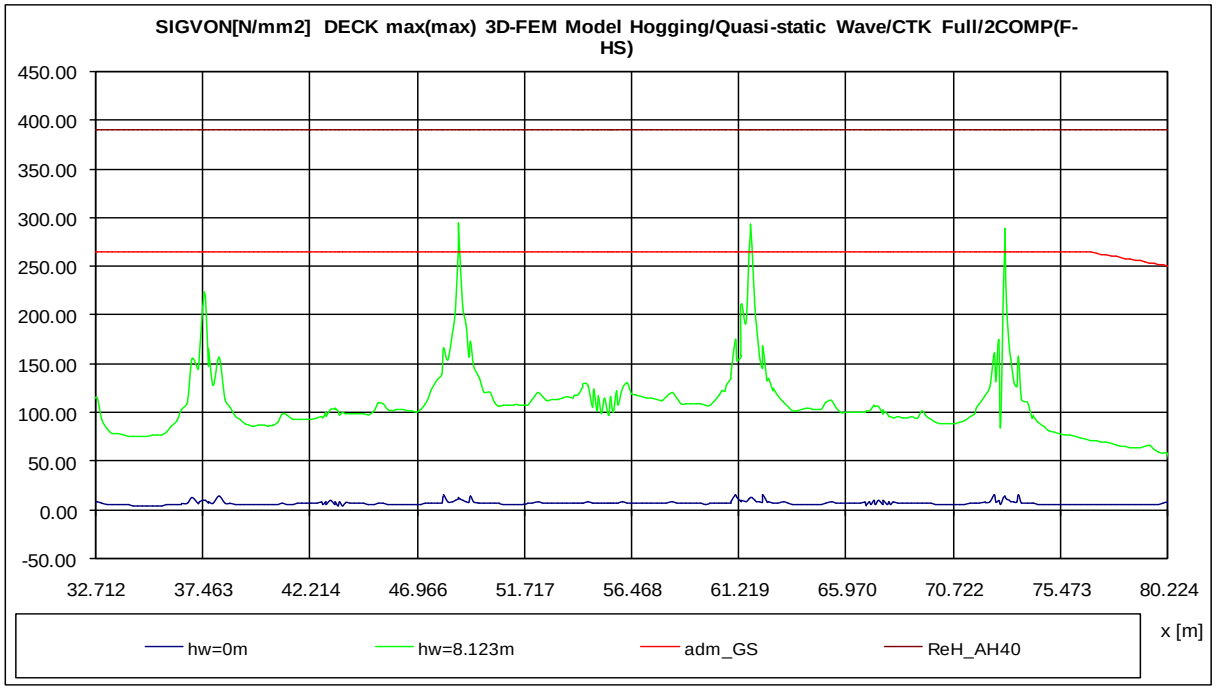

Fig.8.3.12. Maximum Equivalent vonMises Deck Stress, σ_{von} [MPa] in Hogging wave conditions, two cargo holds compartments 3D-FEM fine mesh model, with Hotspot correction (eq 2.3.5.)

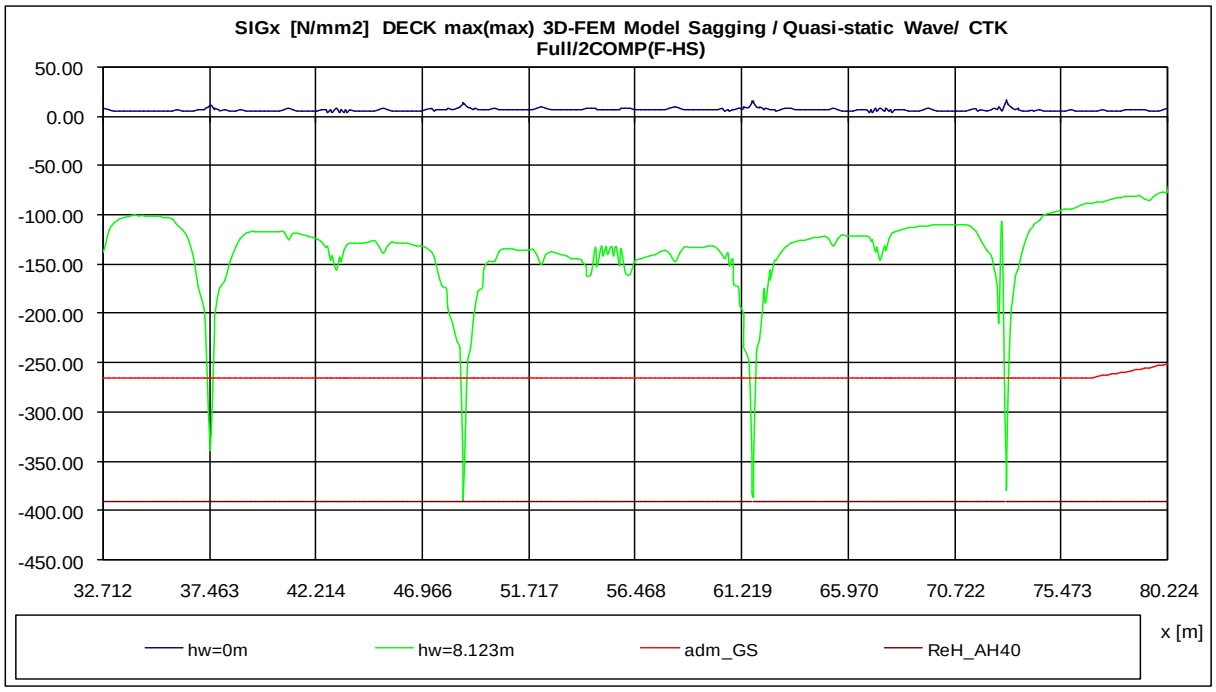

Fig.8.3.13. Maximum Normal Deck Stress, σ_X [MPa] in Sagging wave conditions, two cargo holds compartments 3D-FEM fine mesh model, with Hotspot correction (eq 2.3.5.)

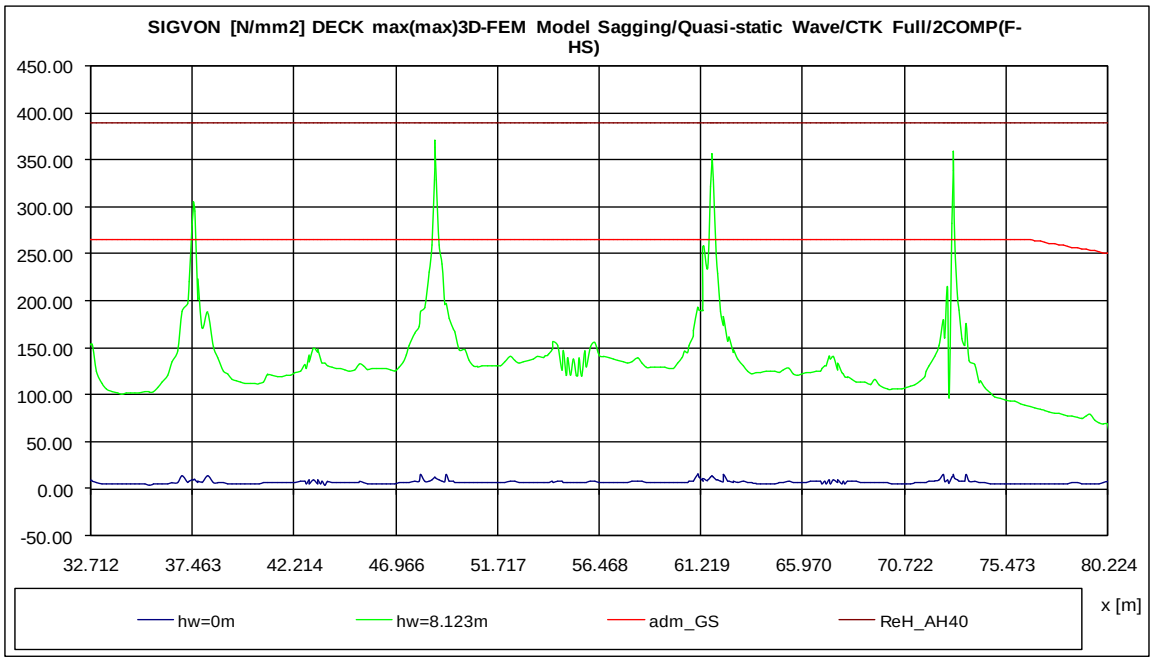

Fig.8.3.14. Maximum Equivalent vonMises Deck Stress, σ_{von} [MPa] in Sagging wave conditions, two cargo holds compartments 3D-FEM fine mesh model, with Hotspot correction (eq 2.3.5.)

Based on the numerical data from the tables (Appendix A8, Tables.A.8.3.1-A.8.3.14) for the reference wave height h_{wBV}=8.123 m it results the following synthesis data:

Table.8.3.16. Maximum Hogging stresses based on two cargo holds compartments 3D-FEM fine mesh model, h_w=8.123 m, with Hotspot correction (eq 2.3.5.)

Panel stress	**Stress 3D [MPa]**	**ReH [MPa]**	$C_s = \frac{ReH}{Stress_{3D}}$	**Stress 1D [MPa]**	$\frac{3D}{1D}$
Maximum σ_x deck	321.57	390	1.213	98.25	3.27
Maximum σ_{vonM} deck	294.76	390	1.323	98.25	3.00
Maximum σ_x bottom	109.30	235	2.150	71.27	1.53
Maximum σ_{vonM} bottom	100.40	235	2.341	71.27	1.41
Panel stress	**τ_{3D} [MPa]**	**τ_{adm} [MPa]**	**3D / adm**	**τ_{1D} [MPa]**	**3D/1D**
Maximum τ_{xz} side	36.52	110	0.332	40.09	0.91

In the Table.8.3.18, Table.8.3.19. and Table.8.3.20 , are compared the maximum values for σ_x , σ_{vonM} and τ_{xz} Stresses at Deck, Bottom and Side, for the 3D FEM full extended model and the two cargo holds compartments 3D-FEM mode with fine mesh size, with Hotspot correction (eq 2.3.5.).

Table.8.3.17. Maximum Sagging stresses based on two cargo holds compartments 3D-FEM fine mesh model, h_w=8.123 m, with Hotspot correction (eq 2.3.5.)

Panel stress	**Stress 3D [MPa]**	**ReH [MPa]**	$C_s = \frac{ReH}{Stress_{3D}}$	**Stress 1D [MPa]**	$\frac{3D}{1D}$
Maximum σ_x deck	389.90	390	1.000	121.17	3.22
Maximum σ_{vonM} deck	371.64	390	1.049	121.17	3.07
Maximum σ_x bottom	120.70	235	1.947	87.90	1.37
Maximum σ_{vonM} bottom	107.80	235	2.180	87.90	1.23
Panel stress	**τ_{3D} [MPa]**	**τ_{adm} [MPa]**	**3D / adm**	**τ_{1D} [MPa]**	**3D/1D**
Maximum τ_{xz} side	42.41	110	0.386	48.27	0.87

Table.8.3.18. Maximum Hogging and Sagging stresses , on Deck elements, based on comparison between the 2 cargo holds compartments 3D-FEM fine mesh and the full extended models, h_w=8.123 m

h_w	**Max σ_x Stress 3D Full [MPa]**	**Max σ_x Stress 3D 2 Comp Fine mesh [MPa]**	**σ_x Fine 2C/3D Full**	**Max σ_{vonM} Stress 3D Full [MPa]**	**Max σ_{vonM} Stress 3D 2 Comp Fine mesh [MPa]**	**σ_{vonM} Fine 2C/3D Full**
Hogging 8.123	241.20	321.57	1.33	217.80	294.76	1.35
Sagging 8.123	329.90	389.90	1.18	297.90	371.64	1.25

Table.8.3.19. Maximum Hogging and Sagging stresses , on Bottom elements, based on comparison between the two cargo holds compartments 3D-FEM fine mesh and the full extended models, h_w=8.123 m

h_w	**Max σ_x Stress 3D Full [MPa]**	**Max σ_x Stress 3D 2 Comp Fine mesh [MPa]**	**σ_x Fine 2C/3D Full**	**Max σ_{vonM} Stress 3D Full [MPa]**	**Max σ_{vonM} Stress 3D 2 Comp Fine mesh [MPa]**	**σ_{vonM} Fine 2C/3D Full**
Hogging 8.123	94.89	109.30	1.15	85.62	100.40	1.17
Sagging 8.123	111.30	120.70	1.08	106.50	107.80	1.01

Table.8.3.20. Maximum Hogging and Sagging stresses , on Side elements, based on comparison between the two cargo holds compartments 3D-FEM fine mesh and the full extended models, h_w=8.123m

h_w	**Maximum τ_{xz} Stress 3D Full [MPa]**	**Maximum τ_{xz} Stress 3D 2 Comp Fine Mesh [MPa]**	$\frac{\tau xz \text{ Fine Mesh 2 } Comp}{\tau xz \ 3D \ Full}$
Hogging 8.123	34.70	36.52	1.05
Sagging 8.123	47.85	42.41	0.89

From Tables 8.3.18, 8.3.19 and 8.3.20, comparing the two cargo holds compartments 3D-FEM fine mesh model, with Hotspot correction (eq 2.3.5.) and the Full extended 3D-FEM model, it results higher stresses: deck 18-35%, bottom 1-17% and side -11 - 5%. The maximum hotspots are again obtained for the deck liquid cargo inlet hatch, being the domain where fatigue should be first analysed.

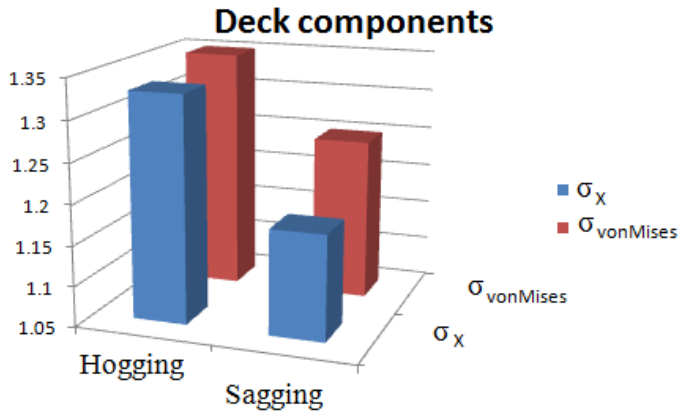

Fig 8.3.15. Hogging and Sagging stresses rapport , on Deck elements, based on comparison between the two cargo holds compartments 3D-FEM fine mesh model and the Full extended 3D-FEM model, h_w=8.123 m

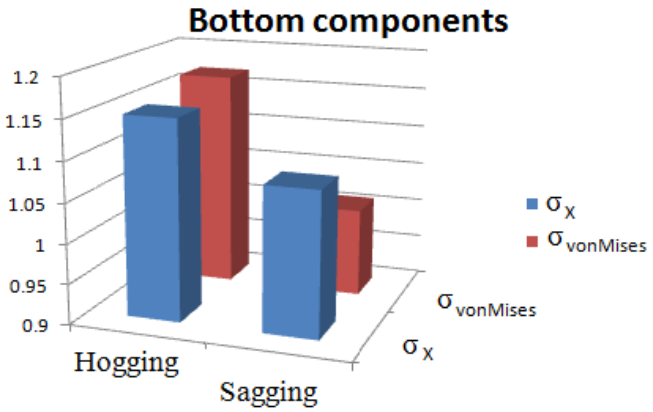

Fig. 8.3.16. Hogging and Sagging stresses rapport , on Bottom elements, based on comparison between the two cargo holds compartments 3D-FEM model and the Full extended 3D-FEM model, h_w=8.123 m

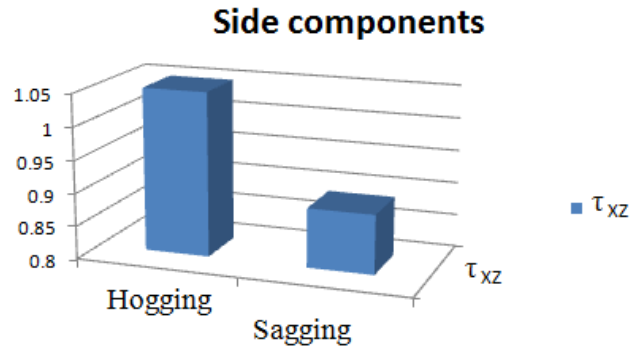

Fig.8.3.17. Hogging and Sagging stresses rapport , on Side elements, based on comparison between the two cargo holds compartments 3D-FEM model and the Full extended 3D-FEM model, h_w=8.123 m

9.COMPARATIVE RESULTS AND CONCLUSIONS

Based on the 1D Equivalent Beam Model and the 3D-FEM Full Extended and Two Cargo Holds Compartments Models numerical analysis that were performed in the previous chapters, the following main conclusions result:

- ✓ The 1D Equivalent Beam Model does not take into account the hotspots areas, but it high lines the most stressed panels in the ship model from the global strength criteria point of view.
- ✓ The 3D-FEM full extended model or the two cargo hold compartments model will lead to similar results, using for equilibrium condition different approaches, if it is used the same mesh-size, same local loads idealization and on the extremities ends of the two cargo hold compartments model the corresponding equivalent global loads are applied. For the two cargo holds compartments 3D-FEM model there were used equilibrium parameters based on the 1D equivalent beam model, instead of directly computed parameters based on full extended 3D-FEM model.
- ✓ The data for a future research in terms of fatigue analysis can be prepared, for the evaluation of the stress hotspot areas, based on the two cargo holds compartments 3D-FEM model, with local refinements (finer mesh size) of the structural components in the specific area.

A comparison between deformations and stress levels obtained with the structural models, having different complexity levels, can be performed based on this study.

Note. In the following tables are used the next marks :

- *1D Beam Model* refers to the numerical results from sub-chapter 5.2, 5.3. and appendix A.5.2, A.5.3.
- *3D-FEM Full Extended Model* refers to the numerical results from sub-chapter 6.4, 6.6. and appendix A.6.1, A.6.2.
- *3D-FEM Two Cargo Holds Compartments Model with Coarse Mesh (2C - coarse)* refers to the numerical results from sub-chapter 7.3. and appendix A.7.
- *3D-FEM Two Cargo Holds Compartments Model with Fine Mesh (2C – fine)* refers to the numerical results from sub-chapter 8.3. and appendix A.8.

Table.9.1. Maximum Hogging stresses based on 1D beam, 3D-FEM full extended and 3D-FEM two cargo holds compartments, coarse and fine mesh, models comparison, reference wave h_{wmax}=8.123 m

Panel stress	Stress 1D Beam [MPa]	Stress 3D FEM Full Extended [MPa]	Stress 3D 2C Coarse Mesh [MPa]	Stress 3D 2C Fine Mesh [MPa]	3D-FEM Full Extended and 1D Beam Stress Ratio	3D-FEM 2C Coarse Mesh and 1D Beam Stress Ratio	3D-FEM 2C Fine Mesh and 1D Beam Stress Ratio
Maximum σ_x deck	98.25	241.20	257.90	321.57	2.45	2.62	3.27
Maximum σ_{vonM} deck	98.25	217.80	233.00	294.76	2.21	2.37	3.00
Maximum σ_x bottom	71.27	94.89	98.01	109.30	1.33	1.38	1.53
Maximum σ_{vonM} bottom	71.27	85.62	88.60	100.40	1.20	1.24	1.41
Maximum τ_{xz} side	40.09	34.70	35.78	36.52	0.86	0.89	0.91

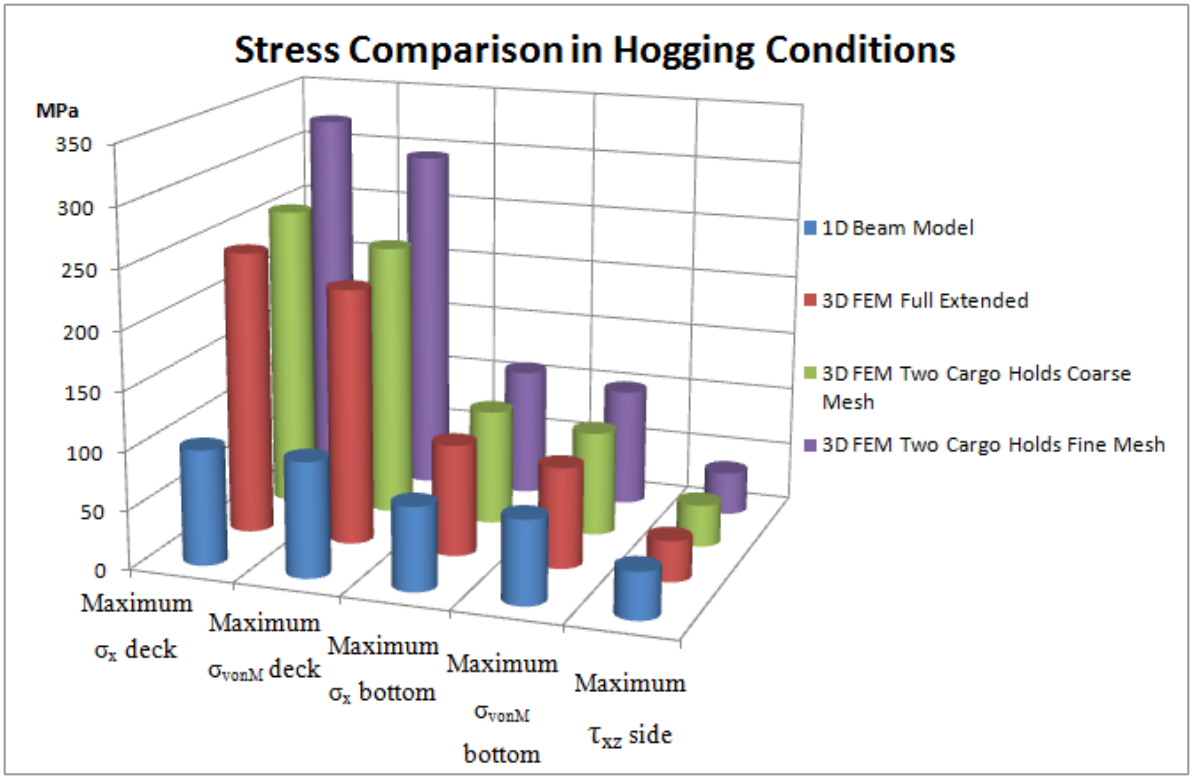

Fig.9.1. Stress comparison on all components for each numerical model analysed in wave Hogging conditions, reference wave h_{wmax}=8.123 m

Table.9.2. Maximum Sagging stresses based on 1D beam, 3D-FEM full extended and 3D-FEM two cargo holds compartments, coarse and fine mesh, models comparison, reference wave h_{wmax}=8.123 m

Panel stress	Stress 1D Beam [MPa]	Stress 3D FEM Full Extended [MPa]	Stress 3D 2C Coarse Mesh [MPa]	Stress 3D 2C Fine Mesh [MPa]	3D-FEM Full Extended and 1D Beam Stress Ratio	3D-FEM 2C Coarse Mesh and 1D Beam Stress Ratio	3D-FEM 2C Fine Mesh and 1D Beam Stress Ratio
Maximum σ_x deck	121.17	329.90	321.30	389.90	2.72	2.65	3.22
Maximum σ_{vonM} deck	121.17	297.90	290.10	371.64	2.46	2.39	3.07
Maximum σ_x bottom	87.90	111.30	118.90	120.70	1.27	1.35	1.37
Maximum σ_{vonM} bottom	87.90	106.50	105.46	107.80	1.21	1.20	1.23
Maximum τ_{xz} side	48.27	47.85	42.36	42.41	0.99	0.88	0.88

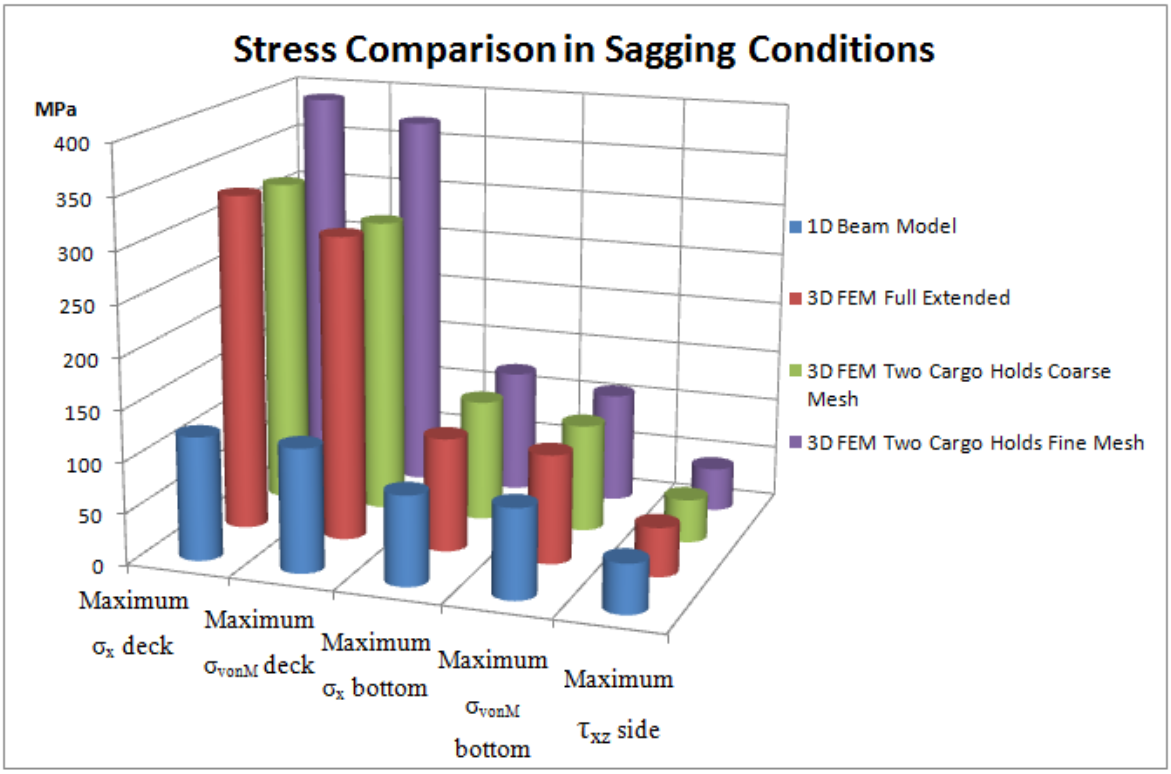

Fig.9.2. Stress comparison on all components for each numerical model analysed in Sagging conditions, reference wave h_{wmax}=8.123 m

From Table.9.1., at the hogging condition, the stress ratio between 3D-FEM two cargo holds compartment model, with coarse mesh size, and 3D-FEM full extended model are: 2.21 - 2.62 for deck, 1.20-1.38 for bottom, pointing out the hotspots occurrence. The side tangential stress ratio is close to 1, values 0.86-0.89, due to the fact that the neutral axis tangential stress coefficient in the 1D equivalent beam model has been obtained as an average value on beam model and because the hot-spots at the side panels are reduced. Comparing the 3D-FEM two cargo holds compartments Coarse Mesh size and Fine mesh Size models, it results that the stresses are higher for the fine mesh with 24.8-26.6 % at deck, 10.8-13.7 % at bottom and very small changes 2.2 % at the side neutral axis (with less hot-spots).

From Table.9.2., at the sagging condition, the stress ratio between 3D-FEM two cargo holds compartment model, with coarse mesh size, and 3D-FEM full extended model are: 2.39-2.72 for deck, 1.20-1.35 for bottom, pointing out the hot-spots occurrence. The side tangential stress ratio is close to 1, values 0.88-0.99, due to the fact that the neutral axis tangential stress coefficient in the 1D equivalent beam model has been obtained as an average value on beam model and because the hot-spots in the side panels are very reduced. Comparing the 3D-FEM two cargo holds compartments Coarse Mesh size and Fine Mesh size models, it results that the stresses are higher for the fine mesh with 21.5-28.4 % at deck, 1.5-2.5 % at bottom and without changes at the side neutral axis (less hot-spots).

As it can be easily observed from the two Figures, 9.1. and 9.2., the results obtained based on the 3D-FEM full extended model and the 3D FEM two cargo holds compartments model, with coarse mesh size, they both have similar stress value for all the analysed components, from deck, bottom and side panels. By this similarity of stresses the boundary conditions and global-local loads used for the 3D FEM two cargo holds compartments model are validated, being applied also for the analysis with 3D FEM two cargo holds compartments model with fine mesh size.

The 3D FEM fine mesh size model is pointing out the hot-spots stress areas which appear on the deck panels around the liquid cargo inlet hatch. The highest stress values were obtain in both hogging and sagging wave condition cases, in the deck elements, the normal stress σ_x components reaching 321.57 MPa in hogging conditions and 389.90 MPa in sagging conditions. Also high values were obtained for the equivalent vonMises stress σ_{von}, 294.76 MPa in hogging and 371.64 MPa in sagging conditions, both stress components values resulting at the cargo inlet hatch stress hot-spots area.

The deck cargo inlet hatch structural region may require further analysis and improvement of the structural elements, by adding additional stiffening and/or increasing the plate thickness.

It can also be observed for the tangential stresses on the side panels that the results are similar within all the analysis performed, including the 1D equivalent beam model. There are minor differences because at the side panels the stress hot-spots are very reduced.

The 1D-equivalent beam model provides the global equilibrium parameters for the 3D-FEM two cargo holds compartments models, both fine and coarse mesh size, with very similar equilibrium parameters values as for the 3D-FEM full extended model. Although it does not include the stress hot-spot areas, the 1D equivalent beam model offers an preliminary global strength analysis and reliable ship-wave equilibrium parameters.

In conclusion, by using the user subroutines developed with Solid Works Cosmos/M 2007 FEM software, the numerical FEM analysis provides reliable data for the ship strength assessment (under equivalent quasi-static head waves), having a good concordance between the structural models developed in this study. For further studies, as fatigue analysis, should combine the advantages of the four structural models analysed in this work, taking into account the sensitivity of the ship hull structure models, for higher risk panels identification.

This work will be further developed by systematic stress hot-spots sensitivity evaluation, as required for local fatigue analysis, based on the 3D-FEM two cargo hold compartments models, with different mesh sizes.

10. ACKNOWLEDGEMENTS

I would like to mention in the beginning that I am very grateful to be part of the Erasmus Mundus Master programme, EMship, which provided me knowledge in ship domain, upgrading from the mechanical engineering domain, and also for the financial support during the studies, providing the scholarship. I would like to have the pleasure of personally transmit my appreciation to all the founders and organisers of the EMship Master course, especially to prof. Philippe Rigo and prof. Andre Hage at Universite de Liege, prof. Pierre Ferrant and prof. Lionel Gentaz at Ecole Centrale du Nantes and prof. Adrian Lungu at University Dunarea de Jos, Galati.

Also many sincere appreciations to my advisor of the master thesis, prof. Domnisoru Leonard, for constant support, indications, advices and technical materials provided during the master thesis development at the University "Dunarea de Jos", of Galati, Naval Architecture Faculty.

I would like to thank to the internship supervisor, Dr. Ionas Ovidiu, for kindly guiding me through the process of ship designing in different stages, and for the technical material provided to develop the model used in the thesis, in the company Ship Design Group, Galati.

This thesis was developed in the frame of the European Master Course in “Integrated Advanced Ship Design” named “EMSHIP” for “European Education in Advanced Ship Design”, Ref.: 159652-1-2009-1-BE-ERA MUNDUS-EMMC.

11. REFERENCES

[1] Baguley D.,Hose D.R.,1997. *How to Interpret Finite Element Results*, NAFEMS, Bell and Bain Ltd, Glasgow

[2] Bathe K.J., 1990. *Finite Elemente Methoden*, Springer Verlag, Berlin

[3] Bidoae R., Ionas O., 2004. *The Naval Architecture*, The Didactic and Pedagogic Publishing House, Bucharest

[4] Bureau Veritas, 2010. *Shipbuilding Classification Society Rules*

[5] Carlos Guedes Soares, Purnendu K. Das (Editors), 2007. *Advancements in Marine Structures*, Taylor& Francis Group, London, ISBN978-0-415-43725-7

[6] Cook R.D.,Malkus D.S.,Plesha M.E., 1989. *Concepts and Applications of Finite Element Analysis*, John Wiley & Sons Inc.,New York

[7] Domnisoru L., 2006. *Structural Analysis and Hydroelasticity of Ships*, The University Foundation „Dunarea de Jos" Publishing House Galati

[8] Domnisoru L., 2001. *The Finite Element Method in Shipbuilding*, The Technical Publishing House, Bucharest

[9] Domnisoru L., Stoicescu L., 2004-2005.*The Analysis of the Global Ship Strengths in Vertical Plane with 1D-Equivalent Girder and 3D-FEM Hull Models. Comparative Study of the two Methods*, WP.2 / Task 2.1.1 Advance Finite Element Modelling and Analysis, Grant EU Marstruct-FP6 Network of Excellence on Marine Structures, Code TNE3-CT-2003-506141

[10] Domnisoru L., Gavan E., Popovici O., 2005. *The Analysis of the Ship Structures with the Finite Element Method*, The Didactic and Pedagogic Publishing House, Bucharest

[11] Frieze, P.A., Shenoi, R.A. (editors) , 2006. *Proceedings of the 16-th International Ship and Offshore Structures Congress - ISSC*, University of Southampton

[12] Hage A.,2011. *Lecture Notes of Ship Design*, EMship Master Course, (University of Liege, ANAST)

[13] Hughes, O.F.,1988. *Ship structural design. A rationally-based, Computer-Aided Optimization Approach*, The Society of Naval Architects and Marine Engineers, New Jersey

[14] Ionas O., Domnisoru L.,Gavrilescu I.,Dragomir D. , 1999. *Calculation Techniques in Shipbuilding*, The Evrika Publishing House, Braila

[15] Modiga M., Dimache A., Olaru D., 2005. *Ship Structures Static*, The Academic Publishing House, Galati

[16] Obreja D., 2005. *Ship Theory. Concepts and methods for the analyse of sailing performances*, The Didactic and Pedagogic Publishing House, Bucharest

[17] Reddy, J.N., 2006. *An Introduction to the Finite Elemenent Method*, McGraw-Hill, New York

[18] Rigo P., Rizzuto E., Analysis and Design of Ship Structure, *Chap 18 of " Ship Design and Construction", Editor T Lamb, SNAME*

[19] Rozbicki, M., Das Purnendu, K., Crow, A., 2001. *The preliminary finite element modelling of a full ship*, International Shipbuilding Progress Delft 48(2), pp.213-225

[20] Servis, D., Voudouris, G., Samuelides, M., Papanikolaou, A., 2003. *Finite element modelling and strength analysis of hold no.1 of bulk carriers*, Marine Structures 16, pp.601-626

[21] Stoicescu L., Domnisoru L., 2007. *Global strength analysis in head waves, for a tanker with longitudinal uniform structure*, The Proceedings of MARSTRUCT 2007, International Conference on Advancements in Marine Structures, Glasgow, Taylor & Francis Group, London, pp.283-294

[22] Technical information regarding the Chemical Tanker 4000 tones prototype ship (2007) Granted by Ship Design Group Galati (www.shipdesigngroup.eu)

[23] Tetsuya, Yao., 2003. *Hull girder strength*, Marine Structures 16, pp.1-13

[24] Zienkiewicz, O.C., Taylor, R.L. , 1988. *The finite element method. Basic formulation and linear problems*, McGraw-Hill Book Company, London

[25] Zienkiewicz, O.C., Taylor, R.L., 1989. *The Finite Element Method. Solid and Fluid Mechanics. Dynamics and Non-Linearity*, McGraw-Hill Book Company, London

- **Analysis Tools:**

P_ACASV version 5, developed at “Dunarea de Jos” University of Galati (Domnisoru, 2006);
Rhinoceros 2006 - academic trial licence;
AutoCAD 2011- academic licence;
Artlantis Studio 4 - academic trial licence;
Solid Works Cosmos/M 2007 - licence at "Dunarea de Jos" University of Galati;

12. APPENDIX

A1.1. Macro-command Files Procedures, Implemented in Solid Works Comos/ M 2007 Software "Press" Hogging/Sagging for Full Extended 3D-FEM Model (Equivalent Wave Hydrostatic Pressure on the Hull Shell)

```
C* **WITH TRIMM
  parassign,Lenght,real,109.6108
  parassign,xFw,real,-0.25
  parassign,Hw,real,-8.123
  parassign,dmax,real,8.6
  parassign,NDpp,int,31061
  parassign,NDpv,int,46016
  CALLMACRO,IN_EL
C*
C* STEP 1 NO TRIMM
C*  (dsw=0.0)
  parassign,dsw,real,3.2
  parassign,RFZpp,real,2.0
  parassign,RFZpv,real,-1.0
  parassign,REZEQ,real,1.0
  parassign,REZEQ1,real,1E+15
#LABEL LAB1
  #if (ABS(REZEQ)>0.1)
       parassign,dsw,real,(dsw+0.05)
       #if (dsw>dmax)
        #GOTO LAB2
       #endif
     CALLMACRO,DEL_press
     CALLMACRO,EG_press,dsw,Lenght,Hw
     A_STATIC,G,
     R_STATIC
     parassign,RFZpp,real,RFZ(1|NDpp|0)
     parassign,RFZpv,real,RFZ(1|NDpv|0)
     parassign,REZEQ,real,(RFZpp+RFZpv)
     parlist,*
     #if (REZEQ<0)
      parassign,dsw,real,(dsw-0.05)+0.05/(REZEQ-REZEQ1)*(0-REZEQ1)
       CALLMACRO,DEL_press
       CALLMACRO,EG_press,dsw,Lenght,Hw
       A_STATIC,G,
       R_STATIC
       parassign,RFZpp,real,RFZ(1|NDpp|0)
       parassign,RFZpv,real,RFZ(1|NDpv|0)
       parassign,REZEQ,real,(RFZpp+RFZpv)
       parassign,REZEQ1,real,REZEQ
      #GOTO LAB2
     #endif
     parassign,REZEQ1,real,REZEQ
```

```
  #else
    #GOTO LAB2
  #endif
#GOTO LAB1
#LABEL LAB2
parlist,*
C*
C* STEP 2 WITH TRIMM
  parassign,RFZpv1,real,RFZpv
  #if (RFZpv>RFZpp)
    parassign,semn1,int,1
  #endif
  #if (RFZpv<RFZpp)
    parassign,semn1,int,-1
  #endif
  #if ((ABS(RFZpv)<0.1) && (ABS(RFZpp)<0.1))
    parassign,semn1,int,0
    parassign,semn,int,0
    #GOTO LAB3
  #endif
C*
   parassign,trimm,real,0.0
#LABEL LAB4
  #if (RFZpv>RFZpp)
    parassign,semn,int,1
  #endif
  #if (RFZpv<RFZpp)
    parassign,semn,int,-1
  #endif
  #if ((ABS(RFZpv)<0.1)&&(ABS(RFZpp)<0.1))
    parassign,semn,int,0
    #GOTO LAB3
  #endif
  #if (semn!=semn1)
 parassign,trimm,real,(trimm-0.001*semn1)+(0.001*semn1)/(RFZpv-RFZpv1)*(0-RFZpv1)
   parassign,dpp,real,dsw-(Lenght/2+xFw)*trimm
   parassign,dpv,real,dsw+(Lenght/2-xFw)*trimm
      CALLMACRO,DEL_press
      CALLMACRO,EG_press2,dpp,dpv,Lenght,Hw
      A_STATIC,G,
      R_STATIC
      parassign,RFZpp,real,RFZ(1|NDpp|0)
      parassign,RFZpv,real,RFZ(1|NDpv|0)
      parassign,REZEQ,real,(RFZpp+RFZpv)
    #GOTO LAB3
  #endif
C*
  parassign,RFZpv1,real,RFZpv
  parassign,trimm,real,trimm+0.001*semn
       #if (ABS(trimm)>0.5)
```

```
        #GOTO LAB3
       #endif
  parassign,dpp,real,dsw-(Lenght/2+xFw)*trimm
  parassign,dpv,real,dsw+(Lenght/2-xFw)*trimm
    CALLMACRO,DEL_press
    CALLMACRO,EG_press2,dpp,dpv,Lenght,Hw
    A_STATIC,G,
    R_STATIC
    parassign,RFZpp,real,RFZ(1|NDpp|0)
    parassign,RFZpv,real,RFZ(1|NDpv|0)
    parassign,REZEQ,real,(RFZpp+RFZpv)
    parlist,*
#GOTO LAB4
#LABEL LAB3
parlist,*
    CALLMACRO,OUT_EL
```

A.1.2 Macro-command Files Procedures, Implemented in Solid Works Comos/ M 2007 Software "EL_DBS" to Select the Shell Plating for the Full Extended 3D FEM Model

```
C* Group Deck 9,10
INITSEL,EL,1,1
ACTSET,SEL,1,
ESELPROP,RC,121,122,1,1
ESELPROP,RC,229,230,1,1
ESELPROP,RC,327,328,1,1
ESELPROP,RC,426,427,1,1
ESELPROP,RC,524,525,1,1
ESELPROP,RC,621,622,1,1
EGROUP,9,SHELL3T,0,0,0,0,0,0,0,0
EPROPCHANGE,1,ELMAX,1,EG,9,8
INITSEL,EL,1,1
ACTSET,SEL,1,
ESELPROP,RC,726,726,1,1
EGROUP,10,SHELL3T,0,0,0,0,0,0,0,0
EPROPCHANGE,1,ELMAX,1,EG,10,8
INITSEL,EL,1,1
C* Bottom 11
ACTSET,SEL,1,
ESELPROP,RC,101,102,1,1
ESELPROP,RC,202,203,1,1
ESELPROP,RC,209,209,1,1
ESELPROP,RC,302,303,1,1
ESELPROP,RC,353,353,1,1
ESELPROP,RC,402,403,1,1
ESELPROP,RC,453,453,1,1
ESELPROP,RC,502,503,1,1
ESELPROP,RC,543,543,1,1
ESELPROP,RC,602,603,1,1
```

```
ESELPROP,RC,604,604,1,1
ESELPROP,RC,701,702,1,1
EGROUP,11,SHELL3T,0,0,0,0,0,0,0,0
EPROPCHANGE,1,ELMAX,1,EG,11,8
C* Side 12
INITSEL,EL,1,2
ACTSET,SEL,2,
ESELPROP,RC,111,112,1,2
ESELPROP,RC,218,218,1,2
ESELPROP,RC,316,316,1,2
ESELPROP,RC,415,415,1,2
ESELPROP,RC,515,515,1,2
ESELPROP,RC,544,544,1,2
ESELPROP,RC,612,613,1,2
ESELPROP,RC,715,717,1,2
EGROUP,12,SHELL3T,0,0,0,0,0,0,0,0
EPROPCHANGE,1,ELMAX,1,EG,12,8
C*
INITSEL,EL,1,1
INITSEL,EL,1,2
C* Nodes selection
INITSEL,EL,1,1
ACTSET,SEL,1,
ESELPROP,EG,9,10,1,1
SELREF,ND,EL,1,ELMAX,1,1
INITSEL,EL,1,2
ACTSET,SEL,2,
ESELPROP,EG,11,11,1,2
SELREF,ND,EL,1,ELMAX,1,1
INITSEL,EL,1,3
ACTSET,SEL,3,
ESELPROP,EG,12,12,1,3
SELREF,ND,EL,1,ELMAX,1,1
C*
INITSEL,EL,1,4
ACTSET,SEL,4,
SELRANGE,EL,0,1,1,1,18.57,99.42,0,6.7504,0,10.0999,4
C*
```

A.1.3. The "Geomacro.mac" File GEO Procedures Library Developed for the Support of GEO Macro-Commands Files

```
C* ***Hydrostatic pressure
C* ***with flat free surface KN/m2
$macro,hst_press
  parassign,Tief,real,0.0
  parassign,density,real,1.025
  parassign,sgn,int,1
  CALLMACRO,hst_shell,Tief,density,sgn
$ENDM

$macro,hst_shell,Tief,density,sgn
parassign,csid,int,0
parassign,i,int,0
#loop LB1 ELMAX
  parassign,i,int,i+1
  #if (exist(EL|i) && listsel(EL|i))
    parassign,fnum,int,0
    parassign,z,real,ZELF(i|fnum|csid)
    parassign,pval,real,((Tief-z)*density*9.81)
    parassign,fnum,int,5
    #if (pval>0)
      parassign,pval,real,(pval*sgn)
      PEL,i,pval,fnum,i,1,4
    #endif
  #endif
#label LB1
$ENDM
C* ***End Hydrostatic pressure

C* ***INOUT Elements Groups
$macro,IN_EL
  INITSEL,EL,1,10
  ESELPROP,EG,2,8,1,10
$ENDM

$macro,OUT_EL
  INITSEL,EL,1,10
$ENDM

$macro,DEL_press
  PEDEL,1,5,ELMAX,1
$ENDM
C* ***End INOUT Elements

C* ***FLUIDS_EQ1_WAVES (NO TRIMM)
$macro,EG_press,dsw,Lenght,Hw
  parassign,sgn,int,1
  CALLMACRO,sin_shell,dsw,Lenght,Hw,sgn
```

```
$ENDM

C* ***Hydrostatic pressure
C* ***sin free surface KN/m2
$macro,sin_press
  parassign,dsw,real,0.0
  parassign,Lenght,real,0.0
  parassign,Hw,real,0.0
  parassign,sgn,int,1
  CALLMACRO,sin_shell,dsw,Lenght,Hw,sgn
$ENDM

$macro,sin_shell,dsw,Lenght,Hw,sgn
parassign,csid,int,0
parassign,i,int,0
#loop LB1 ELMAX
  parassign,i,int,i+1
  #if (exist(EL|i) && listsel(EL|i))
    parassign,fnum,int,0
    parassign,z,real,ZELF(i|fnum|csid)
    parassign,x,real,XELF(i|fnum|csid)
parassign,Tief,real,(dsw+Hw/2*COS((2*PI*x/Lenght)))
    parassign,pval,real,((Tief-z)*1.025*9.81)
    parassign,fnum,int,5
    #if (pval>0)
      parassign,pval,real,(pval*sgn)
      PEL,i,pval,fnum,i,1,4
    #endif
  #endif
#label LB1
$ENDM
C* ******End Fluids EQ1

C* ***FLUIDE_EQ2_WAVES (WITH TRIMM)
$macro,EG_press2,dpp,dpv,Lenght,Hw
  parassign,sgn,int,1
CALLMACRO,sin_shell2,dpp,dpv,Lenght,Hw,sgn
$ENDM

C* ***Hydrostatic pressure (with trimm)  sin free surface KN/m2
$macro,sin_press2
  parassign,dpp,real,0.0
  parassign,dpv,real,0.0
  parassign,Lenght,real,0.0
  parassign,Hw,real,0.0
  parassign,sgn,int,1
CALLMACRO,sin_shell2,dpp,dpv,Lenght,Hw,sgn
$ENDM

$macro,sin_shell2,dpp,dpv,Lenght,Hw,sgn
```

```
parassign,csid,int,0
parassign,i,int,0
#loop LB1 ELMAX
  parassign,i,int,i+1
  #if (exist(EL|i) && listsel(EL|i))
    parassign,fnum,int,0
    parassign,z,real,ZELF(i|fnum|csid)
    parassign,x,real,XELF(i|fnum|csid)
    parassign,Tief,real,dpp+(dpv-dpp)/Lenght*x
 parassign,Tief,real,Tief+Hw/2*COS((2*PI*x/Lenght))
    parassign,pval,real,((Tief-z)*1.025*9.81)
    parassign,fnum,int,5
    #if (pval>0)
      parassign,pval,real,(pval*sgn)
      PEL,i,pval,fnum,i,1,4
    #endif
  #endif
#label LB1
$ENDM
C* ******End Fluids EQ2
```

A.2.1 Macro-command Files Procedures, Implemented in Solid Works Comos/ M 2007 Software "EL_DBS_LE_TK" to Create the Selection of the Plating for the Two Cargo Holds Compartments 3D-FEM Model

```
C* Group Deck 11,12
INITSEL,EL,1,1
ACTSET,SEL,1,
ESELPROP,RC,121,122,1,1
ESELPROP,RC,229,230,1,1
ESELPROP,RC,327,328,1,1
ESELPROP,RC,426,427,1,1
ESELPROP,RC,524,525,1,1
ESELPROP,RC,621,622,1,1
EGROUP,11,SHELL3T,0,0,0,0,0,0,0,0
EPROPCHANGE,1,ELMAX,1,EG,11,8
INITSEL,EL,1,1
ACTSET,SEL,1,
ESELPROP,RC,726,726,1,1
EGROUP,12,SHELL3T,0,0,0,0,0,0,0,0
EPROPCHANGE,1,ELMAX,1,EG,12,8
INITSEL,EL,1,1
C* Bottom 13
ACTSET,SEL,1,
ESELPROP,RC,101,102,1,1
ESELPROP,RC,202,203,1,1
ESELPROP,RC,209,209,1,1
ESELPROP,RC,302,303,1,1
ESELPROP,RC,353,353,1,1
ESELPROP,RC,402,403,1,1
```

```
ESELPROP,RC,453,453,1,1
ESELPROP,RC,502,503,1,1
ESELPROP,RC,543,543,1,1
ESELPROP,RC,602,603,1,1
ESELPROP,RC,604,604,1,1
ESELPROP,RC,701,702,1,1
EGROUP,13,SHELL3T,0,0,0,0,0,0,0,0
EPROPCHANGE,1,ELMAX,1,EG,13,8
C* Side 14
INITSEL,EL,1,2
ACTSET,SEL,2,
ESELPROP,RC,111,112,1,2
ESELPROP,RC,218,218,1,2
ESELPROP,RC,316,316,1,2
ESELPROP,RC,415,415,1,2
ESELPROP,RC,515,515,1,2
ESELPROP,RC,544,544,1,2
ESELPROP,RC,612,613,1,2
ESELPROP,RC,715,717,1,2
EGROUP,14,SHELL3T,0,0,0,0,0,0,0,0
EPROPCHANGE,1,ELMAX,1,EG,14,8
C*
INITSEL,EL,1,1
INITSEL,EL,1,2
C* Nodes selection
INITSEL,EL,1,1
ACTSET,SEL,1,
ESELPROP,EG,11,12,1,1
SELREF,ND,EL,1,ELMAX,1,1
INITSEL,EL,1,2
ACTSET,SEL,2,
ESELPROP,EG,13,13,1,2
SELREF,ND,EL,1,ELMAX,1,1
INITSEL,EL,1,3
ACTSET,SEL,3,
ESELPROP,EG,14,14,1,3
SELREF,ND,EL,1,ELMAX,1,1
C*
```

A.2.2. Macro-command Files Procedures, Implemented in Solid Works Comos/ M 2007 Software "Press" Hogging/Sagging for Two Cargo Holds Compartments 3D-FEM Model (Equivalent Wave Hydrostatic Pressure on the Hull Shell)

```
C* **WITH TRIMM [KN,t,m]

C* - Hw hogg, +Hw sagg
parassign,Hw,real,0.0

parassign,dpp,real,4.26970
parassign,dpv,real,4.57661

C* xpp=0 model has correct position
parassign,Lenght,real,109.611
parassign,xpp,real,0.0
parassign,ro,real,1.025
parassign,NDpp,int,22451
parassign,NDpv,int,22452

C* xpp=31.712m UZpp=0.006580
DND,NDpp,UZ,0,NDpp,1;
DND,NDpp,RY,-0.000089,NDpp,1;

C* xpv=80.224m UZpv=0.005363
DND,NDpv,UZ,-0.001217,NDpv,1;
DND,NDpv,RY,0.000147,NDpv,1;


CALLMACRO,IN_EL
CALLMACRO,sin_shell,dpp,dpv,Lenght,xpp,ro,Hw
CALLMACRO,OUT_EL

A_STATIC,G,
R_STATIC
parlist,*
```

A.3.1 Macro-Command Files Procedures, Implemented in Solid Works Comos/ M 2007 Software "GPoint" to add Points in Nodes for Boundary Conditions (Two Cargo Holds Compartments 3D-FEM Model) "GPOINT.GEO"

```
C* PUT POINTS IN NODES
parassign,i,int,0
parassign,j,int,PTMAX
#loop LB1 NDMAX
  parassign,i,int,i+1
  #if (exist(ND|i) && listsel(ND|i))
```

```
    parassign,j,int,j+1
    PTND,j,i
  #endif
#label LB1
```

A.3.2. Macro-Command Files Procedures, Implemented in Solid Works Comos/ M 2007 Software "Curves.PP" Creates Lines Between Nodes for Two Cargo Holds Compartments 3D-FEM Model

```
 C* PUT CURVES
parassign,PP,int,306
parassign,i,int,0
parassign,j,int,CRMAX
#loop LB1 PTMAX
  parassign,i,int,i+1
  #if (exist(PT|i) && listsel(PT|i))
    parassign,j,int,j+1
    CRLINE,j,PP,i
  #endif
#label LB1
```

A.4. The Plate Thickness for Each Block of the 3D-CAD Model Generation, Chapter 4.

Table.A.4.1. Layers and thickness of block 1

RC	dxf	3D Face	Gross thk.
no.	file	no.	[mm]
Aft Block 1			
101	Z1_102_Bottom_pl_10	184	10.0
102	Z1_103_Bottom_pl_15	31	15.0
103	Z1_110_DB_GD_pd_web_6	14	6.0
104	Z1_111_DB_GD_fl_15	4	15.0
105	Z1_130_DB_Gd_wb_12	38	12.0
106	Z1_131_DB_gd_fl_15	34	15.0
107	Z1_132_DB_Gd_wb_10	4	10.0
108	Z1_133_DB_gd_fl_12	4	12.0
109	Z1_134_DB_GD_wb_8	12	8.0
110	Z1_135_DB_gd_fl_10	24	10.0
111	Z1_201_Shell_pl_12	132	12.0
112	Z1_202_Shell_pl_10	32	10.0
113	Z1_210_Shell_Frame_HP160x9	40	9.0
114	Z1_211_Shel_frame_wb_10	87	10.0
115	Z1_212_Shell_frame_fl_120x12	80	12.0
116	Z1_213_Shell_frame_fl_100x12	20	12.0
117	Z1_214_Shell_frame_wb_12	4	12.0

118	Z1_215_Shell_frame_fl_150x15	8	15.0
119	Z1_230_Shell_gd_wb_10	30	10.0
120	Z1_231_Shell_gd_fl_12	30	12.0
121	Z1_301_Mdk_pl_9	170	9.0
122	Z1_302_MDK_pl_12	31	12.0
123	Z1_310_MDK_fr_wb_10	173	10.0
124	Z1_311_MDK_fr_fl_120x12	72	12.0
125	Z1_320_MDK_GD_wb_10	37	10.0
126	Z1_321_MDK_GD_FL_12	143	12.0
127	Z1_322_MDK_GD_PD_wb_5	5	5.0
128	Z1_330_MDK_long_HP120x8	112	8.0
129	Z1_331_MDK_long_HP140x8	16	8.0
130	Z1_332_MDK_long_PD_HP120x8(pd)	9	4.0
131	z1_401_bhd_FR12_WALL_8	74	8.0
132	Z1_402_BHD_wall_12	61	12.0
133	Z1_403_BHD_Wall_10	336	10.0
134	Z1_404_BHD_wall_15	20	15.0
135	Z1_405_BHD_Wall_12	12	12.0
136	Z1_410_bhd_orizontal_PL_8	132	8.0
137	Z1_411_BHD_vertical_pl8	37	8.0
138	Z1_412_BHD_orizontal_pl_10	88	10.0
139	Z1_413_BHD_vertical_pl_10	28	10.0
140	Z1_414_BHD_vertical_pl_18	4	18.0
141	Z1_416_BHD_vertical_pl_12	4	12.0
142	Z1_417_BHD_vertical_PD_pl_5	15	5.0
143	Z1_420_BHD_frame_wb_8	21	8.0
144	Z1_430_BHD_vertical_HP160x9	98	9.0
145	Z1_431_BHD_vertical_HP120x8	24	8.0
146	Z1_432_BHD_oriz_HP120x8	10	8.0
147	Z1_433_BHD_vertical_PD_HP120x8(pd)	1	4.0

Table.A.4.2. Layers and thickness of block 2

RC	**DXF**	**3D Face**	**Gross thk.**
no.	file	no.	[mm]
Midship Block 2			
201	Z2_100_DB_top_pl_10	157	10.0
202	Z2_101_DB_Bilge_pl_10	58	10.0
203	Z2_102_DB_Bott_pl_10	144	10.0
204	Z2_103_DB_GDcent_12	3	12.0
205	Z2_104_DB_GD_9	55	9.0
206	Z2_105_DB__wall_pl_10	41	10.0
207	Z2_106_DB_Tank_pl_10	81	10.0

208	Z2_107_DB_GDcentPD_6	25	6.0
209	Z2_108_Bott_pl_12	21	12.0
210	Z2_120_DB_Frame_wb_10	41	10.0
211	Z2_122_DB_Frame_wb_9	388	9.0
212	Z2_130_DB_Bilge_longHP160x9	15	9.0
213	Z2_131_DB_bott_longHP_160x9	18	9.0
214	Z2_132_DB_longHp_180x9	100	9.0
215	Z2_133_DB_Bott_longHp_180x9	80	9.0
216	Z2_134_DB_longHP160x9	19	9.0
217	Z2_150_DB_bkt_15	3	15.0
218	Z2_201_Shell__pl_12	261	12.0
219	Z2_210_Shell_Frame_wb_15	239	15.0
220	Z2_211_Shell_Frame_fl_200x20	224	20.0
221	Z2_212_Shell_Frame_wb_12	38	12.0
222	Z2_213_Shell_Frame_fl_200x15	40	15.0
223	Z2_214_Shell_bhd_46_fr_wb_9	42	9.0
224	Z2_230_Shell_longHp160x9	196	9.0
225	Z2_231_Shell_Stringer_wb_12	52	12.0
226	Z2_232_Shell_Stringer_fl_15	24	15.0
227	Z2_250_Shell_Bkt_15	36	15.0
228	Z2_251_Shell_BKT_12	3	12.0
229	Z2_301_MDK_pl_9	119	9.0
230	Z2_302_MDK_pl_12	22	12.0
231	Z2_320_MDK_gd_wb_15	38	15.0
232	Z2_321_MDK_gd_fl_20	139	20.0
233	Z2_322_MDK_Gd_PDwb_7p5	11	7.5
234	Z2_330_MDK_longHP_140x8	91	8.0
235	Z2_340_MDK_Frame_wb_10	91	10.0
236	Z2_341_MDK_Frame_wb_12	93	12.0
237	Z2_342_MDK_Frame_wb_15	16	15.0
238	Z2_343_MDK_Frame_fl_150x12	152	12.0
239	Z2_344_MDK_Frame_fl_250x20	12	20.0
240	Z2_401_BHD_wall_fr46_8	98	8.0
241	Z2_407_BHD46_PL_10	60	10.0
242	Z2_420_BHD46_HP_180x9	38	9.0
243	Z2_421_BHD46_HP_140x8	10	8.0
244	Z2_431_BHD_46_gd_wb_12	7	12.0
245	Z2_432_BHD46_GD_fl_15	17	15.0
246	Z2_436_BHD46_GD_wb_15	7	15.0
247	Z2_437_BHD_46_GD_fl_20	14	20.0
248	Z2_438_BHD_PDweb_6	3	6.0

Tab.A.4.3. Layers and thickness of block 3

RC	DXF	3D Face	Gross thk.
no.	file	no.	[mm]
Midship Block 3			
301	Z3_100_DB_top_pl_10	164	10.0
302	Z3_101_DB_Bilge_pl_10	132	10.0
303	Z3_102_DB_Bott_pl_10	211	10.0
304	Z3_103_DB_GDcent_12	2	12.0
305	Z3_104_DB_GD_9	49	9.0
306	Z3_106_DB_Tank_pl_10	143	10.0
307	Z3_107_DB_GDcentPD_6	36	6.0
308	Z3_120_DB_Frame_wb_10	89	10.0
309	Z3_121_DB_FR_WB_15	41	15.0
310	Z3_122_DB_Frame_wb_9	620	9.0
311	Z3_130_DB_Bilge_longHP160x9	33	9.0
312	Z3_131_DB_bott_longHP_160x9	47	9.0
313	Z3_132_DB_longHp_180x9	125	9.0
314	Z3_133_DB_Bott_longHp_180x9	103	9.0
315	Z3_134_DB_longHP160x9	49	9.0
316	Z3_201_Shell__pl_12	307	12.0
317	Z3_210_Shell_Frame_wb_15	403	15.0
318	Z3_211_Shell_Frame_fl_200x20	380	20.0
319	Z3_212_Shell_Frame_wb_12	52	12.0
320	Z3_213_Shell_Frame_fl_200x15	26	15.0
321	Z3_214_Shell_Frame_wb_9	84	9.0
322	Z3_230_Shell__longHp160x9	222	9.0
323	Z3_231_Shell_Stringer_wb_12	52	12.0
324	Z3_232_Shell_Stringer_fl_15	24	15.0
325	Z3_250_Shell_Bkt_15	59	15.0
326	Z3_251_Shell_BKT_12	2	12.0
327	Z3_301_MDK_pl_9	163	9.0
328	Z3_302_MDK_pl_12	38	12.0
329	Z3_320_MDK_gd_wb_15	58	15.0
330	Z3_321_MDK_gd_fl_20	209	20.0
331	Z3_322_MDK_gd__PDwb_7p5	14	7.5
332	Z3_330_MDK_longHP_140x8	120	8.0
333	Z3_340_MDK_Frame_wb_10	150	10.0
334	Z3_341_MDK_Frame_wb_12	119	12.0
335	Z3_342_MDK_frame_wb_15	29	15.0
336	Z3_343_MDK_Frame_fl_150x12	232	12.0
337	Z3_344_MDK_Frame_fl_250x20_BHD62	12	20.0
338	Z3_401_BHD_wall_fr78_8	85	8.0
339	Z3_402_BHD_wall_fr80_8	85	8.0
340	Z3_403_BHD_wall_fr62_8	33	8.0

341	Z3_404_BHD_wall_fr62_12	12	12.0
342	Z3_405_BHD_fr80_LG_pl_12	8	12.0
343	Z3_406_BHD_fr80_LG_pl_10	22	10.0
344	Z3_407_BHD_pl_fr80_10	110	10.0
345	Z3_408_BHD_fr80_LG_PD_6	8	6.0
346	Z3_420_BHD_fr78_80_Hp_180x9	57	9.0
347	Z3_421_BHD_fr78_80_Hp_140x8	98	8.0
348	Z3_422_BHD_fr62_HP_120x7	17	7.0
349	Z3_430_BHD_fr62__GD_wb_10	28	10.0
350	Z3_431_BHD_fr62__GD_wb_12	10	12.0
351	Z3_432_BHD_fr62_GD_fl_15	32	15.0
352	Z3_433_BHD_fr62_Frame_fl_250x20	6	20.0
353	Z3_Bott_pl_12	45	12.0

Tab.A.4.4. Layers and thickness of block 4

RC	**DXF**	**3D Face**	**Gross thk.**
no.	file	no.	[mm]
Midship Block 4			
401	Z4_100_DB_pl_10	168	10.0
402	Z4_101_DB_Bilge_pl_10	136	10.0
403	Z4_102_DB_Bott_pl_10	214	10.0
404	Z4_104_DB_GD_9	55	9.0
405	Z4_106_DB_Tank_pl_10	154	10.0
406	Z4_107_DB_GDcentPD_6	40	6.0
407	Z4_120_DB_frame_wb_10	40	10.0
408	Z4_121_DB_FR_WB_15	41	15.0
409	Z4_122_DB_Frame_wb_9	662	9.0
410	Z4_130_DB_Bilge_longHP160x9	34	9.0
411	Z4_131_DB_bott_longHP_160x9	48	9.0
412	Z4_132_DB_longHp_180x9	130	9.0
413	Z4_133_DB_Bott_longHp_180x9	104	9.0
414	Z4_134_DB_longHP160x9	48	9.0
415	Z4_201_Shell__pl_12	318	12.0
416	Z4_210_Shell_Frame_wb_15	444	15.0
417	Z4_211_Shell_Frame_fl_200x20	418	20.0
418	Z4_212_Shell_Frame_wb_12	53	12.0
419	Z4_213_Shell_Frame_fl_200x15	26	15.0
420	Z4_214_Shell_frame113_wb9	42	9.0
421	Z4_230_Shell__longHp160x9	225	9.0
422	Z4_231_Shell_Stringer_wb_12	64	12.0
423	Z4_232_Shell_Stringer_fl_15	30	15.0
424	Z4_250_Shell_Bkt_15	65	15.0
425	Z4_251_Shell_BKT_12	2	12.0
426	Z4_301_MDK_pl_9	168	9.0

427	Z4_302_MDK_pl_12	37	12.0
428	Z4_320_MDK_gd_wb_15	60	15.0
429	Z4_321_MDK_gd_fl_20	228	20.0
430	Z4_322_MDK_gd__PDwb_7p5	15	7.5
431	Z4_330_MDK_longHP_140x8	129	8.0
432	Z4_340_MDK_Frame_wb_10	166	10.0
433	Z4_341_MDK_Frame_wb_12	133	12.0
434	Z4_342_MDK_frame_wb_15	29	15.0
435	Z4_343_MDK_Frame_fl_150x12	256	12.0
436	Z4_344_MDK_Frame_fl_250x20_BHD62	12	20.0
437	Z4_401_BHD_wall_fr113_8	104	8.0
438	Z4_403_BHD_wall_fr96_8	33	8.0
439	Z4_404_BHD_wall_fr96_12	12	12.0
440	Z4_407_BHD_fr113_pl_10	86	10.0
441	Z4_408_BHD_113_lg_PD_6	3	6.0
442	Z4_420_BHD_fr113_HP180x9	47	9.0
443	Z4_421_BHD_fr113_HP140x8	10	8.0
444	Z4_422_BHD_fr96_HP_120x7	17	7.0
445	Z4_430_BHD_fr96_GD_wb_10	28	10.0
446	Z4_431_BHD_fr96_GD_wb_12	10	12.0
447	Z4_432_BHD_fr96_GD_fl_15	32	15.0
448	Z4_433_BHD_fr96_Frame_fl_250x20	6	20.0
449	Z4_434_BHD_113_wb_12	7	12.0
450	Z4_435_BHD_113_fl_15	17	15.0
451	Z4_436_BHD_113_wb_15	7	15.0
452	Z4_437_BHD_113_fl_20	14	20.0
453	Z4_Bott_pl_12	45	12.0

Tab.A.4.5. Layers and thickness of block 5

RC	**DXF**	**3D Face**	**Gross thk.**
no.	file	no.	[mm]
Midship Block 5			
501	Z5_100_DB_top_pl_10	93	10.0
502	Z5_101_DB_Bilge_pl_10	68	10.0
503	Z5_102_DB_Bott_pl_10	120	10.0
504	Z5_103_DB_GDcent_12	1	12.0
505	Z5_104_DB_GD_9	28	9.0
506	Z5_106_DB_Tank_pl_10	77	10.0
507	Z5_107_DB_GDcentPD_6	20	6.0
508	Z5_120_DB_Frame130_wb_10	33	10.0
509	Z5_122_DB_Frame_wb_9	344	9.0
510	Z5_130_DB_Bilge_longHP160x9	17	9.0
511	Z5_131_DB_bott_longHP_160x9	16	9.0

512	Z5_132_DB_longHp_180x9	70	9.0
513	Z5_133_DB_Bott_longHp_180x9	62	9.0
514	Z5_134_DB_longHP160x9	16	9.0
515	Z5_201_Shell__pl_12	179	12.0
516	Z5_210_Shell_Frame_wb_15	242	15.0
517	Z5_211_Shell_Frame_fl_200x20	228	20.0
518	Z5_214_Shell_bhd130_fr_wb_9	50	9.0
519	Z5_230_Shell_longHp160x9	17	9.0
520	Z5_231_Shell_Stringer_wb_12	32	12.0
521	Z5_232_Shell_Stringer_fl_15	16	15.0
522	Z5_233_Shell_logHP_220x11	135	11.0
523	Z5_250_Shell_Bkt_15	36	15.0
524	Z5_301_MDK_pl_9	94	9.0
525	Z5_302_MDK_pl_12	16	12.0
526	Z5_320_MDK_gd_wb_15	33	15.0
527	Z5_321_MDK_gd_fl_20	121	20.0
528	Z5_322_MDK_gd__PDwb_7p5	9	7.5
529	Z5_330_MDK_longHP_140x8	72	8.0
530	Z5_340_MDK_Frame_wb_10	91	10.0
531	Z5_341_MDK_Frame_wb_12	67	12.0
532	Z5_342_MDK_frame_wb_15	13	15.0
533	Z5_343_MDK_Frame_fl_150x12	140	12.0
534	Z5_401_BHD_130_wall_8	83	8.0
535	Z5_407_BHD_130_pl_10	59	10.0
536	Z5_421_BHD_130_HP_140x8	21	8.0
537	Z5_423_BHD_130_HP160x8	23	8.0
538	Z5_434_BHD_130_wb_12	7	12.0
539	Z5_435_BHD_130_fl_15	17	15.0
540	Z5_436_BHD_130_wb_15	7	15.0
541	Z5_437_BHD_130_fl_20	14	20.0
542	Z5_438_BHD_130_wb_PD_6	3	6.0
543	Z5_Bott_pl_12	45	12.0
544	Z5_Shell_pl_12	63	12.0

Tab.A.4.6. Layers and thickness of block 6

RC	**DXF**	**3D Face**	**Gross thk.**
no.	file	no.	[mm]
Midship Block 6			
601	Z6_100_DB_top_pl_10	59	10.0
602	Z6_101_DB_Bilge_pl_10	24	10.0
603	Z6_102_DB_Bottom_pl_10	65	10.0
604	Z6_103_Bottom_pl_12	12	12.0
605	Z6_104_DB_GD_9	18	9.0

606	Z6_106_DB_Tank_pl_10	61	10.0
607	Z6_107_DB_GDcentPD_6	13	6.0
608	Z6_122_DB_Frame_wb_9	155	9.0
609	Z6_123_DB_Frame_wb_12	34	12.0
610	Z6_132_DB_longHp_180x9	48	9.0
611	Z6_133_DB_Bott_longHp_180x9	43	9.0
612	Z6_201_Shell_pl_18	111	18.0
613	Z6_202_Shell_pl_10	54	10.0
614	Z6_210_Shell_Frame_wb_15	211	15.0
615	Z6_211_Shell_Frame_fl_200x20	198	20.0
616	Z6_230_Shell_longHp160x9	14	9.0
617	Z6_231_Shell_Stringer_wb_12	28	12.0
618	Z6_232_Shell_Stringer_fl_15	14	15.0
619	Z6_233_Shell_logHP_220x11	105	11.0
620	Z6_250_Shell_Bkt_15	24	15.0
621	Z6_301_MDK_pl_9	75	9.0
622	Z6_302_MDK_pl_12	13	12.0
623	Z6_320_MDK_gd_wb_15	26	15.0
624	Z6_321_MDK_gd_fl_20	91	20.0
625	Z6_322_MDK_gd__PDwb_7p5	5	7.5
626	Z6_330_MDK_longHP_140x8	50	8.0
627	Z6_340_MDK_Frame_wb_10	74	10.0
628	Z6_341_MDK_Frame_wb_12	62	12.0
629	Z6_343_MDK_Frame_fl_150x12	114	12.0

Tab.A.4.7. Layers and thickness of block 7

RC	**DXF**	**3D Face**	**Gross thk.**
no.	file	no.	[mm]
Fore Block 7			
701	Z7_102_bottom_pl_13p5	72	13.5
702	Z7_103_bottom_pl_18	17	18.0
703	Z7_104_DB_wb_10	77	10.0
704	Z7_105_DB_fl_150x15	69	15.0
705	Z7_107_DB_GD_PD_5	137	5.0
706	Z7_120_DB_frame_wb_10	36	10.0
707	Z7_121_DB_plate_10	52	10.0
708	Z7_150_transversal_HP140x8	164	8.0
709	Z7_151_transversal_HP160x9	15	9.0
710	z7_152_transversal_HP120x8	41	8.0
711	Z7_153_Shell_frame_HP_200x11	174	11.0
712	Z7_153_transversal_HP_180x9	8	9.0
713	Z7_170_DB_Bow_wb_12	17	12.0
714	Z7_171_DB_bow_fl_12	23	12.0
715	Z7_201_Shell_pl_18	407	18.0

716	Z7_202_Shell_pl_12	60	12.0
717	Z7_203_Shell_pl_10	43	10.0
718	Z7_210_Shell_frame_wb_10	18	10.0
719	Z7_211_Shell_frame_fl_120x12	50	12.0
720	Z7_212_Shell_frame_wb_12	31	12.0
721	Z7_213_Shell_frame_fl_200x15	10	15.0
722	Z7_214_Shell_frame_fl_150_15	16	15.0
723	Z7_220_Shell_pl_10	186	10.0
724	Z7_230_Shell_GD_wb_10	24	10.0
725	Z7_231_Shell_GD_fl_15	96	15.0
726	Z7_301_MDK_pl_9	90	9.0
727	Z7_310_MDK_gd_wb_10	43	10.0
728	z7_311_mdk_gd_fl_12	44	12.0
729	Z7_340_MDK_frame_wb_10	4	10.0
730	Z7_341_MDK_frame_fl_120x12	16	12.0
731	Z7_342_MDK_frame_wb_12	11	12.0
732	Z7_401_BHD_151_wall_10	20	10.0
733	Z7_402_BHD_155_wall_12	33	12.0
734	Z7_403_BHD_147_wall_10	77	10.0
735	Z7_404_BHD_143_wall_10	142	10.0
736	Z7_420_BHD_frame_wb_10	46	10.0

A.5.1. Table Inputs for the 1D Equivalent Beam Model Numerical Computation

Table A.5.1. Numerical inputs for the 1D Equivalent Beam Mode computation

	m	m^4	m^2	m^2	tm^2/m	m^3	m^3	$1/m^2$
Nr.e	**x**	**Iyy**	**Afz**	**A**	**Jyy**	**WD**	**WB**	**ktnn**
1	0	3.01785	0.17165	0.33692	23.23747	0.70396	0.36392	6.22574
2	0.30	3.09697	0.17440	0.34232	23.84666	0.71781	0.39095	6.21832
3	0.90	3.25520	0.17990	0.35312	25.06503	0.74549	0.44502	6.20348
4	1.50	3.41343	0.18540	0.36391	26.28341	0.77317	0.49908	6.18865
5	2.10	3.57166	0.19090	0.37471	27.50179	0.80085	0.55314	6.17381
6	2.70	3.72989	0.19640	0.38550	28.72016	0.82854	0.60720	6.15897
7	3.30	3.88812	0.20190	0.39630	29.93854	0.85622	0.66127	6.14413
8	3.90	4.04635	0.20740	0.40710	31.15691	0.88390	0.71533	6.12930
9	4.50	4.20458	0.21290	0.41789	32.37529	0.91158	0.76939	6.11446
10	5.10	4.36281	0.21840	0.42869	33.59366	0.93927	0.82345	6.09962
11	5.70	4.52104	0.22390	0.43948	34.81204	0.96695	0.87752	6.08478
12	6.30	4.67927	0.22940	0.45028	36.03042	0.99463	0.93158	6.06995
13	6.90	4.83751	0.23490	0.46107	37.24879	1.02231	0.98564	6.05511
14	7.50	4.99574	0.24040	0.47187	38.46717	1.05000	1.03971	6.04027
15	8.10	5.15397	0.24590	0.48266	39.68554	1.07768	1.09377	6.02543
16	8.70	5.31220	0.25140	0.49346	40.90392	1.10536	1.14783	6.01060
17	9.30	5.47043	0.25690	0.50425	42.12229	1.13304	1.20189	5.99576
18	9.90	5.62866	0.26240	0.51505	43.34067	1.16073	1.25596	5.98092

19	10.50	5.78689	0.26790	0.52585	44.55905	1.18841	1.31002	5.96608
20	11.10	5.94512	0.27340	0.53664	45.77742	1.21609	1.36408	5.95125
21	11.70	6.10335	0.27890	0.54744	46.99580	1.24377	1.41814	5.93641
22	12.30	6.26158	0.28440	0.55823	48.21417	1.27146	1.47221	5.92157
23	12.90	6.41981	0.28989	0.56903	49.43255	1.29914	1.52627	5.90673
24	13.50	6.57804	0.29539	0.57982	50.65092	1.32682	1.58033	5.89190
25	14.10	6.73627	0.30089	0.59062	51.86930	1.35450	1.63440	5.87706
26	14.70	6.89450	0.30639	0.60141	53.08768	1.38218	1.68846	5.86222
27	15.30	7.05273	0.31189	0.61221	54.30605	1.40987	1.74252	5.84738
28	15.90	7.21096	0.31739	0.62301	55.52443	1.43755	1.79658	5.83255
29	16.50	7.36920	0.32289	0.63380	56.74280	1.46523	1.85065	5.81771
30	17.10	7.52743	0.32839	0.64460	57.96118	1.49291	1.90471	5.80287
31	17.70	7.68566	0.33389	0.65539	59.17955	1.52060	1.95877	5.78803
32	18.29	7.83993	0.33926	0.66592	60.36747	1.54759	2.01148	5.77357
33	18.86	7.99025	0.34448	0.67617	61.52493	1.57389	2.06284	5.75947
34	19.43	8.14057	0.34971	0.68643	62.68238	1.60018	2.11420	5.74538
35	20.06	8.30882	0.35555	0.69791	63.97792	1.62962	2.17169	5.72960
36	20.77	8.49501	0.36203	0.71061	65.41155	1.66219	2.23530	5.71214
37	21.48	8.68119	0.36850	0.72331	66.84517	1.69477	2.29892	5.69468
38	22.18	8.86738	0.37497	0.73602	68.27879	1.72734	2.36253	5.67722
39	22.89	9.05356	0.38144	0.74872	69.71241	1.75991	2.42614	5.65976
40	23.59	9.21363	0.38818	0.76196	70.94493	1.79103	2.46904	5.65000
41	24.30	9.37369	0.39493	0.77519	72.17745	1.82214	2.51193	5.64024
42	25.01	9.53376	0.40167	0.78843	73.40997	1.85326	2.55483	5.63048
43	25.71	9.69383	0.40842	0.80167	74.64249	1.88437	2.59772	5.62071
44	26.42	9.85390	0.41516	0.81491	75.87501	1.91549	2.64062	5.61095
45	27.12	10.01396	0.42190	0.82814	77.10753	1.94660	2.68351	5.60119
46	27.83	10.17403	0.42865	0.84138	78.34005	1.97772	2.72640	5.59143
47	28.54	10.33410	0.43539	0.85462	79.57257	2.00883	2.76930	5.58166
48	29.24	10.49417	0.44213	0.86786	80.80509	2.03995	2.81219	5.57190
49	29.95	10.65423	0.44888	0.88109	82.03761	2.07107	2.85509	5.56214
50	30.65	10.81430	0.45562	0.89433	83.27012	2.10218	2.89798	5.55238
51	31.36	10.97437	0.46237	0.90757	84.50264	2.13330	2.94088	5.54261
52	32.11	11.14555	0.46958	0.92173	85.82071	2.16657	2.98675	5.53217
53	32.87	11.31695	0.47680	0.93590	87.14052	2.19989	3.03268	5.52172
54	33.58	11.31695	0.47680	0.93590	87.14052	2.19989	3.03268	5.52172
55	34.28	11.31695	0.47680	0.93590	87.14052	2.19989	3.03268	5.52172
56	34.99	11.31695	0.47680	0.93590	87.14052	2.19989	3.03268	5.52172
57	35.69	11.31695	0.47680	0.93590	87.14052	2.19989	3.03268	5.52172
58	36.40	11.31695	0.47680	0.93590	87.14052	2.19989	3.03268	5.52172
59	37.11	11.31695	0.47680	0.93590	87.14052	2.19989	3.03268	5.52172
60	37.81	11.31695	0.47680	0.93590	87.14052	2.19989	3.03268	5.52172
61	38.52	11.31695	0.47680	0.93590	87.14052	2.19989	3.03268	5.52172
62	39.22	11.31695	0.47680	0.93590	87.14052	2.19989	3.03268	5.52172
63	39.93	11.31695	0.47680	0.93590	87.14052	2.19989	3.03268	5.52172
64	40.64	11.31695	0.47680	0.93590	87.14052	2.19989	3.03268	5.52172
65	41.34	11.31695	0.47680	0.93590	87.14052	2.19989	3.03268	5.52172
66	42.05	11.31695	0.47680	0.93590	87.14052	2.19989	3.03268	5.52172
67	42.75	11.31695	0.47680	0.93590	87.14052	2.19989	3.03268	5.52172
68	43.46	11.31695	0.47680	0.93590	87.14052	2.19989	3.03268	5.52172
69	44.17	11.31695	0.47680	0.93590	87.14052	2.19989	3.03268	5.52172
70	44.87	11.31695	0.47680	0.93590	87.14052	2.19989	3.03268	5.52172

71	45.58	11.31695	0.47680	0.93590	87.14052	2.19989	3.03268	5.52172
72	46.28	11.31695	0.47680	0.93590	87.14052	2.19989	3.03268	5.52172
73	46.99	11.31695	0.47680	0.93590	87.14052	2.19989	3.03268	5.52172
74	47.70	11.31695	0.47680	0.93590	87.14052	2.19989	3.03268	5.52172
75	48.40	11.31695	0.47680	0.93590	87.14052	2.19989	3.03268	5.52172
76	49.11	11.31695	0.47680	0.93590	87.14052	2.19989	3.03268	5.52172
77	49.81	11.31695	0.47680	0.93590	87.14052	2.19989	3.03268	5.52172
78	50.52	11.31695	0.47680	0.93590	87.14052	2.19989	3.03268	5.52172
79	51.23	11.31695	0.47680	0.93590	87.14052	2.19989	3.03268	5.52172
80	51.93	11.31695	0.47680	0.93590	87.14052	2.19989	3.03268	5.52172
81	52.64	11.31695	0.47680	0.93590	87.14052	2.19989	3.03268	5.52172
82	53.34	11.31695	0.47680	0.93590	87.14052	2.19989	3.03268	5.52172
83	54.10	11.31695	0.47680	0.93590	87.14052	2.19989	3.03268	5.52172
84	54.88	11.31695	0.47680	0.93590	87.14052	2.19989	3.03268	5.52172
85	55.64	11.31695	0.47680	0.93590	87.14052	2.19989	3.03268	5.52172
86	56.43	11.31695	0.47680	0.93590	87.14052	2.19989	3.03268	5.52172
87	57.18	11.31695	0.47680	0.93590	87.14052	2.19989	3.03268	5.52172
88	57.89	11.31695	0.47680	0.93590	87.14052	2.19989	3.03268	5.52172
89	58.59	11.31695	0.47680	0.93590	87.14052	2.19989	3.03268	5.52172
90	59.30	11.31695	0.47680	0.93590	87.14052	2.19989	3.03268	5.52172
91	60.00	11.31695	0.47680	0.93590	87.14052	2.19989	3.03268	5.52172
92	60.71	11.31695	0.47680	0.93590	87.14052	2.19989	3.03268	5.52172
93	61.42	11.31695	0.47680	0.93590	87.14052	2.19989	3.03268	5.52172
94	62.12	11.31695	0.47680	0.93590	87.14052	2.19989	3.03268	5.52172
95	62.83	11.31695	0.47680	0.93590	87.14052	2.19989	3.03268	5.52172
96	63.53	11.31695	0.47680	0.93590	87.14052	2.19989	3.03268	5.52172
97	64.24	11.31695	0.47680	0.93590	87.14052	2.19989	3.03268	5.52172
98	64.95	11.31695	0.47680	0.93590	87.14052	2.19989	3.03268	5.52172
99	65.65	11.31695	0.47680	0.93590	87.14052	2.19989	3.03268	5.52172
100	66.36	11.31695	0.47680	0.93590	87.14052	2.19989	3.03268	5.52172
101	67.06	11.31695	0.47680	0.93590	87.14052	2.19989	3.03268	5.52172
102	67.77	11.31695	0.47680	0.93590	87.14052	2.19989	3.03268	5.52172
103	68.48	11.31695	0.47680	0.93590	87.14052	2.19989	3.03268	5.52172
104	69.18	11.31695	0.47680	0.93590	87.14052	2.19989	3.03268	5.52172
105	69.89	11.31695	0.47680	0.93590	87.14052	2.19989	3.03268	5.52172
106	70.59	11.31695	0.47680	0.93590	87.14052	2.19989	3.03268	5.52172
107	71.30	11.31695	0.47680	0.93590	87.14052	2.19989	3.03268	5.52172
108	72.01	11.31695	0.47680	0.93590	87.14052	2.19989	3.03268	5.52172
109	72.71	11.31695	0.47680	0.93590	87.14052	2.19989	3.03268	5.52172
110	73.42	11.31695	0.47680	0.93590	87.14052	2.19989	3.03268	5.52172
111	74.12	11.31695	0.47680	0.93590	87.14052	2.19989	3.03268	5.52172
112	74.83	11.31695	0.47680	0.93590	87.14052	2.19989	3.03268	5.52172
113	75.54	11.31695	0.47680	0.93590	87.14052	2.19989	3.03268	5.52172
114	76.24	11.31695	0.47680	0.93590	87.14052	2.19989	3.03268	5.52172
115	76.95	11.31695	0.47680	0.93590	87.14052	2.19989	3.03268	5.52172
116	77.65	11.31695	0.47680	0.93590	87.14052	2.19989	3.03268	5.52172
117	78.36	11.31695	0.47680	0.93590	87.14052	2.19989	3.03268	5.52172
118	79.07	11.31695	0.47680	0.93590	87.14052	2.19989	3.03268	5.52172
119	79.82	11.31695	0.47680	0.93590	87.14052	2.19989	3.03268	5.52172
120	80.58	11.31695	0.47680	0.93590	87.14052	2.19989	3.03268	5.52172
121	81.28	11.31695	0.47680	0.93590	87.14052	2.19989	3.03268	5.52172
122	81.99	11.31695	0.47680	0.93590	87.14052	2.19989	3.03268	5.52172

123	82.70	11.31695	0.47680	0.93590	87.14052	2.19989	3.03268	5.52172
124	83.40	11.31695	0.47680	0.93590	87.14052	2.19989	3.03268	5.52172
125	84.11	11.31695	0.47680	0.93590	87.14052	2.19989	3.03268	5.52172
126	84.81	11.31695	0.47680	0.93590	87.14052	2.19989	3.03268	5.52172
127	85.52	11.31695	0.47680	0.93590	87.14052	2.19989	3.03268	5.52172
128	86.23	11.15462	0.46996	0.92248	85.89059	2.16834	2.98918	5.53162
129	86.93	10.99229	0.46312	0.90905	84.64067	2.13678	2.94568	5.54152
130	87.64	10.82997	0.45628	0.89563	83.39075	2.10523	2.90218	5.55142
131	88.34	10.66764	0.44944	0.88220	82.14082	2.07367	2.85868	5.56132
132	89.05	10.50531	0.44260	0.86878	80.89090	2.04212	2.81518	5.57122
133	89.76	10.34298	0.43577	0.85535	79.64098	2.01056	2.77168	5.58112
134	90.46	10.18066	0.42893	0.84193	78.39105	1.97901	2.72818	5.59102
135	91.17	10.01833	0.42209	0.82851	77.14113	1.94745	2.68468	5.60092
136	91.87	9.85600	0.41525	0.81508	75.89121	1.91590	2.64118	5.61082
137	92.58	9.69367	0.40841	0.80166	74.64129	1.88434	2.59768	5.62072
138	93.29	9.53135	0.40157	0.78823	73.39136	1.85279	2.55418	5.63062
139	93.99	9.36902	0.39473	0.77481	72.14144	1.82123	2.51068	5.64052
140	94.70	9.20669	0.38789	0.76138	70.89152	1.78968	2.46718	5.65042
141	95.36	9.05356	0.38144	0.74872	69.71241	1.75991	2.42614	5.65976
142	95.99	8.71599	0.37307	0.73230	67.11312	1.70587	2.33036	5.68459
143	96.61	8.37842	0.36471	0.71588	64.51383	1.65183	2.23458	5.70942
144	97.24	8.04085	0.35634	0.69946	61.91453	1.59779	2.13880	5.73424
145	97.86	7.70328	0.34798	0.68303	59.31524	1.54375	2.04301	5.75907
146	98.49	7.36571	0.33961	0.66661	56.71595	1.48971	1.94723	5.78390
147	99.11	7.02814	0.33124	0.65019	54.11666	1.43567	1.85145	5.80873
148	99.74	6.69057	0.32288	0.63377	51.51736	1.38163	1.75567	5.83355
149	100.35	6.36002	0.31469	0.61769	48.97214	1.32872	1.66188	5.85786
150	100.95	6.03595	0.30665	0.60192	46.47682	1.27684	1.56993	5.88170
151	101.55	5.71188	0.29862	0.58616	43.98150	1.22496	1.47798	5.90553
152	102.15	5.38781	0.29059	0.57039	41.48618	1.17308	1.38603	5.92936
153	102.75	5.06375	0.28256	0.55463	38.99085	1.12120	1.29407	5.95320
154	103.35	4.73968	0.27453	0.53887	36.49553	1.06932	1.20212	5.97703
155	103.95	4.41561	0.26650	0.52310	34.00021	1.01745	1.11017	6.00087
156	104.55	4.09154	0.25847	0.50734	31.50489	0.96557	1.01822	6.02470
157	105.15	3.76748	0.25043	0.49157	29.00957	0.91369	0.92627	6.04853
158	105.75	3.44341	0.24240	0.47581	26.51425	0.86181	0.83432	6.07237
159	106.35	3.11934	0.23437	0.46004	24.01893	0.80993	0.74237	6.09620
160	106.95	2.79527	0.22634	0.44428	21.52361	0.75805	0.65042	6.12004
161	107.55	2.47121	0.21831	0.42851	19.02829	0.70618	0.55847	6.14387
162	108.15	2.14714	0.21028	0.41275	16.53297	0.65430	0.46652	6.16770
163	108.75	1.82307	0.20225	0.39698	14.03765	0.60242	0.37456	6.19154
164	109.331	1.50927	0.19447	0.38172	11.62134	0.55218	0.28552	6.21462
165	109.611	1.35803	0.19072	0.37436	10.45686	0.52797	0.24261	6.22574

,where:

I_Y [m^4] = Vertical bending moment of inertia
A_F [m^2]= Vertical Shearing area
J_{yy} [tm^2/m]= the inertial mass moment per unit length
W_D [m^3] =strength modulus at the deck level
W_B [m^3] =strength modulus at the bottom level
k_{tnn} [$1/m^2$] = the coefficient of the tangential shear stress at the neutral axis

A.5.2.Table Results of the 1D Equivalent Beam Model Numerical Computation in Hogging Condition

Table.A.5.2.1. Maximum Normal Deck Stress,σ_X [MPa] in Hogging wave conditions, 1D computation

h_w [m]	Stress max(max) [MPa]	Stress adm_GS [MPa]	ReH [MPa]	max/adm_GS	Cs=ReH/max
0	8.45	265	390	0.032	46.132
1	19.46	265	390	0.073	20.039
2	32.05	265	390	0.121	12.170
3	44.26	265	390	0.167	8.812
4	55.76	265	390	0.210	6.995
5	66.91	265	390	0.252	5.829
6	77.65	265	390	0.293	5.022
7	87.84	265	390	0.331	4.440
8	97.18	265	390	0.367	4.013
8.123	98.25	265	390	0.371	3.969

Table.A.5.2.2. Maximum Normal Bottom Stress,σ_X [MPa] in Hogging wave conditions, 1D computation

h_w [m]	Stress max(max) [MPa]	Stress adm_GS [MPa]	ReH [MPa]	max/adm_GS	Cs=ReH/max
0	6.70	175	235	0.038	35.050
1	14.12	175	235	0.081	16.646
2	23.25	175	235	0.133	10.110
3	32.10	175	235	0.183	7.320
4	40.45	175	235	0.231	5.810
5	48.53	175	235	0.277	4.842
6	56.33	175	235	0.322	4.172
7	63.72	175	235	0.364	3.688
8	70.50	175	235	0.403	3.334
8.123	71.27	175	235	0.407	3.297

Table. A.5.2.3. Maximum Tangential side stress τ_{xz} [MPa] in Hogging wave conditions, 1D computation

h_w [m]	Stress max(max) [MPa]	Stress adm_GS [MPa]	ReH [MPa]	max/adm_GS	Cs=ReH/max
0	6.34	110	235	0.058	37.052
1	8.90	110	235	0.081	26.405
2	13.75	110	235	0.125	17.087
3	18.48	110	235	0.168	12.720
4	22.98	110	235	0.209	10.228
5	27.37	110	235	0.249	8.587
6	31.65	110	235	0.288	7.426
7	35.77	110	235	0.325	6.570
8	39.64	110	235	0.360	5.928
8.123	40.09	110	235	0.364	5.861

A.5.3. Table Results of the 1D Equivalent Beam Model Numerical Computation in Sagging Condition

Table.A.5.3.1. Maximum Normal Deck Stress,σ_X [MPa] in Sagging wave conditions, 1D computation

h_w [m]	Stress max(max) [MPa]	Stress adm_GS [MPa]	ReH [MPa]	max/adm_GS	Cs=ReH/max
0	8.45	265	390	0.032	46.132
1	8.62	265	390	0.033	45.249
2	22.96	265	390	0.087	16.984
3	37.90	265	390	0.143	10.290
4	53.36	265	390	0.201	7.309
5	69.28	265	390	0.261	5.630
6	85.56	265	390	0.323	4.558
7	102.18	265	390	0.385	3.817
8	119.07	265	390	0.449	3.275
8.123	121.17	265	390	0.457	3.219

Table.A.5.3.2. Maximum Normal Bottom Stress,σ_X [MPa] in Sagging wave conditions, 1D computation

h_w [m]	Stress max(max) [MPa]	Stress adm_GS [MPa]	ReH [MPa]	max/adm_GS	Cs=ReH/max
0	6.70	175	235	0.038	35.050
1	6.25	175	235	0.036	37.587
2	16.66	175	235	0.095	14.108
3	27.49	175	235	0.157	8.547
4	38.71	175	235	0.221	6.071
5	50.25	175	235	0.287	4.676
6	62.06	175	235	0.355	3.786
7	74.12	175	235	0.424	3.170
8	86.38	175	235	0.494	2.721
8.123	87.90	175	235	0.502	2.674

Table. A.5.3.3. Maximum Tangential side stress τ_{xz} [MPa] in Sagging wave conditions, 1D computation

hw [m]	Stress max(max) [MPa]	Stress adm_GS [MPa]	ReH [MPa]	max/adm_GS	Cs=ReH/max
0	6.34	110	235	0.058	37.052
1	7.90	110	235	0.072	29.765
2	13.06	110	235	0.119	17.989
3	18.40	110	235	0.167	12.774
4	23.89	110	235	0.217	9.838
5	29.68	110	235	0.270	7.918
6	35.58	110	235	0.323	6.605
7	41.53	110	235	0.378	5.659
8	47.53	110	235	0.432	4.944
8.123	48.27	110	235	0.439	4.868

A.6.1. Table Results of the Numerical Computation in Hogging Conditions, Full Extended 3D-FEM Model

Table.A.6.1.1. Maximum Normal Deck Stress,σ_X [MPa] in Hogging wave conditions, 3D-FEM full extended model, Safety coefficients Cs according to the yield stress limit ReH

h_w [m]	Stress max(max) [MPa]	Stress adm_GS [MPa]	ReH [MPa]	max/adm_GS	Cs=ReH/max
0	22.15	265	390	0.084	17.607
1	43.37	265	390	0.164	8.992
2	75.39	265	390	0.284	5.173
3	105.10	265	390	0.396	3.711
4	133.70	265	390	0.504	2.917
5	161.60	265	390	0.609	2.413
6	188.80	265	390	0.712	2.066
7	214.60	265	390	0.809	1.817
8	238.40	265	390	0.899	1.636
8.123	241.20	265	390	0.910	1.617

Table.A.6.1.2. Maximum Equivalent vonMises Deck Stress, σ_{von} [MPa] in Hogging wave conditions, 3D-FEM full extended model, Safety coefficients Cs according to the yield stress limit ReH

h_w [m]	Stress max(max) [MPa]	Stress adm_GS [MPa]	ReH [MPa]	max/adm_GS	Cs=ReH/max
0	92.16	265	390	0.348	4.232
1	92.16	265	390	0.348	4.232
2	92.16	265	390	0.348	4.232
3	94.87	265	390	0.358	4.111
4	120.60	265	390	0.455	3.234
5	145.70	265	390	0.549	2.677
6	170.10	265	390	0.642	2.293
7	193.40	265	390	0.729	2.017
8	215.30	265	390	0.812	1.811
8.123	217.80	265	390	0.821	1.791

Table.A.6.1.3. Maximum Normal Bottom Stress,σ_X [MPa] in Hogging wave conditions, 3D-FEM full extended model, Safety coefficients Cs according to the yield stress limit ReH

hw [m]	Stress max(max) [MPa]	Stress adm_GS [MPa]	ReH [MPa]	max/adm_GS	Cs=ReH/max
0	37.56	175	235	0.215	6.257
1	36.55	175	235	0.209	6.430
2	38.49	175	235	0.220	6.105
3	48.18	175	235	0.275	4.878
4	57.65	175	235	0.329	4.076
5	66.95	175	235	0.383	3.510
6	76.06	175	235	0.435	3.090
7	84.79	175	235	0.485	2.772
8	92.80	175	235	0.530	2.532
8.123	94.89	175	235	0.542	2.477

Table.A.6.1.4. Maximum Equivalent vonMises Bottom Stress, σ_{von} [MPa] in Hogging wave conditions, 3D-FEM full extended model, Safety coefficients Cs according to the yield stress limit ReH

hw [m]	Stress max(max) [MPa]	Stress adm_GS [MPa]	ReH [MPa]	max/adm_GS	Cs=ReH/max
0	38.96	175	235	0.223	6.032
1	36.73	175	235	0.210	6.398
2	34.84	175	235	0.199	6.745
3	43.69	175	235	0.250	5.379
4	52.39	175	235	0.299	4.486
5	60.96	175	235	0.348	3.855
6	69.36	175	235	0.396	3.388
7	77.40	175	235	0.442	3.036
8	84.78	175	235	0.484	2.772
8.123	85.62	175	235	0.489	2.745

Table.A.6.1.5. Maximum Tangential side stress τ_{xz} [MPa] in Hogging wave conditions, 3D-FEM full extended model, Safety coefficients Cs according to the yield stress limit ReH

hw [m]	Stress max(max) [MPa]	Stress adm_GS [MPa]	ReH [MPa]	max/adm_GS	Cs=ReH/max
0	5.88	110	235	0.053	39.946
1	8.17	110	235	0.074	28.750
2	11.47	110	235	0.104	20.488
3	15.79	110	235	0.144	14.883
4	19.87	110	235	0.181	11.827
5	23.80	110	235	0.216	9.874
6	27.58	110	235	0.251	8.521
7	31.14	110	235	0.283	7.547
8	34.30	110	235	0.312	6.851
8.123	34.70	110	235	0.315	6.772

A.6.2. Table Results of the Numerical Computation in Sagging Conditions, Full Extended 3D-FEM Model

Table.A.6.2.1. Maximum Normal Deck Stress,σ_X [MPa] in Sagging wave conditions, 3D-FEM full extended model, Safety coefficients Cs according to the yield stress limit ReH

h_w [m]	Stress max(max) [MPa]	Stress adm_GS [MPa]	ReH [MPa]	max/adm_GS	Cs=ReH/max
0	14.20	265	390	0.054	27.465
1	31.53	265	390	0.119	12.369
2	71.65	265	390	0.270	5.443
3	112.60	265	390	0.425	3.464
4	153.90	265	390	0.580	2.534
5	195.60	265	390	0.738	1.994
6	237.80	265	390	0.897	1.640
7	280.70	265	390	1.059	1.389
8	324.40	265	390	1.223	1.202
8.123	329.90	265	390	1.244	1.182

Table.A.6.2.2. Maximum Equivalent vonMises Deck Stress, σ_{von} [MPa] in Sagging wave conditions, 3D-FEM full extended model, Safety coefficients Cs according to the yield stress limit ReH

h_w [m]	Stress max(max) [MPa]	Stress adm_GS [MPa]	ReH [MPa]	max/adm_GS	Cs=ReH/max
0	26.19	265	390	0.099	14.891
1	29.13	265	390	0.110	13.388
2	64.78	265	390	0.244	6.020
3	101.80	265	390	0.384	3.831
4	139.10	265	390	0.525	2.804
5	176.80	265	390	0.667	2.206
6	214.90	265	390	0.810	1.815
7	253.60	265	390	0.956	1.538
8	293.00	265	390	1.105	1.331
8.123	297.90	265	390	1.124	1.309

Table.A.6.2.3. Maximum Normal Bottom Stress,σ_X [MPa] in Sagging wave conditions, 3D-FEM full extended model, Safety coefficients Cs according to the yield stress limit ReH

h_w [m]	Stress max(max) [MPa]	Stress adm_GS [MPa]	ReH [MPa]	max/adm_GS	Cs=ReH/max
0	37.56	175	235	0.215	6.257
1	33.86	175	235	0.193	6.940
2	32.78	175	235	0.187	7.169
3	39.96	175	235	0.228	5.881
4	53.06	175	235	0.303	4.429
5	66.27	175	235	0.379	3.546
6	79.64	175	235	0.455	2.951
7	93.19	175	235	0.533	2.522
8	107.00	175	235	0.611	2.196
8.123	111.30	175	235	0.636	2.111

Table.A.6.2.4. Maximum Equivalent vonMises Bottom Stress, σ_{von} [MPa] in Sagging wave conditions,
3D-FEM full extended model, Safety coefficients Cs according to the yield stress limit ReH

h_w [m]	Stress max(max) [MPa]	Stress adm_GS [MPa]	ReH [MPa]	max/adm_GS	Cs=ReH/max
0	38.96	175	235	0.223	6.032
1	38.99	175	235	0.223	6.027
2	44.31	175	235	0.253	5.304
3	53.19	175	235	0.304	4.418
4	62.71	175	235	0.358	3.747
5	72.80	175	235	0.416	3.228
6	83.33	175	235	0.476	2.820
7	94.15	175	235	0.538	2.496
8	105.10	175	235	0.601	2.236
8.123	106.50	175	235	0.609	2.207

Table.A.6.2.5. Maximum Tangential side stress τ_{xz} [MPa] in Sagging wave conditions, 3D-FEM full extended model, Safety coefficients Cs according to the yield stress limit ReH

h_w [m]	Stress max(max) [MPa]	Stress adm_GS [MPa]	ReH [MPa]	max/adm_GS	Cs=ReH/max
0	5.88	110	235	0.053	39.946
1	5.90	110	235	0.054	39.851
2	10.73	110	235	0.098	21.901
3	15.69	110	235	0.143	14.978
4	21.50	110	235	0.195	10.930
5	27.43	110	235	0.249	8.567
6	33.39	110	235	0.304	7.038
7	39.42	110	235	0.358	5.961
8	45.52	110	235	0.414	5.163
8.123	47.85	110	235	0.435	4.911

A.7. Tables Results for the Numerical Computation in Hogging and Sagging Conditions, Two Cargo Holds Compartments 3D-FEM Model, With Coarse Size Mesh

Table.A.7.1. Maximum Normal Deck Stress,σ_X [MPa] in Hogging wave conditions, two cargo holds compartments 3D-FEM model With Coarse Size Mesh, Safety coefficients Cs according to the yield stress limit ReH

h_w [m]	Stress max(max) [MPa]	Stress adm_GS [MPa]	ReH [MPa]	max/adm_GS	Cs=ReH/max
0	12.44	265	390	0.047	31.350
8.123	257.90	265	390	0.973	1.512

Table.A.7.2. Maximum Equivalent vonMises Deck Stress, σ_{von} [MPa] in Hogging wave conditions, two cargo holds compartments 3D-FEM model With Coarse Size Mesh, Safety coefficients Cs according to the yield stress limit ReH

h_w [m]	Stress max(max) [MPa]	Stress adm_GS [MPa]	ReH [MPa]	max/adm_GS	Cs=ReH/max
0	11.32	265	390	0.043	34.452
8.123	233.00	265	390	0.879	1.674

Table. A.7.3. Maximum Normal Bottom Stress,σ_X [MPa] in Hogging wave conditions, two cargo holds compartments 3D-FEM model With Coarse Size Mesh, Safety coefficients Cs according to the yield stress limit ReH

h_w [m]	Stress max(max) [MPa]	Stress adm_GS [MPa]	ReH [MPa]	max/adm_GS	Cs=ReH/max
0	23.94	175	235	0.137	9.816
8.123	98.01	175	235	0.560	2.398

Table. A.7.4. Maximum Equivalent vonMises Bottom Stress, σ_{von} [MPa] in Hogging wave conditions, two cargo holds compartments 3D-FEM model With Coarse Size Mesh, Safety coefficients Cs according to the yield stress limit ReH

h_w [m]	Stress max(max) [MPa]	Stress adm_GS [MPa]	ReH [MPa]	max/adm_GS	Cs=ReH/max
0	21.49	175	235	0.123	10.935
8.123	88.60	175	235	0.506	2.652

Table. A.7.5. Maximum Tangential side stress τ_{xz} [MPa] in Hogging wave conditions, two cargo holds compartments 3D-FEM model With Coarse Size Mesh, Safety coefficients Cs according to the yield stress limit ReH

h_w [m]	Stress max(max) [MPa]	Stress adm_GS [MPa]	ReH [MPa]	max/adm_GS	Cs=ReH/max
0	3.40	110	235	0.031	69.036
8.123	35.78	110	235	0.325	6.568

Table.A.7.6. Maximum Normal Deck Stress,σ_X [MPa] in Sagging wave conditions, two cargo holds compartments 3D-FEM model With Coarse Size Mesh, Safety coefficients Cs according to the yield stress limit ReH

h_w [m]	Stress max(max) [MPa]	Stress adm_GS [MPa]	ReH [MPa]	max/adm_GS	Cs=ReH/max
0	12.44	265	390	0.047	31.350
8.123	321.30	265	390	1.212	1.214

Table.A.7.7. Maximum Equivalent vonMises Deck Stress, σ_{von} [MPa] in Sagging wave conditions, two cargo holds compartments 3D-FEM model With Coarse Size Mesh, Safety coefficients Cs according to the yield stress limit ReH

h_w [m]	Stress max(max) [MPa]	Stress adm_GS [MPa]	ReH [MPa]	max/adm_GS	Cs=ReH/max
0	11.32	265	390	0.043	34.452
8.123	290.10	265	390	1.094	1.344

Table. A.7.8. Maximum Normal Bottom Stress,σ_X [MPa] in Sagging wave conditions, 2 cargo holds compartments 3D-FEM model With Coarse Size Mesh, Safety coefficients Cs according to the yield stress limit ReH

h_w [m]	Stress max(max) [MPa]	Stress adm_GS [MPa]	ReH [MPa]	max/adm_GS	Cs=ReH/max
0	23.94	175	235	0.137	9.816
8.123	118.90	175	235	0.678	1.976

Table. A.7.9. Maximum Equivalent vonMises Bottom Stress, σ_{von} [MPa] in Sagging wave conditions, 2 cargo holds compartments 3D-FEM model With Coarse Size Mesh, Safety coefficients Cs according to the yield stress limit ReH

h_w [m]	Stress max(max) [MPa]	Stress adm_GS [MPa]	ReH [MPa]	max/adm_GS	Cs=ReH/max
0	21.49	175	235	0.123	10.935
8.123	105.40	175	235	0.602	2.230

Table. A.7.10. Maximum Tangential side stress τ_{xz} [MPa] in Sagging wave conditions, 2 cargo holds compartments 3D-FEM model With Coarse Size Mesh, Safety coefficients Cs according to the yield stress limit ReH

hw [m]	Stress max(max) [MPa]	Stress adm_GS [MPa]	ReH [MPa]	max/adm_GS	Cs=ReH/max
0	3.40	110	235	0.031	69.036
8.123	42.36	110	235	0.385	5.548

A.8. Tables Results for the Numerical Computation in Hogging and Sagging Conditions, Two Cargo Holds Compartments 3D-FEM Model, With Fine Mesh Size

Table.A.8.1. Maximum Normal Deck Stress, σ_X [MPa] in Hogging wave conditions, two cargo holds compartments 3D-FEM fine mesh model, Safety coefficients Cs according to the yield stress limit ReH

h_w [m]	Stress max(max) [MPa]	Stress adm_GS [MPa]	ReH [MPa]	max/adm_GS	Cs=ReH/max
0	18.24	265	390	0.069	21.382
8.123	390.00	265	390	1.471	1.000

Table.A.8.2. Maximum Equivalent vonMises Deck Stress, σ_{von} [MPa] in Hogging wave conditions, two cargo holds compartments 3D-FEM fine mesh model, Safety coefficients Cs according to the yield stress limit ReH

h_w [m]	Stress max(max) [MPa]	Stress adm_GS [MPa]	ReH [MPa]	max/adm_GS	Cs=ReH/max
0	16.51	265	390	0.062	23.622
8.123	356.30	265	390	1.344	1.095

Table. A.8.3. Maximum Normal Bottom Stress, σ_X [MPa] in Hogging wave conditions, two cargo holds compartments 3D-FEM fine mesh model, Safety coefficients Cs according to the yield stress limit ReH

h_w [m]	Stress max(max) [MPa]	Stress adm_GS [MPa]	ReH [MPa]	max/adm_GS	Cs=ReH/max
0	28.79	175	235	0.165	8.163
8.123	109.30	175	235	0.625	2.150

Table. A.8.4. Maximum Equivalent vonMises Bottom Stress, σ_{von} [MPa] in Hogging wave conditions, two cargo holds compartments 3D-FEM fine mesh model, Safety coefficients Cs according to the yield stress limit ReH

h_w [m]	Stress max(max) [MPa]	Stress adm_GS [MPa]	ReH [MPa]	max/adm_GS	Cs=ReH/max
0	36.04	175	235	0.206	6.521
8.123	100.40	175	235	0.574	2.341

Table. A.8.5. Maximum Tangential side stress τ_{xz} [MPa] in Hogging wave conditions, two cargo holds compartments 3D-FEM fine mesh model, Safety coefficients Cs according to the yield stress limit ReH

h_w [m]	Stress max(max) [MPa]	Stress adm_GS [MPa]	ReH [MPa]	max/adm_GS	Cs=ReH/max
0	4.51	110	235	0.041	52.164
8.123	36.52	110	235	0.332	6.435

Table.A.8.6. Maximum Normal Deck Stress,σ_X [MPa] in Sagging wave conditions, two cargo holds compartments 3D-FEM fine mesh model, Safety coefficients Cs according to the yield stress limit ReH

h_w [m]	Stress max(max) [MPa]	Stress adm_GS [MPa]	ReH [MPa]	max/adm_GS	Cs=ReH/max
0	18.24	265	390	0.069	21.382
8.123	486.50	265	390	1.835	0.802

Table.A.8.7. Maximum Equivalent vonMises Deck Stress, σ_{von} [MPa] in Sagging wave conditions, two cargo holds compartments 3D-FEM fine mesh model, Safety coefficients Cs according to the yield stress limit ReH

h_w [m]	Stress max(max) [MPa]	Stress adm_GS [MPa]	ReH [MPa]	max/adm_GS	Cs=ReH/max
0	16.51	265	390	0.062	23.622
8.123	435.40	265	390	1.642	0.896

Table. A.8.8. Maximum Normal Bottom Stress,σ_X [MPa] in Sagging wave conditions, two cargo holds compartments 3D-FEM fine mesh model, Safety coefficients Cs according to the yield stress limit ReH

h_w [m]	Stress max(max) [MPa]	Stress adm_GS [MPa]	ReH [MPa]	max/adm_GS	Cs=ReH/max
0	28.79	175	235	0.165	8.163
8.123	120.70	175	235	0.690	1.947

Table. A.8.9. Maximum Equivalent vonMises Bottom Stress, σ_{von} [MPa] in Sagging wave conditions, two cargo holds compartments 3D-FEM fine mesh model, Safety coefficients Cs according to the yield stress limit ReH

h_w [m]	Stress max(max) [MPa]	Stress adm_GS [MPa]	ReH [MPa]	max/adm_GS	Cs=ReH/max
0	36.04	175	235	0.206	6.521
8.123	107.80	175	235	0.616	2.180

Table. A.8.10. Maximum Tangential side stress τ_{xz} [MPa] in Sagging wave conditions, two cargo holds compartments 3D-FEM fine mesh model, Safety coefficients Cs according to the yield stress limit ReH

h_w [m]	Stress max(max) [MPa]	Stress adm_GS [MPa]	ReH [MPa]	max/adm_GS	Cs=ReH/max
0	4.51	110	235	0.041	52.164
8.123	42.41	110	235	0.386	5.541

Table.A.8.11. Maximum Normal Deck Stress,σ_X [MPa] in Hogging wave conditions, two cargo holds compartments 3D-FEM fine mesh model, Safety coefficients Cs according to the yield stress limit ReH, with Hotspot correction

h_w [m]	Stress max(max) [MPa]	Stress adm_GS [MPa]	ReH [MPa]	max/adm_GS	Cs=ReH/max
0	16.47	265	390	0.062	23.675
8.123	321.57	265	390	1.213	1.213

Table.A.8.12. Maximum Equivalent vonMises Deck Stress, σ_{von} [MPa] in Hogging wave conditions, two cargo holds compartments 3D-FEM fine mesh model, Safety coefficients Cs according to the yield stress limit ReH, with Hotspot correction

h_w [m]	Stress max(max) [MPa]	Stress adm_GS [MPa]	ReH [MPa]	max/adm_GS	Cs=ReH/max
0	16.19	265	390	0.061	24.089
8.123	294.76	265	390	1.112	1.323

Table.A.8.13. Maximum Normal Deck Stress,σ_X [MPa] in Sagging wave conditions, two cargo holds compartments 3D-FEM fine mesh model, Safety coefficients Cs according to the yield stress limit ReH, with Hotspot correction

h_w [m]	Stress max(max) [MPa]	Stress adm_GS [MPa]	ReH [MPa]	max/adm_GS	Cs=ReH/max
0	16.47	265	390	0.062	23.675
8.123	389.90	265	390	1.470	1.000

Table.A.8.14. Maximum Equivalent vonMises Deck Stress, σ_{von} [MPa] in Sagging wave conditions, two cargo holds compartments 3D-FEM fine mesh model, Safety coefficients Cs according to the yield stress limit ReH, with Hotspot correction

h_w [m]	Stress max(max) [MPa]	Stress adm_GS [MPa]	ReH [MPa]	max/adm_GS	Cs=ReH/max
0	16.19	265	390	0.061	24.089
8.123	371.64	265	390	1.402	1.049